DISSERTATION

MEASURING AND MODELING TRANSPIRATION AND PHOTOSYNTHESIS IN ZEA MAYS AND HELIANTHUS ANNUUS: LEAF-LEVEL AND SAP FLOW STUDIES

Submitted by

Grace Susanna Lloyd Miner

Department of Soil and Crop Sciences

In partial fulfillment of the requirements

For the Degree of Doctor of Philosophy

Colorado State University

Fort Collins, Colorado

Summer 2016

Doctoral Committee:

Advisor: William Bauerle
Co-Advisor: Jay Ham

Scott Denning
Dale Shaner

Copyright by Grace Susanna Lloyd Miner 2016

All Rights Reserved

ABSTRACT

MEASURING AND MODELING TRANSPIRATION AND PHOTOSYNTHESIS IN ZEA MAYS AND HELIANTHUS ANNUUS: LEAF-LEVEL AND SAP FLOW STUDIES

Methods of estimating the exchanges of CO_2 and water between the land and the atmosphere are critical for predicting the responses of plant communities and field crops to a changing climate. Biological and physical processes are incredibly complex, and efforts to predict assimilation (A_n), stomatal conductance (g_s), or transpiration (T) must strike a balance between predictive accuracy and simplicity of implementation. A common approach is to couple a model of A_n (Farquhar, Caemmerer et al. 1980) to the Ball-Berry model (BB model) of g_s (Ball, Woodrow et al. 1987). A strength of this approach is that the models can be parameterized with relatively few physiological variables and then utilized in leaf-level, regional, and global models. In conjunction with model estimates, there must be accurate and user-friendly tools for validating model estimates and measuring T at the field or watershed scale. This dissertation is divided into four discrete but complimentary chapters centered on (i) evaluation and measurement of key parameters utilized in modeling g_s and A_n and (ii) measuring plant and canopy T with a low-cost open source sap flow tool.

Chapter 1 is a survey of published values of the slope parameter (*m)* in the BB model of g_s, which represents the composite sensitivity of g_s to A_n, CO_2 concentration [CO_2], humidity, and temperature (Ball, Woodrow et al. 1987). Designated values of *m* can have large impacts on simulated T, but there is a lack of synthesis regarding how *m* varies (i) in response to growth conditions or water stress and (ii) between species or plant functional types (PFTs). This chapter examines various measurement techniques for *m* and discusses factors that can influence

estimates. The wide variety of collection methods and differences in the data used to determine *m* likely contributes to variation in published values and obscures clear comparison of values. There is no clear agreement on how *m* changes in response to water stress, and differences in conclusions between studies may be due to the degree and duration of water stress or differences in thresholds of sensitivity between PFTs. The overall mean value of the BB *m* calculated from historical values for C3 vegetation was 10.01 ± 6.43 (n = 227). The mean value dropped to 5.16 ± 2.98 (n = 13) for C4 vegetation. There was a large amount of variation around the mean, with reported values as low as 0.7 to as high as 39.2. Inter-species variation was large for all PFTs, frequently varying by over 100%. Despite this variation, the mean values by PFT generally agreed with those utilized in earth system models (ESMs), although the mean literature values for C3 grasses, C3 crops, C4 crops, and herbaceous species were higher. Interestingly, despite the large variation in collection techniques, the value rankings by PFT largely agree with the recent framework and hypotheses proposed for understanding and predicting the values of *m* across PFTs (Lin, Medlyn et al. 2015).

Chapter 2 examines both the BB slope and the 'residual' g_s as light goes to zero (g_0) for two field crops, maize (*Zea mays L.)* and sunflower (*Helianthus annuus L.*). Both parameters are influential in modeled estimates of transpiration, but the time-intensive nature of leaf-level measurement results in sparse physical data reflecting species-specific values or the response to season or soil moisture stress. This work measured *m* and g_0 seasonally and under different water availability and determined the minimum stomatal settling times needed for robust estimates. In maize, the parameters could be obtained in < 20 minutes per plant by utilizing changes in Photosynthetic Photon Flux Density (PPFD), whereas ≈ 40 minutes per plant was needed in sunflower. Lower g_s under water stress reduced the absolute change in the g_s response, further

decreasing the time needed to obtain parameters. Differences in the statistical method used to determine *m* and g_0 impacted parameter estimates by up to 30%. There was no evidence of a seasonal shift in either parameter in well-watered maize, supporting the use of a single value for modeling across the season. Measurements of leaf traits correlated with *m* also corroborated this finding. Well-watered parameter values for maize ($m = 4.53 \pm 0.65$; $g_0 = 0.017 \pm 0.016$ mol m^{-2} s^{-1}) were similar to those currently utilized in land-surface models for C4 plants, but were higher than values previously reported for maize. The mean *m* value for well-watered sunflower ($m = 8.84 \pm 3.77$) was similar to the value used for C3 plants in land-surface models (i.e., ≈ 9), but varied from values reported elsewhere for sunflower. Sunflower g_0 values were highly variable and were larger ($g_0 = 0.354 \pm 0.226$ mol m^{-2} s^{-1}) than those reported for most plants. However, nighttime gravimetric measurements corroborated that substantial g_s and T occurred when $A_n < 0$. While seasonal changes were not significant for either parameter in sunflower, additional replication may be necessary to detect shifts in g_0. Water stress reduced both parameters in maize. In sunflower, only g_0 values were reduced with water stress, although there was an indication of a decline in *m* under rapid and severe water stress. Our results show that both of the BB parameters must be adjusted downward under water stress in maize, whereas the g_0 term is reduced under water stress in sunflower.

The analysis in Chapter 3 focuses on the maximum electron transport capacity (J_{max}) and the maximum carboxylation capacity (V_{cmax}), two parameters of the Farquhar et al. (1980) model of A_n which represent leaf photosynthetic capacity (P_c). V_{cmax} and J_{max} show genotypic and phenotypic variation and change as a function of growth environment, leaf age, and drought. Failure to incorporate temporal shifts in P_c results in poor model estimates of annual C uptake, but changes are often neglected due to the labor-intensive nature of collecting a sequence of leaf-

level gas exchange measurements for parameter calculations. Data on species-specific seasonal or water stress responses are often scarce, resulting in models using fixed V_{cmax}/J_{max} values for broad classes of PFTs. Given the difficulty of measuring P_c parameters via gas exchange, it is appealing to calculate variations via the relationship between leaf P_c and nitrogen (N) content. General relationships between N – V_{cmax} and N – Chlorophyll (Chl) have been reported across a wide range of PFTs, but the strength of the relationships vary widely. Further, the relationships are often developed by collecting data across strong gradients in environmental variables or across PFTs, and it is less clear if the relationships can describe the temporal effects of leaf age or drought. Knowledge of seasonal linkages between leaf Chl, N and P_c opens the possibility of estimating parameters at large scales if Chl or N can be sensed remotely. In this study we characterized the seasonal variability of V_{cmax}, J_{max} and assimilation (A_{max}) under different water availability for maize and sunflower and coupled these data with measurements of leaf spectral properties, Chl, N and leaf mass per unit area (LMA). We then examined the seasonal relationships between leaf properties and P_c. We observed a significant relationship between SPAD – Chl in maize, but found no seasonal variation in Chl or SPAD values in sunflower. The seasonal Chl - N_a relationship was significant in maize, but with a lower slope than previously reported, while the Chl – N_a relationship was not significant in sunflower. Area based N – V_{cmax} relationships were not significant for either crop. Mass-based relationships were highly significant for maize, whereas the relationship in sunflower was poor. Seasonal variability in P_c was not well described by changes in leaf spectral properties, Chl, or N_a in sunflower. In maize, P_c was highly correlated to changes in LMA and DOY. These results suggest that reliable estimates of P_c from leaf properties may not be successful in well-fertilized field crops and the relationships should be carefully evaluated prior to utilization.

Chapter 4 presents a new low-cost tool for measuring sap flow (SF). SF measurements provide a valuable tool for studying plant water relations. The heat pulse (HP) SF method can provide logistical advantages over other sap flow techniques due to the low power requirements as well as the fact that one gauge can be used on plants varying different stem diameters. In this study we utilize new developments in HP theory, low-cost electronics, and desktop manufacturing to construct, calibrate, and validate an affordable research-grade HP measurement tool. We also compared the performance of the T_{max} HP method to a new HP technique based on the ratio of the temperature maxima measured by a downstream and tangential probe (HR_{max}).

Gauges were fabricated using 3D-printing technology and low-cost electronics to keep materials cost under $25 per gauge. Each gauge included three needle probes that were inserted into the stem periphery. A central needle contained a resistance heater for applying the heat pulse, while two additional needles measured the resulting temperature increases at positions downstream and tangent to the flow direction. The resultant data was used to calculate sap velocity using two techniques. The T_{max} method used the time to temperature maximum (T_{max}) while a novel heat ratio method (HR_{max}) used the ratio of the temperature increase between the downstream and tangent probes. The data acquisition and control systems were built from low-cost Arduino microcontrollers. Prototype SF gauges were tested and calibrated for corn and sunflower in the greenhouse, and once calibrated for a specific gauge design and species, the gauges closely tracked gravimetric measurements of plant transpiration. The T_{max} method performed well under high rates of sap flow (i.e., up to 300 g hr^{-1}) in both sunflower and corn, but the accuracy of measurements was poor at low rates of transpiration. The T_{max} method overestimated sap flow when transpiration fell below ≈ 20 g hr^{-1} (corn) ≈ 50 g hr^{-1} (sunflower). The new HR_{max} method was able to accurately track sap flow at high flows and also performed

remarkably well at tracking nighttime flows as low as 3 g hr^{-1} in corn. The gauges were also deployed in the field on irrigated corn to validate the calibration coefficients determined in the greenhouse. Estimates of transpiration over a two-week period were within 10% of calculated reference evapotranspiration under the new HR_{max} method, whereas the T_{max} method overestimated transpiration due to overestimation of nighttime flows.

The entire measurement system is 5 to 10 times less expensive than commercial alternatives and can be constructed in-house by researchers, producers, or students interested in the technology. The do-it-yourself simplicity and low cost of the approach make it possible to deploy large numbers of gauges in the field to capture spatial variability, compare water use among agronomic plots, or scale-up sap flow to measure canopy transpiration.

ACKNOWLEDGEMENTS

The following paragraphs will be read by only a few individuals, as the acknowledgments section is hardly gripping reading. Hence, it is to those readers that I am writing. Here, on this one page, I get to write the 'ending' to this five-year process.

It has been a convoluted, difficult journey, and I would not be writing these words if not for the dedication of my co-advisors, Dr. Bill Bauerle and Dr. Jay Ham. In the course of this PhD, I lost my brother and became a mother, two major life events that could easily have led me to step away from this endeavor. Instead, I had two mentors who continually bolstered and supported me. Bill – Life and loss has changed both of us these past few years, and I am grateful to know you both as an advisor and a friend. I always knew you were cheering for me, now more than ever. Jay - I am grateful for your authenticity, your scientific rigor, and your friendship. Not many PhD advisors send their students Annie Dillard quotes to remind them that "How we spend our days is, of course, how we spend our lives." Having you as a mentor has truly transformed my thinking and my life. I am also deeply appreciative to the other members of my committee, Dr. Dale Shaner and Dr. Scott Denning. You gave freely of your time and resources, and I have benefited from your guidance.

Blake – your love and support is remarkable. I am more blessed in you than anyone has ever been blessed before. To my parents, and my siblings – each of you is a part of this work and my life's meaning. Michael – thank you for believing in me and being my biggest advocate. I am grateful to have had you as a brother - there are so many things I still needed to ask you. Someday we will be able to sing again? And with that: I am glad I did it, even if I failed a thousand times along the way.

TABLE OF CONTENTS

CHAPTER 1:

ESTIMATING THE SENSITIVITY OF STOMATAL CONDUCTANCE TO PHOTOSYNTHESIS IN THE BALL-BERRY MODEL: A REVIEW

Summary

A common approach for estimating fluxes of CO_2 and water in leaf and canopy models is to couple a biochemical model of photosynthesis (A_n) (Farquhar, Caemmerer et al. 1980) to a semi-empirical model of stomatal conductance (g_s) such as the widely validated and utilized Ball-Berry (BB) model (e.g., Ball, Woodrow et al. 1987). This coupling provides an effective way of predicting transpiration rates at multiple scales, and this strategy is utilized in many leaf and canopy-level physiological models, as well as in regional and global earth system models (ESMs). The designated value of the empirical slope parameter (*m*) in the BB model can have large impacts on simulated transpiration. However, there is a lack of consensus or synthesis regarding how *m* varies between species or plant functional types (PFTs) or in response to growth conditions. Literature values are highly variable, and comparisons are made difficult due to differences in collection methodologies and methods of determining *m*. In this review, we review the various methodologies used to estimate *m* and collate reported values by PFT and in response to elevated CO_2 and water stress.

We found a wide variety of collection techniques for *m*, and posit that differences in measurement techniques can influence the resultant *m* value, particularly if stomata have not reached steady-state. Transparent reporting of the methodology and data used to determine *m* is needed to permit a clearer comparison of values. There was lack of a literature consensus regarding how *m* changes in response to water stress, and differences in results may be obscured

by differences in collection methodologies, the degree and duration of water stress, and different thresholds of sensitivity between PFTs. The mean value for C3 vegetation was 10.01 ± 6.43 (n = 227). The mean value dropped to 5.16 ± 2.98 (n = 13) for C4 vegetation. There was a large amount of variation around the mean, with reported values ranging from as low as 0.7 to as high as 39.2. Inter-species variation was also large for all PFTs, frequently varying by over 100%. While some of this variation is likely due to the differences in collection methodologies, the disparate values obtained for the same or similar species is surprising, and may reflect differences due to distinct ecotypes from hydrologically contrasting sites or climate of origin. The mean *m* by PFT compiled from the literature generally agreed with the values utilized in ESMs, although the mean values for C3 grasses, C3 crops, C4 crops, and herbaceous species were higher. Interestingly, despite the large variations in collection techniques and the value rankings of *m* by PFT largely agree with a recent framework and hypotheses recently proposed for understanding and predicting the values of *m* across PFTs and biomes (Lin, Medlyn et al. 2015).

Introduction

Plant canopies affect the water and energy budgets of the land surface by controlling the passage of water vapor and carbon dioxide (CO_2) through the aperture or conductance of small orifices on the leaf surface called stomata. As a control interface involved in regulating plant water loss, a better understanding of how to model stomatal conductance (g_s) is important for accurate predictions of transpiration (e.g., Bauerle and Bowden 2011). Stomatal responses are also important for larger-scale regional predictions of hydrology, runoff, carbon uptake, and energy fluxes in land surface models (Berry, Beerling et al. 2010). Approximately 40% of the precipitation that falls on land surfaces is returned to the atmosphere via transpiration (T) (Berry,

Beerling et al. 2010), highlighting the importance of accurate stomatal response parameterization in land-atmosphere models. Water vapor exchanges over a range of temporal and spatial scales are complex functions, usually requiring simplifications of biological, chemical, and physical processes. To capture feedbacks that span multiple temporal and spatial scales, land surface models must simulate the response of transpiration to changes in environmental conditions and differences in available soil water.

A common approach for estimating fluxes of CO_2 and water in leaf and canopy models is to couple a biochemical model of photosynthesis (A_n) (Farquhar, Caemmerer et al. 1980) to a semi-empirical model of stomatal conductance (g_s) such as the widely validated and utilized Ball-Berry (BB) model (e.g.,Ball, Woodrow et al. 1987; Ball 1988; Collatz, Ribas-Carbo et al. 1992). Relative to other g_s models, the BB model requires fewer parameters (e.g., Damour, Simonneau et al. 2010). Thus, the coupling of the BB g_s model to A_n provides an efficient and effective way of predicting transpiration rates at multiple scales, and this strategy is utilized in many leaf and canopy-level physiological models, as well as in regional and global earth system models (ESMs) of carbon and water cycling (e.g., Wang and Jarvis 1990; Sellers, Randall et al. 1996; Sellers, Dickinson et al. 1997; Baldocchi and Meyers 1998; Bounoua, Collatz et al. 1999; Oleson, Niu et al. 2008; Kattge, Knorr et al. 2009; Berry, Beerling et al. 2010).

Carbon fluxes are frequently estimated using the A_n model of Farquhar et al. (1980), a mechanistic model that can quantify how A_n responds to changes in environmental variables. The key parameter in the Farquhar et al. (1980) model is the maximum carboxylation rate (V_{cmax}, $\mu mol\ CO_2\ m^{-2}\ s^{-1}$), while other parameters such as the maximum rate of electron transport (J_{max}) and respiration (R_d) can be scaled with V_{cmax} (Wullschleger 1993; Medlyn, Dreyer et al. 2002). The development of a fully mechanistic model of g_s that can be applied across scales has proven

to be more elusive, and our current understanding of the underlying physiological mechanisms of stomatal responses is less than complete. Hence, the majority of the proposed g_s models are empirical or semi-empirical (Damour, Simonneau et al. 2010). Models of g_s can be broadly grouped into three different categories – multiplicative or limiting-factor models (Jarvis 1976), semi-empirical models based on the g_s - A_n relationship (e.g., Ball, Woodrow et al. 1987; Ball 1988; Leuning 1990; Collatz, Ribas-Carbo et al. 1992; Leuning 1995), and process-based water stress response models based on ABA signaling, leaf water potential, or hydraulic control (Tyree and Sperry 1988; Tardieu and Davies 1993). We note that a separate group of g_s models based on economic stomatal optimization theory, i.e. that stomata maximize carbon gain (A) while minimizing water loss (E) (Cowan and Farquhar 1977; Cowan 1982; Mäkelä, Berninger et al. 1996; Katul, Manzoni et al. 2010), has recently been considered for climate models (Medlyn et al., 2011, Heroult et al., 2013, Lin et al. 2015). However, the approach has not yet gained widespread acceptance. Noting the diversity of approaches for modeling g_s (Damour, Simonneau et al. 2010) we focus here on the semi-empirical equation first posited by Ball, Woodrow, and Berry (1987) with the minor modifications thereafter (Leuning 1995; Medlyn, Duursma et al. 2011). We focus on this model as it has been widely adopted in modeling g_s at scales from the leaf to the globe, and has broad appeal due to its accuracy and simplicity ((Buckley and Mott 2013) Other models that couple g_s to A_n utilize different forms of the BB model, but similarly couple the demand for CO_2 with g_s to water vapor and the "logic and limitation are similar in all" (Berry, Beerling et al. 2010). The Ball-Berry (BB) model describes g_s to water vapor as:

$$g_s = m * A_n \frac{H_s}{C_s} + g_o \quad (1)$$

where H_s is the relative humidity at the leaf surface, C_s is the CO_2 concentration [CO_2] at the leaf surface (µmol mol^{-2}), *m* is the slope of the relationship between g_s and A_nH_s/C_s determined via linear regression, and g_0 (mol m^{-2} s^{-1}) is the intercept of the regression, representing minimum g_s (Ball, Woodrow et al. 1987; Ball 1988). The latter group of terms (i.e., A_nH_s/C_s) is hereafter referred to as the Ball Index. This simple model can describe stomatal responses to environmental parameters such as light, CO_2, temperature, and humidity (Ball 1988).

The designated value of the empirical slope parameter in the BB model can have large impacts on simulated transpiration (Leuning, Dunin et al. 1998; Lai, Katul et al. 2000; Bauerle and Bowden 2011; Barnard and Bauerle 2013; Bauerle, Daniels et al. 2013) and on estimates of carbon flux (Luo, Medlyn et al. 2001; Bauerle, Daniels et al. 2013). While the influence of the value of *m* on transpiration estimates has been found to vary between spatial scales and environmental gradients, the effect can be large (Bauerle, Daniels et al. 2013; Dietze, Serbin et al. 2014). For example, Bauerle et al. (2014) examined how modeled transpiration estimates were impacted by using either the mean value of reported *m* values versus using values ± 1 standard deviation from the mean, and found that model estimates were impacted by up to 46%. Despite the parameter's importance, it remains unclear how much *m* varies between plant functional types (PFTs). Species-level differences clearly exist (Ball, Woodrow et al. 1987; Ball 1988; Collatz, Ball et al. 1991) but the values reported in the literature are highly variable between and within species, as well as among studies. In the absence of information providing further resolution, some earth system models use only a few constant *m* values that encompass broad vegetation classes. Typical values utilized are $m = 9$ for C3 vegetation and $m = 4$ for C4 vegetation (Collatz et al. 1991, 1992, Sellers et al. 1996), with some models incorporating slight differentiations by plant functional type. For example, the Community Land Model (CLM)

utilizes a lower value of *m* for needle leaf evergreen trees (*m* = 6) than for broadleaf deciduous trees and crops (*m* = 9) (Oleson, Lawrence et al. 2010). Other models use slightly higher values for crop species (*m* = 10) and temperate broad-leaved forests (*m* = 9.5) and lower values for boreal conifer forests (*m* = 7.5) (Baldocchi and Meyers 1998).

In addition to the lack of information on species-level differences in *m*, there is also controversy surrounding whether *m* changes in response to environmental variables such as moisture stress or elevated [CO_2] (Tenhunen, Serra et al. 1990; Sala and Tenhunen 1996; Medlyn, Barton et al. 2001; Xu and Baldocchi 2003; Leakey, Bernacchi et al. 2006; Wolf, Akshalov et al. 2006; Medlyn, Duursma et al. 2011; Heroult, Lin et al. 2013). This leads to different approaches for representing drought effects in simulation models – some models reduce *m*, whereas other models incorporate drought impacts by scaling back parameters of the A_n model, with a few models including both effects (e.g., Egea, Verhoef et al. 2011; Zhou, Duursma et al. 2013).

A clearer understanding of how *m* varies by species and PFT and whether there is physiological acclimation under drought or elevated [CO_2] is critical for depicting accurate vegetation responses in coupled A_n – g_s models, but there is a lack of consensus or synthesis regarding how *m* varies between species and in response to growth conditions. Comparisons are made more difficult due to differences in collection methodologies, methods of determining *m*, and the differences in the parameter values obtained between various indices (i.e., Ball et al., 1987 vs. Leuning 1995). The overarching objective of this review is to collate reported values and patterns of response by PFT and under variable growth conditions for the BB slope parameter, *m.* A summary and compilation of existing values will be useful as a resource for modelers working at a range of scales. As the g_0 term of the BB g_s model is frequently reported

in studies examining *m*, we also compile g_0 values where available in order to further build on previous reviews (Snyder, Richards et al. 2003; Caird, Richards et al. 2007). A secondary objective is to highlight the differences in collection techniques and methods of estimating the *m* parameter in order to encourage methodologies that allow for comparison of values between PFTs and growing conditions.

We first revisit the original presentation of the BB model of g_s, and review commonly utilized variations of this model. We next outline the original methodology for estimating the two empirical parameters of the model, *m* and g_0, and point out the differences in experimental techniques that can influence parameter estimates and may contribute to the variable values found in the literature. We also offer a brief summary of the non-traditional but novel ways that *m* has been collected. Next, we chronologically explore the historical developments and controversies over the stability of *m* under changing environmental conditions. Finally, we utilize a thorough literature survey to compile reported values of *m* and general patterns of parameter values by PFT.

Background

The first presentation of a semi-empirical model of g_s was published in 1987 (Ball, Woodrow et al. 1987), building upon a previously observed correlation between A_n and g_s that implied some level of regulation between the demand for CO_2 by the chloroplasts and stomatal control of CO_2 supply (Wong, Cowan et al. 1979; Wong, Cowan et al. 1985). Ball et al. (1987) found a linear relationship between g_s and a combined physiological index (A_n* H_s/C_s; i.e., the Ball Index) that held over a broad range of environmental conditions. The slope of this relationship (*m)* represents a composite sensitivity of g_s to A_n, [CO_2], humidity, and temperature (Ball et al., 1987). The model was more fully developed in Ball's PhD dissertation (1988),

which confirmed the robust nature of this empirical relationship for an additional eight species. Ball (1988) reported values of *m* ranging from 2.4 to 16.4 for a variety of C3 and C4 species, with values differing between species and separating distinctly by photosynthetic pathway. The ordinate intercept also varied between species, with some species having intercepts significantly different from zero.

A key finding from this body of work was that *m* represents a "compromise between the costs and benefits of g_s relative to the photosynthetic activity of the leaf" and that instantaneous water-use efficiency (A_n per unit T; W_T) and carbon isotope discrimination (δ^{13} C) during A_n were inversely related to *m*. Ball et al. (1987) and Ball (1988) additionally showed that the empirical model of g_s could be arranged to:

$$\frac{C_i}{C_s} = 1 - \frac{1.6}{H_s * m} \quad (2)$$

High values of *m* corresponded to lower W_T, higher C_i/C_s, and decreased isotope discrimination. We note that the slope parameter *m* is called by other terms in the literature, including g_{fac} (Tenhunen, Serra et al. 1990; Falge, Graber et al. 1996), g_f (Sala and Tenhunen 1996; Van Wijk, Dekker et al. 2000), *k* (Ball, Woodrow et al. 1987; Harley and Tenhunen 1991; Baldocchi and Harley 1995), g_m (Chen, Coughenour et al. 1994), a_1 (Leuning 1995; Leuning, Dunin et al. 1998), b_1 (Dougherty, Bradford et al. 1994), and g_1 (Leuning 1995; Medlyn, Duursma et al. 2011). We refer to the slope parameter as *m*, conserving the definition as a derived slope.

The BB model has not escaped criticism - the most appropriate and accurate form of humidity response is the subject of debate (Damour, Simonneau et al. 2010), with some arguing that mechanistically g_s must be dependent on transpiration instead of relative humidity (Mott and

Parkhurst 1991; Monteith 1995; Oren, Sperry et al. 1999). The BB model also performs poorly in C3 species at sub-ambient concentrations of [CO_2], when rates of photorespiration increase (Leuning 1990; Weber and Gates 1990; Lloyd 1991). Leuning (1990, 1995) proposed an altered version of the BB model by incorporating the CO_2 compensation point (Γ) and replacing H_r with Lohammer's function of vapor pressure deficit (VPD) as a proxy for transpiration (Leuning 1995):

$$g_s = g_0 + \frac{mA_n}{(c_s - \Gamma)\left(1 + \frac{D_s}{D_0}\right)} \tag{3}$$

where D_s is the leaf-to-air VPD (kPa) and D_o is a fitted parameter. Incorporation of Γ in the denominator is necessary at low CO_2 concentrations, as A_n goes to zero at the Γ rather than when C_s goes to zero (Leuning 1990). For C4 plants, the Γ is too low for this alteration to substantially improve the predictive power of the equation (Dougherty 1994). An issue with the Ball-Berry-Leuning (BBL) equation is that *m* and D_o are strongly correlated, suggesting a degree of redundancy. Leuning (1995) pointed out this correlation, noting that the choice of one parameter influences the range of the other. This makes it difficult to estimate parameters with confidence or to clearly interpret differences in parameters among datasets (Medlyn, Berbigier et al. 2005; Medlyn, Duursma et al. 2011).

Medlyn et al. (2011) proposed a model formulation that combines the BB model with the optimal stomatal control model of Cowan and Farquhar (1977):

$$g_s = g_0 + 1.6\left(1 + \frac{m}{\sqrt{D}}\right) * \frac{A_n}{C_s} \tag{4}$$

and that *m* increases linearly with the combination of terms:

$$m \propto \sqrt{\Gamma^* \cdot \lambda} \quad (5)$$

Where Γ^* is the CO_2 compensation point of A_n in the absence of dark respiration and λ is the Lagrangian multiplier of the stomatal optimization theory (if D is expressed in kPa, then *m* has units of $kPa^{0.5}$). The authors call this the "Unified Stomatal Optimization Model" (USO), offering a simple means for quantifying λ using the fitted parameter *m* as a proxy (Medlyn, Duursma et al. 2011). This more recent formulation provides a useful framework for understanding and predicting differences in plant water use strategies and stomatal behavior between PFTs and biomes.

The BBL and USO g_s models have been shown to outperform the BB model for specific data sets (Leuning 1995; Falge, Graber et al. 1996; Medlyn, Duursma et al. 2011), while in other cases the BB model performs in a superior fashion (Baldocchi and Harley 1995; Bunce 1998; Wohlfahrt, Bahn et al. 1998; Gutschick and Simonneau 2002), with some studies reporting negligible differences between g_s models (Mo and Liu 2001; Macfarlane, White et al. 2004). Our purpose is not to review the utility of the various forms of the equation, but rather to report methods of parameter collection and to offer a synthesis of the variation in values within species and by PFT. Given the historical depth of literature surrounding the BB model, we focus primarily on the values reported for the original model and the later BBL formulation, but also note the valuable synthesis provided by the USO model.

Traditional Methods of Deriving the BB slope parameter

In the original derivation of *m* and g_0, Ball (1988) worked under experimentally controlled conditions and varied one of four factors (i.e., the ambient mole fraction of CO_2 (C_a), the ambient mole fraction of water vapor (W_s), photosynthetically active radiation (PAR), and air

temperature (T_a)) while the other factors were held constant. Data were recorded only when A_n and g_s "closely approached steady-state" as the BB g_s model "makes no attempt to describe transient responses. In nature, of course, conditions are constantly changing" (Ball 1988). The slope (*m*) and intercept (g_0) were then derived via regression on g_s versus the Ball Index.

Importance of near steady-state responses

The limitation of recording data only when near steady-state conditions are reached for g_s and A_n is important to note for researchers attempting to measure *m*, and can impose challenges in terms of collection and replication. Stomata respond more slowly than A_n to changes in environmental conditions (e.g., Pearcy 1990) and the time it takes for g_s to approach steady-state conditions after a shift in environmental conditions is dependent on both the species and the variable being altered (Jones 2013). For example, Grantz and Zeiger (1986) found a 5-fold difference in the kinetics of the stomatal half-time responses to changes in light and VPD between soybean and sugarcane, and observed symmetric temporal opening and closing in response to light but asymmetric temporal responses to changes in VPD. Aasamaa and Sober (2011) found that stomatal sensitivities to changes in light intensity, [CO_2], and air humidity were higher in slow-growing temperate deciduous trees than in fast-growing species. Brodribb et al. (2009) studied the kinetics of stomatal light responses for an evolutionary cross-section of vascular land plants, and found that the half-times of stomatal closure after the transition from light (1000 PAR) to dark (0 PAR) varied drastically between families and species (i.e., from 249 seconds to 9902 seconds). The speed of stomatal opening and closure has also been shown to be dependent on guard cell morphology and mechanics, with grasses often displaying a capacity for faster stomatal opening and closure (Franks and Farquhar 2007), and there are additional variations in the kinetics of stomatal response between C3 and C4 grasses (Knapp 1993). Water

stress can decrease the time required for closure in response to variations in light (Knapp and Smith 1990) or humidity (Aasamaa and Sober 2011). In addition, the type of gas exchange system used to induce step-wise changes may influence the required measurement times (i.e., speed of detection, location of the IRGA, etc.). Clearly, the time for stomata to reach semi steady-state conditions also depends heavily on the magnitude of the change in the environmental response variable. Furthermore, the leaf environmental conditions prior to the initiation of measurements will impact settling times – if a leaf is placed in a cuvette and exposed to drastically different light conditions, it may take quite some time for stomata to adjust (Biosciences 2002).

All of these factors influence the time investment needed to obtain accurate estimates of *m*. Preliminary experiments are often necessary to determine the stomatal settling time for near steady-state conditions to occur after a variable is altered. Xu and Baldocchi (2003) utilized light and CO_2 response curves to obtain *m*, and found that a 3-minute settling time for each level resulted in a *m* of 1.6 ($r^2 = 0.13$), whereas when the settling time was increased to 8 minutes, the estimated value of *m* increased to 8.75 ($r^2 = 0.91$). This highlights the apparent but often overlooked fact that, depending on the variable being manipulated and the direction of change, the slope or the intercept can be either over or underestimated if too short of a time step is used. Leuning (1990) also noted this, stating that different values of g_s were observed for a given value A_n "depending on whether irradiance was increasing or decreasing. The stomatal index thus applies only for steady-state."

Another concerning question about reported *m* values is the somewhat arbitrary definition of what constitutes a steady-state or 'stable' measurement of g_s. Useful definitions have been posited – i.e., Brodribb et al. (2009) defined stability as a less than 3% change over 8 minutes,

while Heroult et al. (2013) defined it as the point where the coefficient of variation for A_n and g_s was <1%. Other researchers report a defined time interval, i.e. using settling times of 10, 20, or 30 minutes with each step-wise change in an environmental variable (Leuning 1995; Bunce 2000; Liozon, Badeck et al. 2000; Leakey, Bernacchi et al. 2006), with some reporting up to 1 – 1.5 hours until steady state rates of gas exchanged were achieved (Kellomäki and Wang 1997). These are useful metrics, as they inform how the parameter was collected. However, we find that this information is frequently omitted, causing ambiguity for the reader in the quality and reliability of parameter values. Reporting the time-step used, the direction and magnitude of induced environmental change, and how steady-state conditions were determined is beneficial to modelers and plant biologists alike. Additionally, detailed explanation will give investigators wishing to estimate *m* on similar species a sense of the time required for robust parameter estimations.

Exclusion, inclusion, weighting, and pooling of the data used to obtain m

Another consideration when calculating *m* is that some measurements are usually excluded from the linear regression. For example, Ball (1988) excluded measurement points with C_s<150 µmol mol^{-1} and PAR < 150 µmol m^{-2} s^{-1} as g_s no longer changes linearly with A_n at low photon flux or ambient [CO_2]. While Ball's original derivation defined g_0 as the fit intercept from the least squares regression of g_s on the Ball Index, he acknowledged that the g_s - A_n relationship can deviate from a linear relationship under low light and noted that inclusion of this data results in a situation where "g_s tends to be higher than a linear model would predict" (1988). Failure to exclude such data can result in an inaccurately low estimate of *m.* A clear corollary to this caution is that determining g_0 via linear regression on the same data utilized to determine *m* can result in underestimation of the g_0 parameter. Others also note this physiological reality, and

define g_0 instead as the g_s when A_n goes to zero (Leuning 1990; Leuning 1995). While the focus of this review is on *m*, recent work has highlighted the inaccuracies in g_0 estimates that can occur when the parameter is estimated using linear regression on data collected under condition of high light (Barnard and Bauerle 2013), and a growing body of research also acknowledges the physiological significance of this 'residual' conductance across species and plant functional types (Caird, Richards et al. 2007). Exclusion of the g_0 term (Van Wijk 2000) or forcing or setting the intercept to zero in the regression (McMurtrie et al. 1992*;* Falge et al.1996) can impact estimates of *m* and should be avoided given the current state of knowledge, unless the term has been experimentally determined to not be significantly different from zero (Gimeno, Crous et al. 2015).

Ball (1988) and Collatz et al. (1991) also emphasized that in order to prevent bias, the regression for determining *m* should include data collected under the range of light intensities, $[CO_2]$, temperature, and humidities that occur in the environment of interest. The time and feasibility constraints this poses are significant, and in practice much of the data used to determine *m* in the literature comes from utilizing (or inducing) variations in light intensity. While variations in light are the most diurnally fluctuating factor modulating g_s in many environments (Damour, Simonneau et al. 2010), changes in VPD can also strongly influence g_s (Dang, Margolis et al. 1997) and the type of response data used in the regression can influence estimates of *m.* For example, Dang et al. (1998) calculated *m* using data across a wide range of environmental conditions and found significantly higher values of *m* when the regression utilized only VPD response data *(*m = 8.12) than when all of the environmental response data was used (m = 5.59).

Another factor that can influence estimates of *m* is the distribution of data in the regression – for example, when comparing seasonal or treatment differences in *m*, older plants or plants under environmental stress may show greatly reduced g_s when compared to younger, unstressed plants. In the literature, it is often unclear whether statistically significant differences in *m* between treatments or between measurement periods is due to the presence of higher values of g_s in well-watered or young plants versus lower g_s in water-stressed or older plants. Similar arguments can be made for species comparisons. This is especially true when fitting a linear model to data that shows a curvilinear humidity response between g_s and A_n. Ball (1988) noted that a second order polynomial was significantly better at describing the humidity response of cotton, but justified a linear model, as the bulk of observations occurred under conditions where a linear model would provide a good estimate of g_s. Others have found curvilinearity in the data (Leuning 1990; Gutschick and Simonneau 2002; Heroult, Lin et al. 2013), particularly at the more extreme environmental conditions (Dougherty, Bradford et al. 1994). If high g_s and A_n measurements are not balanced with measurements of low g_s and A_n, even a small amount of curvature in a response can result in a higher slope than would be determined if there was data in lower quadrants to balance the upper curvature.

One solution is to randomly re-sample the data in the regression so that there are approximately equal numbers of data points in similar ranges. While this allows for more accurate comparisons between treatments or species, clustered data within too narrow of a range is another issue altogether, particularly if *m* is derived from diurnal g_s curves under well-watered conditions. In this situation, data can cluster in the high g_s range (cf. 'Non-traditional methods of collecting *m'*). Further, given the time-intensive nature of parameter collection, there is often

insufficient data to randomly re-sample. Hence, we caution against the comparison of results between data sets that contain differences in distribution.

One more methodological difference that can cause small discrepancies in *m* estimates is performing a single regression on combined data, versus separate regressions for each leaf or plant and then compiling these individual *m* values into a mean *m*. While the two methods can lead to similar results, the mean *m* from regression analysis on individual leaves will not be equal to *m* from combined data (Bunce 1998). We note, however, that when the data from individual leaves or plants shows little spread, the differences between regression on combined data and the mean slope from regression on individual leaves can be nominal. For example, when unpublished data from maize was compiled into one regression, the slope was 4.48, whereas the mean slope value obtained via regression on individual leaves (n = 20) averaged 4.31. At the same time, when an identical analysis method was performed on well-watered sunflower, which shows much higher variability in *m*, it resulted in *m* = 11.1 (1.083*)* for the combined regression versus a mean of *m* = 10.3 via regression on individual leaves.

Additional methods used to measure or infer *m*

Instantaneous diurnal or mid-day measurements

The long stomatal settling times that are often necessary when collecting *m* via response curves can limit replication and pose severe time constraints. As an alternative to running controlled response curves, some researchers have relied on natural diurnal fluctuations in environmental conditions to estimate *m.* Here, cuvette conditions are matched to the ambient conditions - the leaf is then inserted into the cuvette until gas exchange rates stabilize. Under this approach, the BB index is computed with the assumption that g_s is already near steady state relative to A_n. The technique has been used on measurements collected diurnally (Falge, Graber

et al. 1996; Gutschick and Simonneau 2002; Medlyn, Berbigier et al. 2005; Heroult, Lin et al. 2013), at mid-day over a seasonal time course (Bunce 2000; Bunce 2004), or when either the maximum and minimum diurnal g_s is expected (Gimeno, Crous et al. (2015). Others have calculated *m* from "branch bag" style cuvettes that open and close at defined time intervals, utilizing diurnal or seasonal variations in A_n, g_s, and environmental conditions to obtain *m* (Medlyn, Berbigier et al. 2005; Launiainen, Katul et al. 2011). Medlyn et al. (2005) estimated *m* from conditions immediately prior to the initiation of CO_2 response curves, as g_s did not change during the curves. While these techniques are appealing due to lower labor and time investment, and might be viable alternatives to the time-intensive nature of collecting *m* via steady-state response curves, a comparison of data from simultaneous measurements via both techniques is lacking.

Shimono et al. (2010) proposed an alternative method to bypass the laborious leaf-level measurement of *m*, instead using steady-state porometers to measure g_s and pairing it with on-site ambient humidity and CO_2 measurements. However, there are distinct gradients in [CO_2] and humidity within and around plant canopies (Jones 2013) that could spatially influence g_s. An additional unknown in Shimono et al. (2010) was that they did not measure A_n, but instead applied a leaf nitrogen content versus PAR relationship to estimate A_n, likely introducing additional sources of variability in *m.*

Inverse modeling approaches

As opposed to bottom-up approaches based on single-leaf measurements, some researchers use a canopy model inversion approach to estimate *m* from a best fit to measured fluxes (i.e., via eddy covariance or sap flow). A benefit of these techniques is that they can potentially integrate whole-canopy processes and account for variation among leaves and plants

(Launiainen, Katul et al. 2011). Furthermore, there is an increasingly abundant amount of long-term micrometeorological flux data (Baldocchi et al. 2001) that can potentially be utilized to obtain estimates of key ecosystem parameters, providing an alternative to the laborious nature of seasonally collecting the BB slope via leaf level gas exchange.

However, micrometeorological and sap flow data are also subject to measurement error (e.g. Baldocchi et al. 2001). In addition, there are potential errors due to simulation model structure or framework, and it can be unclear whether variation in *m* represents a real physiological change or is merely attributable to measurement error or artifacts of model sensitivity or structure (Lai, Katul et al. 2000; Wolf, Akshalov et al. 2006). For example, Van Wijk et al. (2000) calculated *m* by minimizing the difference between transpiration measured via sap flow and transpiration simulated from a process-based forest growth model, but acknowledged that derived values of *m* were specific to the model used in the derivation. Valentini et al. (1995) used eddy covariance techniques to evaluate canopy conductance (g_{sc}) by inverting the Penman-Montieth equation with measurements of latent heat flux and vapor pressure. They found that the slope of g_{sc} versus the Ball Index changed seasonally and postulated that their data could indicate either that *m* changes seasonally at the leaf level or that the balance between plant transpiration and evaporation from the soil changes seasonally. Sala and Tenhunen (1996) solved for *m* across the growing season with an inverse modeling approach and reported strong seasonal changes in the parameter. However, their inversion method to determine *m* was based on single estimated values of leaf area index (LAI) and V_{cmax}, whereas it is now known that these variables change over the season, (e.g., Dang, Margolis et al. 1998; Wilson, Baldocchi et al. 2000; Xu and Baldocchi 2003; Grassi, Vicinelli et al. 2005; Bauerle, Oren et al. 2012). Lai et al., (2000) utilized eddy covariance data to find the optimum values of *m*

required to minimize the root mean square error of measured versus modeled fluxes and their results indicated that the 'optimum' values of *m* varied among measurement periods. While they made some direct measurements of LAI and *m*, measurements of V_{cmax} occurred only twice in a two-year period and V_{cmax} was assumed constant throughout the season. Hence, unaccounted for seasonal variation in V_{cmax} could contribute to observed variation in *m.* Similarly, Wolf et al. (2006) estimated *m* by inverting a modeling paradigm of canopy CO_2 and energy fluxes, and found significant seasonal variation in the *m* estimates (i.e., 15-24*),* but could not explain the discrepancy between the leaf scale and canopy-scale *m* measurements. Ono et al. (2013) utilized canopy-averaged eddy flux measurements of g_s and A_n to calculate *m* by a top-down approach based on a double-source canopy model. Reported *m* values were highly variable across the season.

Yet another approach for calculating *m* is to re-arrange Equation 2 to obtain an 'appropriate' or specified C_i for a given C_a (Harley and Tenhunen 1991).While a typical ratio of C_i/C_a in non-stressed C3 species is approximately 0.7 and 0.3 for C4 plants, this ratio varies between species and under conditions of water stress (Wong et al. 1979; Norman 1982, Farquhar et al., 1989). In a novel utilization of the C_i/C_a ratio, Katul et al. (2000) estimated *m* from the mean C_i/C_a ratio derived from δ^{13} C measurements (neglecting the g_o term), but noted that the constant C_i/C_a approximation does not reflect measured variation in the ratio under variable environmental conditions such as drought. As highlighted by Blum (2005), the C_i/C_a ratio is "often susceptible to misinterpretation, especially when the dynamics of the nominator and denominator are obscure." Variations in the value of C_i/C_a for a given species can occur through changes in g_s, changes in photosynthetic capacity or a combination of both (Condon, Richards et al. 2002). For example, the ratio can decrease under drought due to reductions in stomatal

aperture for a given rate of A_n, but the ratio can also *increase* under drought if non-stomatal limitations cause decreases in A_n. Hence, assuming a constant seasonal value of C_i/C_a for determining *m* can be problematic, particularly under conditions of water stress (Xu and Baldocchi 2003).

The stability of m under changing environmental conditions

Changes in m under elevated CO_2

While only a handful of studies have specifically focused on measuring changes in *m* under elevated CO_2, the results from woody perennial species have been variable. Weber and Gates (1990) found no alteration of *m* as a function of $[CO_2]$ in red oak (*Quercus rubra*). Kellomake and Wang (1997) reported that elevated $[CO_2]$ significantly decreased *m* in Scots pine (*Pinus sylvestris*) by 10% and increased g_o by 12%. Alternatively, Liozon et al. (2000) found no significant differences in *m* or g_0 for beech saplings (*Fagus sylvatica*) grown in chambers under ambient versus elevated $[CO_2]$. Medlyn et al. (2001) analyzed data from various tree species and found that the parameters of the BB model were generally not altered by elevated $[CO_2]$. However, results diverged under conditions of water stress for one species, and they concluded that the $A_n - g_s$ relationship may change in response to a limited water supply. Gimeno et al. (2015) explicitly tested for the effect of elevated $[CO_2]$ on *m* (USO model) in a mature woodland and found the parameter to be conserved even as $[CO_2]$ was increased.

The $[CO_2]$ response of *m* reported in herbaceous annual and perennial species is similarly varied. A $[CO_2]$ response was found in rye grass (*Lolium perenne*) (Nijs et al., 1997), and Harley et al. (1992) found small but significant reductions in *m* for cotton (*Gossypium hirsutum)* grown at elevated $[CO_2]$. Chen et al. (1994) reported a significantly higher slope in response to elevated $[CO_2]$ for a C4 grass (*Andropogon gerardii*). Bunce (1998) reported that variation in growth

temperature alone caused a nearly two-fold variation in the slope for soybean (*Glycine max*) and grain amaranth (*Amaranthus hypochondriacus*) and that *m* also varied significantly as a function of growth [CO_2] and light environment in amaranth. Similarly, Bunce (2004) found that *m* decreased by nearly 50% under elevated [CO_2] for soybean grown in open-topped chambers and reported significant declines in both *m* and g_0 under elevated [CO_2] for three other crop species. These results contrast markedly with those of Leakey et al. (2006) who found no evidence for changes in *m* or g_0 in soybean after long-term growth at elevated [CO_2] in a free-air CO_2 enrichment (FACE) study, suggesting that acclimation of g_s occurs concurrently with photosynthetic acclimation.

While results in the literature are conflicting, the overarching conclusions from long-term FACE studies suggest that the coordination of g_s and A_n is not substantially altered under elevated [CO_2] (Ainsworth and Long 2005; Ainsworth and Rogers 2007; Gimeno, Crous et al. 2015), which supports the maintenance of a constant *m* under elevated [CO_2]. However, the majority of this work has been conducted on angiosperms, and recent evidence suggests that the sensitivity of stomata to changes in [CO_2] varies between plant clades (Brodribb et al. 2009), leaving open the possibility that the parameter responses to changes in [CO_2] may be species-specific.

Changes in m under water stress

The A_n - g_s relationship can be altered under water stress (Brodribb 1996; Condon, Richards et al. 2002; Katul, Leuning et al. 2003; Damour, Simonneau et al. 2010), which can render the BB group of g_s models incapable of capturing water stress responses if values for *m* are static. Numerous proposals have been made to modify the well-watered value of *m* by incorporating empirical functions based on leaf water potential (Ψ_L), soil water potential (Ψ_S), or

soil water content (θ_s) (Tenhunen, Serra et al. 1990; Sala and Tenhunen 1996; Baldocchi 1997; Wang and Leuning 1998; Van Wijk, Dekker et al. 2000; Damour, Simonneau et al. 2010). Others assert that *m* is a constrained parameter, centering around 10 ± 20% for C3 plants, and deviates only under moderate to severe soil moisture deficit (Baldocchi and Meyers 1998; Misson et al. 2004). Consequently, the extent to which *m* changes under water stress is still debated (Baldocchi 1997; Xu and Baldocchi 2003).

Tenhunen et al. (1990) asserted that *m* changes in response to the integrated water stress experienced by plants, but instead of measuring *m*, values reported in the study were estimated by matching model calculations and gas exchange measurements. Moreover, although photosynthetic parameters were adjusted as a function of temperature, they were otherwise held constant across the season. Harley and Tenhunen (1991) varied *m* as a function of $\theta_s$and varied model estimates of *m* until a specified value of C_i per Ca (i.e., ≈ 230 umol mol^{-1} at a C_a of 340 μmol mol^{-1}) was reached. Sala and Tenhunen (1996) correlated *m* with predawn xylem water potential while holding g_o, LAI and V_{cmax} constant seasonally – unmeasured changes in seasonal values of these parameters would thus be expected to contribute to changes in modeled *m.* Baldocchi (1997) incorporated a cumulative drought index to adjust *m* to model estimates of CO_2 and water vapor exchange over a temperate forest during summer drought, again discarding the seasonality of photosynthetic parameters. Still other studies varied *m* in slightly alternative empirical ways (e.g., as a function of plant water status, or θ_s)

Where physical measurements of *m* under water stress have been made, the results have been contradictory. Liozon et al. (2000) took seasonal measurements of *m,* and found that if date of measurement was taken as a factor, there were significant differences in both *m* and g_0. While not explicitly examined, the authors suggest that differences in θ_s between measurement dates

could have contributed to these seasonal shifts in parameter values. Xu and Baldocchi (2003) determined that *m* was relatively constant over the season for blue oak (*Quercus douglasii)* even with leaf age effects and conditions of severe water-stress, concluding that *m* did not need to be modified under water stress conditions. In contrast, Misson et al. (2004) measured significant variation (i.e., 350%) in *m* over the growing season for ponderosa pine (*Pinus ponderosa*) but found no significant relationship between *m* and Ψ_L or θ_s. Instead, they found that g_0 decreased as a function of Ψ_L and subsequently modified this parameter to account for soil water stress. Heroult et al. (2013) hypothesized that the sensitivity of *m* (BBL and USO models) to drought should vary with the climatic origin - of the four eucalyptus species examined, two showed significant reductions in *m* under drought and the other two species showed no difference. However, the authors point out that the slopes converged at low g_s values among all species save one, and examination of the plots suggests that differences between the well-watered and drought responses may be partly due to differences in the distribution of the data coupled with curvilinearity in the well-watered response. Alternatively, Gimeno (2015) found no evidence of a response of *m* (USO model) to changes in water availability in eucalyptus (*Eucalyptus tereticornis*). Zhou et al. (2013) analyzed experimental data sets from published and unpublished literature to examine variation in *m* (USO model) as a function of water stress and reported that the rate of decline of *m* under drought showed considerable variation among species and plant functional types, consistent with the findings of Manzoni et al. (2011) regarding λ of the stomatal optimization theory.

The lack of a consensus in the literature regarding how *m* changes in response to water stress is likely obscured by differences in collection methodologies, the degree and duration of water stress, and different thresholds of sensitivity between PFTs (e.g., Dang et al. 1997).

However, a recent body of work is directed towards understanding and predicting differences in plant water use strategies and stomatal behavior between PFTs and biomes, providing a much needed framework for understanding the response of *m* to water stress (Medlyn, Duursma et al. 2011; Heroult, Lin et al. 2013; Lin, Medlyn et al. 2015).

Variation and patterns in reported values of the Ball-Berry slope

The values of *m* reported in the literature encompass a broad range of species and PFTs. The values presented in Table 1 primarily reflect studies where *m* was physically measured, but we also included parameter values from a few highly cited and influential papers (i.e., Baldocchi and Meyers 1998, Harley and Tenhunen 1991). The value of *m* has been previously reported to center around 10 ± 20% (Baldocchi et al. 1998). The overall mean calculated from compiled historical values for C3 vegetation was similar to this at 10.01 ± 6.43 (n = 227). The mean value dropped to 5.16 ± 2.98 (n = 13) for C4 vegetation. There was a large amount of variation around the mean, with reported values ranging from as low as 0.7 to as high as 39.2 (Table 1). Inter-species variation was also large for all PFTs. For example, published values for the C3 crops soybean (*Glycine max)* and sunflower (*Helianthus annuus)* varied by ≈ 150%. Similarly varied values are reported in evergreen gymnosperms (i.e., 96% variation in *Picea mariana*) and deciduous angiosperms (i.e., 141% variation in *Acer rubrum*). While some of this variation is likely due to the differences in collection methodologies, the disparate values obtained for the same or similar species is surprising, and may reflect differences due to distinct ecotypes from hydrologically contrasting sites or climate of origin (Bauerle, Whitlow et al. 2003; Lin, Medlyn et al. 2015).

Grouping values by PFT resulted in value rankings of *m* that showed both similarities and distinctions from those currently utilized in ESMs. For example, our results showed that the average values of *m* reported in the literature were higher for evergreen and deciduous

angiosperm trees (9.8 ± 4.6 and 8.7± 5.1, respectively) than for evergreen gymnosperm trees (6.7 ± 2.5), similar to the categorical distinctions made in both the CLM and CANVEG models (Oleson et al. 2010; Baldocchi and Meyers 1998). However, the mean historical values compiled for C3 crops (13.3 ± 3.1), C3 grasses (13.5 ± 3.1), and herbaceous perennial species (13.2 ± 4.5) were notably higher than the values currently utilized in ESMs (i.e., 9 – 10). The mean value for C4 crops (5.8 ± 3.8) was also higher than the *m* value frequently used for simulating C4 vegetation (i.e., *m* = 4). Interestingly, the value rankings from our literature survey, which compiled values across multiple collection techniques, largely agree with the recent meta-analysis of Luo et al. (2015), which utilized the USO g_s model to explore variation in *m* by PFT and biome. Luo et al. (2015) observed a more conservative water use strategy (i.e., lower *m)* in gymnosperm trees than in angiosperm trees, and also found that *m* values were largest in C3 grasses and crops.

Conclusions

Accurate simulations of vegetation productivity and transpiration in coupled A_n - g_s models are dependent on robust values of the BB slope parameter, *m.* A clearer understanding of species-level differences in *m* and whether physiological acclimation occurs under drought or elevated [CO_2] is critical for characterizing vegetation responses in coupled A_n- g_s models. The wide range of values summarized in this review highlights the variability in reported values of *m*. Leaf-level quantitative estimates of *m* often require a large time investment and differences in measurement techniques can influence the resultant *m* value, particularly if stomata have not reached steady-state. Comparisons of *m* between treatments or species can also be clouded by differences in the distribution of g_s data. Transparent reporting of the methodology and data used to determine *m* is needed to permit a clearer comparison of values. Although innovative and

creative methods to determine *m* using top-down model inversion techniques bypass the time-intensive nature of leaf-level measurements, they too are accompanied by uncertainties. While only a small body of work has specifically examined variation in *m* under elevated [CO_2], the emerging consensus is that *m* is generally not altered by elevated [CO_2]. However, the response of *m* to water stress varies greatly, likely a function of the duration, severity and PFT sensitivity to water stress (Medlyn et al. 2011; Heroult et al. 2013). The mean *m* by PFT compiled from the literature generally agreed with the values utilized in ESMs, although the mean values for C3 grasses, C3 crops, C4 crops, and herbaceous species were higher. While the large variations in collection techniques for the values compiled in this review prevents statistical comparison of *m* by PFT, the value rankings largely agree with the recent framework and hypotheses recently proposed for understanding and predicting the values of *m* across PFTs and biomes (Medlyn, Duursma et al. 2011; Lin, Medlyn et al. 2015).

Table 1. Values of the slope parameter (*m*) and intercept (g_0) for the Ball Berry (BB), Ball-Berry Leuning (BBL) and USO model of stomatal conductance reported in the literature. Values in parentheses are reported standard errors while values following the ± represent the standard deviation. Collection types are 1 = Light response curve; 2 = CO_2 response curve; 3 = Humidity response curve; 4 = Temperature response curve; 5 = Vapor pressure deficit response curve; 6 = Instantaneous diurnal measurements; 7 = Other methods, including evaluation of published data sets, eddy covariance, sap flow, least squares minimization of modeled versus measured conductance or fluxes, and simulated values. Units are *m*, dimensionless for the BB and BBL models; if D is expressed in kPa, then *m* has units of $kPa^{0.5}$ for the USO model; g_0, mol m^{-2} s^{-1}. *Indicates a value reported as not significantly different than zero.

Species	**Growth Conditions**	**Model**	**Slope (*m*)**	**g_0**	**Collection Method**	**R^2**	**Reference**
Acer buergeranum		BB	10.0 (2.9)	0.075 - 0.211 (0.010 - 0.030)	1, 2		Bowden and Bauerle (2008)
Acer rubrum		BB	9.50	0.0175	1, 2		Harley and Baldocchi (1995)
Acer rubrum		BB	9.85	0.03	1, 2		Bauerle et al. (2004b)
Acer rubrum		BBL	7.72 ± 3.7	0.015 ± 0.018	1		Barnard and Bauerle (2013)
Acer rubrum		BB	5.50	0	1, 2		Bauerle et al. (2004b)
Acer rubrum		BB	6.2 (1.6)	0.159 - 0.279 (0.013 - 0.056)	1, 2		Bowden and Bauerle (2008)
Acer rubrum		BB	1.7 ± 0.3	0.14	1,2		Reynolds et al. (2009)
Acer rubrum cv. Autumn Blaze		BBL	5.56	0.041	1, 2		Bauerle and Bowden (2011)
Acer rubrum cv. October Glory		BBL	5.68	0.046	1, 2		Bauerle and Bowden (2011)
Acer rubrum cv. Red Sunset		BBL	7.14	0.035	1, 2		Bauerle and Bowden (2011)
Acer rubrum cv. Summer Red		BBL	7.52	0.043	1, 2		Bauerle and Bowden (2011)
Acer rubrum cv. Autumn Flame		BBL	6.17	0.048	1, 2		Bauerle and Bowden (2011)
Aegiceras corniculatum		BB	2.30	0.03	2	0.69	Leuning (1995)
Aegiceras corniculatum		BBL	3.30	0.03	2	0.69	Leuning (1995)
Allocasuarina luehmannii		USO	1.99		7		Zhou et al. (2013)
Amaranthus hypochondriacus	[350], 25° C	BB	18.5 (2.1)		5	0.80	Bunce (1998)
Amaranthus hypochondriacus	[525], 25 °C	BB	9.8 (0.7)		5	0.54	Bunce (1998)
Amaranthus hypochondriacus	[700], 25 °C	BB	10.6 (1.6)		5	0.80	Bunce (1998)
Amaranthus hypochondriacus	[350], 30 °C	BB	9 (1)		5	0.47	Bunce (1998)
Amaranthus hypochondriacus	ambient [CO_2], 20 °C	BB	9.3 (2.1)		5	0.83	Bunce (1998)
Amaranthus hypochondriacus	ambient [CO_2], 25 °C, low PPFD	BB	5.3 (0.9)		5	0.26	Bunce (1998)
Amaranthus hypochondriacus	ambient [CO_2], 25 °C	BB	5.1 (1.2)		5	0.27	Bunce (1998)
Amaranthus retroflexus		BB	3.06	0.03	1, 2, 3, 4	0.95	Ball (1988)

Species	Growth Conditions	Model	Slope (*m*)	g_0	Collection Method	R^2	Reference
Andropogon gerardii		BB	4.07	0.0595	1, 4	0.86	Chen et al. (1994)
Andropogon gerardii	elevated [CO2]	BB	6.24	0.0533	1, 4	0.92	Chen et al. (1994)
Andropogon gerardii	Seasonal water stress	BB	4.10		1, 2		Polley et al. (1992)
Arbutu unedo		BB	2.20	0.03	5	0.22	Leuning (1995)
Arbutu unedo		BBL	4.70	0.01	5	0.30	Leuning (1995)
Arbutus unedo		BB	10.00		7		Harley and Tenhunen (1991)
Arbutus unedo		BB	3.30	0.01	5	1.00	Leuning (1995)
Arbutus unedo		BBL	4.60	0	5	0.99	Leuning (1995)
Avicennia marina		BB	2.30	0.02	2	0.97	Leuning (1995)
Avicennia marina		BB	4.60	- 0.06	2	0.87	Leuning (1995)
Avicennia marina		BBL	3.30	0.01	2	0.95	Leuning (1995)
Avicennia marina		BBL	8.80	-0.09	2	0.82	Leuning (1995)
Betula nigra		BBL	8.13 ± 8.73	-0.014 ± 0.041	1		Barnard and Bauerle (2013)
Betula nigra		BB	2.5 ± 0.7	0.69 ± 0.10	1,2		Reynolds et al. (2009)
Betula pendula		BB	9.37	0.084	6	0.15	Medlyn et al. (2001)
Betula pendula	elevated [CO_2]	BB	18.62	- 0.018	6	0.42	Medlyn et al. (2001)
Betula pendula		BBL	8.04	0.061	6		Uddling et al. (2005)
Broussonetia papyrifera		USO	5.88		7		Zhou et al. (2013)
Camissonia brevipes		BB	16.43	- 0.31	1,2,3,4	0.85	Ball (1988)
Capsicum annum		BB	2.00	0.03	2	0.85	Leuning (1995)
Capsicum annum		BBL	3.20	0.03	2	0.85	Leuning (1995)
Carpinus betula		BBL	9.53 ± 2.61	-0.030 ± 0.082	1		Barnard and Bauerle (2013)
Cedrus atlantica		USO	3.18		7		Zhou et al. (2013)
Cercidiphyllum japonicum		BB			6, 7		Kosugi et al. (2003)
Cercidiphyllum japonicum, leaf expansion		BB	6.7	0.045	6, 7		Kosugi et al. (2003)
Cercidiphyllum japonicum, leaf falling		BB	9.70	0.02	6, 7		Kosugi et al. (2003)
Cercidiphyllum japonicum, leaf maturity		BB	5.80	0.058	6, 7		Kosugi et al. (2003)
Cercis Canadensis		BBL	8.16 ± 3.55	-0.030 ± 0.0125	1		Barnard and Bauerle (2013)
Cinnamomum bodinieri		USO	3.11		7		Zhou et al. (2013)
Commelina communis		BB	8.80	0.08	2	0.92	Leuning (1995)

Species	Growth Conditions	Model	Slope (*m*)	g_0	Collection Method	R^2	Reference
Commelina communis		BBL	10.00	0.08	2	0.92	Leuning (1995)
Corylus avellana		BB	2.10	0.02	5	0.85	Leuning (1995)
Corylus avellana		BB	3.00	0.02	5	0.97	Leuning (1995)
Corylus avellana		BBL	3.80	0.02	5	0.86	Leuning (1995)
Corylus avellana		BBL	4.50	0.01	5	0.98	Leuning (1995)
Cucumis sativus		BB	8.38	0.045	6	0.78	Liu et al. (2008)
Dactylis glomerata (Meadow)		BB	13.70	0.0762	6	0.77	Wohlfahrt et al. (1998)
Eucalyptus cladocalyx	well-watered	BBL	11.27 (3.15)	0.169 (0.026)	6	0.61	Heroult et al. (2013)
Eucalyptus cladocalyx	drought	BBL	16.4 (7.99)	0.083 (0.015)	6	0.61	Heroult *et al.* (2013)
Eucalyptus cladocalyx	well-watered	USO	2.46 (0.30)	0.135 (0.024)	6	0.65	Heroult et al. (2013)
Eucalyptus cladocalyx	drought	USO	2.94 (0.39)	0.056 (0.014)	6	0.76	Heroult et al. (2013)
Eucalyptus crebra		USO	4.30	set at 0	4		Lin et al. (2012)
Eucalyptus delegatensis		BB	11.98 (1.0)	0.016 (0.016)*	6	0.72	Medlyn et al. (2011)
Eucalyptus delegatensis		BBL	14.43 (2.37)	0.001 (0.01)*	6	0.80	Medlyn et al. (2011)
Eucalyptus delegatensis		USO	3.48 (0.29)	-0.007 (0.014)*	6	0.79	Medlyn et al. (2011)
Eucalyptus dunnii	well-watered	BBL	22.13	-0.020 (0.027)	6	0.84	Heroult et al. (2013)
Eucalyptus dunnii	drought	BBL	5.74 (1.76)	0.047 (0.01)	6	0.84	Heroult et al. (2013)
Eucalyptus dunnii	well-watered	USO	5.17 (0.36)	-0.055 (0.029)	6	0.82	Heroult et al. (2013)
Eucalyptus dunnii	drought	USO	1.33 (0.22)	0.042 (0.005)	6	0.73	Heroult et al. (2013)
Eucalyptus globulus		BB	6.42	0.0102	6	0.81	Macfarlane et al. (2004)
Eucalyptus globulus		BBL	6.22	0.0119	6	0.79	Macfarlane et al. (2004)
Eucalyptus grandis	no fertilization, no irrigation	BB	7.20	0.01	1,2,3,4		Leuning (1990)
Eucalyptus grandis	no fertilization, irrigation	BB	8.40	0.01	1,2,3,4		Leuning (1990)
Eucalyptus grandis	fertilization, irrigation	BB	7.50	0.01	1,2,3,4		Leuning (1990)
Eucalyptus grandis	no fertilization, irrigation	BB	11.10	0.01	1,2,3,4		Leuning (1990)
Eucalyptus grandis	fertilization, irrigation	BB	10.40	0.01	1,2,3,4		Leuning (1990)
Eucalyptus grandis		BB	10.30	0.01	1,2,3,4		Leuning (1990)
Eucalyptus grandis	varying nutrient & light levels	BB	9.3 - 18.0	fixed at 0.01	1,2,3,4	0.77	Leuning (1990)
Eucalyptus grandis	varying nutrient & light levels	BBL	20.5 - 42.2	fixed at 0.01	1,2,3,4	0.78	Leuning (1995)
Eucalyptus milliodora	well-watered	BBL	8.63 (0.88)	0.002 (0.015)	6	0.83	Heroult et al. (2013)

Species	Growth Conditions	Model	Slope (*m*)	g_0	Collection Method	R^2	Reference
Eucalyptus milliodora	drought	BBL	5.49 (.926)	0.056 (0.018)	6	0.83	Heroult et al. (2013)
Eucalyptus milliodora	well-watered	USO	3.26 (0.20)	0.005	6	0.82	Heroult et al. (2013)
Eucalyptus milliodora	drought	USO	2.63 (0.22)	0.043 (0.013)	6	0.84	Heroult et al. (2013)
Eucalyptus parramattensis		BB	15.27 (1.03)	0.016 (0.007)	6	0.70	Medlyn et al. (2011)
Eucalyptus parramattensis		BBL	68.7 (103)*	0.014 (0.007)	6	0.70	Medlyn et al. (2011)
Eucalyptus parramattensis		USO	6.88 (0.61)	0.008 (0.007)*	6	0.68	Medlyn et al. (2011)
Eucalyptus pauciflora		BB	5.10	0.03	2	0.91	Leuning (1995)
Eucalyptus pauciflora		BB	2.30	0.02	2	0.95	Leuning (1995)
Eucalyptus pauciflora		BBL	8.10	0.03	2	0.89	Leuning (1995)
Eucalyptus pauciflora		BBL	5.70	0.01	2	0.93	Leuning (1995)
Eucalyptus pilularis		USO	2.22		7		Zhou et al. (2013)
Eucalyptus populnea		USO	3.15		7		Zhou et al. (2013)
Eucalyptus saligna	well-watered	BBL	8.22(0.41)	-0.033 (0.10)	6	0.88	Heroult et al. (2013)
Eucalyptus saligna	drought	BBL	5.44 (0.24)	0.009(0.005)	6	0.88	Heroult et al. (2013)
Eucalyptus saligna	well-watered	USO	3.41 (0.18)	-0.001 (0.011)	6	0.82	Heroult et al. (2013)
Eucalyptus saligna	drought	USO	2.08 (0.14)	0.007 (0.004)	6	0.90	Heroult et al. (2013)
Eucalyptus tereticornis	ambient & elevated [CO_2],variable precipitation	USO	4.275 (0.132)	-0.038 (0.007)	6		Gimeno et al. (2015)
Fagus sylvatica	ambient & elevated [CO_2]	BB	3.81 (0.84)	0.02 (0.01)	1	0.91	Liozon et al. (2000)
Fagus sylvatica	`	BBL	5.17 (1.46)	0.02 (0.01)	1	0.91	Liozon et al. (2000)
Fagus sylvatica		BB	12.70	-0.02	6	0.95	Medlyn et al. (2001)
Fagus sylvatica	elevated [CO_2]	BB	12.10	-0.003	6	0.91	Medlyn et al. (2001)
Fagus sylvatica		BB	11.24 (0.88)	-0.002(0.015)*	6	0.88	Medlyn et al. (2011)
Fagus sylvatica		BBL	8.17 (1.94)	-0.06 (0.04)*	6	0.78	Medlyn et al. (2011)
Fagus sylvatica		USO	3.94 (0.58)	-0.049 (0.025)*	6	0.78	Medlyn et al. (2011)
Ficus tikoua		USO	6.17		7		Zhou et al. (2013)
forest, boreal conifer		BB	7.50	0.01	7		Baldocchi and Meyers (1998)
forest, temperate broad leaved		BB	9.50	0.01	7		Baldocchi and Meyers (1998)
forest, tropical rainforest		BB	4.9 ± 1.1	0.04 ± 0.02	6		Kumagai et al. (2006)
Glycine max	ambient & elevated [CO_2]	BB	12.58		2,4,5		Wilson and Bunce 1997
Glycine max		BB	10.00	0.01	7		Baldocchi and Meyers (1998)
Glycine max	[350], 25 °C	BB	33.2 (4.7)		5	0.55	Bunce (1998)

Species	Growth Conditions	Model	Slope (*m*)	g_0	Collection Method	R^2	Reference
Glycine max	[525], 25 °C	BB	35.5 (2.8)		5	0.63	Bunce (1998)
Glycine max	[700], 25 °C	BB	31 (1.5)		5	0.70	Bunce (1998)
Glycine max	[350], 30 °C	BB	32.4 (2.8)		5	0.69	Bunce (1998)
Glycine max	[350], 20 °C	BB	22.7 (2.7)		5	0.66	Bunce (1998)
Glycine max	[350], 25 °C, low PPFD	BB	37.4 (3.9)		5	0.76	Bunce (1998)
Glycine max	[350], 25 °C	BB	22.8 (1.7)		5	0.31	Bunce (1998)
Glycine max		BBL	82.78	0.336	6	0.44	Yu et al. (2004)
Glycine max		BB	11.00	0.01	6	0.77	Bunce (2004)
Glycine max	elevated [CO_2]	BB	5.60	0.08	6	0.78	Bunce (2004)
Glycine max		BB	10.60	0.008*	1,2,3		Leakey et al. (2006)
Glycine max	elevated [CO_2]	BB	10.90	0.007*	1,2,3		Leakey et al. (2006)
Glycine max		USO	3.74		7		Zhou et al. (2013)
Glycine max		USO	3.77		7		Zhou et al. (2013)
Glycine max		BB	9.29	0.008	1,2,3,4	0.97	Ball (1988)
Gossypium hirsutum		BB	9.58				Harley et al. 1992
Gossypium hirsutum	elevated [CO_2]	BB	8.92				Harley et al. 1992
Gossypium hirsutum		BB	2.30	0.08	5	0.99	Leuning (1995)
Gossypium hirsutum		BBL	3.60	0.06	5	0.93	Leuning (1995)
Gossypium hirsutum cv. Alcala		BB	8.01	0.03	1, 2, 3, 4	0.90	Ball (1988)
Gossypium hirsutum cv. Delcot		BB	8.04	0.005	1, 2, 3, 4	0.91	Ball (1988)
grassland, C3 Tallgrass prairie		BB	10.00		6		Hanan et al. (2005)
grassland, C4 grasses	seasonal water stress	BB	3.62 (0.15)	0.045 (0.005)	1,2	0.85	Polley et al. (1992)
grassland, C4 tallgrass prairie		BB	3.40		6		Hanan et al. (2005)
grassland, forbe steppe		BB	15.4 - 23.8		7		Wolf et al. (2006)
grassland, mixed		BB	9.76	0.031	7	0.72	Carlson (2000)
grassland, temperate, season 1		BB	6.43	0.056	7	0.60	Wever et al. (2002)
grassland, temperate, season 2		BB	12.10	0.026	7	0.52	Wever et al. (2002)
grassland, temperate, season 3		BB	14.76	0.025	7	0.63	Wever et al. (2002)
Hedera helix		BB	7.34		3, 4		Aphalo and Jarvis (1993)
Hedera helix		BB	5.75		3, 4		Aphalo and Jarvis (1993)

Species	Growth Conditions	Model	Slope (*m*)	g_0	Collection Method	R^2	Reference
Helianthus annuus		BB	2.30	0.11	2	0.76	Leuning (1995)
Helianthus annuus		BBL	3.80	0.11	2	0.74	Leuning (1995)
Helianthus annuus		USO	4.64		7		Zhou et al. (2013)
Helianthus annuus, season 1		BB	20.61	0.434	6	0.47	Gutschick and Simonneau (2002)
Helianthus annuus, season 1		BBL	18.19	0.478	6	0.38	Gutschick and Simonneau (2002)
Helianthus annuus, season 2		BB	14.35	0.174	6	0.67	Gutschick and Simonneau (2002)
Helianthus annuus, season 2		BBL	14.43	0.11	6	0.38	Gutschick and Simonneau (2002)
Hordeum vulgare		BB	6.50	0	6	0.80	Thorgeirsson and Soegaard (1999)
Hordeum vulgare	[350]	BB	10 (2.0)	0.088 (0.051)	6	0.55	Bunce (2000)
Hordeum vulgare	[525]	BB	8.3 (1.7)	0.080 (0.034)	6	0.55	Bunce (2000)
Hordeum vulgare	[700]	BB	6.26 (2.2)	0.104 (0.040)	6	0.30	Bunce (2000)
Juniperus monosperma	reduced precipitation	BB	8.404 (0.304)	0.0084	6	0.79	Limousin et al. (2013)
Juniperus monosperma	ambient precipitation	BB	7.416 (0.257)	0.0102	6	0.81	Limousin et al. (2013)
Juniperus monosperma	irrigated	BB	7.487 (0.225)	0.0148	6	0.74	Limousin et al. (2013)
Koeleria pyramidata (Pasture)		BB	10.60	0.022	6	0.52	Wohlfahrt et al. (1998)
Liquidambar styraciflua		BB	9.80	0.019	6	0.80	Gunderson et al. (2002)
Liquidambar styraciflua	elevated [CO_2]	BB	8.90	0.001	6	0.81	Gunderson et al. (2002)
Liriodendron tulipifera, leaf expansion		BB	26.1	0.052	6, 7		Kosugi et al. (2003)
Liriodendron tulipifera, leaf falling		BB	18.90	0.064	6, 7		Kosugi et al. (2003)
Liriodendron tulipifera, leaf maturity		BB	9.30	0.063	6, 7		Kosugi et al. (2003)
Lupinus arizonicus		BB	7.40	0.04	5	0.73	Leuning (1995)
Lupinus arizonicus		BBL	13.40	-0.01	5	0.68	Leuning (1995)
Malus domestica		BBL	9.99 ± 0.59	0.020 ± 0.010	1		Barnard and Bauerle (2013)
Malvastrum rotundifolium		BB	11.70	0.02	1, 2 ,3 ,4	0.89	Ball (1988)
Malvastrum rotundifolium		BB	8.00	0.16	5	0.92	Leuning (1995)
Malvastrum rotundifolium		BBL	14.80	0.12	5	0.90	Leuning (1995)

Species	Growth Conditions	Model	Slope (*m*)	g_0	Collection Method	R^2	Reference
Deciduous shrubs		USO	4.82		7		Zhou et al. (2013)
Evergreen shrubs		USO	4.72		7		Zhou et al. (2013)
Mediterranean herbs		USO	4.72		7		Zhou et al. (2013)
Mixed forest, deciduous		BB	7.80	0.01	2, 6	0.85	Wilson et al. (2001)
Mixed forest		BB	4 - 10		7		Reichstein et al. (2002)
Mixed forest, deciduous and evergreen		BB	6 - 12	0.005 - 0.001	6, 7		Tanaka et al. (2002)
Nardus stricta		BB	16.00	0.0219	6	0.74	Wohlfahrt et al. (1998)
Nerium oleander		BB	10.62	0.07	1, 2, 3, 4	0.85	Ball (1988)
Nerium oleander		BB	1.50	0.07	5	0.95	Leuning (1995)
Nerium oleander		BBL	2.30	0.06	5	0.90	Leuning (1995)
Olea europaea var. Chemlali		USO	2.72		7		Zhou et al. (2013)
Olea europaea var. Meski		USO	3.16		7		Zhou et al. (2013)
Oryza sativa		BBL	27.4 - 53.0	assumed 0.006	7		Ono et al. (2010)
Oryza sativa		BB	3.7 - 13	-0.0488	7	0.74	Shimono et al. (2010)
Oryza sativa	elevated [CO_2]	BB	2.8 - 11.0	0.0149	7	0.73	Shimono et al. (2010)
Oryza sativa		BB	17.9 - 63.3		7		Ono et al. (2013)
Panicum virgatum	seasonal water stress	BB	3.80		1, 2		Polley et al. (1992)
Paulownia elongata		BB	5. 8 ± 1.1	0.14 ± 0.0	1, 2		Reynolds et al. (2009)
Pennisitum glaucum	T_{leaf} <35 °C	BB	4.76	0.18	6	0.53	Boegh et al. (1999)
Pennisitum glaucum	T_{leaf} > 35 °C	BB	3.65	0.09	6	0.61	Boegh et al. (1999)
Pennisitum glaucum	T_{leaf} <35 °C	BBL	7.36	0.16	6	0.60	Boegh et al. (1999)
Pennisitum glaucum	T_{leaf} > 35 °C	BBL	6.53	0.08	6	0.67	Boegh et al. (1999)
Perityle emoryl		BB	10.13	0.06	1, 2, 3, 4	0.89	Ball (1988)
PFT, C3 crop		USO	5.79 (0.04)	assumed 0	7		Lin et al. (2015)
PFT, C3 grass		USO	5.25 (0.13)	assumed 0	7		Lin et al. (2015)
PFT, C4 grass		USO	1.62 (0.03)	assumed 0	7		Lin et al. (2015)
PFT, deciduous angiosperm trees		USO	4.64 (0.04)	assumed 0	7		Lin et al. (2015)
PFT, deciduous savanna trees		USO	2.98 (0.39)	assumed 0	7		Lin et al. (2015)
PFT, evergreen angiosperm trees		USO	3.37 (0.03)	assumed 0	7		Lin et al. (2015)
PFT, evergreen gymnosperm		USO	2.35 (0.02)	assumed 0	7		Lin et al. (2015)

Species	Growth Conditions	Model	Slope (*m*)	g_0	Collection Method	R^2	Reference
trees							
PFT, evergreen savanna trees		USO	7.18 (0.25)	assumed 0	7		Lin et al. (2015)
PFT, shrubs		USO	3.32 (0.05)	assumed 0	7		Lin et al. (2015)
PFT, tropical Rainforest trees		USO	3.77 (0.06)	assumed 0	7		Lin et al. (2015)
Phaseolus vulgaris		BB	13.1 (NS)	0.57 (NS)	6	0.11	Bunce (2004)
Phaseolus vulgaris	elevated [CO_2]	BB	15.50	0.26	6	0.32	Bunce (2004)
Phillyrea angustifolia		BB	10.09	0.033	6	0.66	Medlyn et al. (2001)
Phillyrea angustifolia	elevated [CO_2]	BB	1.85	0.048	6	0.22	Medlyn et al. (2001)
Phillyrea angustifolia; Pistacia lentiscus		BB	9.09 (0.92)	0.038 (0.008)*	6	0.68	Medlyn et al. (2011)
Phillyrea angustifolia; Pistacia lentiscus		BBL	14.7 (10.1)*	0.03 (0.01)	6	0.63	Medlyn et al. (2011)
Phillyrea angustifolia; Pistacia lentiscus		USO	3.11 (0.56)	0.027 (0.01)	6	0.61	Medlyn et al. (2011)
Picea abies	Site 1 (younger trees)	BB	9.80	forced to zero	6	0.78	Falge et al. (1996)
Picea abies	Site 1 (younger trees)	BB	10.00	-0.0006	6	0.78	Falge et al. (1996)
Picea abies	Site 2 (older trees)	BB	6.50	forced to zero	6	0.41	Falge et al. (1996)
Picea abies	Site 2 (older trees)	BB	4.40	0.0084	6	0.55	Falge et al. (1996)
Picea abies		BB	2.93	0.054	6	0.67	Medlyn et al. (2001)
Picea abies	elevated [CO_2]	BB	4.56	0.032	6	0.53	Medlyn et al. (2001)
Picea abies		BB	6.00	0.025			Zheng et al. (2002)
Picea abies		BB	3.50	0.034	6		Medlyn et al. (2005)
Picea abies		USO	1.45 (0.39)	0.04 (0.004)	6		Uddling and Wallin (2012)
Picea abies	elevated [CO_2]	USO	2.44 (0.29)	0.44 (0.009)	6		Uddling and Wallin (2012)
Picea mariana	22 °C day/ 14 or 16 °C night	BBL	5.22	0.0565	1, 2, 3, 4		Way et al. (2011)
Picea mariana	30 °C day/22 or 24 °C night	BBL	8.22	0.0106	1, 2, 3, 4		Way et al. (2011)
Picea mariana	22 °C day/ 14 or 16 °C night	BB	2.85	0.0974	1, 2, 3, 4		Way et al. (2011)
Picea mariana	30 °C day/22 or 24 °C night	BB	8.10	0.0336	1, 2, 3, 4		Way et al. (2011)
Picea mariana		BB	4.79	0.016	1, 2, 4, 5	0.82	Dang et al. (1998)
Picea mariana		BB	6.62	0.014	5	0.91	Dang et al. (1998)

Species	Growth Conditions	Model	Slope (*m*)	g_0	Collection Method	R^2	Reference
Picea sitchensis		BB	6.44	0.043	6	0.20	Medlyn et al. (2001)
Picea sitchensis	elevated [CO_2]	BB	7.63	0.023	6	0.74	Medlyn et al. (2001)
Picea sitchensis		BB	5.19	0.027	6	0.71	Medlyn et al. (2001)
Picea sitchensis	elevated [CO_2]	BB	7.05	0.009	6	0.83	Medlyn et al. 2001
Picea sitchensis		BBL	6.33	0.037	6		Medlyn et al. (2005)
Picea sitchensis (Sitka A)		BB	4.55 (0.38)	0.0039 (0.004)	6	0.65	Medlyn et al. (2011)
Picea sitchensis (Sitka A)		BBL	7.35 (0.92)	0.038 (0.003)	6	0.72	Medlyn et al. (2011)
Picea sitchensis (Sitka A)		USO	0.87 (0.09)	0.031 (0.003)	6	0.74	Medlyn et al. (2011)
Picea sitchensis (Sitka B)		BB	5.17 (0.67)	0.027 (0.008)	6	0.70	Medlyn et al. (2011)
Picea sitchensis (Sitka B)		BBL	5.36 (2.24)	0.024 (0.01)	6	0.73	Medlyn et al. (2011)
Picea sitchensis (Sitka B)		USO	1.24 (0.27)	0.0.20 (0.008)	6	0.73	Medlyn et al. (2011)
Pinus banksiana		BB	5.59	0.016	1, 2, 4, 5	0.81	Dang et al. (1998)
Pinus banksiana		BB	8.16	0.01	5	0.90	Dang et al. (1998)
Pinus contorta		BB	9.75	0.00752	6		Nikolov et al. (1995)
Pinus edulis	reduced precipitation	BB	6.877 (.207)	0.0045	6	0.85	Limousin et al. (2013)
Pinus edulis	ambient precipitation	BB	6.808 (.234)	0.0051	6	0.81	Limousin et al. (2013)
Pinus edulis	irrigated	BB	7.924 (0.170)	0.0087	6	0.85	Limousin et al. (2013)
Pinus flexilis		BB	8.70	0.0184	6		Nikolov et al. (1995)
Pinus pinaster		BBL	8.63	0.015	6		Medlyn et al. (2005)
Pinus ponderosa	well-watered and drought	BB	4 to 18	0.0-0.12	2		Misson et al. (2004)
Pinus radiata		BB	16.40	fixed at 0	6	0.91	McMurtrie et al. (1992)
Pinus sylvestris		BBL	3.22 - 3.91	0.0374 - 0.0532	1, 2		Kellomäki and Wang (1997)
Pinus sylvestris	elevated [CO_2]	BBL	2.90 - 3.55	0.0528 - 0.0596	1, 2		Kellomäki and Wang (1997)
Pinus sylvestris		BB	6.89	0.001	6	0.88	Launiainen et al. (2011)
Pinus sylvestris		BBL	6.46	0.001	6		Launiainen et al. (2011)
Pinus taeda		BB	5.90		6		Katul et al. (2000)
Pinus taeda		BBL	4.00		6		Katul et al. (2000)
Pinus taeda		BB	≈ 4 to 9		6		Lai et al. (2000)
Pinus taeda		BB	3.42 ± 0.30	0.04 (0.01)	6		Katul et al. (2010)
Pinus taeda	elevated [CO_2]	BB	3.56 ± 0.44	0.03 (0.01)	6		Katul et al. (2010)
Pinus taeda		BBL	3.52	0.016 (0.006)	6		Katul et al. (2010)
Pinus taeda	elevated [CO_2]	BBL	4.71	-0.006 (0.01)	6		Katul et al. (2010)

Species	Growth Conditions	Model	Slope (*m*)	g_0	Collection Method	R^2	Reference
Pinus taeda		BB	7.14 (1.36)	0.057(0.019)	6	0.17	Medlyn et al. (2011)
Pinus taeda		BBL	10.96 (2.67)	0.007(0.02)*	6	0.52	Medlyn et al. (2011)
Pinus taeda		USO	2.82 (0.31)	-0.011(0.013)*	6	0.52	Medlyn et al. (2011)
Pistacia lentiscus		BB	8.16	0.042	6	0.73	Medlyn et al. (2011)
Pistacia lentiscus	elevated [CO_2]	BB	13.41	0.028	6	0.50	Medlyn et al. (2001)
Pistacia vera		BB	3.50	0.05	5	0.99	Leuning (1995)
Pistacia vera		BBL	5.20	0.04	5	0.99	Leuning (1995)
Plantago atrata (abandoned area)		BB	9.80	0.0761	6	0.66	Wohlfahrt et al. (1998)
Plantago atrata (meadow)		BB	13.80	0.07	6	0.63	Wohlfahrt et al. (1998)
Plantago atrata (pasture)		BB	14.10	0.0793	6	0.61	Wohlfahrt et al. (1998)
Plantago media (Pasture)		BB	10.80	0.0911	6	0.49	Wohlfahrt et al. (1998)
Platanus orientalis, leaf expansion		BB	17.8	0.102	6, 7		Kosugi et al. (2003)
Platanus orientalis, leaf falling		BB	8.00	0.089	6, 7		Kosugi et al. (2003)
Platanus orientalis, leaf maturity		BB	9.80	0.061	6, 7		Kosugi et al. (2003)
Platanus x acerifolia		BB	13.0 (1.6)	0.131 - 0.210 (0.030 - 0.065)	1, 2		Bowden and Bauerle (2008)
Platycarya longipes		USO	5.85		7		Zhou et al. (2013)
Polygonum viviparum (meadow)		BB	11.90	0.057	6	0.63	Wohlfahrt et al. (1998)
Polygonum viviparum (pasture)		BB	8.90	0.0412	6	0.75	Wohlfahrt et al. (1998)
Polygonum. viviparum (abandoned area)		BB	12.00	0.0545	6	0.46	Wohlfahrt et al. (1998)
Populus tremuloides		BB	13.50	0.0733	6		Nikolov et al. (1995)
Portulaca oleraceae		BB	2.40	0.13	1, 2, 3, 4	0.92	Ball (1988)
Potentilla aurea (abandoned area)		BB	24.70	0.13	6	0.70	Wohlfahrt et al. (1998)
Potentilla aurea (meadow)		BB	17.00	0.12	6	0.63	Wohlfahrt et al. (1998)

Species	Growth Conditions	Model	Slope (*m*)	g_0	Collection Method	R^2	Reference
Potentilla aurea (pasture)		BB	10.60	0.0746	6	0.61	Wohlfahrt et al. (1998)
Prunus armeniaca		BB	6.70	-0.01	5	0.92	Leuning (1995)
Prunus armeniaca		BBL	14.00	-0.05	5	0.92	Leuning (1995)
Prunus dulcis		BB	2.50	0.04	5	0.91	Leuning (1995)
Prunus dulcis		BBL	4.00	0.03	5	0.86	Leuning (1995)
Prunus serrulata		BB	13.8 (1.7)	0.213 - 0.384 (0.017 - 0.050)	1, 2		Bowden and Bauerle (2008)
Prunus x yedoensis		BB			6, 7		Kosugi et al. (2003)
Prunus x yedoensis		BB	4.5 (0.7)	0.231 - 0.288 (0.008 - 0.048)	1, 2		Bowden and Bauerle (2008)
Prunus x yedoensis (leaf expansion)		BB	11.5	0.071	6, 7		Kosugi et al. (2003)
Prunus x yedoensis (leaf falling)		BB	16.10	0.081	6, 7		Kosugi et al. (2003)
Prunus x yedoensis (leaf maturity)		BB	6.90	0.094	6, 7		Kosugi et al. (2003)
Pseudotzuga menziesii		USO	3.13		7		Zhou et al. (2013)
Psudotsuga menziesii		BB	7.70		7		Van Wijk et al. (2000)
Psudotsuga menziesii		BBL	16.57		7		Van Wijk et al. (2000)
Pteroceltis tatarinowii		USO	3.70		7		Zhou et al. (2013)
Quercus alba		BB	9.50	0.0175	1, 2		Harley and Baldocchi (1995)
Quercus coccifera		USO	6.06		7		Zhou et al. (2013)
Quercus douglasii	seasonal water stress	BB	8.88	0.006	1, 2	0.88	Xu and Baldocchi (2003)
Quercus ilex		BB	6.23	0.024	6	0.52	Medlyn et al. 2001
Quercus ilex	elevated [CO_2]	BB	3.28	0.029	6	0.35	Medlyn et al. 2001
Quercus ilex		USO	6.12		7		Zhou et al. (2013)
Quercus ilex (ridge top, shade)		BB	16.00	set at 0.005	7		Sala and Tenhunen (1996)
Quercus ilex (ridge top, sun)		BB	15.60	set at 0.005	7		Sala and Tenhunen (1996)
Quercus ilex (valley bottom, shade)		BB	6.20	set at 0.005	7		Sala and Tenhunen (1996)
Quercus ilex (valley bottom, sun)		BB	6.40	set at 0.005	7		Sala and Tenhunen (1996)

Species	Growth Conditions	Model	Slope (*m*)	g_0	Collection Method	R^2	Reference
Quercus nuttallii		BB	3.3 ± 0.9	0.15 ± 0.0	1, 2		Reynolds et al. (2009)
Quercus phellos		BB	2.4 ± 0.7	0.11 ± 0.0	1, 2		Reynolds et al. (2009)
Quercus rubra	ambient & elevated [CO_2]	BB	1.122 (0.012)	0.015 (0.002)*		0.95	Weber and Gates (1990)
Quercus suber		BB	4.90	0.01	5	0.97	Leuning (1995)
Quercus suber		BBL	6.90	0.01	5	0.96	Leuning (1995)
Quercus suber		USO	7.55		7		Zhou et al. (2013)
Rinanthus alectorolophus (Meadow)		BB	18.30	0.1931	6	0.54	Wohlfahrt et al. (1998)
Rosa cymosa		USO	3.07		7		Zhou et al. (2013)
Savanna		BB	13.62 (0.89)	0.048 (0.015)	6	0.76	Medlyn et al. (2011)
Savanna		BBL	141.3 (524)*	0.023 (0.02)*	6	0.77	Medlyn et al. (2011)
Savanna		USO	6.55 (0.61)	-0.007 (0.021)*	6	0.68	Medlyn et al. (2011)
sedge-dominated fen		BB	9.00	0.04	7		Soegaard and Nordstroem (1999)
serpentine grassland (April)		BB	0.7*	0.0025	7	0.78	Valentini et al. (1995)
serpentine grassland (February)		BB	3.298*	0.0042	7	0.68	Valentini et al. (1995)
serpentine grassland (May)		BB	1*	0.0012	7	0.65	Valentini et al. (1995)
Solanum tuberosum		BB	10.00	0.01	7		Baldocchi and Meyers (1998)
Solanum tuberosum		BB	25.30	-0.36	6	0.85	Bunce (2004)
Solanum tuberosum	elevated [CO_2]	BB	20.80	-0.18	6	0.77	Bunce (2004)
Solanum tuberosum		BB	39.18		6	0.62	Ahmadi et al. (2009)
Solanum tuberosum		BB	16.57	0.07	6		Liu et al. (2009)
Sorghastrum nutans	seasonal water stress	BB	3.50		1,2		Polley et al. (1992)
Sorghum bicolor		BB	10.90	-0.33	6	0.93	Bunce (2004)
Sorghum bicolor	elevated [CO_2]	BB	11.60	-0.21	6	0.84	Bunce (2004)
Southern Old Aspen Site		BB	8.50		7		Wang et al. (2009)
Southern Old Aspen Site		BBL	15.50		7		Wang et al. (2009)
Southern Old Black Spruce Site		BB	8.70		7		Wang et al. (2009))
Southern Old Black Spruce Site		BBL	17.60		7		Wang et al. (2009)

Species	Growth Conditions	Model	Slope (*m*)	g_0	Collection Method	R^2	Reference
Southern Old Jack Pine Site		BB	7.80		7		Wang et al. (2009)
Southern Old Jack Pine Site		BBL	16.30		7		Wang et al. (2009)
Trifolium montanum (Pasture)		BB	13.50	0.0426	6	0.76	Wohlfahrt et al. (1998)
Trifolium pratense (Meadow)		BB	6.90	0.0252	6	0.92	Wohlfahrt et al. (1998)
Trisetum flavescens (Meadow)		BB	17.00	0.0754	6	0.60	Wohlfahrt et al. (1998)
Triticum aestivum		BB	10.00	0.01	7		Baldocchi and Meyers (1998)
Triticum aestivum		BBL	11.00		7		Wang and Leuning (1998)
Triticum aestivum	[350]	BB	9.6 (2.0)	0.203 (0.063)	6	0.50	Bunce (2000)
Triticum aestivum	[525]	BB	18.4 (2.0)	-0.024 (0.038)	6	0.87	Bunce (2000)
Triticum aestivum	[700]	BB	9.4 (1.3)	0.084 (0.029)	6		Bunce (2000)
Triticum aestivum		BB	9.00		6		Hanan et al. (2005)
Trollius europaeus, lower leaves (Abandoned area)		BB	12.80	0.0706	6	0.64	Wohlfahrt et al. (1998)
Trollius europaeus, lower leaves (Meadow)		BB	13.40	0.067	6	0.56	Wohlfahrt et al. (1998)
Trollius europaeus, lower leaves (Pasture)		BB	9.10	0.0815	6	0.50	Wohlfahrt et al. (1998)
Trollius europaeus, upper leaves (Abandoned area)		BB	20.20	0.0947	6	0.81	Wohlfahrt et al. (1998)
Trollius europaeus, upper leaves (Meadow)		BB	19.20	0.0292	6	0.85	Wohlfahrt et al. (1998)
Trollius europaeus, upper leaves (Pasture)		BB	9.40	0.0327	6	0.84	Wohlfahrt et al. (1998)
Vaccinium myrtillus		BB	10.50	0.0117	6	0.74	Wohlfahrt et al. (1998)
Vitis		BB	7.3 - 27.5		6		Schultz et al. (1998)
Vitis vinifera		BBL	5.2 - 7.3		7		Prieto et al. (2012)
Zea mays		BB	3.23	0.06	1, 2, 3, 4	0.89	Ball (1988)
Zea mays		BB	3.06	0.08	1, 2	0.93	Collatz et al. (1992)
Zea mays		BB	3.13	0.08	1, 2, 3, 4		Collatz et al. (1992)
Zea mays		BBL	6.502 - 9.482	0.113 - 0.146	6		Yu et al. (2001)

Figures

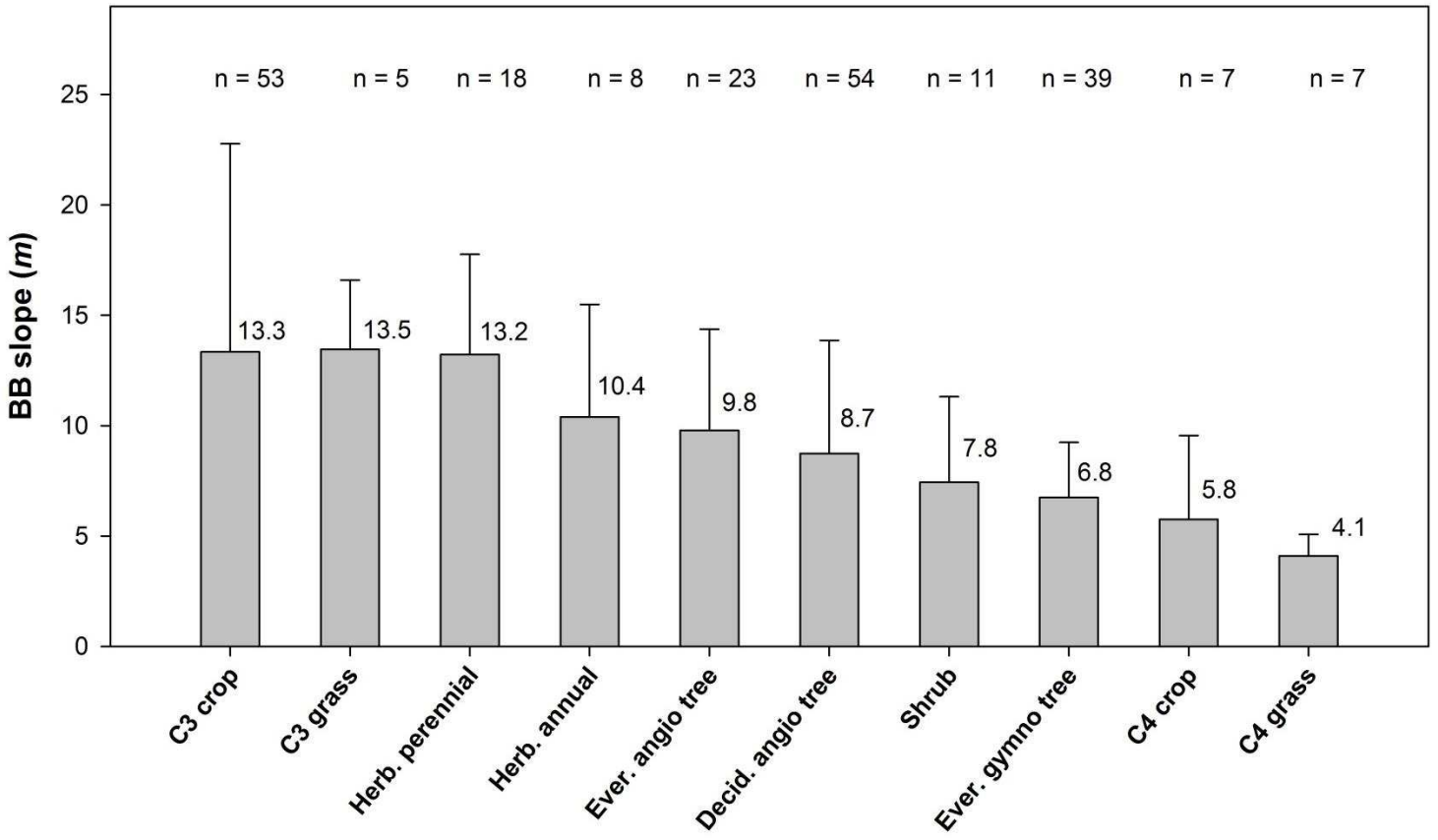

Figure 1. Mean values of the *m* parameter of the Ball-Berry model of stomatal conductance by plant functional type. Each bar represents the mean reported literature value ± 1 SD. The sample size (n) reflects the number of distinct values reported, including instances where multiple values of *m* were measured in response to changing environmental conditions or season. Data from mixed canopies and grasslands is excluded, as well as data from Ono et al. (2012).

CITATIONS

Aasamaa, K. and Sõber, A., 2011. Stomatal sensitivities to changes in leaf water potential, air humidity, CO2 concentration and light intensity, and the effect of abscisic acid on the sensitivities in six temperate deciduous tree species. Environmental and Experimental Botany, 71(1): 72-78.

Ahmadi, S.H., Andersen, M.N., Poulsen, R.T., Plauborg, F. and Hansen, S., 2009. A quantitative approach to developing more mechanistic gas exchange models for field grown potato: a new insight into chemical and hydraulic signalling. Agricultural and forest meteorology, 149(9): 1541-1551.

Ainsworth, E.A. and Long, S.P., 2005. What have we learned from 15 years of free-air CO2 enrichment (FACE)? A meta-analytic review of the responses of photosynthesis, canopy properties and plant production to rising CO2. New Phytologist, 165(2): 351-372.

Ainsworth, E.A. and Rogers, A., 2007. The response of photosynthesis and stomatal conductance to rising [CO2]: mechanisms and environmental interactions. Plant, cell & environment, 30(3): 258-270.

Aphalo, P.J. and Jarvis, P.G., 1993. An Analysis of Ball's Empirical Model of Stomatal Conductance. Annals of Botany, 72(4): 321-327.

Baldocchi, D., 1997. Measuring and modelling carbon dioxide and water vapour exchange over a temperate broad-leaved forest during the 1995 summer drought. Plant Cell and Environment, 20(9): 1108-1122.

Baldocchi, D. and Harley, P., 1995. Scaling carbon dioxide and water vapour exchange from leaf to canopy in a deciduous forest. II. Model testing and application. Plant, Cell & Environment, 18(10): 1157-1173.

Baldocchi, D. and Meyers, T., 1998. On using eco-physiological, micrometeorological and biogeochemical theory to evaluate carbon dioxide, water vapor and trace gas fluxes over vegetation: a perspective. Agricultural and Forest Meteorology, 90(1-2): 1-25.

Ball, J.T., 1988. An Analysis of Stomatal Conductance, Stanford University, Stanford.

Ball, J.T., Woodrow, I.E. and Berry, J.A., 1987. A model predicting stomatal conductance and its contribution to the control of photosynthesis under different environmental conditions, pp. 221-224.

Barnard, D. and Bauerle, W., 2013. The implications of minimum stomatal conductance on modeling water flux in forest canopies. Journal of Geophysical Research: Biogeosciences, 118(3): 1322-1333.

Bauerle, W.L. and Bowden, J.D., 2011a. Predicting transpiration response to climate change: Insights on physiological and morphological interactions that modulate water exchange from leaves to canopies. HortScience, 46(2): 163-166.

Bauerle, W.L. and Bowden, J.D., 2011b. Separating foliar physiology from morphology reveals the relative roles of vertically structured transpiration factors within red maple crowns and limitations of larger scale models. Journal of experimental botany, 62(12): 4295-4307.

Bauerle, W.L., Bowden, J.D., McLeod, M.F. and Toler, J.E., 2004a. Modeling intra-crown and intra-canopy interactions in red maple: assessment of light transfer on carbon dioxide and water vapor exchange. Tree physiology, 24(5): 589-597.

Bauerle, W.L., Daniels, A.B. and Barnard, D.M., 2013. Carbon and water flux responses to physiology by environment interactions: a sensitivity analysis of variation in climate on photosynthetic and stomatal parameters. Climate Dynamics: 1-16.

Bauerle, W.L. et al., 2012. Photoperiodic regulation of the seasonal pattern of photosynthetic capacity and the implications for carbon cycling. Proceedings of the National Academy of Sciences, 109(22): 8612-8617.

Bauerle, W.L., Toler, J.E. and Wang, G.G., 2004b. Stomatal conductance of Acer rubrum ecotypes under varying soil and atmospheric water conditions: predicting stomatal responses with an abscisic acid-based model. Tree physiology, 24(7): 805-811.

Bauerle, W.L., Whitlow, T., Setter, T., Bauerle, T. and Vermeylen, F., 2003. Ecophysiology of Acer rubrum seedlings from contrasting hydrologic habitats: growth, gas exchange, tissue water relations, abscisic acid and carbon isotope discrimination. Tree Physiology, 23(12): 841-850.

Berry, J.A., Beerling, D.J. and Franks, P.J., 2010. Stomata: key players in the earth system, past and present. Current opinion in plant biology, 13(3): 232-239.

Biosciences, L., 2002. Using the LI-6400 portable photosynthesis system. Li-Cor Biosciences Inc.: Lincoln, NE.

Blum, A., 2005. Drought resistance, water-use efficiency, and yield potential—are they compatible, dissonant, or mutually exclusive? Crop and Pasture Science, 56(11): 1159-1168.

Boegh, E., Søgaard, H., Friborg, T. and Levy, P., 1999. Models of CO< sub> 2</sub> and water vapour fluxes from a sparse millet crop in the Sahel. Agricultural and forest meteorology, 93(1): 7-26.

Bounoua, L. et al., 1999. Interactions between vegetation and climate: radiative and physiological effects of doubled atmospheric CO2. Journal of Climate, 12(2): 309-324.

Bowden, J.D. and Bauerle, W.L., 2008. Measuring and modeling the variation in species-specific transpiration in temperate deciduous hardwoods. Tree Physiology, 28(11): 1675-1683.

Brodribb, T., 1996. Dynamics of changing intercellular CO2 concentration (ci) during drought and determination of minimum functional ci. Plant Physiology, 111(1): 179-185.

Brodribb, T.J., McAdam, S.A., Jordan, G.J. and Feild, T.S., 2009. Evolution of stomatal responsiveness to CO2 and optimization of water-use efficiency among land plants. New Phytologist, 183(3): 839-847.

Buckley, T.N. and Mott, K.A., 2013. Modelling stomatal conductance in response to environmental factors. Plant, cell & environment, 36(9): 1691-1699.

Bunce, J.A., 1998. Effects of environment during growth on the sensitivity of leaf conductance to changes in humidity. Global Change Biology, 4(3): 269-274.

Bunce, J.A., 2000. Responses of stomatal conductance to light, humidity and temperature in winter wheat and barley grown at three concentrations of carbon dioxide in the field. Global Change Biology, 6(4): 371-382.

Bunce, J.A., 2004. Carbon dioxide effects on stomatal responses to the environment and water use by crops under field conditions. Oecologia, 140(1): 1-10.

Caird, M.A., Richards, J.H. and Donovan, L.A., 2007. Nighttime stomatal conductance and transpiration in C3 and C4 plants. Plant Physiology, 143(1): 4-10.

Carlson, P.J., 2000. Seasonal and inter-annual variation in carbon dioxide exchange and carbon balance in a mixed grassland, Lethbridge, Alta.: University of Lethbridge, Faculty of Arts and Science, 2000.

Chen, D.-X., Coughenour, M., Knapp, A. and Owensby, C., 1994. Mathematical simulation of C< sub> 4</sub> grass photosynthesis in ambient and elevated CO< sub> 2</sub>. Ecological Modelling, 73(1): 63-80.

Collatz, G.J., Ball, J.T., Grivet, C. and Berry, J.A., 1991. Physiological and environmental regulation of stomatal conductance, photosynthesis and transpiration - a model that includes a laminar boundary layer. Agricultural and Forest Meteorology, 54(2-4): 107-136.

Collatz, G.J., Ribas-Carbo, M. and Berry, J., 1992. Coupled photosynthesis-stomatal conductance model for leaves of C4 plants. Functional Plant Biology, 19(5): 519-538.

Condon, A., Richards, R., Rebetzke, G. and Farquhar, G., 2002. Improving intrinsic water-use efficiency and crop yield. Crop Science, 42(1): 122-131.

Cowan, I., 1982. Regulation of water use in relation to carbon gain in higher plants, Physiological Plant Ecology II. Springer, pp. 589-613.

Cowan, I. and Farquhar, G., 1977. Stomatal function in relation to leaf metabolism and environment, Symposia of the Society for Experimental Biology, pp. 471.

Damour, G., Simonneau, T., Cochard, H. and Urban, L., 2010. An overview of models of stomatal conductance at the leaf level. Plant, Cell & Environment, 33(9): 1419-1438.

Dang, Q.-L., Margolis, H.A. and Collatz, G.J., 1998. Parameterization and testing of a coupled photosynthesis–stomatal conductance model for boreal trees. Tree Physiology, 18(3): 141-153.

Dang, Q.-L., Margolis, H.A., Coyea, M.R., Sy, M. and Collatz, G.J., 1997. Regulation of branch-level gas exchange of boreal trees: roles of shoot water potential and vapor pressure difference. Tree Physiology, 17(8-9): 521-535.

Dietze, M.C. et al., 2014. A quantitative assessment of a terrestrial biosphere model's data needs across North American biomes. Journal of Geophysical Research: Biogeosciences, 119(3): 286-300.

Dougherty, R.L., Bradford, J.A., Coyne, P.I. and Sims, P.L., 1994. Applying an empirical model of stomatal conductance to three C-4 grasses. Agricultural and Forest Meteorology, 67(3): 269-290.

Egea, G., Verhoef, A. and Vidale, P.L., 2011. Towards an improved and more flexible representation of water stress in coupled photosynthesis–stomatal conductance models. Agricultural and Forest Meteorology, 151(10): 1370-1384.

Falge, E., Graber, W., Siegwolf, R. and Tenhunen, J., 1996. A model of the gas exchange response ofPicea abies to habitat conditions. Trees, 10(5): 277-287.

Farquhar, G., Caemmerer, S. and Berry, J., 1980. A biochemical model of photosynthetic CO 2 assimilation in leaves of C 3 species. Planta, 149(1): 78-90.

Franks, P.J. and Farquhar, G.D., 2007. The mechanical diversity of stomata and its significance in gas-exchange control. Plant Physiology, 143(1): 78-87.

Gimeno, T.E. et al., 2015. Conserved stomatal behaviour under elevated CO2 and varying water availability in a mature woodland. Funct. Ecol.

Grantz, D.A. and Zeiger, E., 1986. Stomatal responses to light and leaf-air water vapor pressure difference show similar kinetics in sugarcane and soybean. Plant Physiology, 81(3): 865-868.

Grassi, G., Vicinelli, E., Ponti, F., Cantoni, L. and Magnani, F., 2005. Seasonal and interannual variability of photosynthetic capacity in relation to leaf nitrogen in a deciduous forest plantation in northern Italy. Tree Physiology, 25(3): 349-360.

Gunderson, C. et al., 2002. Environmental and stomatal control of photosynthetic enhancement in the canopy of a sweetgum (Liquidambar styraciflua L.) plantation during 3 years of CO2 enrichment. Plant, Cell & Environment, 25(3): 379-393.

Gutschick, V.P. and Simonneau, T., 2002. Modelling stomatal conductanceof field-grown sunflower under varying soil water content and leafenvironment: comparison of three models of stomatal response toleaf environment and coupling with an abscisic acid-based modelof stomatal response to soil drying. Plant, Cell & Environment, 25(11): 1423-1434.

Hanan, N.P. et al., 2005. Testing a model of CO 2, water and energy exchange in Great Plains tallgrass prairie and wheat ecosystems. Agricultural and Forest Meteorology, 131(3): 162-179.

Harley, P. and Baldocchi, D., 1995. Scaling carbon dioxide and water vapour exchange from leaf to canopy in a deciduous forest. I. Leaf model parametrization. Plant, Cell & Environment, 18(10): 1146-1156.

Harley, P. and Tenhunen, J., 1991. Modeling the photosynthetic response of C3 leaves to environmental factors. Modeling crop photosynthesis–from biochemistry to canopy: 17-39.

Harley, P., Thomas, R., Reynolds, J. and Strain, B., 1992. Modelling photosynthesis of cotton grown in elevated CO2. Plant, Cell & Environment, 15(3): 271-282.

Heroult, A., Lin, y.Ä., Bourne, A., Medlyn, B.e. and Ellsworth, D.s., 2013. Optimal stomatal conductance in relation to photosynthesis in climatically contrasting Eucalyptus species under drought. Plant, Cell & Environment, 36(2): 262-274.

Jarvis, P.G., 1976. The interpretation of the variations in leaf water potential and stomatal conductance found in canopies in the field. Philosophical Transactions of the Royal Society of London. B, Biological Sciences, 273(927): 593.

Jones, H.G., 2013. Plants and microclimate: a quantitative approach to environmental plant physiology. Cambridge University Press.

Kattge, J., Knorr, W., Raddatz, T. and Wirth, C., 2009. Quantifying photosynthetic capacity and its relationship to leaf nitrogen content for global-scale terrestrial biosphere models. Global Change Biology, 15(4): 976-991.

Katul, G., Ellsworth, D. and Lai, C.T., 2000. Modelling assimilation and intercellular CO2 from measured conductance: a synthesis of approaches. Plant, Cell & Environment, 23(12): 1313-1328.

Katul, G., Leuning, R. and Oren, R., 2003. Relationship between plant hydraulic and biochemical properties derived from a steady-state coupled water and carbon transport model. Plant, Cell & Environment, 26(3): 339-350.

Katul, G., Manzoni, S., Palmroth, S. and Oren, R., 2010. A stomatal optimization theory to describe the effects of atmospheric CO2 on leaf photosynthesis and transpiration. Annals of Botany, 105(3): 431-442.

Kellomäki, S. and Wang, K.-Y., 1997. Photosynthetic responses of Scots pine to elevated CO2 and nitrogen supply: Results of a branch-in-bag experiment. Tree Physiology, 17(4): 231-240.

Knapp, A.K., 1993. Gas Exchange Dynamics in C3 and C4 Grasses: Consequence of Differences in Stomatal Conductance. Ecology: 113-123.

Knapp, A.K. and Smith, W.K., 1990. Contrasting stomatal responses to variable sunlight in two subalpine herbs. Am. J. Bot.: 226-231.

Kosugi, Y., Shibata, S. and Kobashi, S., 2003. Parameterization of the CO2 and H2O gas exchange of several temperate deciduous broad-leaved trees at the leaf scale considering seasonal changes. Plant, Cell & Environment, 26(2): 285-301.

Kumagai, T. et al., 2006. Modeling CO2 exchange over a Bornean tropical rain forest using measured vertical and horizontal variations in leaf-level physiological parameters and leaf area densities. Journal of Geophysical Research: Atmospheres (1984–2012), 111(D10).

Lai, C.T., Katul, G., Oren, R., Ellsworth, D. and Schäfer, K., 2000. Modeling CO2 and water vapor turbulent flux distributions within a forest canopy. Journal of Geophysical Research: Atmospheres (1984–2012), 105(D21): 26333-26351.

Launiainen, S., Katul, G.G., Kolari, P., Vesala, T. and Hari, P., 2011. Empirical and optimal stomatal controls on leaf and ecosystem level CO2and H2O exchange rates. Agricultural and Forest Meteorology, 151(12): 1672-1689.

Leakey, A.D., Bernacchi, C.J., Ort, D.R. and Long, S.P., 2006. Long-term growth of soybean at elevated [CO2] does not cause acclimation of stomatal conductance under fully open-air conditions. Plant, Cell & Environment, 29(9): 1794-1800.

Leuning, R., 1990. Modelling stomatal behaviour and and photosynthesis of eucalyptus grandis. Functional Plant Biology, 17(2): 159-175.

Leuning, R., 1995. A critical-appraisal of a combined stomatal-photosynthesis model for C3 plants. Plant Cell and Environment, 18(4): 339-355.

Leuning, R., Dunin, F. and Wang, Y.-P., 1998. A two-leaf model for canopy conductance, photosynthesis and partitioning of available energy. II. Comparison with measurements. Agricultural and Forest Meteorology, 91(1): 113-125.

Limousin, J. et al., 2013. Regulation and acclimation of leaf gas exchange in a piñon–juniper woodland exposed to three different precipitation regimes. Plant, cell & environment, 36(10): 1812-1825.

Lin, Y.-S. et al., 2015. Optimal stomatal behaviour around the world. Nature Climate Change.

Lin, Y.-S., Medlyn, B.E. and Ellsworth, D.S., 2012. Temperature responses of leaf net photosynthesis: the role of component processes. Tree physiology, 32(2): 219-231.

Liozon, R., Badeck, F.-W., Genty, B., Meyer, S. and Saugier, B., 2000. Leaf photosynthetic characteristics of beech (Fagus sylvatica) saplings during three years of exposure to elevated CO2 concentration. Tree physiology, 20(4): 239-247.

Liu, F., Andersen, M.N. and Jensen, C.R., 2009. Capability of the 'Ball-Berry'model for predicting stomatal conductance and water use efficiency of potato leaves under different irrigation regimes. Scientia Horticulturae, 122(3): 346-354.

Liu, Z., Zhang, Z., Wang, Z. and Shu, Q., 2008. Measuring and modeling stomatal conductance of cucumber crop in solar greenhouse in Northeast China. Scientia horticulturae, 117(2): 103-108.

Lloyd, J., 1991. Modeling stomatal responses to environment in macadamia-integrifolia. Aust. J. Plant Physiol., 18(6): 649-660.

Luo, Y. et al., 2001. Gross primary productivity in Duke Forest: modeling synthesis of CO2 experiment and eddy-flux data. Ecol. Appl., 11(1): 239-252.

Macfarlane, C., White, D. and Adams, M., 2004. The apparent feed-forward response to vapour pressure deficit of stomata in droughted, field-grown Eucalyptus globulus Labill. Plant, Cell & Environment, 27(10): 1268-1280.

Mäkelä, A., Berninger, F. and Hari, P., 1996. Optimal control of gas exchange during drought: theoretical analysis. Annals of Botany, 77(5): 461-468.

McMurtrie, R.E., Leuning, R., Thompson, W.A. and Wheeler, A.M., 1992. A model of canopy photosynthesis and water-use incorporating a mechanistic formulation of leaf CO2 exchange. Forest Ecology and Management, 52(1-4): 261-278.

Medlyn, B. et al., 2001. Stomatal conductance of forest species after long-term exposure to elevated CO2 concentration: A synthesis. New Phytologist, 149(2): 247-264.

Medlyn, B. et al., 2002. Temperature response of parameters of a biochemically based model of photosynthesis. II. A review of experimental data. Plant, Cell & Environment, 25(9): 1167-1179.

Medlyn, B.E. et al., 2005. Carbon balance of coniferous forests growing in contrasting climates: Model-based analysis. Agricultural and Forest Meteorology, 131(1): 97-124.

Medlyn, B.E. et al., 2011. Reconciling the optimal and empirical approaches to modelling stomatal conductance. Global Change Biology, 17(6): 2134-2144.

Misson, L., Panek, J.A. and Goldstein, A.H., 2004. A comparison of three approaches to modeling leaf gas exchange in annually drought-stressed ponderosa pine forests. Tree Physiology, 24(5): 529-541.

Mo, X. and Liu, S., 2001. Simulating evapotranspiration and photosynthesis of winter wheat over the growing season. Agricultural and Forest Meteorology, 109(3): 203-222.

Monteith, J., 1995. A reinterpretation of stomatal responses to humidity. Plant, Cell & Environment, 18(4): 357-364.

Mott, K. and Parkhurst, D., 1991. Stomatal responses to humidity in air and helox. Plant, Cell & Environment, 14(5): 509-515.

Nikolov, N.T., Massman, W.J. and Schoettle, A.W., 1995. Coupling biochemical and biophysical processes at the leaf level: an equilibrium photosynthesis model for leaves of C< sub> 3</sub> plants. Ecological Modelling, 80(2): 205-235.

Oleson, K.W. et al., 2010. Technical description of version 4.0 of the Community Land Model (CLM).

Oleson, K.W. et al., 2008. Improvements to the Community Land Model and their impact on the hydrological cycle. J. Geophys. Res, 113: G01021.

Ono, K. et al., 2013. Canopy-scale relationships between stomatal conductance and photosynthesis in irrigated rice. Global Change Biology.

Oren, R. et al., 1999. Survey and synthesis of intra-and interspecific variation in stomatal sensitivity to vapour pressure deficit. Plant, Cell & Environment, 22(12): 1515-1526.

Pearcy, R.W., 1990. Sunflecks and photosynthesis in plant canopies. Annu. Rev. Plant Biol., 41(1): 421-453.

Polley, H. et al., 1992. Leaf gas exchange of Andropogon gerardii Vitman, Panicum virgatum L., and Sorghastrum nutans (L.) Nash in a tallgrass prairie. Journal of Geophysical Research: Atmospheres (1984–2012), 97(D17): 18837-18844.

Prieto, J.A. et al., 2012. A leaf gas exchange model that accounts for intra-canopy variability by considering leaf nitrogen content and local acclimation to radiation in grapevine (Vitis vinifera L.). Plant, Cell & Environment, 35(7): 1313-1328.

Reichstein, M. et al., 2002. Severe drought effects on ecosystem CO2 and H2O fluxes at three Mediterranean evergreen sites: revision of current hypotheses? Global Change Biology, 8(10): 999-1017.

Reynolds, R.F., Bauerle, W.L. and Wang, Y., 2009. Simulating carbon dioxide exchange rates of deciduous tree species: evidence for a general pattern in biochemical changes and water stress response. Annals of botany, 104(4): 775-784.

Sala, A. and Tenhunen, J.D., 1996. Simulations of canopy net photosynthesis and transpiration in Quercus ilex L under the influence of seasonal drought. Agricultural and Forest Meteorology, 78(3-4): 203-222.

Schultz, H.R., Lebon, E. and Rousseau, C., 1998. Suitability of the Ball, Woodrow, Berry model for the description of stomatal coupling to photosynthesis of different vitis species and vitis vinifera cultivars in different climatic regions at various levels of water deficit, I ISHS Workshop on Water Relations of Grapevines 493, pp. 17-30.

Sellers, P.J. et al., 1997. Modeling the exchanges of energy, water, and carbon between continents and the atmosphere. Science, 275(5299): 502.

Sellers, P.J. et al., 1996. A revised land surface parameterization (SiB2) for atmospheric GCMs. Part I: Model formulation. Journal of Climate, 9(4): 676-705.

Shimono, H., Okada, M., Inoue, M., Nakamura, H. and Kobayashi, K., 2010. Diurnal and seasonal variations in stomatal conductance of rice at elevated atmospheric CO2 under fully open-air conditions. Plant, cell and environment, 33(3): 322-331.

Snyder, K., Richards, J. and Donovan, L., 2003. Night-time conductance in C3 and C4 species: do plants lose water at night? Journal of Experimental Botany, 54(383): 861-865.

Soegaard, H. and Nordstroem, C., 1999. Carbon dioxide exchange in a high-arctic fen estimated by eddy covariance measurements and modelling. Global Change Biology, 5(5): 547-562.

Tanaka, K., Kosugi, Y. and Nakamura, A., 2002. Impact of leaf physiological characteristics on seasonal variation in CO< sub> 2</sub>, latent and sensible heat exchanges over a tree plantation. Agricultural and forest meteorology, 114(1): 103-122.

Tardieu, F. and Davies, W., 1993. Integration of hydraulic and chemical signalling in the control of stomatal conductance and water status of droughted plants. Plant, Cell & Environment, 16(4): 341-349.

Tenhunen, J.D., Serra, A.S., Harley, P.C., Dougherty, R.L. and Reynolds, J.F., 1990. Factors influencing carbon fixation and water-use by mediterranean sclerophyll shrubs during summer drought. Oecologia, 82(3): 381-393.

Thorgeirsson, H. and Soegaard, H., 1999. Simulated carbon dioxide exchange of leaves of barley scaled to the canopy and compared to measured fluxes. Agricultural and forest meteorology, 98: 479-489.

Tyree, M.T. and Sperry, J.S., 1988. Do woody plants operate near the point of catastrophic xylem dysfunction caused by dynamic water stress? Answers from a model. Plant physiology, 88(3): 574-580.

Uddling, J., Hall, M., Wallin, G. and Karlsson, P.E., 2005. Measuring and modelling stomatal conductance and photosynthesis in mature birch in Sweden. Agricultural and Forest Meteorology, 132(1): 115-131.

Uddling, J. and Wallin, G., 2012. Interacting effects of elevated CO2 and weather variability on photosynthesis of mature boreal Norway spruce agree with biochemical model predictions. Tree physiology: tps086.

Valentini, R., Gamon, J.A. and Field, C.B., 1995. Ecosystem gas exchange in a California grassland: seasonal patterns and implications for scaling. Ecology: 1940-1952.

Van Wijk, M. et al., 2000. Modeling daily gas exchange of a Douglas-fir forest: comparison of three stomatal conductance models with and without a soil water stress function. Tree Physiology, 20(2): 115-122.

Wang, S., Yang, Y. and Trishchenko, A.P., 2009. Assessment of canopy stomatal conductance models using flux measurements. Ecological Modelling, 220(17): 2115-2118.

Wang, Y.-P. and Leuning, R., 1998. A two-leaf model for canopy conductance, photosynthesis and partitioning of available energy I:: Model description and comparison with a multi-layered model. Agricultural and Forest Meteorology, 91(1): 89-111.

Wang, Y.P. and Jarvis, P.G., 1990. Description and validation of an array model - maestro. Agricultural and Forest Meteorology, 51(3-4): 257-280.

Way, D.A., Oren, R., Kim, H.S. and Katul, G.G., 2011. How well do stomatal conductance models perform on closing plant carbon budgets? A test using seedlings grown under current and elevated air temperatures. Journal of Geophysical Research: Biogeosciences, 116(G4).

Weber, J. and Gates, D., 1990. Gas exchange in Quercus rubra (northern red oak) during a drought: analysis of relations among photosynthesis, transpiration, and leaf conductance. Tree Physiology, 7(1-2-3-4): 215-225.

Wever, L.A., Flanagan, L.B. and Carlson, P.J., 2002. Seasonal and interannual variation in evapotranspiration, energy balance and surface conductance in a northern temperate grassland. Agricultural and Forest Meteorology, 112(1): 31-49.

Wilson, K., Baldocchi, D. and Hanson, P., 2001. Leaf age affects the seasonal pattern of photosynthetic capacityand net ecosystem exchange of carbon in a deciduous forest. Plant, Cell & Environment, 24(6): 571-583.

Wilson, K.B., Baldocchi, D.D. and Hanson, P.J., 2000. Spatial and seasonal variability of photosynthetic parameters and their relationship to leaf nitrogen in a deciduous forest. Tree Physiology, 20(9): 565-578.

Wohlfahrt, G., Bahn, M., Horak, I., Tappeiner, U. and Cernusca, A., 1998. A nitrogen sensitive model of leaf carbon dioxide and water vapour gas exchange: application to 13 key species from differently managed mountain grassland ecosystems. Ecological Modelling, 113(1): 179-199.

Wolf, A., Akshalov, K., Saliendra, N., Johnson, D.A. and Laca, E.A., 2006. Inverse estimation of Vcmax, leaf area index, and the Ball-Berry parameter from carbon and energy fluxes. Journal of Geophysical Research: Atmospheres (1984–2012), 111(D8).

Wong, S., Cowan, I. and Farquhar, G., 1979. Stomatal conductance correlates with photosynthetic capacity.

Wong, S.C., Cowan, I.R. and Farquhar, G.D., 1985. Leaf conductance in relation to rate of CO2 assimilation 1. Influence of nitrogen nutrition, phosphorus-nutrition, photon flux-density, and ambient partial-pressure of CO2 during ontogeny. Plant Physiology, 78(4): 821-825.

Wullschleger, S.D., 1993. Biochemical limitations to carbon assimilation in C3 plants,Äîa retrospective analysis of the A/Ci curves from 109 species. Journal of Experimental Botany, 44(5): 907-920.

Xu, L. and Baldocchi, D.D., 2003. Seasonal trends in photosynthetic parameters and stomatal conductance of blue oak (Quercus douglasii) under prolonged summer drought and high temperature. Tree Physiology, 23(13): 865-877.

Yu, G.-R., Zhuang, J. and Yu, Z.-L., 2001. An attempt to establish a synthetic model of photosynthesis-transpiration based on stomatal behavior for maize and soybean plants grown in field. J. Plant Physiol., 158(7): 861-874.

Yu, Q., Zhang, Y., Liu, Y. and Shi, P., 2004. Simulation of the stomatal conductance of winter wheat in response to light, temperature and CO2 changes. Annals of Botany, 93(4): 435-441.

Zheng, D., Freeman, M., Bergh, J., Røsberg, I. and Nilsen, P., 2002. Production of Picea abies in south-east Norway in response to climate change: a case study using process-based model simulation with field validation. Scand. J. For. Res., 17(1): 35-46.

Zhou, S., Duursma, R.A., Medlyn, B.E., Kelly, J.W. and Prentice, I.C., 2013. How should we model plant responses to drought? An analysis of stomatal and non-stomatal responses to water stress. Agricultural and Forest Meteorology, 182: 204-214.

CHAPTER 2:

SEASONAL VARIABILITY OF THE PARAMETERS OF THE BALL-BERRY MODEL OF STOMATAL CONDUCTANCE IN MAIZE (ZEA MAYS L.) AND SUNFLOWER (HELIANTHUS ANNUUS L.) UNDER WELL-WATERED AND WATER-STRESSED CONDITIONS

Summary

The Ball-Berry (BB) model of stomatal conductance (g_s) is frequently coupled with a biochemical model of photosynthesis to estimate fluxes of carbon dioxide (CO_2) and water in plant canopy models. The BB model contains two empirical parameters, the slope proportionality constant (*m),* and 'residual' g_s (g_0), and both parameters are highly influential to transpiration estimates. However, the time-intensive nature of leaf-level parameter collection results in only sparse physical data reflecting species-specific values or the responses of *m* and g_0 to season or soil moisture stress. Here, we measured and characterize *m* and g_0 seasonally and under different water availability for two economically important field crops, maize and sunflower, and determined the minimum stomatal settling times needed for robust parameter estimates. We also compare two different methods for estimating the BB parameters. We found that estimates of the BB parameters could be obtained in < 20 minutes per plant in maize by utilizing changes in Photosynthetic Photon Flux Density (PPFD), whereas ≈ 40 minutes per plant was needed in sunflower. Lower rates of g_s under water stress reduced the absolute change in the g_s response to PPFD, further lowering the time needed to obtain values. However, the statistical method used to estimate *m* and g_0 impacted values by up to 25 - 30% in both crops. We found no evidence of a

seasonal shift in *m* or g_0 in well-watered maize, supporting the use of a single value for modeling across the season. Measurements of leaf traits correlated with *m* also corroborated this finding. Well-watered parameter values for maize (*m* = 4.53 ± 0.65 and g_0 = 0.017 ± 0.016 mol m^{-2} s^{-1}) were similar to those currently utilized in land-surface models for C4 plants, but were higher than values previously reported for maize. The mean *m* value for well-watered sunflower (*m* = 8.84 ± 3.77) was similar to the value used for C3 plants in land-surface models (i.e., ≈ 9), but varied from the *m* values reported elsewhere for sunflower. Sunflower g_0 values exhibited a high degree of variability and g_0 values were substantially higher (g_0 = 0.354 ± 0.226 mol m^{-2} s^{-1}) than those reported for most plants. However, nighttime gravimetric measurements corroborated that substantial g_s and transpiration occurred when A_n <0. While seasonal changes in parameters were not significant in sunflower, additional replication may be necessary to detect seasonal shifts in the g_0 parameter. Water stress resulted in significant reductions in both *m* and g_0 in maize. In sunflower, only g_0 values were reduced under water stress, although there an indication of a decline in *m* under rapid and severe water stress. Our results show that both of the BB parameters must be adjusted downward under water stress in maize, whereas the g_0 term is reduced under water stress in sunflower.

Introduction

Plant canopies affect the water and energy budgets of the land surface by controlling the passage of water vapor and CO_2 through the aperture or conductance of small orifices on the leaf surface called stomata. As a control interface involved in regulating water loss, stomata play a key role in how plants adapt to changing environmental conditions. A better understanding of how to model stomatal conductance (g_s) is important for accurate predictions of plant water use (Bauerle and Bowden, 2011) as well for larger-scale regional predictions of hydrology, runoff,

carbon uptake, and energy fluxes in land surface models (Berry et al. 2010). Water vapor exchanges over a range of temporal and spatial scales are complex functions, usually requiring simplifications of biological, chemical, and physical processes. To capture feedbacks that span multiple temporal and spatial scales, models must simulate the sensitivity of transpiration to changes in environmental conditions and differences in available soil water. Moreover, differences in available soil water adversely impact plant growth and productivity, and changes in climate and water availability exacerbate the need for accurate methods of modeling seasonal variation in plant water use in both natural and managed systems.

A common approach for estimating fluxes of CO_2 and water in leaf and canopy models is to couple a mechanistic biochemical model of photosynthesis (A_n) (Farquhar et al., 1980) to a model of g_s (Ball, 1988; Ball et al., 1987; Collatz et al., 1992) or slight modifications of this model (e.g., Leuning 1995; Leuning et al. 1991). This method is routinely utilized in leaf-level physiological models, as well as in regional and global hydrologic and climate models (Berry et al., 2010; Sellers et al., 1997; Sellers et al., 1996). These models require only a few empirical parameters and can easily be incorporated into vegetation models, providing an efficient and effective way of predicting rates of A_n and transpiration at multiple scales (Baldocchi and Meyers, 1998; Bounoua et al., 1999; Damour et al., 2010; Oleson et al., 2008; Sellers et al., 1996). These two models form the foundation of many contemporary models of terrestrial carbon and water cycling (Leakey et al., 2006).

The majority of proposed g_s models are empirical or semi-empirical, as the current understanding of the physiological mechanisms of stomatal responses is less than complete (Damour et al., 2010). One of the most commonly used semi-empirical models of g_s is the Ball-Berry (BB) model (Ball et al., 1987) or slight modifications of this model (Leuning, 1995;

Leuning et al., 1991). The BB model describes g_s to water vapor as a function of net assimilation (A_n), relative humidity at the leaf surface (H_s), CO_2 concentration at the leaf surface (C_s), g_s when A_n approaches zero (g_0) and a slope proportionality constant (m):

$$g_s \cong m * A_n \frac{H_s}{C_s} + g_0 \qquad (1)$$

The slope proportionality constant (*m)* is the slope of the relationship between g_s and A_nH_s/C_s (hereafter referred to as the Ball Index), traditionally fit via linear regression. The slope *m* represents a "compromise between the costs and benefits of g_s relative to the photosynthetic activity of the leaf" (Ball, 1988). Instantaneous water-use efficiency (A_n per unit T; W_T) and carbon isotope discrimination (δ^{13} C) during A_n are inversely related to *m*, while *m* increases in conjunction with the ratio of intercellular to atmospheric CO_2 concentration (C_i/C_a). The intercept of the BB model, g_0, encompasses both cuticular conductance ($g_{cuticular}$) and residual g_s, and is commonly defined as either (i) a fit parameter extrapolated as the intercept of the least squares regression between g_s and the Ball Index (Ball, 1988; Ball et al., 1987; Collatz et al., 1991) or as the residual or base conductance when $A_n \leq 0$ (e.g., Leuning, 1995). The g_s - A_n relationship is not always linear at low PPFD (Ball, 1988), and g_0 values measured in the dark or via regression on data collected at very low levels of PPFD can vary from values measured when g_0 is estimated as a fitted value with measurements taken under higher PPFD (Barnard and Bauerle, 2013; Collatz et al., 1992; Leuning, 1995). Additional confusion occurs due to the fact that true nighttime measurements of g_s are also referred to as g_0 throughout the literature. For clarity throughout this paper, we refer to intercept estimates obtained via regression as g_{0_reg} and to true nighttime measurements of g_s as g_{0_night}. While the g_0 parameter may be small or not

significantly different from zero in some species (Gimeno et al., 2015; Leakey et al., 2006), many species show substantial conductance when $A_n \leq 0$ (Barnard and Bauerle, 2013; Caird et al., 2007; Cavender-Bares et al., 2007; Howard and Donovan, 2007; Snyder et al., 2003; Zeppel et al., 2012), and inclusion of the term has been shown to be necessary to accurately model transpiration (Barnard and Bauerle, 2013).

Both *m* and g_0 are highly influential on modeled estimates of transpiration (Barnard and Bauerle, 2013; Bauerle and Bowden, 2011). Species-level differences in *m* and g_0 clearly exist (Ball, 1988; Barnard and Bauerle, 2013; Collatz et al., 1991; Leuning, 1995; Medlyn et al., 2011), but many models assume a static or generic value across plant functional types (e.g., Krinner et al., 2005). The time-intensive nature of leaf-level parameter collection results in only sparse physical data reflecting species specific parameter values, or the responses of *m* and g_0 to season or soil moisture stress. Considerable time and effort are often needed to collect robust parameter estimates. For example, in the original derivation of the BB g_s model, Ball (1988) worked under experimentally controlled conditions and varied one of four factors (i.e., the ambient mole fraction of CO_2 (C_a), the ambient mole fraction of water vapor (W_s), photosynthetically active radiation (PAR), and air temperature (T_a)) while the other factors were held constant. Data were recorded only when A_n and g_s approached steady-state. The necessity of recording data only when a near steady-state conditions are reached for both g_s and A_n can impose challenges in terms of parameter collection and replication. Stomata respond more slowly than A_n to changes in environmental conditions (e.g., Pearcy, 1990) and the time it takes for g_s to approach steady-state conditions after a shift in environmental conditions is dependent on the species, the variable being altered, and the magnitude of the change in conditions (Aasamaa and Sõber, 2011; Franks and Farquhar, 2007; Grantz and Zeiger, 1986; Jones, 2013).

It can take several hours to collect the quantity and spread of data necessary to determine *m* (Barnard and Bauerle, 2013; Xu and Baldocchi, 2003). An additional investment of time is needed if g_0 is determined via regression only on data collected under low PPFD (Leuning 1995) or at night (Barnard and Bauerle, 2013)

A drawback to the BB model is that it does not capture the response to water stress without modification (Damour et al., 2010) There have been numerous studies that attempt to adapt the BB model to capture water stress as empirical functions of soil or plant water status in order to improve simulations of plant water use under drought (Kirschbaum, 1999; Misson et al., 2004; Sala and Tenhunen, 1996; Tenhunen et al., 1990; Tuzet et al., 2003). However, very few studies have physically measured how the BB slope is altered under drought (Medlyn et al., 2011), and even less attention has been given to the impacts of drought on g_0 (Barnard and Bauerle, 2013). Similarly, many of the studies that report seasonal variations in *m* did not physically measure *m*, but instead calculated the parameter via top-down approaches that minimize the difference between observed fluxes and model simulations (Lai et al., 2000; Ono et al., 2013; Valentini et al., 1995; Wolf et al., 2006). Some authors have reported that *m* changes over the course of the season (Misson et al., 2004), whereas others have found a constant seasonal value (Xu and Baldocchi, 2003). When careful attention has been given to examining the response of *m* to water stress, the results have been contradictory, with some studies reporting that the parameter is relatively stable under water stress (Gimeno et al., 2015) even when water stress is severe (Xu and Baldocchi, 2003) whereas others have reported a distinct response of the parameter to water stress (Heroult et al., 2013; Zhou et al., 2013). Others have found that the g_0 term rather than *m* shifts as soil moisture potential is reduced (Misson et al., 2004), whereas other studies have failed to find a response of g_0 to changes in soil moisture

(Barnard and Bauerle, 2013). Additionally, the majority of the studies examining *m* or g_0 have occurred in perennial species (Barnard and Bauerle, 2013; Falge et al., 1996; Gimeno et al., 2015; Heroult et al., 2013; Kirschbaum, 1999; Medlyn et al., 2005; Medlyn et al., 2011; Misson et al., 2004; Xu and Baldocchi, 2003), with only a few instances of careful examination for annual field crops (Bunce, 2000; Collatz et al., 1992; Gutschick and Simonneau, 2002; Leakey et al., 2006). Recent efforts to couple crop models with climate models to predict fluxes from croplands (Lokupitiya et al., 2009) highlight the need for estimates of *m* and g_0 that are specific to crops.

There is a clear need for continued research into species-specific estimates of the BB model parameters, as well as investigation of whether values are static seasonally and under water stress. The objectives of this research were to physically measure and characterize *m* and g_0 (i) seasonally, and (ii) under different water availability for two economically important field crops, maize and sunflower. Specifically, we measured changes in the BB parameters for five different ontogenic stages and under well-watered and water-stressed conditions, and determined the minimum stomatal settling times needed for robust parameter estimates. We also compared estimates of g_0 obtained from linear regression on all data, versus regression on data at low PPFD. Next, we examined the relationship of the BB parameters with other water relations parameters, soil volumetric water content (θ_v) and leaf water potential (Ψ_{Leaf}) to see if these variables could be used to scale parameters under water stress. Measurements of $\delta^{13}C$ and W_T were compared with changes in *m* and g_{0_reg} to compare and confirm temporal trends. In sunflower, we compared the parameter values obtained from gradually imposed seasonal water stress to the values obtained from rapidly induced water stress and compared daytime versus nighttime estimates of g_0.

Materials and Methods

Site description

The primary measurements for this study were conducted during the 2013 growing season in the greenhouse facilities at Colorado State University, Fort Collins, CO. Ancillary field measurements were made at the USDA-ARS Limited Irrigation Research Farm (LIRF) in northern Colorado, USA (40°26′57″ N, 104°38′12″ W, Elev. 1427 m).

Greenhouse Experiment

Seeds of sunflower (Syngenta hybrid 2495 NS/CL/DM) and maize (Dekalb hybrid DKC52-04 RIV) were planted on June 10, 2013 (DOY 161) into 26 L pots. Pots were filled with 8.8 kg of air-dried soilless substrate consisting of a 1:1:3 by volume ratio of Greens Grade™, Turface® Quick Dry®, and Fafard 2SV. Briefly, Greens Grade™ consists of a minimum of 60% medium – course sand, 20-30% of particles ranging from fine sand to clay, and less than 10% very course sand. Turface® Quick Dry® is a fine, calcined, non-swelling illite and silica clay, with a cation exchange capacity (CEC) of 33.6 meq/100 g. Fafard 2SV is a mix of peat moss and fine vermiculite. Our intent was to create a soilless substrate that could be readily replicated, and that had a particle size distribution, porosity, CEC, and a water release curve that was more similar to soil than typical soilless mixes. Accurate soil moisture sensor readings require good contact with the medium, so we avoided potting mixtures with large air spaces and voids. Volumetric water content (θ_v) at field capacity (0.33 MPa) as determined via soil water release curves was approximately 49%.

Plants of similar sizes within a species were randomly assigned to either a well-watered or water-stressed treatment. Measurements were performed in approximately 2-week intervals, beginning in the mid to late vegetative stage and continuing until plant senescence. All plants

were kept well-watered until after the first measurement period, after which a water stress treatment was imposed. A total of five measurement periods occurred for well-watered plants and four for the water stressed, as the water-stress treatment induced early senescence. Measurement dates and accompanying growth stages for each crop are given in Table 1. For ease of reference, we refer to measurement periods in lieu of day of year (DOY). Five plants per treatment were tracked over the season for changes in m and g_0.

Table 1. Dates of measurement and corresponding developmental stages for well-watered maize and sunflower grown under greenhouse conditions. Maize growth stages were determined when at least one-half of the plants had reached a stage as determined by the leaf collar method and visual indicators of kernel development. Sunflower growth stages were delineated following the methods of Schneiter and Miller (1981).

Measurement Period	Day of Year	Growth Stage
---- Maize ----		
Period 1	198 - 199	Vegetative; Eight leaf collared (V8)
Period 2	210 - 211	Vegetative; Fourteenth leaf collared (V14)
Period 3	217 - 218	Reproductive; Silking (R1)
Period 4	233 - 234	Reproductive; Blister (R2)
Period 5	247	Reproductive; Dent (R5)
--- SUNFLOWER ---		
Period 1	197 - 199	Vegetative; Thirteen true leaves (V13)
Period 2	211 - 212	Reproductive; Floral head (R1)
Period 3	218 - 220	Reproductive; Inflorescence opening (R4)
Period 4	231 - 232	Reproductive; Head 90% in flower (R5.9)
Period 5	253	Reproductive; Bracts senescing (R8)
Rapid dry-down	238 - 240	Reproductive; R6

Soil moisture sensors

Soil moisture sensors were installed in five pots per treatment to monitor θ_v (cm^{-3} cm^{-3}) (Decagon 5TM sensors; Decagon Devices, Inc., Pullman, WA). In addition, we assessed the accuracy of the sensors in the substrate from near saturation to the permanent wilting point, as studies have demonstrated that errors are introduced in soil moisture readings if substrate-specific calibrations are not performed (Varble and Chávez, 2011). Hence, a substrate-specific

calibration was developed and applied over a measured volumetric water content of 0.20 – 0.58. This calibration curve (R^2 = 0.95) was then used to calculate θ_v in lieu of the generic manufacturer's calibration. While variability of soil, roots, and rocks in field conditions can result in inaccuracies of manufacturer calibrations, our material was thoroughly homogenized, and we were able to produce a precise and accurate calibration for the substrate.

Soil moisture treatments

Irrigation emitters (PPC Spray Stake, Netafilm Inc., Fresno, CA, USA) were placed in each pot, and the pots were sealed with Glad® Press 'n Seal to eliminate evaporation from the soil surface. Each pot had a 180° spray stake operating at a flow rate of 12 L h^{-1} (PPC Spray Stake, Netafilm Inc., Fresno, CA, USA). To prevent preferential flow of water, the soil moisture sensors were installed horizontally, mid-way between the plant and the pot sidewall. A wireless sensor network providing local set point control was used to manage irrigations (Lea-Cox et al., 2013). Briefly, the system consisted of data loggers (Decagon nR5-DC; Decagon Devices, Inc., Pullman, WA) for monitoring Decagon 5TM sensors and controlling 12V direct current solenoids. A software interface automated the wireless sensor network irrigation (Kohanbash et al., 2013). The system was programmed to monitor the soil moisture content of five replicates per species at 15-minute intervals, compile the measurements into an average value of θ_v, and irrigate with a pre-set amount of water when the average θ_v was below the target set point. This type of dynamic irrigation control permitted automated application of water to maintain a target θ_v in the face of variable environmental conditions and increased water consumption due to crop growth.

While there was some initial fluctuation in θ_v as irrigation regimes were being established, substrate moisture content was then kept at a daily average target θ_v of 0.40 for the

well-watered treatment and 0.24 for the water-stressed treatment (Fig 1). Seasonal daily treatment averages of θ_v were 0.39 ± 0.02 for well-watered maize, 0.23 ± 0.01 for water-stressed maize, 0.40 ± 0.03 for well-watered sunflower, and 0.24 ± 0.02 for water-stressed sunflower. Target stress levels were determined by lowering θ_v until water limitations induced strong mid-day leaf curling in maize and leaf wilting in sunflower. The target θ_v had to be raised slightly over the season in both treatments to support increased canopy biomass under elevated summer temperatures. To ensure adequate plant nutrition, Peters' Excel Cal-Mag (15-5-15) was applied at a strength of 200 ppm N via the irrigation lines (Kottkamp et al., 2010).

Environmental conditions and meteorological measurements

Supplemental lighting was provided for a period of 13 hours (6:00 – 19:00). Photosynthetic photon flux (PPF; µmol m^{-2} s^{-1}), air temperature (T_{air}; °C), and relative humidity (RH; %) were measured every minute using EHT RH/temperature sensors and AQO-S PAR photon flux sensors mounted at the top of the canopy (Decagon Devices, Pullman, WA) (Fig 1). Sensors were moved as the plants grew to maintain top-of-canopy location.

Greenhouse conditions were programmed to permit the maximum amount of light interception (i.e., shade cloth was only pulled during days where intense solar radiation and temperatures demanded additional cooling efforts). Daytime temperatures over the experimental period averaged 26.5 °C, but in some instances maximum daytime temperatures climbed higher despite continuous cooling. Supplemental humidity was provided to keep relative humidity around 50%, and the daytime vapor pressure deficit (VPD) averaged 1.8 kPa.

Gas exchange measurements

Two portable steady-state photosynthetic systems (Model Li-6400; LI-COR Inc., Lincoln, NE, USA) were used to measure gas exchange on expanded sunlit leaves near the top of

the canopy. Response curves of A_n versus the incident PPFD were conducted on five tracked plants per treatment during each measurement period. Only well-watered plants were measured at period five, as water stressed caused early leaf senescence in the stress treatment. Leaves were acclimated in the chamber with a target leaf temperature of 25 °C (sunflower) or 31 °C (maize), a controlled CO_2 concentration [CO_2] of 400 μmol mol^{-1} and a PPFD of 2000 μmol m^{-2} s^{-1} for several minutes. Humidity levels in the cuvette were initially set at 55%, corresponding to a vapor pressure deficit (VPD) of ≈ 2 kPa for maize and ≈ 1.5 kPa for sunflower. After several minutes of acclimation to these cuvette conditions, the [CO_2] of air entering the chamber was stabilized at 400 μmol mol^{-1} while PPFD was sequentially lowered (2000, 1500, 1200, 1000, 800, 600, 400, 200, 100, 50, 25 and 0 μmol m^{-2} s^{-1}). Between 1200 and 200 PPFD, each level was held for 12 minutes for sunflower and 8 minutes for maize. At 100 PAR and below, each PPFD level was held for 3-6 minutes. A full A/Q_p response curve took a minimum of 90 minutes for sunflower and 60 minutes for maize. Large swings in chamber humidity were minimized by manually adjusting the flow of air through a dessicant column. The reduced rates of g_s and plant transpiration under low light and as a function of leaf age and water stress resulted in decreases in cuvette humidity. Some spread in relative humidity is desirable when calculating the BB Index (Ball et al. 1988) so while we ensured that values did not climb too high, the incoming air was not humidified. The relative humidity for the well-watered treatment ranged from 40.4 - 66.6 %, averaging 52.9 ± 4.7 %, with a slightly smaller range in the water stressed treatment (40 – 56.7%; 51. 3 ± 3.65).

Leaf water potential and $\delta^{13}C$

Daytime leaf water potential (Ψ_L) was measured on the same leaf immediately after the completion of the light response curves with a pressure chamber (PMS Instrument Company;

Corvallis, Oregon). Prior to excision with a razor blade, leaves were wrapped in a plastic bag. Ten leaf tissue discs of known area were taken from the leaf with a cork borer, with care taken to avoid large veins. There were fewer observations for sunflower due to lack of data in the first measurement period. Discs for determination of $\delta\ ^{13}C$ were dried at 60 °C for ≥ 72 hours and then weighed for dry mass determination. The tissue was then placed in glass vials and powder ground with a steel ball-mill grinder. Two replicates per sample of Total N and C composition were determined via mass spectrometry. The N and C analyses were conducted using a Europa Scientific automated nitrogen carbon analyzer (ANCA/NT) with a Solid/Liquid Preparation Module (Dumas combustion sample preparation system) coupled to a Europa 20-20 Stable isotope analyzer.

Rapid dry-down of sunflower plants

A rapid three-day dry down was performed on a separate group of mature sunflower plants (n = 6) from DOY 238 to 240 when plants were at the R6 growth stage. All plants were well-watered up until the initiation of the rapid-dry down, but no additional water was added after the experiment was underway. The soil surface of each pot was sealed to prevent evaporation from the soil surface, and sunflower heads were bagged. Each plant was weighed during pre-dawn hours and at 20:00 to obtain estimates of nighttime and daytime transpiration rates (Adam CBK, Adam Equipment Inc., Bletchley Milton Keynes, UK). Daytime measurements of m and g_0 were obtained with A_n - PPFD curves in the same manner as noted above. To obtain measures of nighttime g_0, predawn measurements were made starting around 4:30 AM. Green safety headlamps were used to avoid stomatal opening. The chamber light level was set to 0 μmol m^{-2} s^{-1}, and the flow was set to 120 - 150 μmol s^{-1}. Prior to measuring gas exchange, measurements were made with an empty chamber to assess instrument error.

Estimates of g_s in the empty cuvette ranged from 0.0006 – 0.0027 mol m^{-2} s^{-1}, and were always less than 5% of the g_{0_night} values obtained. The conductance values provided by the LICOR-6400 are a total of both g_s and $g_{cuticular}$ in parallel. We did not take measurements of $g_{cuticular}$, so the values reported include both pathways. However, minimum nighttime g_s of sunflower species has been measured and found to be five times greater than $g_{cuticular}$ (Howard and Donovan 2007). Sample and reference infrared gas analyzer were matched prior to every measurement. Gas exchange readings were logged every 30 seconds, and were typically stable within 1-3 minutes. Pre-dawn Ψ_L was taken on a leaf immediately adjacent to the measurement leaf following gas exchange measurements.

Ancillary Field Measurements

To ensure that the physiology and growth parameters of greenhouse-grown plants were similar to field-grown plants, ancillary field measurements were made at the USDA-ARS LIRF field site. The same genotypes of maize and sunflower used in the greenhouse experiments were grown in the field under drip irrigation, with water applied to meet the full demands of evapotranspiration. A full description of the site and experimental design can be found in DeJonge et al. (2015). Field measurements were taken immediately following irrigation events. Light response curves were run on a sample of well-watered maize plants (n = 11) over a three-week period (DOY 205-226). A similar number of curves were run on sunflower plants at the V17-19 (DOY 206) and R4 (DOY 226) growth stages. However, a portion of the sunflower curves had to be discarded due to a faulty thermocouple on the LiCor 6400, leaving a smaller number of curves for comparison of the parameter values of field-grown versus greenhouse grown plants (n = 4).

Statistical Analyses

We were interested in comparing the results of two different methods of estimating the parameters of the BB model. In method one (M1), the slope (*m*) and intercept (g_0) were determined via linear least squares regression on each individual leaf using the REG procedure of SAS (SAS Institute, Cary, NC, USA). Each tracked plant was an experimental unit and treated as a replicate (n = 5) for each treatment. Only data collected via 200 and 1200 PAR, with a minimum settling time of 6-minutes per light level were used to determine *m*. The mean slope and intercept values for each treatment and and/or measurement period were then compared using repeated measures ANOVA in the MIXED procedure of SAS with measurement period and treatment as fixed effects, and plant as a random effect. Means were compared using Tukey's honestly significant difference test. Results were considered significant when $p < 0.05$. T-tests were used to compare differences between field-grown versus greenhouse-grown plants. A benefit of this method is that is accounts for the variance structure (i.e., the fact that data points collected on the same plant should be correlated).

A second method (M2) of determining the BB parameters is to run one regression on compiled leaf-level measurements (i.e., compiling all data by treatment). To compare the results of compiling treatment means from individual leaf measurements versus performing a regression on all data by treatment, an ANCOVA analysis with dummy variables was used to compare the regression lines of data compiled for each treatment, both in terms of the slope and intercept parameters. A drawback to this method is that standard statistical methods assume independent observations and using repeat observations per leaf or plant violates this assumption.

Repeated measures in the MIXED procedure of SAS was used to evaluate differences in $\delta\,^{13}C$,W_T, and C_i/C_a between periods and treatments. Regression analyses in the REG procedure of SAS were used to determine the association among BB parameters and Ψ_{Leaf} and θ_v. Where

relationships were weak or not clearly linear, the CORR procedure in SAS was used to evaluate Pearson product moment correlations and Spearman rank-order correlations.

Results

Maize

Mean well-watered values and seasonal variability

In well-watered maize, steady g_s readings typically occurred only 1 - 2 minutes after a 200 umol m^{-2} s^{-1} change in PPFD, indicating rapid stomatal adjustment. In addition, there was only a very small (i.e., <5%) reduction in the *m* estimate obtained by waiting six versus three minutes. In water-stressed maize, utilizing a 3-minute versus 6-minute settling time at each light level did not significantly change the values obtained for *m* or g_0.

The overall seasonal mean well-watered greenhouse values for the BB slope and intercept (obtained via linear regression on data where PAR $\geq$ 200) were $m = 4.53 \pm 0.65$ and $g_0 = 0.017 \pm 0.016$ mol m^{-2} s^{-1} (n = 25). Seasonal differences in the well-watered *m* values were significant only between measurement periods two and five (P = 0.0022), and there were no seasonal changes in the well-watered value of g_0 (Fig 2). However, if only data from lower g_s was utilized (i.e., <0.225 mol m^{-2} s^{-1}), there were no significant differences between any measurement periods for *m* or g_0 in well-watered maize, and the mean value of *m* dropped slightly to 4.23 ± 0.52.

If a single regression is run on all well-watered data (i.e., instead of compiled means) the result is $y = 4.94x + 0.009$, with an R^2 of 0.91. Hence, utilizing method 1 versus method 2 results in an approximately 10% estimate difference of *m* and a 50% difference in g_0.

Well-watered versus water-stressed values

Water-stress significantly reduced both *m* and g_0. Comparison of compiled treatment means from measurement periods two through four shows that water stress reduced *m* from a

well-watered value of 4.76 ± 0.62 to a value of 3.63 ± 0.41 (P = <0.0024) (Fig 3). Water-stress also reduced g_0 from a well-watered value of 0.0169 ± 0.0166 to 0.0008 ± 0.0006, a value not significantly different than zero. Utilizing an ANCOVA analysis on compiled leaf-level measurements by treatment also results in the conclusion that both *m* and g_0 are reduced under water stress (P = <0.0001).

Estimates of g_0 via regression on low versus high PPFD

Data from periods two through four were used to compare the values of g_0 obtained via regression on data collected at low light levels (i.e., ≤ 100 PAR; $g_{0\_lowPPFD}$) versus the values obtained via the same linear regression used to determined *m* (i.e., 200 – 1200 PAR; $g_{0\_highPPFD}$). Well-watered g_0 values were slightly higher when determined via regression on low light (0.0399 ± 0.0130) versus high light levels (0.0255 ± 0.0154) (p = 0.009). Differences in g_0 values between methods were also different in the water-stressed treatment ($g_{0\_lowPPFD=}$ 0.00774 ± 0.00311 versus $g_{0\_highPPFD}$ = 0.000793 ± 0.00597) (p = 0.0012), although these values are essentially zero, as they are within the range of instrument error.

Relationship of the BB parameters with Ψ_L and θ_v

There was no significant relationship between Ψ_L and *m*, Ψ_L and $g_{0\_reg,}$ or θ_v and g_{0_reg} in maize. The slope did show a weak relationship with θ_v (y = 0.0423 (θ_v) + 2.79; R^2 = 0.32). Removal of three points from the last measurement period markedly improves the regression to an R^2 of 0.51 (Figure 4).

Changes in $\delta^{13}C$, Ci/Ca, and W_T seasonally and under water stress

There were no significant differences in W_T over the season for the well-watered treatment, while W_T increased in a sustained fashion under water stress after measurement period

one (Fig 5; panel a). The ratio of C_i/C_a stayed relatively constant over the season in well-watered maize, dropping only at the final measurement period, whereas the ratio fell and stayed depressed after water-stress was applied (Fig 5; panel b). Patterns in the BB slope generally followed the changes in C_i/C_a and were inversely related to changes in W_T (Figure 5; panel c). Carbon isotope $\delta^{13}C$ values changed seasonally and as a function of treatment, with a significant interaction between the two main effects, but the patterns were not consistent (Fig 5; panel d).

Greenhouse versus Field values

Comparison of values from well-watered greenhouse plants to those obtained in irrigated field plants showed interesting similarities and differences. The values of *m* and g_0 from field-grown maize showed no significant differences between the three measurement times, similar to the steady seasonal values found in greenhouse plants. However, even after normalizing to ensure that data from the field was constrained to the same range as greenhouse data, the mean value of *m* obtained in the field ($m = 3.72 \pm 0.63$) was lower than the mean greenhouse value obtained during similar growth stages (i.e., 4.76 ± 0.62) ($p = <0.0001$). The value of g_{0_reg} for field grown maize ($g_{0\_reg} = 0.022 \pm 0.17$, $n = 11$) was not significantly different than the value obtained in the greenhouse.

Sunflower

Well-watered sunflower plants had exceptionally high values of g_s that frequently stayed elevated despite long-settling times, resulting in very large values for the g_{0_reg}. Sample g_s data is shown for a representative plant in Figure 6 (panel a) as a function of minute and light level to highlight the difficulty of defining 'steady-state', as g_s appears to stabilize for several minutes and then oscillates (i.e., see further data for 600 and 400 PAR). Comparison of the value of *m* and g_0 after 5, 10, 15, and 20-minute settling times is shown in Fig 6 (panel b) to demonstrate

that the parameters of the BB model were typically not impacted by settling times longer than 5 - 6 minutes. Data from periods 2 - 4 was used to compare the values of the slope and intercept obtained after a 2, 4, 6, or 8-minute settling time. In well-watered sunflower, estimates of *m* and g_0 changed up until 6 minutes, but there were no differences between utilizing a 6-minute versus 8-minute settling time (P = 0.99). In water-stressed sunflower, there were no significant differences in the parameter estimates obtained between 2, 4, 6, or 8-minute settling times.

Mean well-watered values and seasonal variability

In well-watered greenhouse sunflower the overall seasonal mean values for *m* and g_{0_reg} were *m* = 9.27 ± 3.78 and g_{0_reg} = 0.354 ± 0.226 mol m^{-2} s^{-1} (n = 25). Although the mean slope value dropped to 6.01 ± 3.76 at period 5, we could detect no significant difference in well-watered *m* between measurement periods (p = 0.14) likely due to the high amount of variability between plants. Visual examination of the data (Fig 7) highlights that it is the intercept that appears to get progressively lower over the season. However, the high degree of variability prevented the detection of seasonal differences in g_0, although some seasonal differences were significantly different at P = 0.1 (i.e., P = 0.0550 for periods 1 versus 4, and P = 0.08 for period 1 vs. 5). If a single regression on all well-watered data was utilized instead of a compilation of means from individual leaf regressions (i.e., M2) the resulting equation is y = 14.36x + 0.170 (R^2 = 0.63). In the case of sunflower, utilizing M1 versus M2 to estimate the BB parameters results in a 35% difference in estimates of *m* and a 25% difference in the estimates of g_{0_reg}.

Well-watered versus water-stressed values

Comparison of compiled treatment means from measurement periods two through four (Fig 8) shows that the *m* values for well-watered sunflower (10.16 ± 3.81) were not significantly different than water-stressed values (*m* = 8.94 ± 2.04) (P = 0.13). Analysis via ANCOVA also

showed no evidence that the slopes differed between treatments (P = 0.21). However the mean intercept was strongly impacted by water stress (P = <0.001). The mean well-watered value of g_{0_reg} was 0.340 ± 0.237, whereas this value fell to 0.018 ± 0.057 under water stress. There were no seasonal differences in *m* or g_{0_reg} in plants under water stress.

A single regression on the same data compiled by treatment (i.e., statistical method 2) results in a slope of 12.14 and intercept of 0.263 (R^2 = 0.59) for well-watered sunflower and slope and intercept of 10.76 and -0.023 for water-stressed sunflower, where the intercept is not significantly different than zero (R^2 = 0.84).

g_0 estimates via regression on low versus high PPFD

There were no differences in the estimates of g_0 obtained via linear regression on high PPFD (i.e., > 200 µmol m^{-2} s^{-1}) versus low light levels (i.e., >100 µmol m^{-2} s^{-1}) for well-watered sunflower (p = 0.84) or water-stressed sunflower (P = 0.0548).

g_o as a function of maximum daytime conductance

Daytime maximum g_s at 1000 PAR ($g_{s\_1000PAR}$) declined seasonally in a near-linear fashion (Fig 9; a). We compared $g_{s\_1000PAR}$ to the daytime estimate of g_0 obtained via linear regression. Daytime g_{0_reg} values were correlated to the maximum $g_{s\_1000PAR}$, although the relationship was not significant under water stress (Fig 9; panel b). Combination of seasonal data across treatments into one regression resulted in $g_0 = 0.547g_s - 0.105$ (R^2 = 0.60). The relationship between A_n and g_s was also highly linear under water stress (R^2 = 0.88, but poorer under well-watered conditions (R^2 = 0.65) (data not shown).

Relationship of the BB parameters with Ψ_L and θ_v

We found no significant relationships between the BB slope and Ψ_{Leaf} or θ_v in sunflower. However, the intercept showed a positive correlation with θ_v (P = <0.0001) and a weak negative correlation with Ψ_{Leaf} (P = <0.0001). The Spearman correlation coefficient for $g_0 - \Psi_{Leaf}$ was r = 0.74 while the Pearson correlation coefficient was r = 0.63. The Spearman correlation coefficient for $g_0 - \theta_v$ was r = 0.63, whereas the Pearson correlation coefficient was r = 0.52 (Fig 10). The seasonal trend towards declines in g_{0_day} values even under well-watered conditions may add to the scatter observed at higher Ψ_{Leaf}, and clouds clear interpretation of these relationships.

Changes in $\delta^{13}C$, Ci/Ca, and W_T seasonally and under water stress

W_T did not change between measurement periods in the well-watered treatment, but W_T increased after water stress was applied (P-values all <0.0001) (Fig 11; panel a). The W_T values in well-watered sunflower (i.e., 2 mmol mol^{-1}) were at the lower range of the W_T reported for herbaceous C3 plants (Lambers 2008), but rose to the upper range (i.e., 5 mmol mol^{-1} under water stress). The ratio of C_i/C_a stayed relatively constant over the season in well-watered sunflower, dropping only slightly towards the end of the season (Fig 11; panel b), whereas the ratio fell and stayed depressed after water-stress was applied, rising slightly at measurement period 4 (Fig 11; panel b). Carbon isotope $\delta^{13}C$ values changed significantly seasonally and as a function of treatment (Fig 11; panel d). Leaf δ^{13} C initially increased under water stress and then converged with well-watered values at period four. The lack of data at the first measurement period is unfortunate, but the fact that treatment means had not separated by the second measurement period highlights the time-integrated nature of the $\delta^{13}C$ signature. Patterns in g_{0_reg} generally followed the changes in C_i/C_a and showed a loose inverse relation to changes in W_T.

Greenhouse versus Field values

Values of the BB slope obtained for well-watered sunflower in the field were comparable to greenhouse values, but showed similarly high variability, with a mean slope of 8.59 ± 3.68. The estimate for the intercept was extremely high at 0.585 ± 0.264 µmol m^{-2} s^{-1}. Conductance values were large, and in some cases showed virtually no detectable change despite long settling times (i.e., > 10 minutes per light level), and additional settling time resulted in only slight reductions in the intercept rather than the slope (Figure 12). Correlation coefficients for regressions run on individual leaves were all > R^2 = 0.90, but a single regression on combined data instead of individual leaves resulted in R^2= 0.66 (y = 9.32x + 0.560) (data not shown).

Rapid-dry down of Sunflower

Plants in the rapid-dry down were nearly at physiological maturity, with lower values of g_s and A_n than plants in pre or early reproductive stages (Cechin and de Fátima Fumis, 2004). Despite watering the plants to pot capacity the evening prior to the experiment, there were already signs of mild water stress occurring mid-afternoon on day one. The large amount of plant biomass coupled with limited soil volume resulted in the onset of water stress. After three days of withholding water, the leaves of three of the six plants in the rapid-dry down experiment were no longer measurable due to severe desiccation, and by day four zero plants were viable for measurement.

On day one, the mean value for the BB slope and intercept was *m* = 9.93 ± 3.16 and g_0 = 0.105 ± 0.072 mol m^{-2} s^{-1} (Figure 13). A single regression on all data points for day one resulted in y = 11.94x + 0.042; R^2 = 0.70. By day two, mean slope and intercept values dropped to *m* = 8.02 ± 2.71 and g_0 = 0.050 mol m^{-2} s^{-1}. Simple linear regression on combined data from day two resulted in y = 10.79x - 0.013 where the intercept was not significantly different from zero (Fig

12; R^2 = 0.89). Only three plants were viable for measurement on day three, with a mean slope of 7.20 ± 1.30 and a g_{0_reg} value of 0.003 ± 0.024 mol m^{-2} s^{-1}, which was not significantly different from zero. Combining data into one regression for day three resulted in y = 6.68 + 0.013 (R^2 = 0.98). The close matching of slope and intercept values between statistical M1 and M2 on day three illustrates that when the data is not highly variable the two methods can converge on comparable values.

Despite the downward trend in parameter values of the BB model with progressive water limitation, ANOVA analysis indicated that the slopes and intercepts were not significantly different between measurement days at the 5% level (P = 0.08).

Measured nighttime g_0 values decreased with water stress (Figure 14; a), and nighttime g_0 values were different at Day 1 versus Day 3 (p = 0.0073). Daytime g_0 values showed a consistent decrease as a function of decreasing Ψ_{Leaf} (Fig 14; b). A similar decrease in g_0 (fit via regression) with predawn Ψ_{Leaf}, was also reported by Misson et al. (2004), who modeled this relationship as:

$$g'_0 = \frac{g_x}{1+\left(\frac{\Psi_p}{\Psi_0}\right)^n} \qquad (2)$$

where g_0, Ψ_0, and n are fitted parameters calculated via a nonlinear-algorithm. This function fit our daytime g_0 observations reasonably well (g_x = 0.203, Ψ_o = 0.89 and n = 5.91), but the relationship between nighttime measurements of g_0 and predawn Ψ_{Leaf} was linear (Fig 14; a).

Average nighttime g_0 values on day one of the dry down were only 60% of the daytime g_{0_reg} values calculated via linear regression (i.e., 0.081 ± 0.024 at night versus 0.126 ± 0.056 during the day). However, on day two, predawn g_0 estimates (0.056 ± 0.016 mol m^{-2} s^{-1}) were higher than daytime estimates (0.022 ± .021 mol m^{-2} s^{-1}). By day three, g_{0_reg} estimates were not

significantly different than zero (0.011 ± 0.01 mol m^{-2} s^{-1}) and predawn estimates were .030 ± 0.009 mol m^{-2} s^{-1}, similar to the values of $g_{cuticular}$ reported for sunflower (Donovan and Howard 2007). Empty cuvette readings taken each day averaged .002 ± 0.001 mol m^{-2} s^{-1}.

Gravimetric measures indicated that nighttime transpirational losses were a significant portion of total transpiration. Water loss via transpiration on the first night of the experiment averaged 0.59 ± 0.14 kg $plant^{-1}$, whereas daytime values averaged 2.75 ± 0.44 kg $plant^{-1}$. Water loss dropped slightly during the second night to 0.51 ± 0.12 kg $plant^{-1}$,with daytime averages of 2.41 ± 0.20 kg $plant^{-1}$. By the third night, nighttime transpiration dropped to an average of 0.41 ± 0.17 kg $plant^{-1}$, but comparisons with daytime transpiration was not possible as several of the plants were fully senesced with crumbling leaves.

Discussion

Minimum time required to obtain parameter estimates

One of the impediments to collecting species-specific estimates of *m* and g_0 is the time investment required to obtain the quantity and quality of data needed for least squares estimates of the parameters. The time required is dependent on how quickly stomata equilibrate to changes in environmental variables such as PPFD. Stomatal response times are dependent on the environmental variable being altered, the direction of change, and on the magnitude change of g_s (Jones, 2013; Woods and Turner, 1971). Additionally, stomatal sensitivities vary drastically between families and species (Brodribb et al., 2009). Stomatal response times to changes in light have been found to vary from 8-minutes ((Xu and Baldocchi, 2003) to 36-minutes (Woods and Turner, 1971) in tree species, and stomatal sensitivities and kinetics vary as a function of plant functional type and evolutionary history (Brodribb et al., 2009).

The stomatal responses to step changes in light we observed were consistent with the response times to light reported for other field crops. For example, Grantz and Zeiger (1986) reported a two-minute halftime response to a 350 µmol m^{-2} s^{-1} decrease in PAR in sugarcane, a C4 grass, and a nine-minute halftime response in soybean, a C3 crop. We found that near steady-state g_s readings in maize typically occurred only one to two minutes after a 200 µmol m^{-2} s^{-1} change in light. In well-watered maize, there was only a 5% difference in the parameter estimates obtained with a three-minute versus six minute settling time. Water stress has been shown to decrease the time required for closure in response to variations in light in some species, conserving water during periods of limited soil water and influencing seasonal patterns of water use and carbon gain (Knapp and Smith, 1990). Concurrent with these previous findings, stomatal adjustments to a change in light occurred more rapidly in maize under water stress, and less than three-minutes per level was needed before semi-steady state conditions were reached. In well-watered sunflower, a six-minute settling time was needed for well-watered plants, but the necessary settling time was reduced to two-minutes under water stress. It is important to note that water-stressed plants were operating within a smaller range of g_s than well-watered plants, and hence the absolute magnitude change in g_s in response to a change in light was smaller.

Our results indicate that estimates of m and g_0 can be collected in less than twenty minutes in maize by utilizing step changes in PPFD (i.e., six levels in this study). The rapid stomatal adjustments in maize are likely explained by the morphology and mechanics of dumb-bell shaped stomata of grasses, which maximize the ability of stomata to track changes in environmental conditions compared to non-grass species (Franks and Farquhar, 2007; Hetherington and Woodward, 2003). While sunflower displays a high amount of plant-to-plant variability in g_s values, estimates of m and g_0 can be collected in thirty-five to forty minutes in

well-watered sunflower by utilizing variations in PPFD, and shorter settling times occur under water stress, further reducing the time investment.

Variation in parameter estimates between statistical methods

The statistical method used to estimate m and g_{0_day} substantially impacted the parameter estimates in sunflower. If seasonal well-watered data was compiled into a single regression (method 2) instead of compiling means for regressions on individual leaves (method 1), the estimate of m increased by 30% and the estimate of g_0 decreased by 25%. This highlights the fact that methodological differences in how the BB parameters are determined can result in different values for the estimates. When the data from individual leaves or plants shows little spread, as in the case of maize, the differences between (i) performing separate regressions for each leaf or plant and then compiling these individual values into a mean versus (ii) regression on combined data can be nominal (Bunce, 1998). However, in the case of a plant with high variability like sunflower, the two analyses result in different values.

Values of the BB model parameters

The well-watered parameter values we obtained for maize (m = 4.53 ± 0.65 and g_{0_reg} = 0.017 ± 0.016 mol m^{-2} s^{-1}) are similar to the values of m = 4.0 and g_{0_reg} = 0.04 mol m^{-2} s^{-1} utilized in the literature to parameterize the physiology of C4 crops such as field maize (Houborg et al., 2013; Sellers et al., 1996). Version 4.0 of the Community Land Model (Oleson et al., 2010) utilizes a value of m = 5 for C4 grass and g_{0_reg} = 0.02 mol m^{-2} s^{-1}, and our data is in close agreement with these values. The mean value we obtained for m was ≈ 30% higher than the values of 3.23 and 3.06 reported by Ball (1988) and Collatz et al. (1992) for maize. Conversely, the mean g_{0_reg} value was lower than the values of 0.06 mol m^{-2} s^{-1} and 0.08 mol m^{-2} s^{-1} reported in the same studies (Ball, 1988; Collatz et al., 1992). Well-watered g_0 values were approximately

30% higher when determined via regression on low light versus high light, consistent with the observed non-linear response of g_s to light as $A_n \rightarrow 0$ (Ball 1988; Leuning 1995; Barnard and Bauerle 2013). The magnitude of g_0 values in maize are surprising, given the importance of the C4 pathway as an adaptive mechanism to survival in hot and dry climates, but night-time water loss has been documented in other C4 species from warm desert climates (i.e., approx. 0.02 – 0.05 mol m^{-2} s^{-1}), similar to the magnitude of the values we obtained.

The rapid kinetic response of stomata to changes in light make it feasible to measure $g_{0\_lowPPFD}$ with only a small time investment, which would likely improve daytime estimate of transpiration (Barnard and Bauerle 2013). However, it is important to highlight that we did not measure true 'nightime' g_s values in maize. Collatz et al. (1992) reported that the minimum value of g_0 measured in the dark in maize was smaller than the fitted value of g_0, and suggested that the minimum value of g_s may be dependent to some extent on light. If nighttime g_0 values are indeed substantially lower than daytime values, this could result in an overestimation of transpiration at night unless some sort of a 'day-night switch' is incorporated to obtain a lower minimum value of g_s at night (Collatz et al., 1992). In contrast, Barnard and Bauerle (2013) found that nighttime g_0 values were higher than the estimates obtained from least squares regression, and reported that model estimates of total transpiration were more accurate when g_{0_night} values were used in lieu of g_{0_reg} values. Additional investigation is needed to determine whether there are disparities between (*i*) the daytime estimates of g_0 collected via linear regression, (*ii*) estimates of g_0 collected during the day when PPFD = 0, and (*iii*) the measurements collected at night.

While our measurements only reflect values for one modern genotype of maize, the results raise the question of whether over three decades of plant breeding and selection for higher productivity may have resulted in increases in the value of *m*. In areas with regular rainfall or

supplemental irrigation during the growing season, crop genotypes with lower W_T and higher *m* values frequently have higher yields of biomass and grain. For example, high W_T in cereals is associated with conservative water use, but also results in conservative growth even in the absence of water stress (Condon et al., 2004). Hence in crop genotypes bred for yield under irrigated or high moisture environments, the slope of the BB model could be expected to increase in a slow yet methodical fashion with selection for higher productivity.

However, the lower *m* values measured in field-grown maize prevent the simple conclusion that slope values may have increased due to breeding. The differences in *m* between greenhouse and field-grown maize suggests either that there are artifacts associated with growing the plants in the greenhouse, or that irrigated field plants experienced some degree of water stress. Some studies have found differences in the degree of stomatal adaptation and response to decreasing leaf or soil water potential for plants grown in controlled environments versus the field (Jones, 2013). However, field-grown plants such as cotton typically show *lower* stomatal sensitivity to water deficits than greenhouse grown plants (Jordan and Ritchie, 1971). One possibility for the higher greenhouse values is that greenhouse plants were irrigated at multiple times throughout the day, perhaps dampening the degree of diurnal stomatal response that occurred in the field as water in the vicinity of the root zone is depleted. However, the greenhouse plants also had a constricted root zone in comparison to field grown plants. Another possibility is that despite cuvette-level control of VPD, field-grown plants were experiencing higher VPDs than greenhouse plants, eliciting reductions in g_s.

Sunflower plants displayed a high degree of variability in parameter values. The seasonal well-watered greenhouse *m* value we obtained ($m = 8.84 \pm 3.77$) was substantially higher than the slope of $m = 2.30$ published by Leuning (1995), but lower than the values of $m = 14.35$ and

m = 20.61 reported elsewhere (Gutschick and Simonneau, 2002). The mean value for field-grown sunflower was nearly identical to the mean greenhouse value, (8.59 ± 3.68) but there was similarly large plant-to-plant variability. Daytime maximum g_s value of approximately 1.5 mol m^{-2} s^{-1} have been reported for greenhouse-grown sunflower (Howard and Donovan, 2007), corroborating the exceptionally high g_s we observed in domesticated sunflower. The seasonal mean well-watered greenhouse g_{0_reg} value (g_0 = 0.389 ± 0.228 umol m^{-2} s^{-1}) was higher than the value found by Leuning (1995), but Gutschick and Simonneau (2002) reported similarly high g_{0_reg} values in field grown sunflower (i.e., g_0 = 0.434 and 0.174 for two field seasons). True 'nighttime' g_s values of nearly 0.4 mol m^{-2} s^{-1} have been measured in greenhouse-grown sunflower (Howard and Donovan, 2007). While our g_{0_night} values during the rapid dry-dawn were substantially lower (i.e., 0.081 ± 0.024 at the well-watered baseline), these measurements were made when plants were late in the reproductive stage. Howard and Donovan (2007) found a significant effect of plant reproductive stage on g_{0_night}, where pre-reproductive plants had much higher g_{0_night} than reproductive plants. Snyder et al.(2003) reported similar g_{0_night} in sunflower of measured late in the season under water limitations (i.e., approx. 0.100 mol m^{-2} s^{-1}). Even at the late growth stages in sunflower, nighttime transpirational losses averaged >20% of daytime transpiration, highlighting the importance of quantifying this 'residual' conductance when modeling plant water use.

Comparisons of the g_0 values obtained at night versus daytime g_{0_reg} estimates were varied. On day one, where water stress was minimal, g_{0_night} values were lower than g_{0_reg} estimates, which is the opposite of the pattern observed by Barnard and Bauerle (2013). On day two, where water stress was clearly evident, the pattern was reversed, and predawn g_0 estimates were higher than daytime estimates. This may have been due to the progression of water stress in

the intervening hours. However, additional studies are needed to probe the differences between nighttime and daytime estimates of g_0.

Seasonal alteration of values

While not many studies exist, the literature findings regarding seasonal variations in *m* and g*0* are inconsistent, and we know of only a few studies that have explicitly examined seasonal changes in the BB parameters independently of water stress responses. Misson et al., (2004) reported a substantial seasonal variation in the value of *m (*i.e., over a 3-fold difference), but water stress also increased seasonally. In contrast, Xu and Baldocchi (2003) found that the seasonal value of *m* in oak was relatively consistent, even under substantial water stress. Ono et al. (2013) reported higher values of *m* in the early and late portions of the growing seasons of rice, and Lai et al. (2000) argued that incorporation of seasonal changes in *m* may be necessary to accurately model carbon uptake in forest canopies. Barnard and Bauerle (2013) found no seasonal evidence of a seasonal change in g_0 in several tree species, whereas Howard and Donovan (2007) found that g_{0_night} varied across plant reproductive stages in sunflower. These studies highlight the disparities in the reports surrounding seasonal variability in *m* and g_0.

We found no significant seasonal differences in either of the BB model parameters in well-watered greenhouse-grown and field-grown maize or sunflower, lending support to the use of a single value of *m* and g_0 for modeling g_s across the growing season in these crops. While the data for both crops suggests that *m* may need to be adjusted downward towards the very end of the season during late reproduction, more replication is necessary to verify this. In sunflower, the high degree of variability in the data likely prevented the detection of seasonal differences in g_{0_reg}. While some seasonal differences in g_{0_reg} were significantly different at P = 0.1, further

studies with more replication are needed to verify whether or not g_0 values should be seasonally downscaled.

Daytime rates of g_s in sunflower declined over the season in a near-linear fashion, a pattern also reported by others for sunflower (Cechin and de Fátima Fumis, 2004). We found g_{0_reg} estimates to be highly correlated with daytime g_s, which provides a possible method of downscaling well-watered g_{0_reg} values. While we know of no studies reporting a correlation between the Ball-Berry g_{0_reg} parameter and daytime g_s values, Snyder et al. (2003) found night-time g_s to be correlated with daytime g_s in species with a range of life histories and native habitats. Correlations between nightime and daytime g_s have also been reported in conifers (Jordan et al., 2005) and in several species of oak (Cavender-Bares et al., 2007). This again highlights the need to investigate the potential linkages between nighttime versus daytime values of g_0.

Responses to water stress

The extent to which *m* changes under water stress is still debated (Baldocchi, 1997; Xu and Baldocchi, 2003). The A_n - g_s relationship can be altered under water stress (Brodribb, 1996; Condon et al., 2002; Damour et al., 2010; Katul et al., 2003), but the thresholds of response and rate of decline of *m* under drought shows variability among species and plant functional types (Zhou et al., 2013). While numerous proposals have been made to modify the well-watered value of *m* by incorporating empirical functions based on Ψ_{Leaf}, Ψ_{Soil}, or θ_v (Baldocchi, 1997; Damour et al., 2010; Sala and Tenhunen, 1996; Tenhunen et al., 1990; Van Wijk et al., 2000; Wang and Leuning, 1998), only a handful of studies have physically examined changes in *m* under water stress, with some reporting a decline in *m* under water stress (Heroult et al., 2013) whereas others have found no response (Gimeno et al., 2015; Xu and Baldocchi, 2003).

We found a distinct response of *m* to water stress in maize, with parameter declines of nearly 25% with reductions in available soil water. Changes in *m* were correlated with declines in θ_v, confirming that this is a valid scaling method in maize. Leaf level W_T increased significantly under water stress and inversely mirrored the seasonal trends in *m*, whereas C_i/C_a fell after water stress was imposed (Ball 1988). However, while $\delta^{13}C$ values initially separated between treatments, with an initial increase in $\delta^{13}C$ values under water stress, over time the $\delta^{13}C$ values of water-stressed plants dropped below the values of well-watered plants. One possible explanation for this is that water stress can lead to pronounced decreases in mesophyll conductance ((Monti et al., 2006; Seibt et al., 2008). While $\delta^{13}C$ is often a good proxy for W_T, under conditions where g_s and mesophyll conductance are not strongly correlated the relationship between d13C and W_T may break down (Lambers et al., 2008). In contrast to maize, we could detect no significant decline in *m* due to water stress in sunflower, although mean values were slightly lower in the stressed treatment. Values also decreased during the rapid-dry down, but trends were not significant. Values of W_T and $\delta^{13}C$ increased under water stress, whereas C_i/C_a declined, suggesting that gains in water use efficiency were occurring despite a failure to detect significant declines in *m.*

Maize g_{0_reg} values were also reduced under water stress to a value not significantly different than zero. In sunflower, the intercept was strongly impacted by water stress, declining to values near zero. These results suggest that residual conductance can be controlled in both of these crops, and that model estimates of g_{0_reg} should be reduced to near zero under water stress. Daytime g_{0_reg} values in sunflower showed a consistent decrease as a function of decreasing $\Psi_{Leaf.}$, although compilation of seasonal data may obscure seasonal trends in the shape of the response (i.e., g_{0_reg} values appear to change both seasonally and under water stress). A similar

decrease in g_{0_reg} with predawn Ψ_{Leaf}, was reported by Misson et al. (2004) in ponderosa pine. Measured nighttime g_0 values also decreased with decreasing Ψ_{Leaf} , although the shape of the relationship varied from the daytime measurements. Our findings are in contrast to those of Barnard and Bauerle (2013), who found no response of g_0 to water stress in trees, but in agreement with other studies that have found a distinct response of the g_0 parameter to water stress (Cavender-Bares et al., 2007; Howard and Donovan, 2007; Zeppel et al., 2012).

Conclusions

Accurate estimates of the *m* and g_0 parameters of the BB g_s model are important for modeling transpiration, but often require substantial time investments. Only a few studies have measured parameter values in field crops -- even less attention has been given to measuring parameter variation seasonally or under water stress, and results from limited studies are conflicting. We found that rapid stomatal adjustments in maize permitted robust estimates of the BB parameters to be obtained in less than twenty minutes per plant, whereas ≈ forty minutes per plant was needed in sunflower. Lower rates of g_s under water stress reduced the absolute change in the g_s response to a change in PPFD, further lowering the time needed to obtain parameter values. However, the statistical method used to estimate *m* and g0 substantially impacted the parameter estimates in both crops. We found no evidence of a seasonal shift in *m* or g_0 in well-watered maize, supporting the use of a single value for modeling across the season. Parameter values were similar to those currently utilized in CLMs. Well-watered sunflower showed no significant seasonal change in *m* or g_0, but more replication may be necessary to detect changes due to the high variability in the data. Values of *m* in well-watered sunflower varied substantially from the values reported elsewhere for sunflower, but were similar to the generic value used for C3 plants in CLMs. g_0 values in well-watered sunflower were extremely large, concurrent with

recent studies that have found substantial residual g_s in multiple species and plant functional types (e.g., Caird et al., 2007; Cavender-Bares et al., 2007; Howard and Donovan, 2007; Ogle et al., 2012; Snyder et al., 2003). Nighttime gravimetric measurements in sunflower confirmed that transpirational losses when light and $A_n \leq 0$ averaged over 20% of daytime transpiration, highlighting the importance of quantifying this 'residual' conductance when modeling plant water use. Our results suggest that species-specific characterization of g_0 may be needed to accurately predict water fluxes in crop canopies.

Water stress decreased *m* in maize, and was significantly correlated with decreases in θ_v. Sunflower data showed a high degree of plant-to-plant variability, and while *m* showed a trend towards decline under both long-term and rapidly induced water stress, results were not significant. The g_0 parameter decreased under water stress for both species. Reductions in g_0 were dramatic in water-stressed sunflower, and declines were correlated with decreases in Ψ_{Leaf}. While changes in nighttime conductance due to water stress have been documented in various species, a significant downscaling of the BB g_0 parameter due to water stress is rarely reported, but may improve transpiration estimates under water stress. Daytime g_{0_reg} values were highly correlated to the maximum daytime $g_{s\_1000PAR}$, providing a potential means of downscaling g_0. Our results corroborate the need for downscaling of the *m* and g_0 in maize under conditions of limited water, whereas in sunflower, the g_0 parameter should be reduced under water stress.

Figures

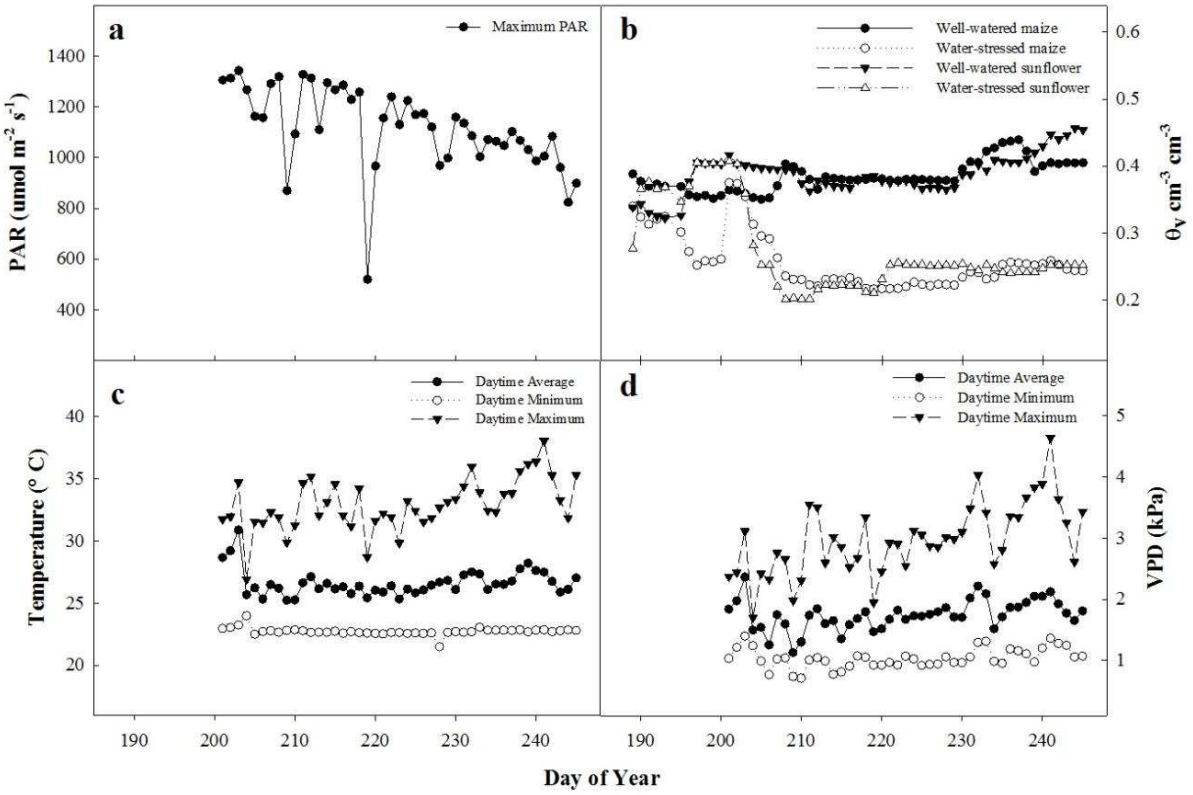

Figure 1. Seasonal variation in daily daytime maximum photosynthetically active radiation (PAR) (a), average daily soil volumetric water content (θ_v) (b), daytime minimum, maximum, and average air temperatures (c), and daytime average, minimum, and maximum vapor pressure deficit (VPD) (d). Daytime values were calculated for the period between sunrise and sunset.

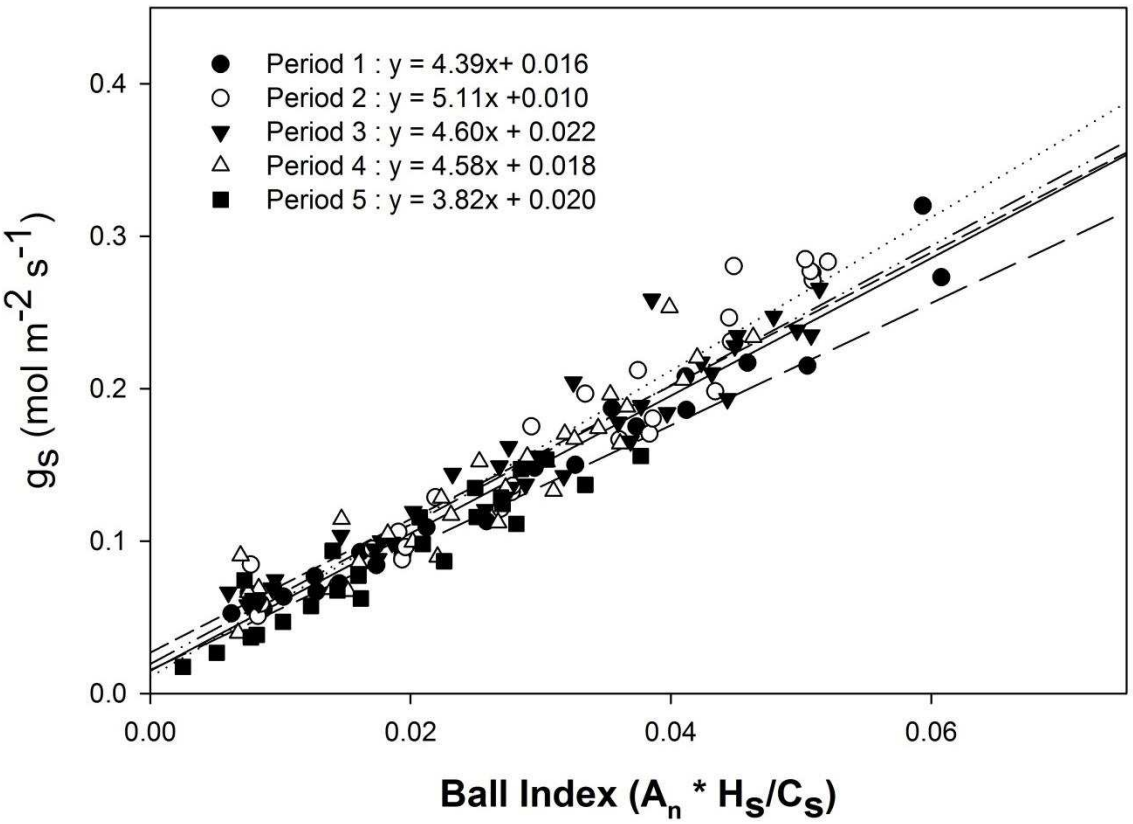

Figure 2. Relationship of stomatal conductance (g_s) with the product of net CO_2 assimilation (An, µmol m-2 s-1) and fractional relative humidity at the leaf surface (Hs, unitless) divided by the CO2 concentration at the leaf surface (Cs) for fully expanded sunlit leaves of well-watered greenhouse maize. Points represent individual leaf measurements. Data are only included for which PPFD $\geq$ 200 µmol m^{-2} s^{-1}. Regression lines represent the treatment means (n = 4-5) of linear functions fitted to data from individual leaves. Differences in the slope are only significant between periods 2 and 5. If only data from lower g_s is compared (i.e., <0.225 mol m^{-2} s^{-1}), there are no significant differences in the slope or intercept between measurement periods.

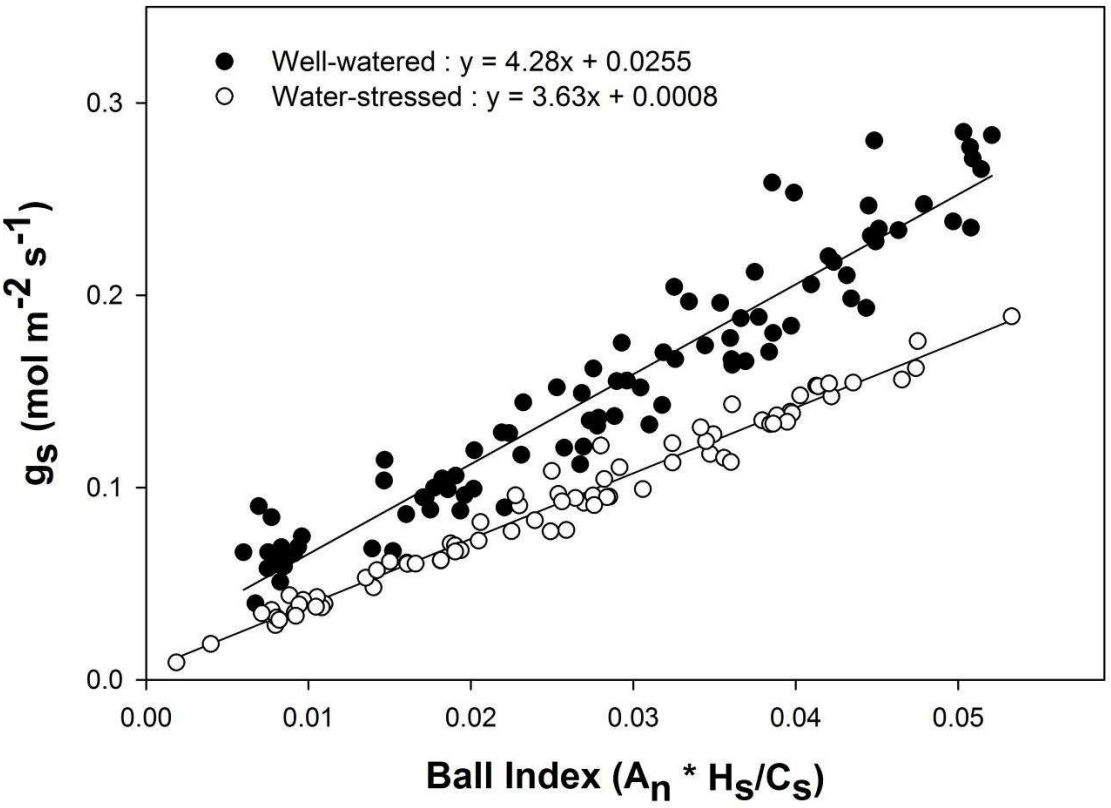

Figure 3. Relationship of stomatal conductance (g_s) with the product of net CO_2 assimilation (A_n, µmol m^{-2} s^{-1}) and the fraction of relative humidity at the leaf surface (H_s, unitless) divided by the concentration of CO_2 at the leaf surface (C_s) for fully expanded sunlit leaves of well-watered and water-stressed greenhouse maize for measurement periods 2 – 4. Regression lines represent the treatment means of linear functions fitted to data at high light levels (200 – 1200 umol m-2 s-1) from individual leaves. A t-test of the means of the slopes and intercepts of individual leaves indicates a significant influence of treatment at P = 0.05.

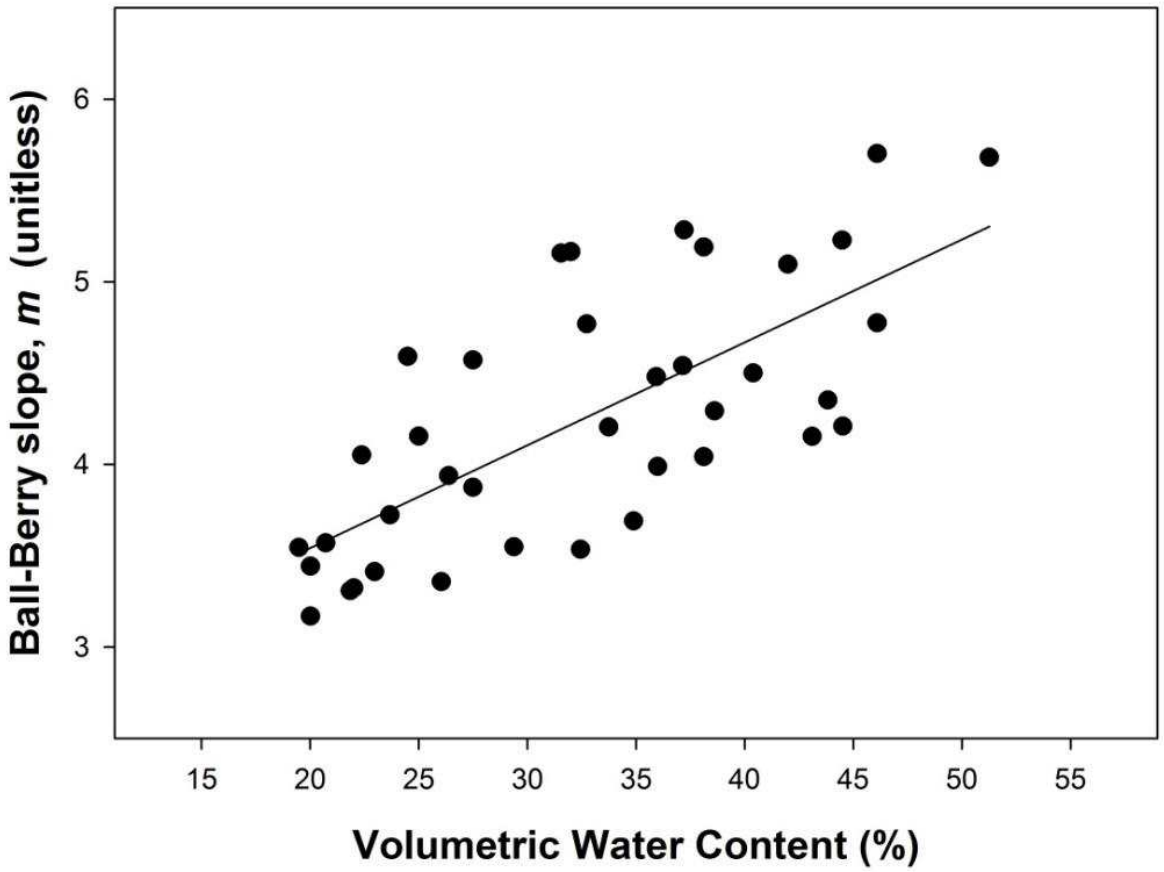

Figure 4. Relationship between the Ball-Berry slope (m) and volumetric water content (θv) for greenhouse maize. The linear regression equation is $m = 0.0563\ (\theta v) + 2.42$; $R^2 = 0.51$.

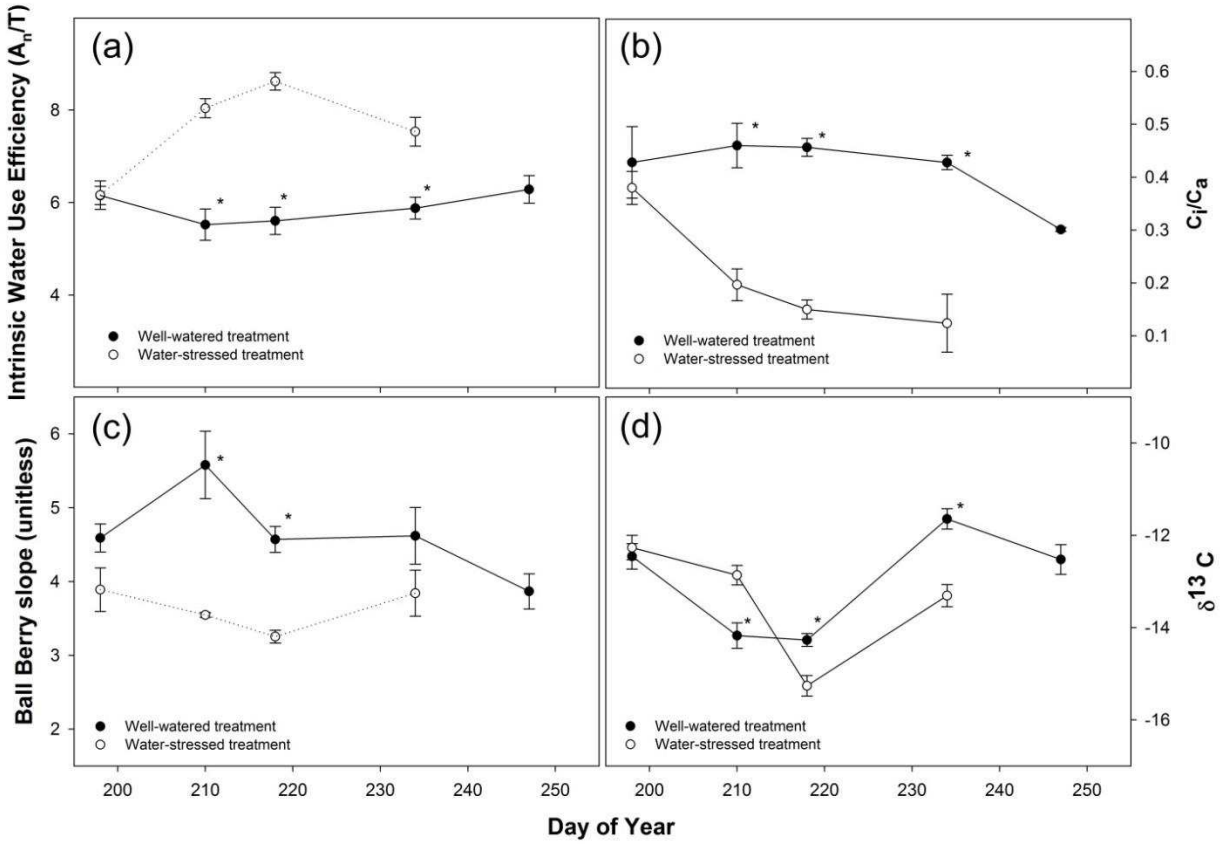

Figure 5. Seasonal changes in intrinsic water use efficiency (mmol mol^{-1}), the ratio of intercellular to atmospheric CO_2 concentration (C_i/C_a), the Ball-Berry slope *m*, and carbon isotope $\delta^{13}C$ values in maize under well-watered and water-stressed conditions. Error bars represent ± SE. Asterisks indicate a significant differences between treatments on that date at $P < 0.05$ (Tukey's HSD).

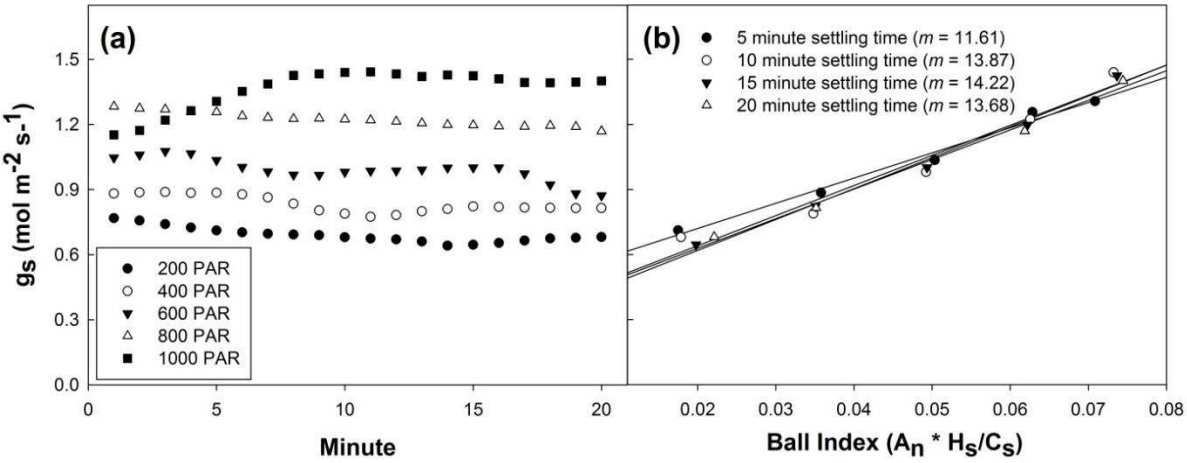

Figure 6. Stomatal conductance (g_s) as a function of light level and settling time (a) and g_s versus the Ball Index as a function of a five, ten, fifteen, or twenty minute settling time at each light level used in the regression (b). Data is for a representative well-watered sunflower plant during the first measurement period.

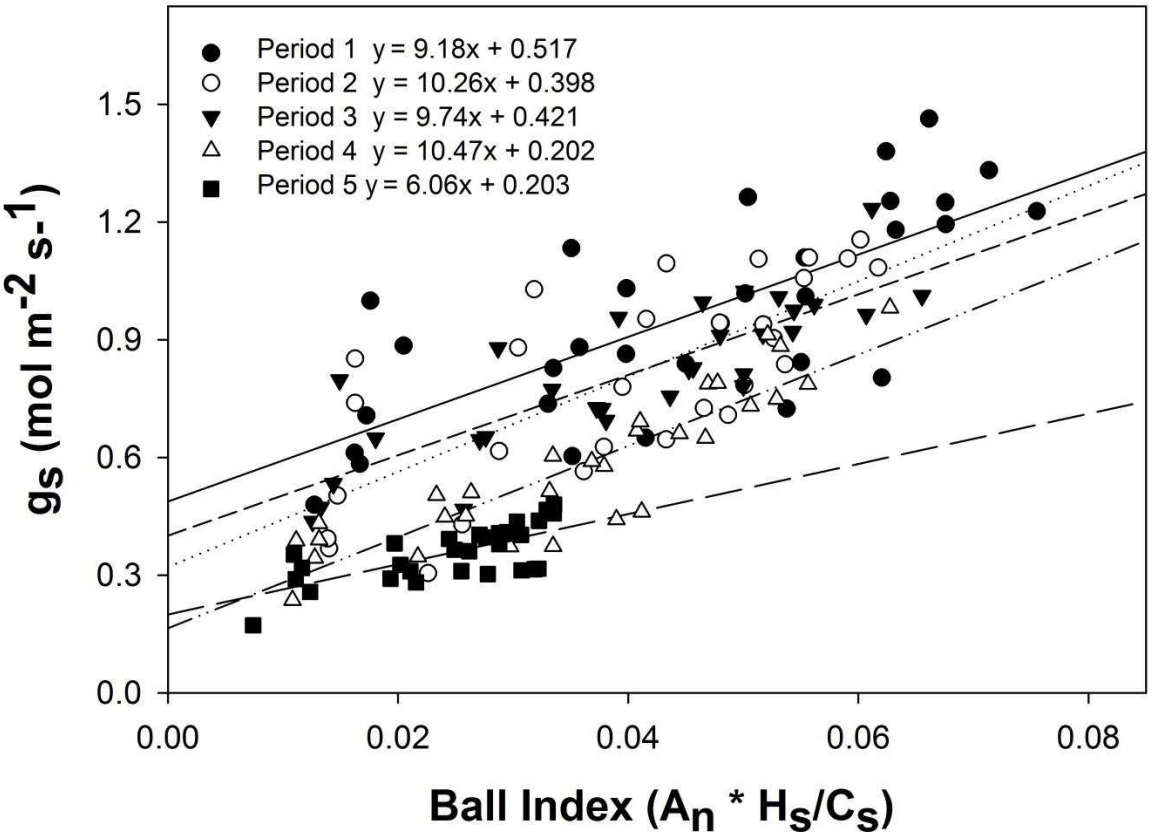

Figure 7. Relationship of stomatal conductance (g_s) with the product of net CO_2 assimilation (An, µmol m^{-2} s^{-1}) and fractional relative humidity at the leaf surface (H_s, unitless) divided by the CO_2 concentration at the leaf surface (C_s) for fully expanded sunlit leaves of well-watered greenhouse sunflower. Points represent individual leaf measurements. Data are only included for which PPFD ≥ 200 µmol m^{-2} s^{-1}. Regression lines represent the treatment means (n = 4-5) of linear functions fitted to data from individual leaves. R^2 values for individual leaf regressions averaged 0.89 ± 0.15. Analysis of Variance on the mean of the slopes and intercepts of individual leaves indicates no significant differences between measurement periods.

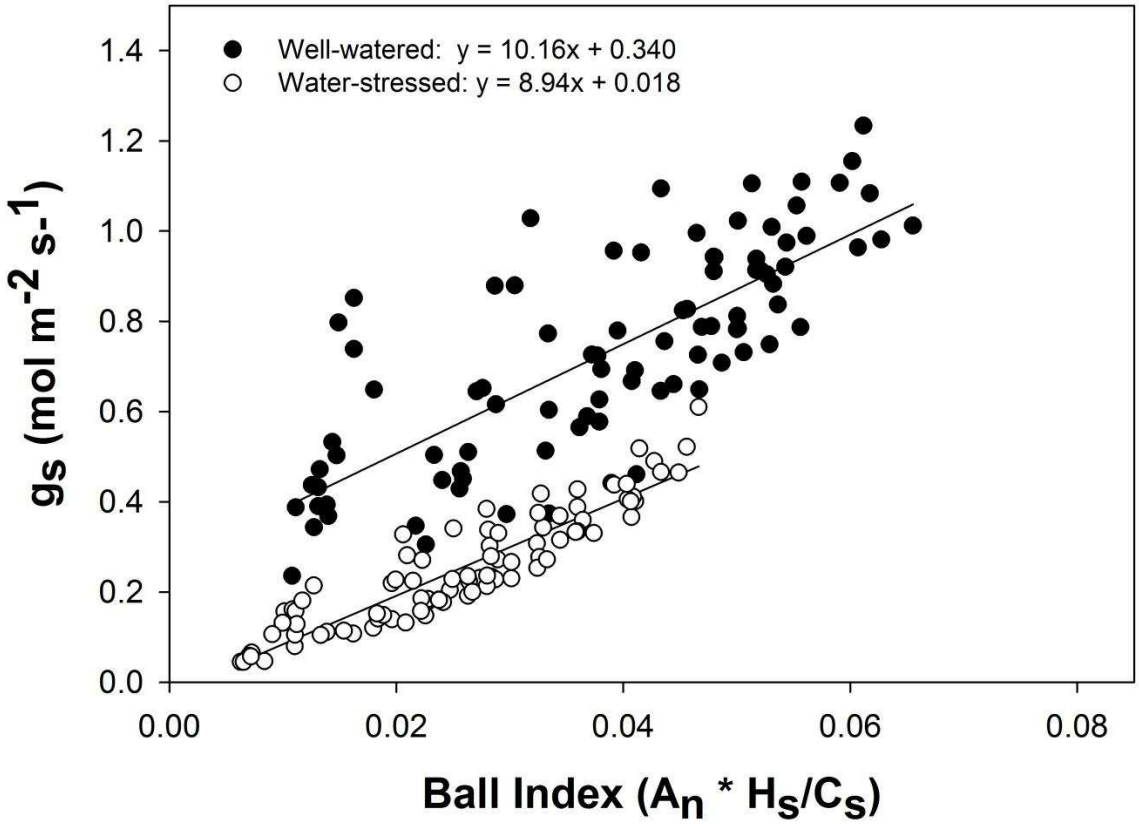

Figure 8. Relationship of stomatal conductance (g_s) with the product of net CO_2 assimilation (A_n, µmol m^{-2} s^{-1}) and fractional relative humidity at the leaf surface (H_s, unitless) divided by the CO_2 concentration at the leaf surface (C_s) for fully expanded sunlit leaves of well-watered and water-stressed greenhouse sunflower for measurement periods 2 – 4. Regression lines represent the treatment means of linear functions fitted to data at high light levels (200 – 1200 µmol m^{-2} s^{-1}) from individual leaves. Analysis of variance on the mean of the intercepts of individual leaves indicates a significant influence of treatment at P = 0.05.

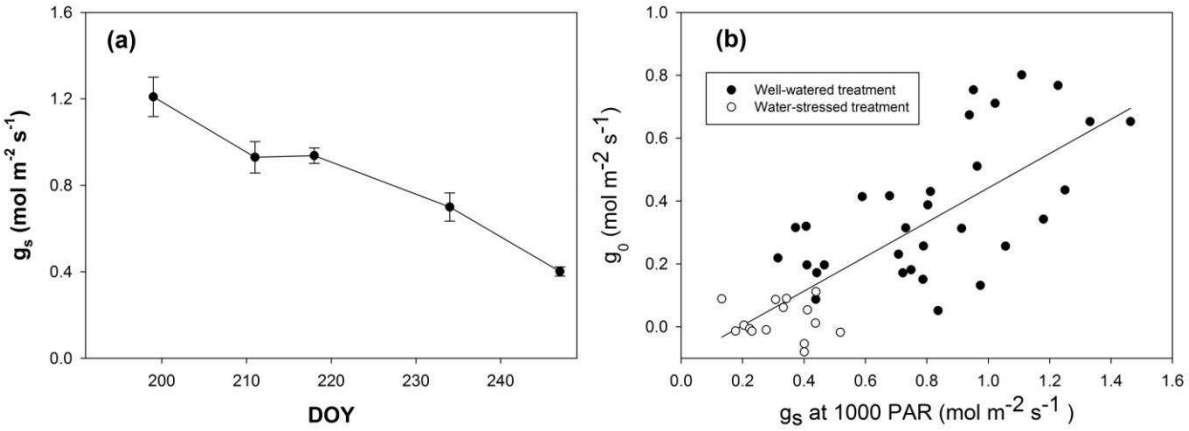

Figure 9. Daytime stomatal conductance (g_s) at 1000 PAR versus Day of Year (DOY) for well-watered sunflower (a) and g0 versus gs at 1000 PAR for well-watered and water stressed sunflower. The regression in panel b is g_0 = 0.547gs – 0.105; R2 = 0.60.

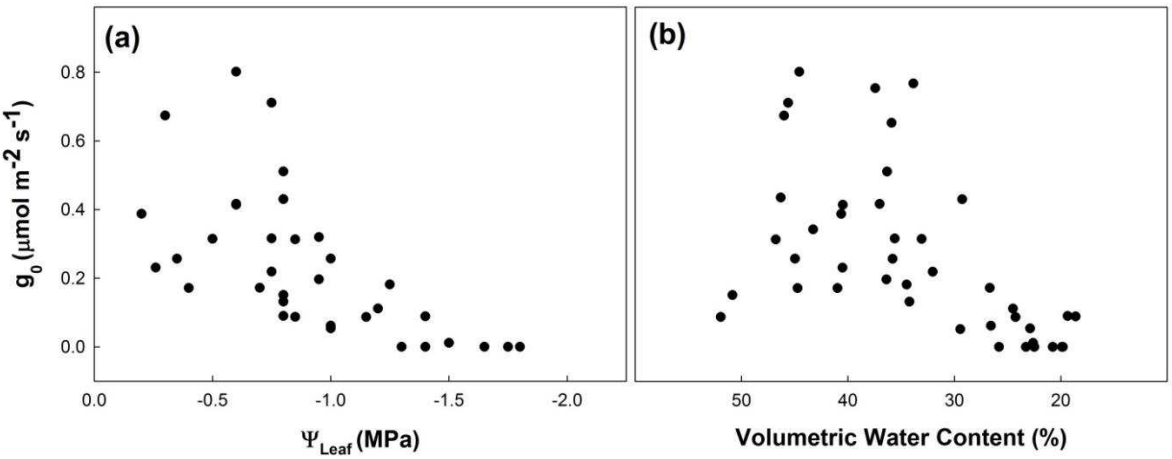

Figure 10. Relationship of residual stomatal conductance (g_0) via linear regression at light levels 200 – 1200 µmol m^{-2} s^{-1} and leaf water potential at the time of measurement (Ψ_{Leaf}) (a) and volumetric water content (θ_v) (b). Slightly negative values of g_0 that were not significantly different than zero were set to zero, as negative conductance values are not physiologically possible. The Spearman correlation coefficient for $g0 - \Psi_{Leaf}$ is r = 0.74 and the Pearson correlation coefficient is r = 0.63. The Spearman correlation coefficient for $g_0 - \theta_v$ is r = 0.63, whereas the Pearson correlation coefficient is r = 0.52.

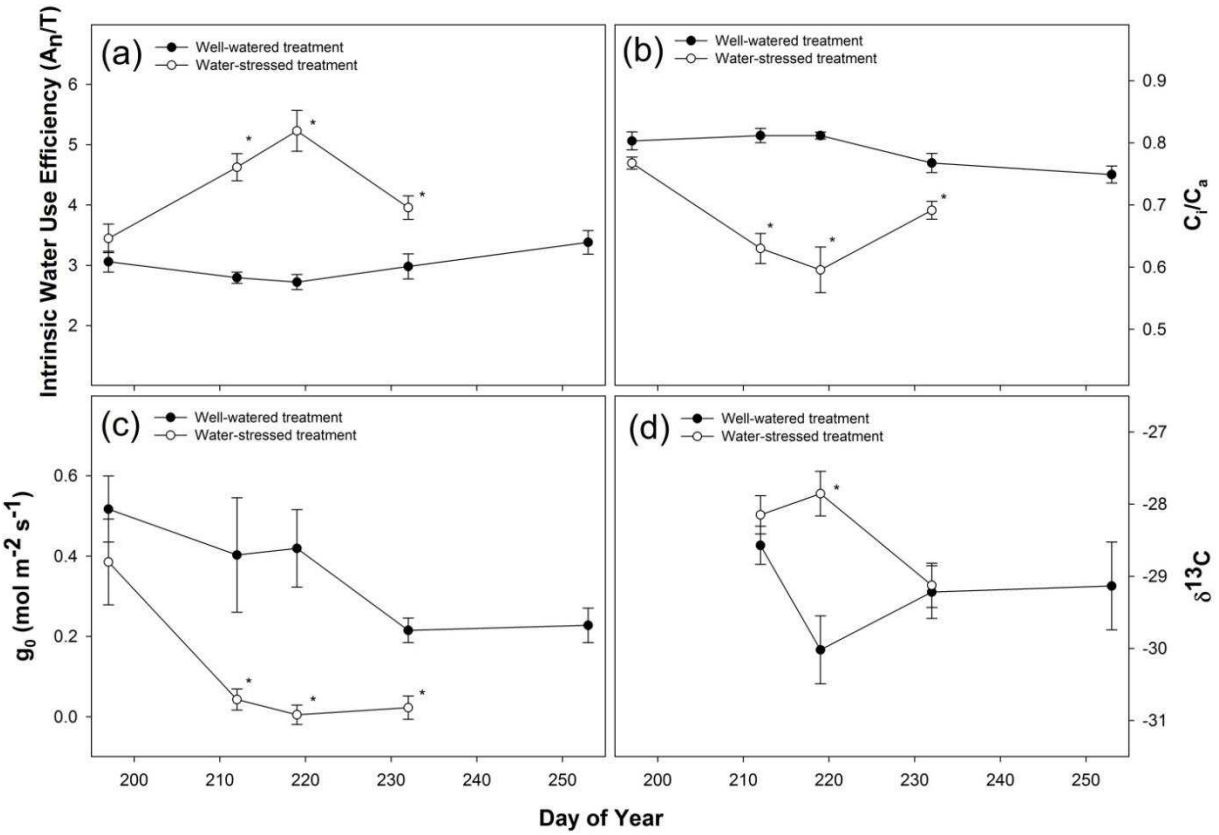

Figure 11. Seasonal changes in water use efficiency (mmol mol^{-1}), the ratio of intercellular to atmospheric CO_2 concentration (C_i/C_a), the Ball-Berry intercept (g_0), and carbon isotope $\delta^{13}C$ values in sunflower under well-watered and water-stressed conditions. Error bars represent ± SE. Asterisks indicate a significant differences between treatments on that date at P = <0.05 (Tukey's HSD).

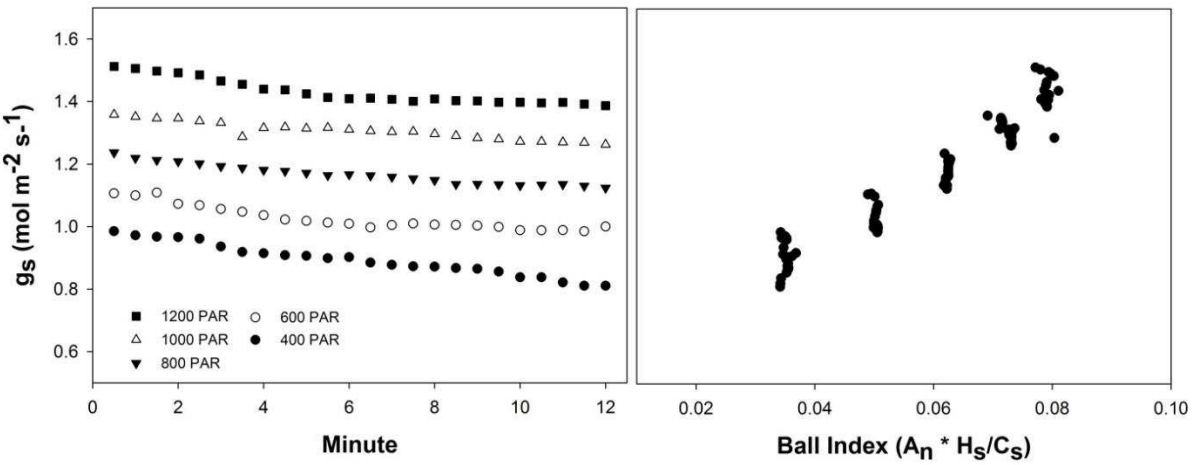

Figure 12. Stomatal conductance (g_s) as a function of light level and settling time (left panel) and g_s over 12 minutes at each light level versus the Ball Index (right panel). Data is for a representative field plant under well-watered conditions.

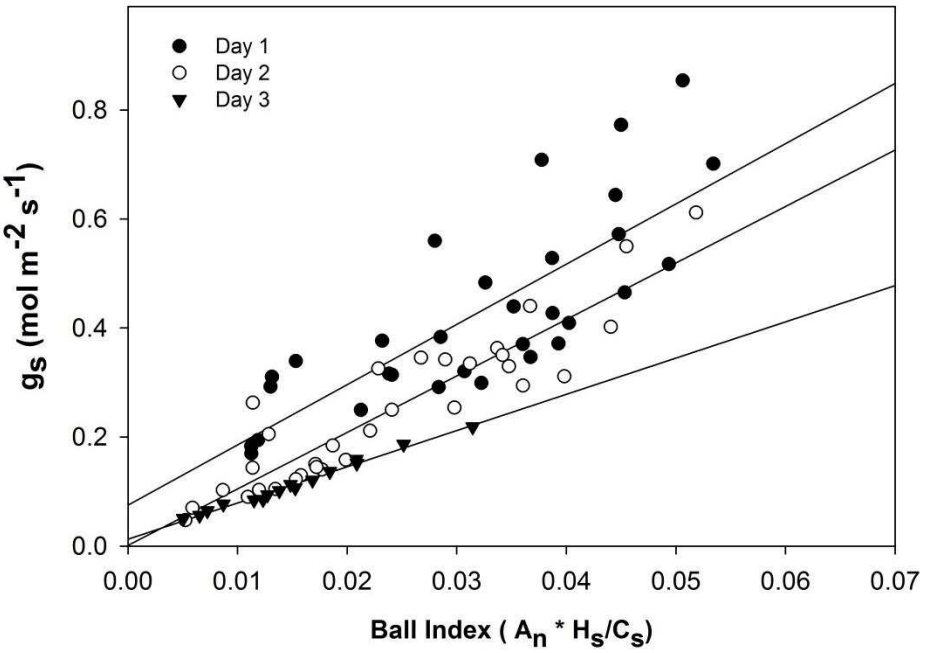

Figure 13. Relationship of stomatal conductance (gs) with the product of net CO2 assimilation (An, µmol m-2 s-1) and fractional relative humidity at the leaf surface (Hs, unitless) divided by the CO2 concentration at the leaf surface (Cs) for fully expanded sunlit sunflower leaves during a rapid soil dry-down. Regression lines represent the treatment means of linear functions fitted to data at high light levels 200 – 1200 µmol m-2 s-1 from individual leaves. Analysis of Variance on the mean of the slopes of individual leaves indicates no significant influence of day at P = 0.05.

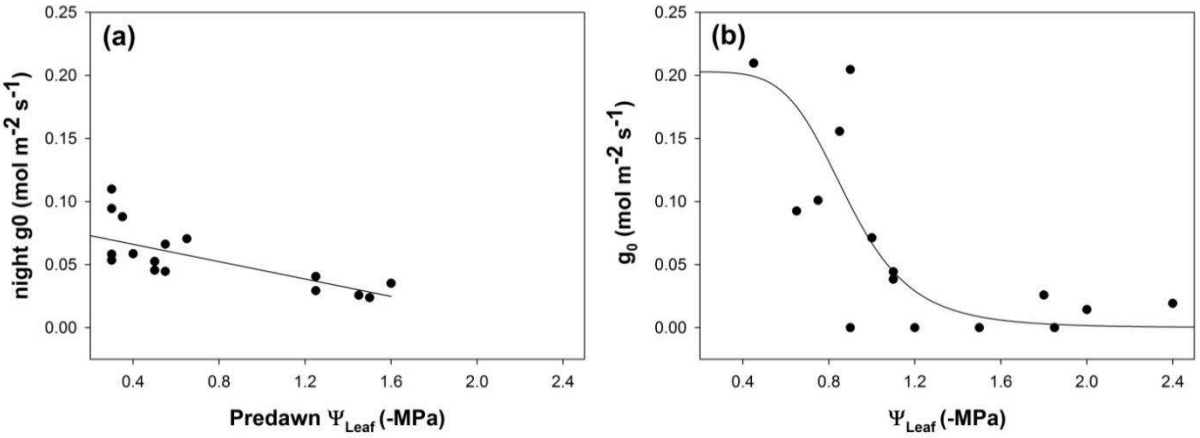

Figure 14. Relationship between night time g_0 values and predawn leaf water potential (Ψ_{Leaf}) (a), and daytime g_0 and Ψ_{Leaf} at the time of measurement (b). Slightly negative values of g_0 that were not significantly different than zero were set to zero, as negative conductance values are not physiologically possible. If linear regression is used (a), the result is $y = 0.080x - 0.034$ ($R^2 = 0.50$). The line in panel b was calculated with equation 2.

CITATIONS

Aasamaa, K. and Sõber, A., 2011. Stomatal sensitivities to changes in leaf water potential, air humidity, CO2 concentration and light intensity, and the effect of abscisic acid on the sensitivities in six temperate deciduous tree species. Environmental and Experimental Botany, 71(1): 72-78.

Baldocchi, D., 1997. Measuring and modelling carbon dioxide and water vapour exchange over a temperate broad-leaved forest during the 1995 summer drought. Plant Cell and Environment, 20(9): 1108-1122.

Baldocchi, D. and Meyers, T., 1998. On using eco-physiological, micrometeorological and biogeochemical theory to evaluate carbon dioxide, water vapor and trace gas fluxes over vegetation: a perspective. Agricultural and Forest Meteorology, 90(1-2): 1-25.

Ball, J.T., 1988. An Analysis of Stomatal Conductance, Stanford University, Stanford.

Ball, J.T., Woodrow, I.E. and Berry, J.A., 1987. A model predicting stomatal conductance and its contribution to the control of photosynthesis under different environmental conditions, pp. 221-224.

Barnard, D. and Bauerle, W., 2013. The implications of minimum stomatal conductance on modeling water flux in forest canopies. Journal of Geophysical Research: Biogeosciences, 118(3): 1322-1333.

Bauerle, W.L. and Bowden, J.D., 2011. Predicting transpiration response to climate change: Insights on physiological and morphological interactions that modulate water exchange from leaves to canopies. HortScience, 46(2): 163-166.

Berry, J.A., Beerling, D.J. and Franks, P.J., 2010. Stomata: key players in the earth system, past and present. Current opinion in plant biology, 13(3): 232-239.

Bounoua, L. et al., 1999. Interactions between vegetation and climate: radiative and physiological effects of doubled atmospheric CO2. Journal of Climate, 12(2): 309-324.

Brodribb, T., 1996. Dynamics of changing intercellular CO2 concentration (ci) during drought and determination of minimum functional ci. Plant Physiology, 111(1): 179-185.

Brodribb, T.J., McAdam, S.A., Jordan, G.J. and Feild, T.S., 2009. Evolution of stomatal responsiveness to CO2 and optimization of water-use efficiency among land plants. New Phytologist, 183(3): 839-847.

Bunce, J.A., 1998. Effects of environment during growth on the sensitivity of leaf conductance to changes in humidity. Global Change Biology, 4(3): 269-274.

Bunce, J.A., 2000. Responses of stomatal conductance to light, humidity and temperature in winter wheat and barley grown at three concentrations of carbon dioxide in the field. Global Change Biology, 6(4): 371-382.

Caird, M.A., Richards, J.H. and Donovan, L.A., 2007. Nighttime stomatal conductance and transpiration in C3 and C4 plants. Plant Physiology, 143(1): 4-10.

Cavender-Bares, J., Sack, L. and Savage, J., 2007. Atmospheric and soil drought reduce nocturnal conductance in live oaks. Tree Physiology, 27(4): 611-620.

Cechin, I. and de Fátima Fumis, T., 2004. Effect of nitrogen supply on growth and photosynthesis of sunflower plants grown in the greenhouse. Plant Sci., 166(5): 1379-1385.

Collatz, G.J., Ball, J.T., Grivet, C. and Berry, J.A., 1991. Physiological and environmental regulation of stomatal conductance, photosynthesis and transpiration - a model that includes a laminar boundary layer. Agricultural and Forest Meteorology, 54(2-4): 107-136.

Collatz, G.J., Ribas-Carbo, M. and Berry, J., 1992. Coupled photosynthesis-stomatal conductance model for leaves of C4 plants. Functional Plant Biology, 19(5): 519-538.

Condon, A., Richards, R., Rebetzke, G. and Farquhar, G., 2002. Improving intrinsic water-use efficiency and crop yield. Crop Science, 42(1): 122-131.

Condon, A., Richards, R., Rebetzke, G. and Farquhar, G., 2004. Breeding for high water-use efficiency. Journal of Experimental Botany, 55(407): 2447-2460.

Damour, G., Simonneau, T., Cochard, H. and Urban, L., 2010. An overview of models of stomatal conductance at the leaf level. Plant, Cell & Environment, 33(9): 1419-1438.

DeJonge, K.C., Taghvaeian, S., Trout, T.J. and Thomas, L.H., 2015. Comparison of canopy temperature-based water stress indices formaize.

Falge, E., Graber, W., Siegwolf, R. and Tenhunen, J., 1996. A model of the gas exchange response ofPicea abies to habitat conditions. Trees, 10(5): 277-287.

Farquhar, G., Caemmerer, S. and Berry, J., 1980. A biochemical model of photosynthetic CO 2 assimilation in leaves of C 3 species. Planta, 149(1): 78-90.

Franks, P.J. and Farquhar, G.D., 2007. The mechanical diversity of stomata and its significance in gas-exchange control. Plant Physiology, 143(1): 78-87.

Gimeno, T.E. et al., 2015. Conserved stomatal behaviour under elevated CO2 and varying water availability in a mature woodland. Funct. Ecol.

Grantz, D.A. and Zeiger, E., 1986. Stomatal responses to light and leaf-air water vapor pressure difference show similar kinetics in sugarcane and soybean. Plant Physiology, 81(3): 865-868.

Gutschick, V.P. and Simonneau, T., 2002. Modelling stomatal conductanceof field-grown sunflower under varying soil water content and leafenvironment: comparison of three models of stomatal response toleaf environment and coupling with an abscisic acid-based modelof stomatal response to soil drying. Plant, Cell & Environment, 25(11): 1423-1434.

Heroult, A., Lin, y.Ä., Bourne, A., Medlyn, B.e. and Ellsworth, D.s., 2013. Optimal stomatal conductance in relation to photosynthesis in climatically contrasting Eucalyptus species under drought. Plant, Cell & Environment, 36(2): 262-274.

Hetherington, A.M. and Woodward, F.I., 2003. The role of stomata in sensing and driving environmental change. Nature, 424(6951): 901-908.

Houborg, R., Cescatti, A., Migliavacca, M. and Kustas, W.P., 2013. Satellite retrievals of leaf chlorophyll and photosynthetic capacity for improved modeling of GPP. Agricultural and Forest Meteorology, 177: 10-23.

Howard, A.R. and Donovan, L.A., 2007. Helianthus nighttime conductance and transpiration respond to soil water but not nutrient availability. Plant Physiology, 143(1): 145-155.

Jones, H.G., 2013. Plants and microclimate: a quantitative approach to environmental plant physiology. Cambridge University Press.

Jordan, G.J., Brodribb, T.J. and Loney, P.E., 2005. Water loss physiology and the evolution within the Tasmanian conifer genus Athrotaxis (Cupressaceae). Aust. J. Bot., 52(6): 765-771.

Jordan, W.R. and Ritchie, J.T., 1971. Influence of soil water stress on evaporation, root absorption, and internal water status of cotton. Plant physiology, 48(6): 783-788.

Katul, G., Leuning, R. and Oren, R., 2003. Relationship between plant hydraulic and biochemical properties derived from a steady-state coupled water and carbon transport model. Plant, Cell & Environment, 26(3): 339-350.

Kirschbaum, M.U.F., 1999. CenW, a forest growth model with linked carbon, energy, nutrient and water cycles. Ecological Modelling, 118(1): 17-59.

Knapp, A.K. and Smith, W.K., 1990. Contrasting stomatal responses to variable sunlight in two subalpine herbs. Am. J. Bot.: 226-231.

Kohanbash, D., Kantor, G., Martin, T. and Crawford, L., 2013. Wireless sensor network design for monitoring and irrigation control: User-centric hardware and software development. HortTechnology, 23(6): 725-734.

Kottkamp, J., Varjabedian, A., Ross, J., Eddy, R. and Hahn, D.T., 2010. Optimizing Greenhouse Corn Production: What Is the Best Fertilizer Formulation and Strength? Purdue Methods for Corn Growth: 14.

Krinner, G. et al., 2005. A dynamic global vegetation model for studies of the coupled atmosphere-biosphere system. Global Biogeochem. Cycles, 19(1): 33.

Lai, C.T., Katul, G., Oren, R., Ellsworth, D. and Schäfer, K., 2000. Modeling CO2 and water vapor turbulent flux distributions within a forest canopy. Journal of Geophysical Research: Atmospheres (1984–2012), 105(D21): 26333-26351.

Lambers, H., Chapin III, F.S. and Pons, T.L., 2008. Plant water relations. Springer.

Lea-Cox, J.D. et al., 2013. Advancing wireless sensor networks for irrigation management of ornamental crops: An overview. HortTechnology, 23(6): 717-724.

Leakey, A.D., Bernacchi, C.J., Ort, D.R. and Long, S.P., 2006. Long-term growth of soybean at elevated [CO2] does not cause acclimation of stomatal conductance under fully open-air conditions. Plant, Cell & Environment, 29(9): 1794-1800.

Leuning, R., 1995. A critical-appraisal of a combined stomatal-photosynthesis model for C3 plants. Plant Cell and Environment, 18(4): 339-355.

Leuning, R., Cromer, R. and Rance, S., 1991. Spatial distributions of foliar nitrogen and phosphorus in crowns of Eucalyptus grandis. Oecologia, 88(4): 504-510.

Lokupitiya, E. et al., 2009. Incorporation of crop phenology in Simple Biosphere Model (SiBcrop) to improve land-atmosphere carbon exchanges from croplands. Biogeosciences, 6(6): 969-986.

Medlyn, B.E. et al., 2005. Carbon balance of coniferous forests growing in contrasting climates: Model-based analysis. Agricultural and Forest Meteorology, 131(1): 97-124.

Medlyn, B.E. et al., 2011. Reconciling the optimal and empirical approaches to modelling stomatal conductance. Global Change Biology, 17(6): 2134-2144.

Misson, L., Panek, J.A. and Goldstein, A.H., 2004. A comparison of three approaches to modeling leaf gas exchange in annually drought-stressed ponderosa pine forests. Tree Physiology, 24(5): 529-541.

Monti, A., Brugnoli, E., Scartazza, A. and Amaducci, M., 2006. The effect of transient and continuous drought on yield, photosynthesis and carbon isotope discrimination in sugar beet (Beta vulgaris L.). Journal of Experimental Botany, 57(6): 1253-1262.

Ogle, K. et al., 2012. Differential daytime and night-time stomatal behavior in plants from North American deserts. New Phytologist, 194(2): 464-476.

Oleson, K.W. et al., 2010. Technical description of version 4.0 of the Community Land Model (CLM).

Oleson, K.W. et al., 2008. Improvements to the Community Land Model and their impact on the hydrological cycle. J. Geophys. Res, 113: G01021.

Ono, K. et al., 2013. Canopy-scale relationships between stomatal conductance and photosynthesis in irrigated rice. Global Change Biology.

Pearcy, R.W., 1990. Sunflecks and photosynthesis in plant canopies. Annu. Rev. Plant Biol., 41(1): 421-453.

Sala, A. and Tenhunen, J.D., 1996. Simulations of canopy net photosynthesis and transpiration in Quercus ilex L under the influence of seasonal drought. Agricultural and Forest Meteorology, 78(3-4): 203-222.

Schneiter, A. and Miller, J., 1981. Description of sunflower growth stages. Crop Science, 21(6): 901-903.

Seibt, U., Rajabi, A., Griffiths, H. and Berry, J.A., 2008. Carbon isotopes and water use efficiency: sense and sensitivity. Oecologia, 155(3): 441-454.

Sellers, P.J. et al., 1997. Modeling the exchanges of energy, water, and carbon between continents and the atmosphere. Science, 275(5299): 502.

Sellers, P.J. et al., 1996. A revised land surface parameterization (SiB2) for atmospheric GCMs. Part I: Model formulation. Journal of Climate, 9(4): 676-705.

Snyder, K., Richards, J. and Donovan, L., 2003. Night-time conductance in C3 and C4 species: do plants lose water at night? Journal of Experimental Botany, 54(383): 861-865.

Tenhunen, J.D., Serra, A.S., Harley, P.C., Dougherty, R.L. and Reynolds, J.F., 1990. Factors influencing carbon fixation and water-use by mediterranean sclerophyll shrubs during summer drought. Oecologia, 82(3): 381-393.

Tuzet, A., Perrier, A. and Leuning, R., 2003. A coupled model of stomatal conductance, photosynthesis and transpiration. Plant, Cell & Environment, 26(7): 1097-1116.

Valentini, R., Gamon, J.A. and Field, C.B., 1995. Ecosystem gas exchange in a California grassland: seasonal patterns and implications for scaling. Ecology: 1940-1952.

Van Wijk, M. et al., 2000. Modeling daily gas exchange of a Douglas-fir forest: comparison of three stomatal conductance models with and without a soil water stress function. Tree Physiology, 20(2): 115-122.

Varble, J.L. and Chávez, J., 2011. Performance evaluation and calibration of soil water content and potential sensors for agricultural soils in eastern Colorado. Agricultural water management, 101(1): 93-106.

Wang, Y.-P. and Leuning, R., 1998. A two-leaf model for canopy conductance, photosynthesis and partitioning of available energy I:: Model description and comparison with a multi-layered model. Agricultural and Forest Meteorology, 91(1): 89-111.

Wolf, A., Akshalov, K., Saliendra, N., Johnson, D.A. and Laca, E.A., 2006. Inverse estimation of Vcmax, leaf area index, and the Ball-Berry parameter from carbon and energy fluxes. Journal of Geophysical Research: Atmospheres (1984–2012), 111(D8).

Woods, D.B. and Turner, N.C., 1971. Stomatal response to changing light by four tree species of varying shade tolerance. New Phytologist, 70(1): 77-84.

Xu, L. and Baldocchi, D.D., 2003. Seasonal trends in photosynthetic parameters and stomatal conductance of blue oak (Quercus douglasii) under prolonged summer drought and high temperature. Tree Physiology, 23(13): 865-877.

Zeppel, M.J. et al., 2012. Nocturnal stomatal conductance responses to rising [CO2], temperature and drought. New Phytologist, 193(4): 929-938.

Zhou, S., Duursma, R.A., Medlyn, B.E., Kelly, J.W. and Prentice, I.C., 2013. How should we model plant responses to drought? An analysis of stomatal and non-stomatal responses to water stress. Agricultural and Forest Meteorology.

CHAPTER 3:

SEASONAL AND WATER STRESS RESPONSES OF PHOTOSYNTHETIC PARAMETERS IN *ZEA MAYS* AND *HELIANTHUS ANNUUS* AND THEIR RELATIONSHIP WITH LEAF NITROGEN AND CHLOROPHYLL CONTENT

Summary

Methods of estimating seasonal variations in photosynthetic capacity (P_c) are critical for modeling the time course of water and carbon (C) fluxes. Given the difficulty of calculating P_c parameters via leaf-level measurements, it is appealing to calculate parameter variation via changes in leaf chlorophyll (Chl) and nitrogen (N) content by assuming that P_c scales with these variables. While seasonal changes in P_c as well as leaf-level relationships between N and P_c have been evaluated in forest canopies, there is only scarce data on seasonal parameter values in field crops, nor is it clear if P_c can be estimated from leaf-level properties. In this study we characterized the seasonal variability of the maximum rates of carboxylation (V_{cmax}), electron transport (J_{max}), and assimilation (A_{max}) under different water availability for maize (*Zea mays L.)* and sunflower (*Helianthus annuus*) and coupled these data with measurements of leaf spectral properties, Chl, N and leaf mass per unit area (LMA). We then examined the seasonal relationships between leaf properties and P_c. We observed a significant relationship between SPAD – Chl in maize, but found no seasonal variation in Chl or SPAD values in sunflower. The seasonal Chl - N_a relationship was significant in maize, but with a lower slope than previously reported, while the Chl – N_a relationship was not significant in sunflower. Area based N – V_{cmax} relationships were not significant for either crop. Mass-based relationships were highly

significant for maize, whereas the relationship in sunflower were poorer. Seasonal variability in P_c was not well described by changes in leaf spectral properties, Chl, or N_a in sunflower. In maize, P_c was highly correlated to changes in LMA and DOY. Reliable estimates of P_c from leaf properties may not be successful in all field crops and the relationships should be carefully evaluated prior to utilization.

Introduction

Efforts to accurately simulate or remotely sense the time course of exchanges of water and carbon between vegetation and the atmosphere require accurate estimation of the seasonal variability in the parameters and processes controlling these fluxes (Houborg et al., 2013). Photosynthesis (A_n) and transpiration are a complex function of factors such as canopy architecture, leaf angle and area, solar radiation, photosynthetic capacity (P_c), and stomatal conductance (g_s). While a wide variety of approaches are used to model fluxes of CO_2 and water vapor, the dominant method is to couple a mechanistic model of A_n (Farquhar et al., 1980) to a semi-empirical model of g_s, particularly the widely validated and utilized Ball-Berry model (e.g., Ball, 1988; Ball et al., 1987; Collatz et al., 1991; Collatz et al., 1992; Egea et al., 2011; Houborg et al., 2013; Sellers et al., 1996b). This approach is routinely employed in leaf-level physiological models, as well as in regional and global hydrologic and climate models (Berry et al., 2010; Sellers et al., 1996a; Sellers et al., 1996b). Simultaneously solving the Ball-Berry model of g_s and the Farquhar et al. (1980) model of A_n provides an efficient and effective way of predicting rates of A_n and transpiration. Derivations of these two leaf-level models are at the center of numerous large-scale models of terrestrial cycling of C and water (e.g., Egea et al., 2011; Sellers et al., 1996a; Sellers et al., 1996b). While a noted strength of these models is that

they can be parameterized with relatively few physiological parameters, the values used are often fixed and broadly assigned by plant functional type.

The Farquhar et al. (1980) model calculates leaf-level CO_2 assimilation rates by considering two potential rate-limiting factors: the ribulose 1,5-bisphosphate (RuBP) saturation rate under low intercellular concentrations of CO_2 (C_i), or the rate of regeneration of RuBP at high internal CO_2 concentrations. The model can quantify how A_n responds to changes in environmental variables such as light, temperature, CO_2, O_2 and leaf nitrogen (N) (Xu and Baldocchi, 2003). Two key parameters in this model, the maximum electron transport capacity (J_{max}) and the maximum carboxylation capacity (V_{cmax}) show genotypic and phenotypic variation (Farquhar et al., 1980). Studies have shown that these parameters are highly correlated (Wullschleger, 1993), but their values change over time and as a function of species type, growth environment, leaf age, drought, and photoperiod (Bauerle et al., 2012; Bauerle, 2011; Medlyn et al., 2002; Wilson et al., 2001; Wilson et al., 2000; Xu and Baldocchi, 2003). In particular, V_{cmax} has been shown to be a highly influential parameter in the A_n model (Dang et al., 1998). Failure to incorporate seasonal trends in P_c results in poor model estimates of annual C uptake (Tanaka et al., 2002; Wilson et al., 2001), but temporal changes in P_c are often neglected due to the time and labor intensive nature of collecting a sequence of leaf-level gas exchange measurements for V_{cmax} and J_{max} calculations. Moreover, data on species-specific seasonal or water stress responses are often scarce, resulting in models using fixed V_{cmax}/J_{max} values for broad classes of plant functional types (e.g., Ali et al., 2015; Houborg et al., 2013; Kattge et al., 2009). Measurements of the maximum assimilation rate under saturating light and ambient CO_2 concentrations (A_{max}) are more frequently available due to the relative simplicity of the measurement, but A_{max} values do not always clearly reflect the intrinsic P_c of the leaf, as the response of stomata to

environmental factors can affect the CO_2 availability at the carboxylation sites (Ali et al., 2015; Grassi et al., 2005; Wilson et al., 2000; Xu and Baldocchi, 2003). However, knowledge of the A_{max} - V_{cmax} relationship can be useful for estimating or constraining estimates of V_{cmax} and J_{max} when V_{cmax} and J_{max} data are not available (Kattge et al., 2009).

The recognition of the importance of scaling parameters has resulted in efforts to develop more mechanistic models in functional forms that constrain the number of needed inputs (Medvigy et al. 2013). Various approaches have been developed with the shared goal of developing a simple representation of seasonal P_c that is applicable at the global scale (Bauerle et al., 2012, Ali et al., 2015, Kattge et al., 2009).

Given the difficulty of continuously measuring P_c parameters in the field via leaf-level gas exchange, it is appealing to attempt to calculate seasonal variations in leaf characteristics from the well-established relationships between leaf P_c and N content (Evans, 1989; Field and Mooney, 1986).

Soluble proteins of the Calvin cycle, dominated by the enzyme ribulose 1,5-bisphosphate carboxylase (Rubisco), represent a large proportion of leaf N. V_{cmax} is related to the photosynthetic limitation by Rubisco, resulting in a relationship between leaf N, A_{max}, and V_{cmax} (Evans 1989). A second major fraction of leaf N is found in the Chl containing pigment-protein reaction center complexes of the thylakoid membrane. While Chl itself does not contain large amounts of N, the proteins that comprise the pigment are high in N, resulting in correlations between leaf Chl and N (Evans 1989).

General relationships between N – A_{max} and N – V_{cmax} have been reported across a wide range of plant functional types (Field and Mooney, 1986; Kattge et al., 2009; Medlyn et al., 1999; Reich et al., 1998) and linkages have been established in temperate, tropical, and boreal

forests (Ollinger et al., 2008; Reich et al., 1997). While a linear relationship is often reported (Le Roux et al., 1999; Leuning et al., 1991; Medlyn et al., 1999; Niinemets and Tenhunen, 1997; Wilson et al., 2000; Xu and Baldocchi, 2003) the strength of the relationship and the reported regression coefficients vary widely by species and functional group. Further, these relationships are often developed by collecting data across strong gradients in environmental variables such as light or nutrient availability or across functional types, and it is less clear if the relationships can describe the temporal effects of leaf age or drought within species (Grassi et al., 2005; Wilson et al., 2001; Wilson et al., 2000). Despite these discrepancies, V_{cmax} values are frequently parameterized in terrestrial models by assuming a linear relationship with N that is often presumed static and unresponsive to changes in plant phenology, leaf structure, and environmental conditions (Ali et al., 2015; Houborg et al., 2013; Kattge et al., 2009; Medlyn et al., 1999; Thornton and Zimmermann, 2007). Similarly, while V_{cmax} and J_{max} are frequently tightly coupled, allowing J_{max} to be estimated from values of V_{cmax}, the ratio between the two variables is not always constant temporally or across species (Medlyn et al., 1999; Wullschleger, 1993). These oversimplifications cause seasonal errors in model simulations of land-atmosphere exchanges, and thus warrant efforts towards refining parameter value responses to changes in the season and environment (Ali et al., 2015; Bauerle et al., 2012).

Knowledge of seasonal linkages between leaf Chl, N and P_c opens the possibility of estimating parameters at large scales, particularly if Chl or N can be sensed remotely (Houborg et al., 2013; Ollinger et al., 2008; Ollinger and Smith, 2005). Integration of field sampling methods, imaging spectroscopy, remote sensing, and CO_2 flux measurements have demonstrated that ecosystem CO_2 uptake capacity scales with whole-canopy N concentration in temperate and boreal forests (Ollinger et al., 2008). Recent work has also proposed the utilization of satellite-

based estimates of Chl for deriving seasonal dynamics in V_{cmax} and constraining model estimates in maize (Houborg et al. 2013).

The coupling of remote sensing data with physiological models has clear applications for agricultural management such as yield forecasting, quantification of regional transpiration, and drought monitoring. However, there is still a need to evaluate the interrelations between Chl, N, and P_c in field crops (Ollinger et al., 2008), as most of the research related to the scaling of V_{cmax} and J_{max} with N or seasonal changes in values has been conducted on evergreen and deciduous forest tree species (Bauerle et al., 2012; Grassi et al., 2005; Medlyn et al., 1999; Ollinger and Smith, 2005; Xu and Baldocchi, 2003). For example, in a recent meta-analysis of the $N_a - A_{max} - V_{cmax}$ relationship that utilized data from dozens of studies, encompassing nearly a hundred different data sets, only one data set was from a C3 crop, presumably due to scarce availability of crop-specific data (Kattge et al., 2009). Another recent analysis explicitly excluded row crops due to their potential to confound the relationships being explored (Ali et al., 2015). The relationship between P_c and leaf-level properties could be different in managed field crops, as N dynamics and patterns of allocation are often distinctly different in grain or oilseed crops as compared to natural ecosystems (Hay and Porter, 2006).

In this study we characterized the seasonal variability of the parameters A_{max}, V_{cmax} and J_{max} under different water availability along with leaf-level measurements of SPAD, Chl, N, and LMA for two field crop species. Our first objective was to assess and compare the seasonal variability in leaf P_c and leaf properties in relation to (i) crop species, (ii) crop ontogeny, and (iii) water stress. Our second objective was to use seasonal measurements of leaf reflectance, Chl, and N to assess the strength and utility of these leaf-level relationships for predicting variability in P_c using seasonal regressions.

Materials and Methods

Site description

The primary measurements for this study were conducted during the 2013 growing season in the greenhouse facilities at Colorado State University, Fort Collins, CO. Ancillary field measurements were made at the USDA-ARS Limited Irrigation Research Farm (LIRF) in northern Colorado, USA (40°26′57″ N, 104°38′12″ W, Elev. 1427 m).

Greenhouse Experiment

Seeds of sunflower (Syngenta hybrid 2495 NS/CL/DM) and maize (Dekalb hybrid DKC52-04 RIV) were planted on June 10, 2013 (DOY 161) into 26 L pots. Pots were filled with 8.8 kg of air-dried soilless substrate consisting of a 1:1:3 by volume ratio of Greens Grade™, Turface® Quick Dry®, and Fafard 2SV. Briefly, Greens Grade™ consists of a minimum of 60% medium – course sand, 20-30% of particles ranging from fine sand to clay, and less than 10% very course sand. Turface® Quick Dry® is a fine, calcined, non-swelling illite and silica clay, with a cation exchange capacity (CEC) of 33.6 meq/100 g. The Fafard 2SV mix is a mix of peat moss and fine vermiculite. Our intent was to create a soilless substrate that could be readily replicated, and that had a particle size distribution, porosity, CEC, and a water release curve that was more similar to soil than typical soilless mixes. Accurate soil moisture sensor readings require good contact with the medium, so we avoided potting mixtures with large air spaces and voids. Volumetric water content (θ_v) at field capacity (0.33 MPa) as determined via soil water release curves was approximately 49%.

Plants of similar sizes within a species were randomly assigned to either a well-watered or water-stressed treatment. Measurements were performed in 2-week intervals, beginning in the mid to late vegetative stage and continuing until plant senescence. All plants were kept well-

watered until after the first measurement period, after which a water stress treatment was imposed. A total of five measurement periods occurred for well-watered plants and four for the water stressed, as the water-stress treatment induced early senescence. Measurement dates and accompanying growth stages for each crop are given in Table 1. For ease of reference, we refer to measurement periods in lieu of day of year (DOY). It is important to note that while we utilize the agronomically useful concept of observable 'growth stages', the growth stages visible to the naked eye in crops like maize are temporally disconnected from physiological transitions – for example, by the time the tassel is visible (the final stage in vegetative development in maize), the stem apex has already transitioned to reproductive development weeks prior (Hay and Porter, 2006).

Each crop treatment contained fourteen plants at the beginning of the experiment, with a destructive harvest of aboveground biomass occurring in 2-week intervals throughout the season. Five plants per treatment were tracked continuously over the season for changes in P_c and leaf properties.

Table 1. Dates of measurement and corresponding developmental stages for well-watered maize and sunflower grown under greenhouse conditions.

Measurement Period	Day of Year	Growth Stage
---- *Maize* ----		
Period 1	198-199	Vegetative; Eight leaf collared (V8)
Period 2	210-211	Vegetative; Fourteenth leaf collared (V14)
Period 3	217-218	Reproductive; Silking (R1)
Period 4	233-234	Reproductive; Blister (R2)
Period 5	247	Reproductive; Dent (R5)
--- *Sunflower* ---		
Period 1	197-199	Vegetative; Thirteen true leaves (V13)
Period 2	211-212	Reproductive; Floral head (R1)
Period 3	218-220	Reproductive; Inflorescence opening (R4)
Period 4	231-232	Reproductive; Head 90% in flower (R5.9)
Period 5	253	Reproductive; Bracts senescing (R8)

Soil moisture sensors

Soil moisture sensors were installed in five pots per treatment to monitor θ_v (cm^{-3} cm^{-3}) (Decagon 5TM sensors; Decagon Devices, Inc., Pullman, WA). In addition, we assessed the accuracy of the sensors in the substrate from near saturation to the permanent wilting point, as studies have demonstrated that errors are introduced in soil moisture readings if substrate-specific calibrations are not performed (Varble and Chávez, 2011). Hence, a substrate-specific calibration was developed and applied over a measured volumetric water content of 0.20 – 0.58. This calibration curve (R^2 = 0.95) was then used to calculate θ_v in lieu of the generic manufacturer's calibration. While variability of soil, roots, and rocks in field conditions can result in inaccuracies of manufacturer calibrations, our material was thoroughly homogenized, and we were able to produce a precise and accurate calibration for the substrate.

Soil moisture treatments

Irrigation emitters (PPC Spray Stake, Netafilm Inc., Fresno, CA, USA) were placed in each pot, and the pots were sealed with Glad® Press 'n Seal to eliminate evaporation from the soil surface. Each pot had a 180° spray stake operating at a flow rate of 12 L h^{-1} (PPC Spray Stake, Netafilm Inc., Fresno, CA, USA). To prevent preferential flow of water, the soil moisture sensors were installed horizontally, mid-way between the plant and the pot sidewall. The soil moisture content of five replicates per species and treatment was monitored continuously throughout the season. Sensors were used to trigger irrigations once the θ_v readings dropped below a pre-determined threshold. A wireless sensor network providing local set point control was used to manage irrigations (Lea-Cox et al., 2013). Briefly, the system consisted of data loggers (Decagon nR5-DC; Decagon Devices, Inc., Pullman, WA) for monitoring Decagon 5TM sensors and controlling 12V direct current solenoids. A software interface automated the wireless

sensor network irrigation (Kohanbash et al., 2013). The system was programmed to monitor the soil moisture content of five replicates per species at 15-minute intervals, compile the measurements into an average value of θ_v, and irrigate with a pre-set amount of water when the average θ_v was below the target set point. This type of dynamic irrigation control permitted automated application of water to maintain a target θ_v in the face of variable environmental conditions and increased water consumption due to crop growth.

While there was some initial fluctuation in θ_v as irrigation regimes were being established, substrate moisture content was then kept within a daily average target θ_v of 0.40 for the well-watered treatment and 0.24 for the water-stressed treatment. Seasonal daily treatment averages of θ_v were 0.39 ± 0.02 for well-watered maize, 0.23 ± 0.01 for water-stressed maize, 0.40 ± 0.03 for well-watered sunflower, and 0.24 ± 0.02 for water-stressed sunflower. Target stress levels were determined by lowering θ_v until water limitations induced strong mid-day leaf curling in maize and leaf wilting in sunflower. The target θ_v had to be raised slightly over the season in both treatments to support increased canopy biomass under elevated summer temperatures. To ensure adequate nutrients, Peters' Excel Cal-Mag (15-5-15) was applied at a strength of 200 ppm N via the irrigation lines (Kottkamp et al., 2010).

Environmental conditions and meteorological measurements

Supplemental lighting was provided for a period of 13 hours (6:00 – 19:00). Photosynthetic photon flux (PPF; µmol m^{-2} s^{-1}), air temperature (T_{air}; °C), and relative humidity (RH; %) were measured every minute using EHT RH/temperature sensors and AQO-S PAR photon flux sensors mounted at the top of the canopy (Decagon Devices, Pullman, WA) (Fig 1). Sensors were moved as the plants grew to maintain top-of-canopy location.

The target daytime greenhouse temperature was set to 27 °C, a trade-off between the temperature optimum of sunflower and the higher temperature optimum of maize (Kim et al., 2007). Greenhouse conditions were programmed to permit the maximum amount of light interception (i.e., shade cloth was only pulled during days where intense solar radiation and temperatures demanded additional cooling efforts). Daytime temperatures over the experimental period averaged 26.5 °C, but on some days the maximum daytime temperatures climbed higher despite continuous cooling. Supplemental humidity was provided to keep relative humidity around 50%, and the daytime vapor pressure deficit (VPD) averaged 1.8 kPa.

Biophysical measurements

Maize growth stages were determined when at least one-half of the plants had reached a stage as determined by the leaf collar method and visual indicators of kernel development. Sunflower growth stages were delineated following the methods of Schneiter and Miller (1981). During periods of destructive harvest, total laminar area per plant was measured with a leaf area meter (LICOR 3100, Li-Cor, Lincoln, NE). Plant biomass was dried in a forced-air oven at 60 °C for ≥ 72 hours and then weighed for determination of dry weight. The five tracked plants in each treatment were measured non-destructively over the season by taking length (L) and width (W) measurements of individual leaves and developing ratios and regression estimators, similar to the method outlined in Stewart and Dwyer (1999) and Rouphael et al. (2007). To develop the regressions, the length (L) and width (W) of individual leaves of field-grown plants were measured and then run through a leaf area meter. An equation of the form of leaf area = $a + b$LW was developed, where a and b are fitted coefficients. The r^2 values of the regression of measured versus calculated values were 0.96 and 0.97 for maize and sunflower, respectively. Leaves tended to shrink and become more brittle during senescence, which made leaf area measurements

less accurate. Hence, comparisons of leaf area measurements for tracked plants were made prior to the initiation of leaf senescence using developed regression equations. At the end of the study, tracked plants were destructively harvested to obtain biomass.

Gas exchange measurements

Two portable steady-state photosynthetic systems (Model Li-6400; LI-COR Inc., Lincoln, NE, USA) were used to measure gas exchange on expanded sunlit leaves near the top of the canopy. Response curves of leaf photosynthesis versus CO_2 concentration (A/C_i) and photosynthetically active radiation (A/Q_p) were conducted on five tracked plants per treatment during each measurement period. For the A/C_i curves, leaves were acclimated in the chamber at 25 °C (sunflower) or 31 °C (maize) at a controlled CO_2 concentration (400 μmol mol^{-1}) and light level (2000 μmol m^{-2} s^{-1}) for several minutes. Humidity levels in the cuvette were set at 55%, corresponding to a VPD of ≈ 2 kPa for maize and <1.5 kPa for sunflower. The CO_2 response curve was then initiated, with nine levels of CO_2 used to generate the A/C_i curves (400, 300, 200, 100, 50, 400, 500, 800, 1000, and 1500 μmol CO_2 mol^{-1}). After the completion of the A/C_i curve, CO_2 concentration was kept constant at 400 μmol mol^{-1} and Q_p was sequentially lowered from 2000 to 1500,1200, 1000, 800, 600, 400, 200, 100, 50, 25 and 0 μmol m^{-2} s^{-1}.

Leaf water potential

Daytime leaf water potential (Ψ_L) was measured on the same leaf immediately after the completion of the light response curves with a pressure chamber (PMS Instrument Company; Corvallis, Oregon). Prior to excision with a razor blade, leaves were wrapped in a plastic bag. Limited pre-dawn Ψ_L measurements were taken during measurement periods four and five to compare the recovery of the water-stressed plants with those in the well-watered treatment.

Leaf-level determination of leaf optical properties, Chlorophyll content, Nitrogen, and LMA

A Minolta SPAD-502 meter (Spectrum Technologies, Inc.) was used for non-destructive estimates of leaf optical properties and Chl content. The SPAD meter outputs a non-dimensional SPAD value (0 - 99) representing the transmittance in the near infrared, where absorbance is insignificant, and transmittance in the red, where light absorbance by Chl is high. Five readings were taken and averaged per leaf from the same leaves and in the same area as that of leaf gas exchange.

After the SPAD and Ψ_L measurement, ten leaf tissue discs of known area were taken from the leaf with a cork borer (13.25 mm inner diameter), with care taken to avoid large veins. Additional discs were taken from the same leaf for total N determination. Discs for Chl content were stored at -80 °C within 1- 2 minutes of collection until extraction. Discs for determination of leaf N, C, and LMA were dried at 60 °C for $\geq$ 72 hours and then weighed for dry mass determination. The tissue was then placed in glass vials and powder ground with a steel ball-mill grinder. Two replicates per sample of Total N and C composition were determined via mass spectrometry. The N and C analyses were conducted using a Europa Scientific automated nitrogen carbon analyzer (ANCA/NT) with a Solid/Liquid Preparation Module (Dumas combustion sample preparation system) coupled to a Europa 20-20 Stable isotope analyzer continuous flow isotope ratio mass spectrometer (Europa Scientific Ltd., Crewe, England). Measurements of LMA were used to convert leaf N and gas exchange parameters from an area to a mass basis. There were fewer observations of LMA and N_a for sunflower due to lack of data in the first measurement period.

For Chl extraction, samples were incubated in the dark with 40 mL of 95 % ethanol (v/v) at 25 °C for 24 hours, at which time discs were cleared of pigment. Ethanol is a safer solvent than acetone or methanol, and there are practical and economic advantages to using it (Ritchie,

2006). While others have reported that incubation time is not always positively correlated with extraction efficiency and that extracts can lose stability over time (Pompelli et al., 2013), a simple test of extraction times found less than a 2% difference between readings taken after 22, 24, 28, or 48 hour extraction times for either crop tissue. Tait and Hik (2003) also reported that a duration of incubation beyond 7 hours had little effect on extraction efficiency for sunflower tissue extracted with DMSO or 80% acetone.

4 mL of the extract was transferred to a 1 cm light path cuvette and analyzed using a dual beam spectrophotometer (Thermo Scientific GENESY 10S UV-Vis) at $A_{664.2}$, $A_{648.6}$, and A_{470} (Lichtenthaler, 1987). Absorbance at 750 nm was recorded on each sample to check and correct for turbidity, as Chls *a* and *b* and carotenoids do not absorb in this region. If absorbance was too high, samples were diluted to ensure that absorbance was less than 0.85, and typically below 0.7. All procedures were performed under dim fluorescent laboratory light with the samples covered to minimize light-associated degradation of chlorophylls. Chl *a*, Chl *b* and total Chl were determined using the equations of Lichtenthaler (1987) and Lichtenthaler et al., (2001).

Calculation of C3 and C4 Photosynthesis Parameters

For sunflower, a non-linear curve-fitting routine was used to estimate the parameters V_{cmax} and J_{max} from A/C_i curves (Sharkey et al., 2007). A_n is frequently assumed to be limited by the properties of Rubisco at a low C_i (Farquhar et al., 1980), whereas at higher C_i, assimilation is typically limited by the RuBP regeneration via electron transport. V_{cmax} was estimated from the lower region of A/C_i curves, where C_i was less than 20 Pa, while J_{max} and TPU were estimated when C_i was greater than 30 Pa. Data at the transition from the Rubisco to RuBP limited regeneration portion was excluded from the analysis. A_{max} was determined from A/Q_p curves, and was defined as the rate of A_n at ambient CO_2 concentration (400 μmol mol^{-1}) and Q_p of 2000

μmol m^{-2} s^{-1}. While we defined this as A_{max}, we were surprised to note that early in the season the light response curves of sunflower did not always show full saturation even at this high light level, but we were limited to this definition of A_{max} by the maximum light intensity of the controlled light source. This observation also refines our definition of J_{max} to the rate of electron transport supporting $NADP^+$ reductions for RuBP regeneration at the measurement light intensity (2000 PAR). Values of the ratio of intercellular to atmospheric CO_2 concentration (C_i/C_a) were also obtained from A/Q_p curves.

SAS PROC NLIN (version 9.4, SAS Institute Inc., Cary, NC, USA) was used to fit a simplified version of the biochemical model of C4 photosynthesis (Kim et al., 2007; Von Caemmerer, 2000). Maximum PEP carboxylase activity (V_{pmax}) was estimated from the initial slope of the A/C_i curves, while the rate saturated region was used to estimate maximum Rubisco activity (V_{cmax}). A/Q_p curves were used to estimate the maximum electron transport rate (J_{max}) as well as C_i/C_a. Values for A_{max} and the C_i/C_a ratio were determined from A/Q_p curves. A_{max} was defined as the rate of photosynthesis at ambient CO_2 concentration (400 μmol mol^{-1}) and Q_p of 2000 μmol m^{-2} s^{-1}. We note that maize, a C4 plant, does not always fully saturate at these light levels, but were limited to this definition by capabilities of the controlled light source.

Ancillary Field Measurements

To ensure that the physiology and growth parameters of greenhouse-grown plants were similar to field-grown plants, ancillary field measurements were made at the USDA-ARS LIRF field site. The same genotypes of maize and sunflower used in the greenhouse experiments were grown in the field under drip irrigation, with water applied to meet the full demands of evapotranspiration. A full description of the site and experimental design can be found in DeJonge et al. (2015). A/C_i and A/Q curves were run on a sample of well-watered maize plants

(n = 11) over a three-week period (DOY 205-226). SPAD and leaf nitrogen measurements were taken following curve completion in the same fashion as in the greenhouse. A similar number of curves were run on sunflower plants at the V17-19 (DOY 206) and R4 (DOY 226) growth stages. However, a portion of the sunflower curves had to be discarded due to a faulty thermocouple on the LiCor 6400, leaving a smaller number of curves for comparison of the parameter values of field-grown versus greenhouse grown plants (n = 5).

Statistical Analyses

Analysis of variance was performed to determine seasonal and treatment effects on biophysical variables. Each tracked greenhouse plant was an experimental unit and treated as a replicate (n = 5) for each treatment. Physiological parameters and leaf tissue samples were analyzed as repeated measures using the SAS MIXED procedure. Results were considered significant when $p < 0.05$. Regression analyses were used to determine the association among measured leaf variables (SPAD – Chl, Chl – N), and P_c parameters (N – A_{max}, N – V_{cmax}, A_{max} – V_{cmax}, V_{cmax} – J_{max},). Area-based and mass based linear regressions were performed, with A_{max} or V_{cmax} as the dependent variable against leaf N and/or LMA. Significant differences between slopes and intercepts as a function of treatment were evaluated by analyses of covariance. Multiple stepwise regression analysis was also used to more fully assess the relationships between V_{cmax} and other environmental and leaf variables (Ψ_L, θ_v, DOY, N_a, and LMA) with $\alpha = 0.05$ used as the criteria for entry into the model.

Results

Seasonal changes in A_{max}, V_{cmax}, and J_{max} and C_i/C_a in maize

A_{max} values declined over the season in both well-watered and water-stressed plants ($p = <0.0001$) (Figure 2; panel a). In the well-watered treatment, values were high and relatively

constant during the late vegetative and early reproductive stages (43.8 ± 5.6 μmol m^{-2} s^{-1}), and then fell off significantly below all previous measurements in late reproduction (25.2 ± 5.6 μmol m^{-2} s^{-1}). A_{max} values collected in the field under well-watered conditions (41.2 ± 3.0) were nearly identical to greenhouse values for similar growth stages. The water-stressed treatment showed steady declines in A_{max} immediately following water limitation (Figure 2; panel a). Water stress in maize was moderate to severe, resulting in 50% reduction in total dry matter allocated to stems and ears (Table 2). Severe water stress (i.e., Ψ_L at the time of measurement - 1.8 – 2.0 MPa) sometimes resulted in completely unresponsive leaves, with A_n values reaching near zero due to stomatal limitations, similar to the threshold of complete inhibition of A_n reported by Westgate and Boyer for maize (1985). Thus, A_Q curves were deemed invalid for several water-stressed plants, particularly during the third measurement period, resulting in a lower number of measurements of A_{max} under water stress. Despite the lower replication, treatment differences in A_{max} were evident by period three ($p = 0.0017$) and increased at period four ($p = 0.0002$).

Table 2**.** Biomass and leaf area of maize plants grown under well-watered and water-stressed conditions.

Parameter	Unit	Well-watered Maize	Water-stressed Maize	SE_{diff}	P
Total aboveground biomass	g $plant^{-1}$	325.1	190.9	13.3	<0.0001
Leaf biomass	g $plant^{-1}$	52.8	44.9	2.0	0.0039
Stem and ear biomass	g $plant^{-1}$	272.3	146.0	12.1	<0.0001
Leaf area	m^2 $plant^{-1}$	0.744	0.742	0.031	0.950

P is the probability that the difference between treatments is not significantly different from zero. Results were considered significant when $P < 0.05$. SE_{diff} represents one standard error of the difference between treatments.

V_{cmax} values were highest at the first measurement period for both treatments of maize, and declined seasonally thereafter ($p = <0.0001$) (Fig 2; panel b). Well-watered values decreased by

35% over the course of our seasonal measurements, from a high of 58.3 ± 3.3µmol m^{-2} s^{-1} during mid-vegetative growth to 37.7 ± 4.2 µmol m^{-2} s^{-1} during the dent stage. Values from field grown maize were closely comparable to greenhouse values for similar growth stages, averaging 54.0 ± 5.5 µmol m^{-2} s^{-1}. There were significant seasonal differences in well-watered V_{cmax} values for period one versus periods four and five, period two versus versus periods four and five, and period three versus periods four and five. Seasonal differences in the water-stressed treatment were significant for periods one and two versus period four. There was also an overall treatment effect ($p = <0.0001$), with treatment differences in V_{cmax} values evident at periods one, three, and four. Under water stress severe enough to induce complete mid-day leaf curling and reduce total seasonal biomass by 55%, the measured apparent V_{cmax} values were only reduced by 10 – 16 % at any period. Treatment differences at period one were unexpected, but examination of the soil θ_v data (Fig 1; panel b) shows a reduced θ_v for the water-stress treatment in the first measurement period, whereas the intent of the irrigation schedule was for all plants to remain well-watered until after the first set of measurements (Fig 1; panel b). Plants were growing rapidly during this period, and irrigation thresholds were difficult to determine. The water-stressed treatments of both crops were placed further from the evaporative cooler, with the well-watered treatment blocking airflow. Unfortunately, the microclimate in the greenhouse could not be blocked for due to the elaborate set-up of soil moisture sensors and automatic irrigation as well as space limitations

J_{max} values also showed significant seasonal variability, declining after the first measurement period for both treatments ($p = 0.0044$) (Fig 2; panel c). Similar to the pattern observed in V_{cmax}, well-watered J_{max} values declined 40% over the course of the season, from a high of 299.6 ± 40.6 µmol m^{-2} s^{-1} during the late vegetative to a low of 171.5 ± 28.8 µmol m^{-2} s^{-1}

during the dent reproductive stage. J_{max} values collected in the field under well-watered conditions (265.1 µmol m^{-2} s^{-1} ± 28.0) were closely comparable to greenhouse values for similar growth stages. There were significant seasonal differences in J_{max} at period one versus periods four and five, period two versus periods four and five and period three versus five. Water-stressed plants showed significant seasonal differences in J_{max} between period one and the three subsequent measurement periods and a treatment effect by period ($p = 0.0433$).

Seasonal C_i/C_a values in well-watered maize stayed constant until the last measurement period, at which point they dropped significantly (Fig 3; panel d). In the water stress treatment there were apparent reductions in the C_i/C_a ratio immediately after water was limited.

The seasonal relationship between J_{max} and V_{cmax} was strong for well-watered maize ($y = 5.81x – 31.27$; $r^2 = 0.79$, $p = <0.0001$), and while the slope and intercept for seasonally combined data did not change significantly between well-watered and water-stressed plants, the r^2 was lower for combined treatment data ($r^2 = 0.65$) (Fig 3). The slopes and the intercepts of the seasonal V_{cmax} - A_{max} relationship were not significantly different between treatments, so data was again combined over treatment into one seasonal regression (data not shown) ($y = 0.59x + 24.5$; $r^2 = 0.49$, $p = < 0.0001$).

Seasonal changes in A_{max}, V_{cmax}, J_{max}, and C_i/C_a in sunflower

There was an effect of measurement period ($p = <0.0001$) and treatment ($p = < 0.0001$) on A_{max} in sunflower as well as an interaction between these two main effects ($p = 0.0383$) (Fig 2; panel e). A_{max} values for well-watered plants were highest during the late vegetative period (45.2 ± 2.0 µmol m^{-2} s^{-1}), declined slightly during the early and mid-reproductive periods (37.2 ± 0.7 µmol m^{-2} s^{-1}), and then fell off in the late reproductive stage (22.5 ± 1.14 µmol m^{-2} s^{-1}). Values from field-grown plants at the late vegetative stage (49.5 µmol m^{-2} s^{-1} ± 3.5) were similar

to those measured in the greenhouse at a similar stage. Treatment differences were significant for the first three measurement periods, where A_{max} values for water-stressed plants were 20 – 28% below well-watered values. Differences at the first measurement period were again unexpected, but most likely due to reasons previously discussed. Water stress was strong enough in sunflower plants to cause severe reductions in leaf area and biomass, as well as lower total aboveground biomass (Table 3). By period four, A_{max} values for water-stressed plants appeared to recover, and were not significantly different than well-watered values.

V_{cmax} showed an effect of measurement period ($p = <0.0001$), treatment ($p = 0.0211$) and an interaction between these variables ($p = 0.0025$) (Fig 3; panel f). Average well-watered values varied by 20% during the first four measurement periods, gradually increasing from the late vegetative stage and early reproductive stages to a high of 210.4 ± 8.73 μmol m^{-2} s^{-1} at the R4 reproductive stage. Values declined at the R5.8 stage (170.8 ± 23.5 μmol m^{-2} s^{-1}) and then decreased another 30% to a low of 118.75 ± 12.5 during the R8 stage. The values obtained from field plants at the late vegetative stage (233.5 ± 18.8 μmol m^{-2} s^{-1}) were similar to but slightly higher than those obtained from greenhouse plants. Seasonal effects were not significant in the water-stressed treatment. Treatment differences in V_{cmax} were only significant after nearly three weeks of strong water limitation – leaves of plants in the water-stressed treatment appeared to completely lose turgor pressure at midday and rapidly senesced lower-canopy leaves. Values for the two treatments converged at period four, despite Ψ_L values in the water-stressed plants that averaged 0.5 – 0.6 MPa below the well-watered plants.

J_{max} followed a similar seasonal pattern as V_{cmax} (Fig 2; panel g), but showed only a 7% variation from the late vegetative through mid-reproduction stage (259.4 – 281.6 μmol m^{-2} s^{-1}). Values then declined during late heading at the R8 stage (185.5 ± 23.5 μmol m^{-2} s^{-1}). Seasonal

declines in the well-watered treatment were only significant at the final measurement period, when values were significantly lower than all other measurement periods. Measured values in field plants were again nearly identical to greenhouse values from similar growth stages (298.0 ± 19.1 µmol m^{-2} s^{-1}). Like V_{cmax}, seasonal changes in J_{max} were not significant in the water-stressed treatment. J_{max} values were only significantly different between treatments at period three.

There were no significant seasonal differences in the calculated C_i/C_a ratio for well-watered sunflower (Fig 3; panel h). The ratio was significantly lowered under water stress, falling sharply during periods two and three. At period four, C_i/C_a values increased significantly from the previous measurement period ($p = 0.0049$).

Correlations between $J_{max} - V_{cmax}$ and $V_{cmax} - A_{max}$ for Sunflower

The seasonal relationship between $J_{max} - V_{cmax}$ was highly significant in sunflower (Fig 3). There were no significant differences in the slope or intercept as a function of treatment, so data were combined. The positive intercept we observed has also been reported by others (Grassi et al., 2005; Wullschleger, 1993) (add Wilson et al. 2001).

The V_{cmax} - A_{max} relationship was significant for the well-watered treatment of sunflower (data not shown) ($y = 2.98x + 67.7$; $r^2 = 0.48$, $p = <0.0001$). While the slope and intercept were not significantly different between treatments, the predictive ability of the model was lower when treatments were pooled ($y = 2.37x + 95.2$; $r^2 = 0.36$, $p = <0.0001$).

Leaf mass per area, Area-based leaf N, Chlorophyll, and SPAD in maize

LMA increased in a linear fashion seasonally for both treatments of maize (Fig 4; panel a) with an effect of measurement period ($p = <0.001$) and treatment ($p = 0.0196$). The LMA of water-stressed maize dropped below well-watered values after approximately a month of water

stress ($p = 0.0065$). While dry matter allocation to the leaves was lower under water stress, there was not a treatment effect on leaf area.

In comparison to LMA, N_a showed only small seasonal increases, but the effects of both measurement period ($p = 0.0123$) and treatment ($p = <0.0001$) were significant, and there were differences in N_a between treatments at periods one, three, and four (Fig 4; panel b). Well-watered values for greenhouse maize ranged from 1.77 – 1.95 g N m^{-2} over five measurement periods, averaging 1.86 ± 0.12 g m^{-2}. Values of N_a from field plants were very similar (1.67 – 2.03 g m^{-2}) to values in greenhouse plants, averaging 1.84 ± 0.13 g m^{-2}. Peak well-watered N_a values occurred three weeks after peak values for A_{max}, V_{cmax}, and J_{max}.

There was an effect of measurement period ($p = 0.0003$) and treatment ($p = 0.0003$) on total Chl (*a* + *b*) content in maize, as well as an interaction between the two main effects ($p = 0.0002$). Changes in Chl content did not always match temporal changes in N_a. Well-watered Chl increased by 18% between the first and second measurement periods in well-watered plants, whereas N_a values showed no increase. Total Chl in well-watered plants increased an additional 25% between periods two and three, while N_a increased by only 9%. Chl levels then stayed elevated for the duration of the experiment, showing no sign of decline even as leaves showed evidence of physiological decline as indicated by reductions in A_{max}, V_{cmax}, and J_{max} (Fig 4; panel *c* and Fig. 2 panels *a-c*). Total Chl was significantly lower in water-stressed plants at period three and period four. Declines in Chl content under water stress were temporally matched to declines in N_a, but Chl declined more strongly than N_a under water stress at period four. Leaf concentrations of Chl *a* and Chl *b* followed similar patterns as total Chl, with an overall seasonal average of 63.1 and 14.2 ug cm^{-2}, respectively. The ratio of Chl *a:b* did not change over the season in maize, and although it was lowered by water stress, the results were not significant ($p =$

0.0675). The overall seasonal average of the Chl *a:b* ratio was 4.5 ug cm^{-2}, similar to the ratio reported by Kim et al., (2006) for another genotype of maize, but markedly higher than those reported by Makino et al., (2003).

Seasonal patterns of SPAD values generally followed changes in total Chl (Fig 4; panel d) but showed some temporal discontinuities. For example, well-watered SPAD values increased significantly at period four, whereas total Chl stayed constant. At period three, total Chl content in well-watered plants increased from the previous period by 25%, whereas SPAD readings showed no change. At period four well-watered SPAD readings increased 7% percent as total Chl stayed steady, whereas at period five total Chl declined 7% while SPAD values declined only 0.5%. Field SPAD values were in a similar range for comparable growth stages as greenhouse values (56.8 ± 4.0).

Leaf mass per area, Area-based leaf N, Chlorophyll, and SPAD in sunflower

In sunflower, LMA initially increased over the season in both treatments and then stayed steady (Fig 4; panel e), with an effect of measurement period ($p = <0.001$), a borderline effect of treatment ($p = 0.0636$) and an interaction between period and treatment ($p = <0.0001$). Water stressed sunflower leaves had higher LMA than well-watered leaves at period two, but by period three new leaves were no longer emerging, and reductions in A_n likely curbed further increases in LMA.

N_a showed an effect of measurement period ($p = <0.0001$), as well as a significant interaction between period and treatment ($p = 0.0015$). Well-watered values for greenhouse sunflower ranged from 2.12 – 3.2 g m^{-2} with a seasonal average of 2.58 g m^{-2} ± 0.53. Leaf N_a levels from well-watered field sunflower plants were similar to greenhouse values, ranging from 2.30 – 2.78 g m^{-2} (DOY 206 – 226), and averaging 2.52 ± 0.21 g m^{-2}. N_a increased during the

vegetative and head-filling period, and declined at the late reproductive stage (Fig 4; panel f). Water-stressed plants showed higher N_a than well-watered plants after three weeks of water stress, but N_a levels between treatments converged after a month of stress.

In contrast to maize, total Chl did not increase seasonally in well-watered sunflower (Fig 4; panel g), and did not track changes in N_a or P_c parameters. Total Chl did show small but significant declines under water stress (Fig 4; panel g). Interestingly, Chl *a* levels showed no effect of measurement period ($p = 0.2280$), but were lowered under water stress at periods two and three ($p = 0.0031$), while Chl b levels were not influenced by treatment ($p = 0.3945$) but were influenced by measurement period ($p = < 0.0001$). The ratio of Chl *a:b* decreased significantly over the course of the season and was further lowered by water stress. There were no changes in SPAD readings seasonally ($p = 0.1934$) or by treatment ($p = 0.4231$) in sunflower. SPAD values from field-grown plants (38.09 ± 4.58) were in a similar range as greenhouse plants (42.3 ± 2.1).

Correlations between Leaf Properties

Total SPAD – Chl

Exponential equations are frequently used to convert SPAD measurements into leaf Chl content, as the relationship deviates from linearity in the high and low ranges of SPAD values (Maxwell et al., 1995, Houborg et al., 2009). An overlay of an exponential equation developed by Houborg et al. (2009) shows that our maize data conforms to their equation, but the smaller spread of our observed values did not warrant an exponential fit (Fig. 5). We obtained a linear correlation of $r^2 = 0.60$ for maize (Fig 5, inset), similar to but lower than the correlations reported in other studies (Houborg et al., 2009; Markwell et al., 1995). Although some studies have reported significant differences in the SPAD –Tot Chl relationship for well-watered versus

water-stressed plants (Schepers et al., 1996; Schlemmer et al., 2005) our regression coefficients for seasonally combined data were not significantly altered by water stress.

Markwell et al. (1994) found that the same exponential equations developed for maize and soybean could be applied to determine leaf Chl concentration of field grown sorghum and *Arabidopsis thaliana* plants, and that the determination of Chl per unit area was relatively independent of species. Hence, the Houborg et al., (2009) equation could also be expected to describe the Chl content of sunflower. While our data clusters on the equation, we obtained virtually no spread in our SPAD or Chl values, and hence no significant relationship, despite repeated sampling over the course of two months as plants moved from the late vegetative to late reproductive stages.

Total Chl – N_a

We found the correlation between total Chl and N_a to be relatively poor for maize, with N_a showing only small changes in comparison to Tot Chl (Fig 6). Schlemmer et al. (2013) reported a strong linear relationship between leaf N content and leaf Chl in maize in combined seasonal data (r^2 = 0.73) although the slope varied throughout the growing season. Our weaker correlation does not appear to be solely due to a lack of spread in our data, as lower or higher leaf N contents would not necessarily change the weak slope of the relationship we observed. No significant correlation between N_a – Chl was observed for sunflower (Fig 6). Total Chl stayed constant in sunflower and did not follow seasonal changes in N_a (Fig 4; panels f and g).

Correlations between Leaf Properties and Photosynthetic Parameters

Leaf Chl – N – A_{max} – V_{cmax}

There were no significant seasonal relationships between Chl content and V_{cmax} (data not shown). The relationship between N_a – A_{max} and N_a –V_{cmax} for seasonally combined data was

also not significant for either crop (Fig 7; panels a-d). Visual inspection of the data shows that the lack of correlation was due to opposite patterns between crops. N_a in maize showed a comparatively small increase over the season when compared to sunflower, but steady increases in LMA (Fig 4; panel a-b). N_a increased weakly but significantly with LMA in maize, but was not impacted by treatment until period four, hence one regression pooled over treatment best described this relationship (Fig 7; panel e). In sunflower, changes in N_a were large and closely tracked changes in LMA in the late vegetative and early reproductive growth stages (Fig 4; panels e-f). This resulted in a highly significant relationship between N_a and LMA in sunflower for both treatments for the second and third measurement periods (DOY 197 – 232) (Fig 7; panel f). However, in the last two measurement periods, the LMA of some well-watered sunflowers stayed high even as N_a declined. This resulted in points with high leverage in the regression as indicated by leverage plots. Exclusion of well-watered data from periods four and five (designated by filled triangles) improved the coefficient of variation from an r^2 of 0.53 to an r^2 of 0.72.

There was a highly significant negative correlation between N_m and LMA in maize due to increases in LMA with only small increases in N_a, (Fig. 4; panels a-b), resulting in a linear seasonal reduction in N_m (Fig 8; panel a). The slope of the N_m – LMA relationship was lowered under water stress ($p = 0.03$) as was the intercept ($p = <0.0001$), but the correlations were strong for both the well-watered and water-stressed treatments ($R^2 = 0.90$ and 0.80, respectively). The C/N ratios of the leaf tissue also showed a linear seasonal increase, indicating that increases in LMA were due largely to increases in carbon containing compounds (Fig 9). Interestingly, examination of leaf C also shows a marked decline under well-watered conditions after the third measurement period, which was at the beginning of the reproductive growth (R1) stage,

suggesting export of stored assimilate to the grain. This large drop in % C is not seen in the water stressed treatment, which could be due to decreased carbohydrate export (Chaves et al., 2002).

Mass-based relationships between leaf N – A_{max} (R^2 = 0.88) and leaf N – V_{cmax} (R^2 = 0.80) were highly significant in maize (Fig 8, panels c and e). The slopes and intercepts were not significantly different between treatments for either variable, so the data were combined into one regression.

In sunflower, the significance of the mass-based N_m – LMA relationship was dependent on inclusion of the same points that were excluded to improve the N_a –LMA relationship (Fig. 8; panel b). When only four well-watered points with high-leverage from DOY 253 are excluded, there is no significance. Regression on all data results in a poor but significant relationship (y = -854.18x + 95.03; R^2= 0.32). In contrast to the linear decline in % N under water stress in maize, leaf % N increased under water stress in sunflower, and showed an initial increase and then decrease in well-watered plants (Fig 9; panel e). Leaf C declined in parallel with N, resulting in very little seasonal change of the C/N ratio (Fig 8; panel f).

The N_m - A_{max} relationship was weak but significant for combined sunflower data (R^2 = 0.26) (Fig 8; panel d). Exclusion of water stressed data improved the regression (R^2 = 0.50), however, the strength again hinged on the inclusion of high leverage data points from late in the season. Exclusion of points from DOY 253 resulted in a weak but significant correlation (R^2 = 0.24).

Prediction of V_{cmax} from environmental variables and leaf properties

Maize

Stepwise regression showed that for well-watered maize, the inclusion of LMA alone explained 83% of the variation in V_{cmax} (y = -1.01x + 93.64). No other variable met the

significance level for entry into the model. N_a was not a significant predictor of V_{cmax} in well-watered plants. The tight correlation between LMA and DOY in maize (r = 0.93) allowed either LMA or DOY to be used with the same predictive ability. Measurements of Ψ_L grew more negative towards the end of the season even in the well-watered treatment. Mid-day Ψ_L potential measurements for maize grown under well-watered field conditions (where rooting depths and water were not limited) also become more negative towards the end of the season (Louise Comas, USDA-ARS, personal correspondence). The relationships between Ψ_L and V_{cmax} was weak but significant in the well-watered treatment (V_{cmax} – r^2= 0.33; p = 0.0064)

For the water-stressed data, Ψ_L alone explained 70% of the variability in V_{cmax} (y = -1.15x + 59.06), and no other variables were significant. For data combined over treatment, LMA explained 53 % of the variation in V_{cmax}. N_a was not a significant stand-alone predictor of V_{cmax}, but the best two-variable model on combined data included both LMA and N_a (r^2= 0.72; Table 5), with no other variables meeting significance for entry into the model. The mass-based V_{cmax} – N_{leaf} relationship was stronger than the area-based model (Table 4).

Sunflower

Data for sunflower was much more convoluted than for maize, as seasonal trends in LMA and N_a diverged by treatment. Significant predictor variables of V_{cmax} in well-watered sunflower via simple linear regression were DOY (R^2 = 0.70), LMA (r^2 = 0.41), and Ψ_L (R^2 = 0.29). In step-wise regression, DOY alone explained 70% of the variability in V_{cmax}, with no other variables meeting the criteria for entry into the model. All variables showed high and significant Pearson correlations with DOY except for θ_v. In water stressed sunflower, V_{cmax} could not be predicted by any variable via simple linear regression or step-wise regression, although N_a was nearly a significant predictor (p = 0.07). For combined sunflower data, only DOY met the

significant level for entry into the model (R^2 = 0.48). Pearson correlations were significant between V_{cmax} and Ψ_L (r = -0.40; p = 0.01), V_{cmax} and LMA (r = -0.51; p = .002), and V_{cmax} and DOY (r = -0.59; p = <0.0001). Correlations were also significant between DOY and Ψ_L (r = 0.42; p = 0.01), DOY and LMA (r = 0.82; p = <0.001) and DOY and N_a (r = 0.52; p = 0.001).

Table 3. Regression coefficients for V_{cmax} versus N_a and LMA, and the mass-based coefficients (V_{cmax_m} versus N_m) for well-watered and water-stressed maize combined (n=36). Significance of the slopes and non-zero intercepts were P < 0.05 (*), P < 0.01 (**), P <0.001 (***). Units: V_{cmax} = μmol m^{-2} s^{-1}; V_{cmax_m} = μmol g^{-1} s^{-1}; N_a= g N m^{-2}; N_m = g g^{-1}; LMA = g m^{-2}.

	$V_{cmax} = b_0 + b_1N_a$	$V_{cmax} = b_0 + b_1LMA$	$V_{cmax} = b_0+b_1N_a + b_2LMA$	$V_{cmax\_m} = b_0 + b_1N_m$
b_0	52.47	80.69***	46.67***	-1.17***
b_1	-2.67	-0.77***	26.40***	54.92***
b_2	na	na	-1.08***	na
R^2	0.00	0.53	0.72	0.83

The mass-based V_{cmax} – N_{leaf} relationship was significant for well-watered sunflower (r^2 = 0.40; p = 0.003), but there was no significant relationship in water-stressed sunflower and a poor relationship for combined data (R^2 = 0.20; p = <0.01).

Discussion

Seasonal Variability in P_n parameters

Values of V_{cmax} and J_{max} are typically higher for agricultural species than for trees or other plant functional types, and our values reflect this (Wullschlger 1993; Leuning 1998; Medlyn 1999). While literature values for maize P_c parameters are scarce, our observed values of A_{max},V_{cmax}, and J_{max} are similar to values reported for maize (Kim et al. 2006) and the range of our V_{cmax} values encompasses the values currently utilized in several climate models. For example, the crop specific version of the Simple Biosphere Model (SiBcrop) utilizes a V_{cmax} value of 54 μmol m^{-2} s^{-1} (Lokupitiya et al., 2009) while the Community Land Model sets V_{cmax} at

57 μmol m^{-2} s^{-1}, and adjusts the value down under N limitations (CLM4, http://www.cesm.ucar.edu/models/ccsm4.0/clm). The literature is similarly sparse on parameter values for sunflower, with seemingly disparate findings. The values for *Helianthus annuus* in the seminal Wullschleger (1993) paper vary by a factor of five – average V_{cmax} values range from 29 – 163 μmol m^{-2} s^{-1}, and J_{max} values range from 113 – 259 μmol m^{-2} s^{-1}. The values we obtained are similar to but slightly higher than the values published by Sobrado and Turner (1986).

The general reported pattern of seasonal changes in V_{cmax} and J_{max} is characterized by an increase in values during leaf development, a maximum in spring or early summer, a steady state or gradual decline during summer, and a further decline during leaf senescence (Xu and Baldocchi, 2003, Medvigy, Grassi et al. 2005, Wilson et al. 2000, Bauerle et al. 2012). In maize, our peak values were observed in the V8 growth stage, and declined thereafter, whereas the pattern of V_{cmax} in well-watered sunflower showed more of the characteristic bell-shaped seasonal response. Our measurements did not encompass the earliest growth stages for either crop, and did not capture the early season increase in LMA and V_{cmax} frequently observed in new leaves that are building physiological and structural capacity (Xu and Baldocchi 2003). Well-watered J_{max} values closely tracked V_{cmax} in both crops, resulting in a positive seasonal relationship between J_{max} and V_{cmax} similar to that reported for trees (Grassi et al. 2005; Wilson Baldocchi and Hansen et al. 2000). While the slope values obtained via regression are slightly different than ratios calculated from average literature values, the calculated ratios are useful for comparison. The slope of the relationship between $J_{max} - V_{cmax}$ we observed in maize is similar to the ratio of 5.2 calculated from the mean values in Kim et al. (2006), and lower than the ratio of 6.6 calculated from generic C4 model parameters (Von Caemmerer, 2000). In sunflower, seasonal patterns of changes in J_{max} also closely tracked changes in V_{cmax}, and the overall

seasonal ratio of J_{max}: V_{cmax} was 1.43 ± 0.14. This ratio is slightly lower than the average values reported for C3 species (Wullschleger 1993; Medlyn et al. 2002). J_{max} : V_{cmax} ratios of published mean values for sunflower (i.e., with no information on the intercept) range from 1.62 – 4.6 (Wullschleger 1993).

Others have found the ratio of J_{max}:V_{cmax} to changes by as much as 30 - 60% seasonally, suggesting that N allocation to electron transport and Rubisco does not always occur in parallel (Xu and Baldocchi; Wilson et al. 2000), while some studies have found no evidence of a significant seasonal trend in the ratio (Grassi et al. 2005; Medlyn et al. 2002). While we did not have enough observations at each measurement period to run individual regressions, the mean ratio of J_{max}: V_{cmax} only varied by around 15% between measurement periods for both crops, suggesting that a constant ratio could be utilized seasonally to estimate J_{max} from V_{cmax} for these field crops.

A_{max} is not always a good measure of photosynthetic capacity, but when V_{cmax} data is not available, knowledge of the A_{max} – V_{cmax} relationship can be useful for estimating V_{cmax} (Kattge et al. 2009). Area-based A_{max} values were significantly related to V_{cmax} for both crops, but correlations were not generally as strong as the correlations reported in trees (Xu and Baldocchi 2003), which could result in propagation of errors if A_{max} is used to estimate V_{cmax} (Ali et al. 2015).

Field crops undergo rapid and large ontological changes, where crops like maize and sunflower can progress from seedling emergence to senescence in 100 to 120 days. Alternately, net productivity may extend for 200 – 250 days of the year in forest species (Wilson et al., 2001; Xu and Baldocchi, 2003). Utilization of seasonal values of physiological parameters instead of average or peak values better captures temporal shifts in productivity (Medvigy et al., 2013).

This is particularly important when modeling changes in growth or productivity, such as yield forecasting. For example, Houborg et al., (2013) found that while using a set value of V_{cmax} in model simulations of maize provided a good fit to observations during the vegetative stage, a static value caused significant overestimations in gross primary productivity during the reproductive and senescence stages. Our measurements support the seasonality of parameter values in maize and sunflower and indicate that peak P_c values in these crops last for less than two weeks.

Changes in P_n parameters under water stress

The effects of drought on P_c are notably diverse and sometimes contradictory, with some supporting g_s limitations to A_n and others concluding that P_c is impacted under moderate stress (Chaves and Oliveira, 2004; Lawlor and Tezara, 2009). Although species type, growth conditions, and experimentation methods all influence the relative effects of stomatal versus metabolic limitation, responses are also dependent on the magnitude and duration of the stress. For example, it is widely known that responses to rapidly induced water stress differ from plant responses to gradually imposed or long-term water shortages (e.g., Chaves et al., 2003; Lawlor and Tezara, 2009), and it is likely that both limitations were present in this experiment.

V_{cmax} values in maize were reduced by water stress, but the overall seasonal declines were larger than the apparent reductions induced by drought. The reductions in leaf area and increases in N_a that occurred in water stressed sunflower were not observed for maize - instead, water stress resulted in significantly lower N_a with no changes in leaf area. The lack of a water stress impact on leaf area in maize is likely due to the timing of the imposed stress. Cell division is inhibited under water stress, leading to smaller leaves, and leaf enlargement in maize has been shown to be sensitive to water stress (Boyer 1970). However, leaf appearance in maize is

visually delayed, insofar as the leaf tip must extend beyond the previous leaf sheath. Vegetative phytomers would already have been largely formed by the time water stress was imposed (Hay and Porter, 2006) which resulted in no reduction of leaf area.

Reductions in the C_i/C_a ratio occurred in maize immediately after the imposition of water stress, pointing to stomatal limitations, which are often an initial water-stress limitation to A_n. The observed declines in C_i/C_a make it unclear whether there were corresponding changes in P_c too. While the declines in V_{cmax} under water stress may have been initially driven solely via stomatal limitations, long-term water stress in corresponded with declines in N_a, strong declines in Chl, and eventual declines in LMA, suggesting that long-term stress affected both the structural and biochemical leaf properties. Declines in Chl and N content under water stress could have been due to a limitation of chloroplast synthesis, to chloroplast degradation with subsequent remobilization of proteins, to changes in leaf Rubisco content, or to reductions in in N uptake (Buchanan et al., 2000).

In sunflower, drought stress resulted in an initial reduction in both V_{cmax} and J_{max}, but after prolonged drought there was no significant difference between treatments. Overall seasonal declines in V_{cmax} and J_{max} were greater than declines under water stress. Both short-term and long-term responses to water stress appeared to be present in sunflower (Lawlor and Tezara 2009). Stomatal limitations were evident via reductions in the C_i/C_a ratio. Sunflower leaves were still forming and expanding when water limitation occurred, which resulted in a reduction in leaf area – sunflower leaf expansion is very sensitive to water stress and inhibited under mild stress levels that have nominal impacts on A_n (Boyer, 1970). However, while leaves that formed and expanded under water stress were smaller, they showed increases in N_a and LMA, similar to patterns reported by Penuelas et al. (1994). Increases in N_a and LMA permit better light

interception and water use efficiency (Chaves et al., 2002) and likely contributed to a recovery in P_c and smaller reductions in A_n even with reduced photosynthetic area. The ratio of C_i/C_a increased after prolonged water stress, suggesting the same pattern of recovery from or acclimation to water stress as other P_c parameters. These results suggest that reductions in A_n under long-term water stress in sunflower may be due to lower total photosynthetic leaf area rather than strong reductions in P_c capacity.

If drought induced changes to mesophyll resistance (g_m), the apparent reductions in V_{cmax} we observed under water stress could be influenced by changes in g_m, as we assumed this to be constant (i.e., the small reductions under water stress may be even less than measured). Increases in the resistance to CO_2 diffusion in the mesophyll can occur under water stress, and if resistance is sufficiently large to decrease the CO_2 concentration from the intercellular spaces (C_i) to the sites of carbon assimilation in the chloroplast, overestimation of the metabolic limitations can occur (Chaves and Oliveira, 2004; Flexas et al., 2008).

Criticisms surrounding measurements of V_{cmax} under water stress also often focus on the confounding effect that patchy g_s can have on interpretations of A/C_i curves. Patchy g_s is the term used to describe the variations in spatial and temporal response of stomata in adjacent areas of a leaf – a 'patchy' distribution of stomatal behavior can produce artifacts in gas exchange calculations (Buckley et al., 1997; Mott and Buckley, 2000; Terashima et al., 1988). Patchiness can cause ambiguity as to whether reductions in A_n are due to changes in the pattern of stomatal opening or true reductions in P_c (i.e., stomatal limitations vs. the biochemical inhibition of photosynthesis). With stomatal patchiness, C_i calculations are impacted – A_n is less than it would be if g_s patterns were homogenous, and hence calculated values for C_i are inaccurate (Buckley et al., 1997; Terashima et al., 1988). There is still active debate about the conditions under which

patchy g_s influences gas exchange data, as not all cases of heterogeneous conductance produce large differences in C_i (Buckley et al., 1997; Mott, 1995). One leading proposed cause of patchy g_s is that it is a consequence of leaf hydraulic architecture, where the vascular flow dynamics caused by the reticulate vein network in dicot leaf tissues cause variation in resistance pathways, contributing to patchy stomatal closure (Mott and Buckley, 2000). Given the uniform monocot veination pattern of maize, it is unlikely that hydraulically driven patchiness occurred. We cannot discount that patchiness could have occurred in sunflower, as some of the earliest studies on this phenomenon utilized sunflower plants to demonstrate the artificial depression in C_i that could be induced by application of ABA (Terashima et al. 1988). Sunflower has been found to show strong diurnal variation in extravascular leaf resistance modulated by changes in circadian rhythms and light levels (Nardini et al., 2005). However, others have observed no inhomogeneities in stomatal apertures in field-grown sunflower, with patchiness only induced by severing the tap root to allow rapid drying of the leaf (Wise et al., 1991).

Whatever the mechanism of reduction in P_c under water stress, modeling seasonal water stress responses will likely require incorporation of multiple limitations (i.e., stomatal, biochemical, and diffusive) as well as methods of downscaling parameters under stress (Egea et al., 2011). Some models account for water stress via parameter dependence on soil water potential or θ_v whereas others use Ψ_L (Egea et al., 2011). Experiments in maize have shown that stomatal responses to water stress are frequently more closely linked to soil moisture and chemical signals originating from the roots, rather than to leaf water status (Chaves et al., 2002; Tardieu et al., 1991). Maize exhibits isohydric behavior by reducing g_s to limit transpiration, resulting in Ψ_L that does not depend strongly on soil water status until water stress becomes moderate to severe. The lack of correlation between θ_v and reductions in P_c parameters in maize

and the significant negative correlation with Ψ_L under water stress is likely a function of our experimental design, wherein the θ_v stayed relatively constant between plants within a treatment, even as plants grew larger and atmospheric demand increased. Sunflower, on the other hand, is an anisohydric species, maintaining g_s and A_n at the expense of declines in Ψ_L (Tardieu and Simonneau, 1998). The significant but poor correlation in water-stressed sunflower between V_{cmax} and Ψ_L suggests that this may not always be a useful variable for downscaling V_{cmax} in response to water stress, despite the typically anisohydric behavior of sunflower.

Leaf-level relationships for predicting photosynthetic parameters

Chl-SPAD

Seasonal patterns of Chl and SPAD generally followed each other in maize, showing only small temporal incongruities in the direction and magnitude of change between measurement periods. The small spread of our observed values for SPAD and Chl is likely due to the conditions of high fertility during growth. SPAD - Chl relationships are frequently developed over intentional gradients in fertility and water availability. For example, Houborg et al. (2009) derived an empirical SPAD - Chl relationship with maize leaves sampled over two seasons from different plots with varying N fertilization and obtained SPAD values as low as 25 and leaf Chl ranging from around 10 - 90 ug cm^{-2}. Others have reported maximum Chl contents in maize of only 60 ug cm^{-2} (Schlemmer et al. 2013). In comparison, our greenhouse SPAD values ranged from 45 -75 and our Chl content ranged from approximately 46 - 100 µg cm^2.

We observed no significant relationship between Chl - SPAD in sunflower, as values for both variables did not change over the season. Other studies have found only small variation in canopy profiles of SPAD values for sunflower, which suggests that sunflower maintains high Chl contents in leaves throughout the canopy. Sadras et al. (2000) examined leaf SPAD as a function

of leaf node position and reproductive stage in sunflower, and reported values from upper canopy leaves that hovered around 40 despite repeated sampling for six weeks after flowering. The lack of spread in our values is likely due to high fertility growth conditions. This does not imply that the Chl - SPAD relationship is not potentially useful, but rather that our values did not indicate seasonal variation.

N_a – Chl

While the N_a - Chl relationship was significant in maize, the slope was much lower than observed by others (Houborg et al. 2009; Schlemmer et al. 2013). The slope of the N_a – Chl relationship can change as a function of developmental stage (Baret et al. 2007), with a higher slope reported in early growth stages, presumably due to N uptake outpacing the production of Chl (Schlemmer et al. 2013). However, the bulk of our measurements were taken after the late vegetative growth stage as growth rates become linear, at which point the slope of the relationship is reported to be relatively stable (Schlemmer et al. 2013). Our comparatively poor correlation may be due to a leveling off of the slope at high rates of fertilization, as our leaf N_a and Chl values are as large or larger than the values reported elsewhere (Schlemmer et al., 2013; Houborg 2009). Many crop species have potential to accumulate N in the form of organic N or nitrate at levels well above the critical minimums required for maximum growth rate (Hay and Porter 2006). High levels of fertilization may have resulted in saturated levels of leaf N even as the amount of total Chl changed. Leaf N and Chl content also typically peak or show a broad maximum around the ear node in maize (Hay and Porter, Sadras et al. 2006), which is where the bulk of our measurements were taken.

Our seasonal compilation of values into one regression for maize may have masked some important temporal incongruities in N_a and Chl. For example, well-watered maize leaves

continued investment in the production of Chl during the vegetative and early reproductive stages, whereas N_a values showed only nominal increases during this period. Towards the end of the season the reverse pattern was observed, with N_a declining more rapidly than Chl.

One possible reason for divergence of the Chl - N_a relationship relates to the 'stay-green' trait. Modern plant breeding has tended to select for enhanced functional life of upper canopy crop leaves, as there is typically a positive correlation between the duration of green leaf area and yield (Hay and Porter 2002). Stay-green characteristics can be achieved via delayed senescence, a slower rate of senescence after initiation, or a cosmetic retention of Chl even as senescence is proceeding normally within the leaf (Thomas and Howarth 2000). In maize, stay-green characteristics have been identified in which Chl is retained even as levels of photosynthetic enzymes decline (Thomas and Howarth 1993). Alteration of Chl catabolism that results in retention of Chl even as Rubisco and other soluble stroma proteins are degraded and remobilized could cause errors in the Chl-N relationship late in the season. There is also evidence that some 'stay-green' lines show elevated Chl in comparison to lines that lack the stay-green trait (Thomas and Howarth 2000), thus maintaining end of season greenness by virtue of having a higher point from which Chl levels must fall. This could presumably contribute to continued investment in Chl even after peak P_c was reached.

In sunflower, total Chl showed virtually no change over the season, but the ratio of Chl *a:b* decreased significantly and was further decreased under water stress. Variations in this ratio are frequently reported as adaptations to gradients in light availability within the canopy (Lambers et al., 2008). The light harvesting antenna complexes contain both Chls *a* and *b*, whereas only Chl *a* is contained in the light reaction centers. Shade tolerant or shade-acclimated plants compensate for low light by increased investment in light harvesting complexes, resulting

in a lower ratio of Chl *a:b*. The seasonal decrease in the ratio of Chl *a:b* we observed may reflect a response to the prevailing light environment, as day length and available PAR decreased throughout the study. Yang et al. (2014) found small seasonal variations in the ratio of Chl *a:b* in a white oak dominated canopy, but we know of no other study that has reported such strong variations in the Chl a:b ratio for sunlit leaves, and thus do not know how common this response is in crop plants. Chl *b* is synthesized from Chl *a*, and the fact that there were no changes in Total Chl suggests the conversion of existing Chl *a* into Chl *b* rather than Chl catabolism and regeneration (Buchanan et al., 2000).

Total Chl stayed constant in sunflower, even as N_a varied, and total Chl did not follow any of the seasonal changes in P_c parameters. Total Chl also stayed high during the final measurement period, even as well-watered values for N_a and V_{cmax} declined by 15 % and 30%, respectively. Total Chl does not appear to be a useful indicator of N_a or P_c in sunflower.

N – V_{cmax}

Expressing N per unit ground area is more relevant for models driven by remotely sensed data than mass-based expressions (Ollinger et al. 2008). If changes in P_c were determined solely by changes in N_a, a single regression of V_{cmax} against N_a would suffice for the entire season. However, we found the area-based V_{cmax} – N relationship to be non-significant for both maize and sunflower. Area-based relationships are sometimes poorer than mass-based relationships, particularly if there are large seasonal changes in LMA (Leuning et al., 1991; Reich et al., 1998; Reich et al., 1997). Conversely, some studies have found stronger area-based than mass-based relationships – this has been reported when variability in P_c is due to species or canopy position (Grassi et al. 2005; Wilson et al. 2001). For example, when variations in both V_{cmax} and N_a are mostly a result of vertical changes in LMA, significant area-based relationships can occur even

as N_m stays fairly constant throughout the canopy. In contrast, temporal changes in V_{cmax} are not always well described by changes in leaf N_a, and the strength of the relationship is sometimes affected by both leaf ontogeny and drought (Grassi et al. 2005, Wilson et al. 2000).

The lack of an area-based relationship may be partly due to fertilization. Grassi et al. (2005) found that the area-based V_{cmax} – N relationship tended to flatten at high N_a values, concluding that the photosynthetic return per unit N decreases when N is abundant in the leaf. In many natural ecosystems, the availability of N represents a key constraint to productivity (Olinger et al. 2008), whereas in agriculture systems N is often applied at saturating levels. For example, Hay and Porter (2006) argue that it is unlikely that serious limitation to A_n are experienced under the levels of N found in the radiation rich top of the canopy of most agronomic systems.

Our results suggest that N_a cannot be used as a standalone predictor of P_c in well-fertilized maize or sunflower. In sunflower, N_a values continued to increase even as P_c showed only small variations, and then peaked only after declines in V_{cmax} were already evident. Even though sunflower LMA and N_a were highly correlated, indicating that additional tissue was high in N, V_{cmax} did not follow a seasonal trend with these two variables. Seasonal changes in N_a were small in both maize treatments, except for very early and or late in the season, and N_a was only a significant predictor of V_{cmax} when it was included in a model alongside LMA or DOY. While we did not capture the early increases in LMA that occur during leaf expansion, LMA increased steadily from the mid vegetative to late reproductive stages in both treatments of maize. This linear pattern of increase in LMA is different than patterns of increase reported in perennial species, where LMA increases rapidly during the spring and remains constant or increases very gradually during the summer and declines towards the end of the season (Xu and Baldocchi

2003; Grassi et al. 2005). Maize LMA increased steadily over the season even as N_m declined, indicating that while leaves were thickening, the additional tissue was not high in N. Seasonal variations in LMA rather than N_a primarily drove changes in maize N_m. Others have also found linear seasonal increases in LMA in maize that only level off towards the end of the season (Plénet et al., 2000).

The high correlation between LMA and DOY in maize makes it unclear which variable is more mechanistically appropriate to use for seasonal downscaling. LMA continued to increase throughout the season until our last measurement (R5), whereas peak physiological activity occurred seven weeks earlier. This suggests that structural development or storage continued even as physiological activity declined, which is the opposite pattern as that observed in many forest canopies (Xu and Baldocchi 2003). While continued increases in LMA are sometimes taken as a surrogate indicator for the timing of physiological maturity, this is clearly not the case for maize. Sugars and starch are produced and stored in vegetative structures of maize for later mobilization to the grain (Westgate and Boyer 1985), which may contribute to the observed continued increases in LMA. However, if P_c declined due to changes in the fraction of N allocated to Rubisco with leaf age (Rey and Jarvis, 1998; Wilson et al., 2000) or to increases in g_m with increasing lignin content (Flexas et al., 2008) than DOY may be the more appropriate predictor variable for describing seasonal changes. Photoperiod has also been identified as an important driver of changes in P_c, but responses to photoperiod are complex and varied in modern genotypes of maize. Domestication of maize from tropical to temperate regions required adaptation to longer day length, and temperate varieties show substantially reduced photoperiod sensitivity (Coles et al., 2010). Another interesting possibility is that starch accumulation in the leaf may create a feedback limitation to Rubisco synthesis (Rey and Jarvis 1998), in which case

LMA may be the more useful predictor. The mechanism(s) underlying seasonal variation in P_c in both maize and sunflower merit further examination.

Conclusions

Croplands are managed agroecosystems with high net primary productivity during the growing season that impact the exchanges of carbon and water and play a role in large-scale climate feedbacks (Lokupitiya et al., 2009). Accurate representations of crop physiology are necessary for predicting carbon and water vapor exchange in agriculture systems. While studies in forested canopies and grasslands have shown that accurate simulations of fluxes require the incorporation of seasonal shifts in V_{cmax} and J_{max} (Bauerle et al., 2012; Grassi et al., 2005; Wang et al., 2008; Wang et al., 2004; Wilson et al., 2001; Wolf et al., 2006; Xu and Baldocchi, 2003), little data on the magnitude or temporality of seasonal shifts in P_c exists for field crops. However, leaf-level measurements of P_c are difficult and rarely feasible to do over meaningful time or spatial scales, making it appealing to utilize Chl and N as remotely sensed scaling variables.

We observed a progressive seasonal decline in P_c in both well-watered and water-stressed maize from the mid-vegetative stage through late senescence, supporting the need for seasonal downscaling of V_{cmax} and J_{max}. In well-watered sunflower, measured P_c increased from the late vegetative to the early reproductive stages, with a strong decline late in reproduction. Measured P_c parameters for both crops were reduced under drought stress, with apparent reductions initially due to stomatal limitations as indicated from C_i/C_a values. While it may be convenient to use Chl as a proxy for N in some species due to the ability to sense it via satellite reflectance, our results suggest that this approach would not be useful or accurate for tracking seasonal changes in N_a for sunflower. Utilization of Chl as a proxy for N content in maize will require further understanding

of both the temporal discontinuities between the two variables as well as knowledge of changes in the linear slope relationship, which may depend on genotype or fertility. Equations developed utilizing variable N nutrition may not always be applicable in crops grown at high fertilization, where the slope may be diminished or non-existent. The area-based V_{cmax} – N relationship for seasonally combined data remained insignificant for both maize and sunflower, whereas the mass based relationship was highly significant in maize due to seasonal changes in LMA.

Figures

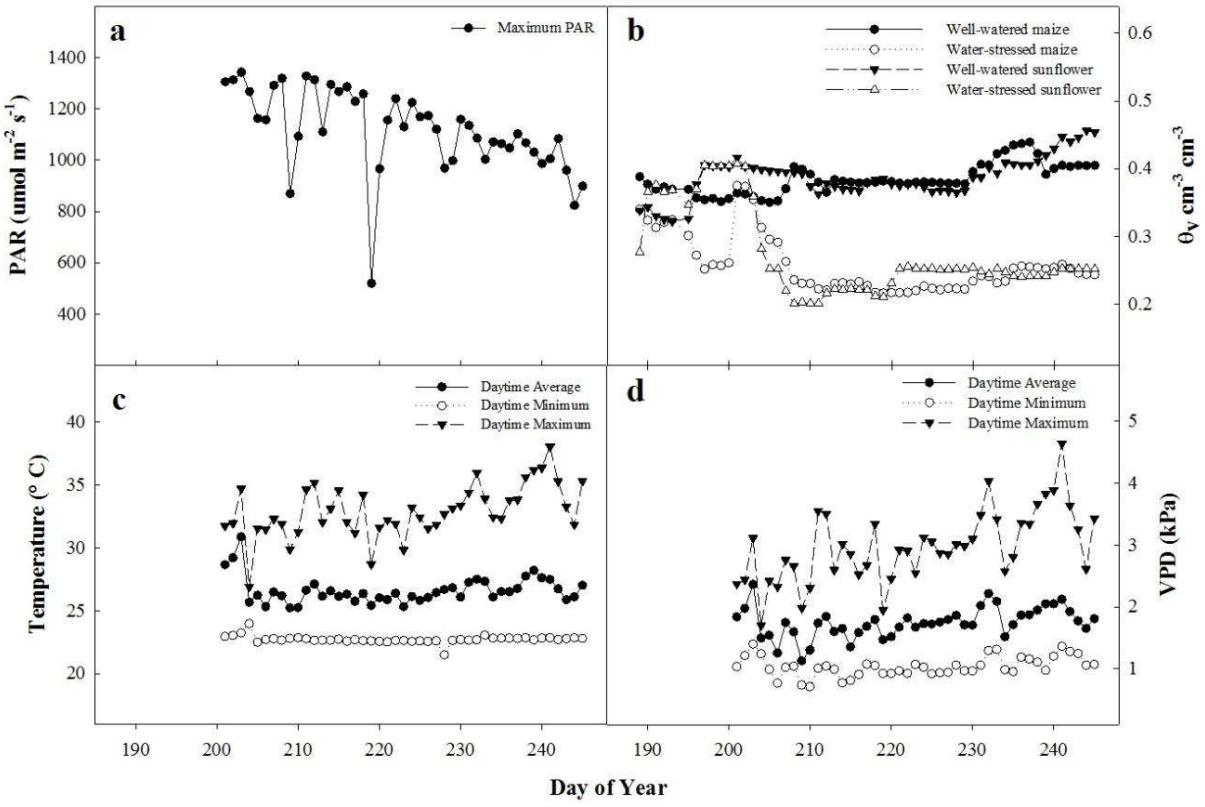

Figure 1. Seasonal variation in daily daytime maximum photosynthetically active radiation (PAR) (panel a), average daily soil volumetric water content (θ_v) (panel b), daytime minimum, maximum, and average air temperatures (panel c), and daytime average, minimum, and maximum vapor pressure deficit (VPD) (panel d). Daytime values were calculated for the period between sunrise and sunset.

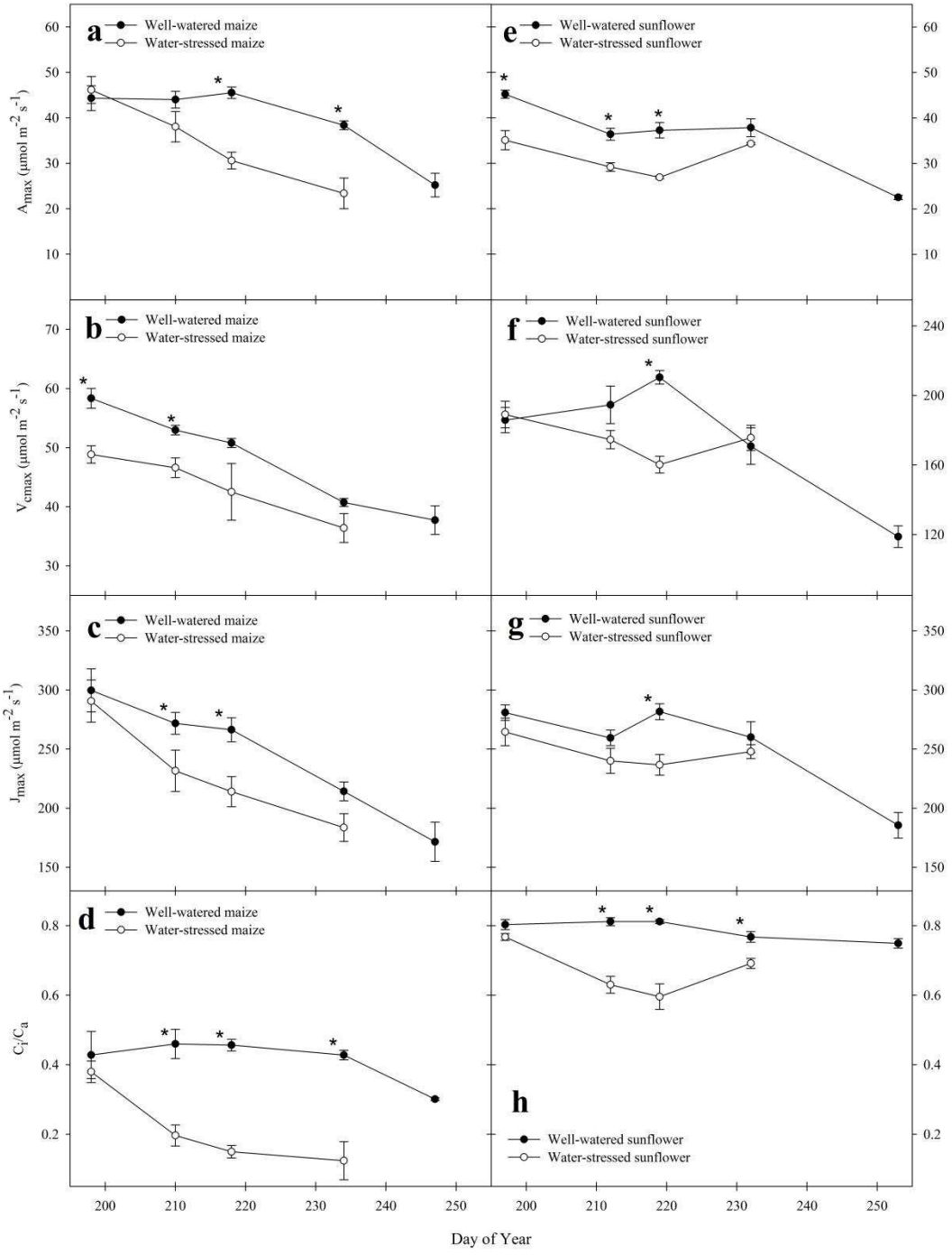

Figure 2. Seasonal changes in the maximum rate of assimilation at 2000 PAR (A_{max}), the maximum rate of carboxylation (V_{cmax}), the maximum rate of electron transport (J_{max}), and the ratio of intercellular to atmospheric CO2 concentration (C_i/C_a) on an area basis for sunflower and maize under well-watered and water-stressed conditions. Error bars represent ± SE. Asterisks indicate a significant differences between treatments on that date (Tukey's HSD). Note the difference in scales between panels b and f.

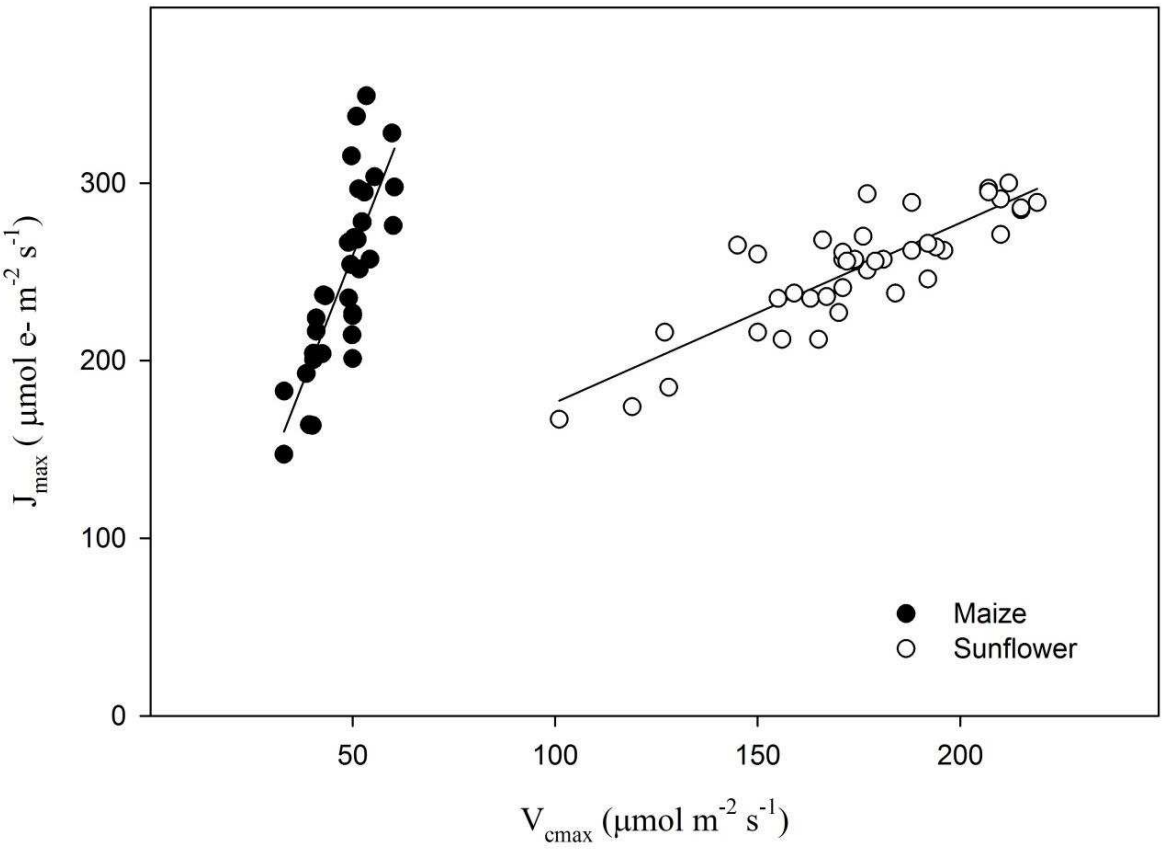

Figure 3. Relationship between the maximum rate of carboxylation (V_{cmax}) and the maximum rate of electron transport (J_{max}) for maize and sunflower. The linear regression equation for maize is $J_{max} = 5.84x - 32.64$ ($r^2 = 0.65$, $p < 0.0001$), and the intercept is not significantly different from zero ($p = 0.3662$). The linear regression for sunflower is $J_{max} = 1.01x + 75.2$ ($r^2 = 0.72$, $p < 0.0001$). Forcing the intercept to zero in sunflower results in a slope of 1.43. Values were compiled from the whole season and over treatment for each crop.

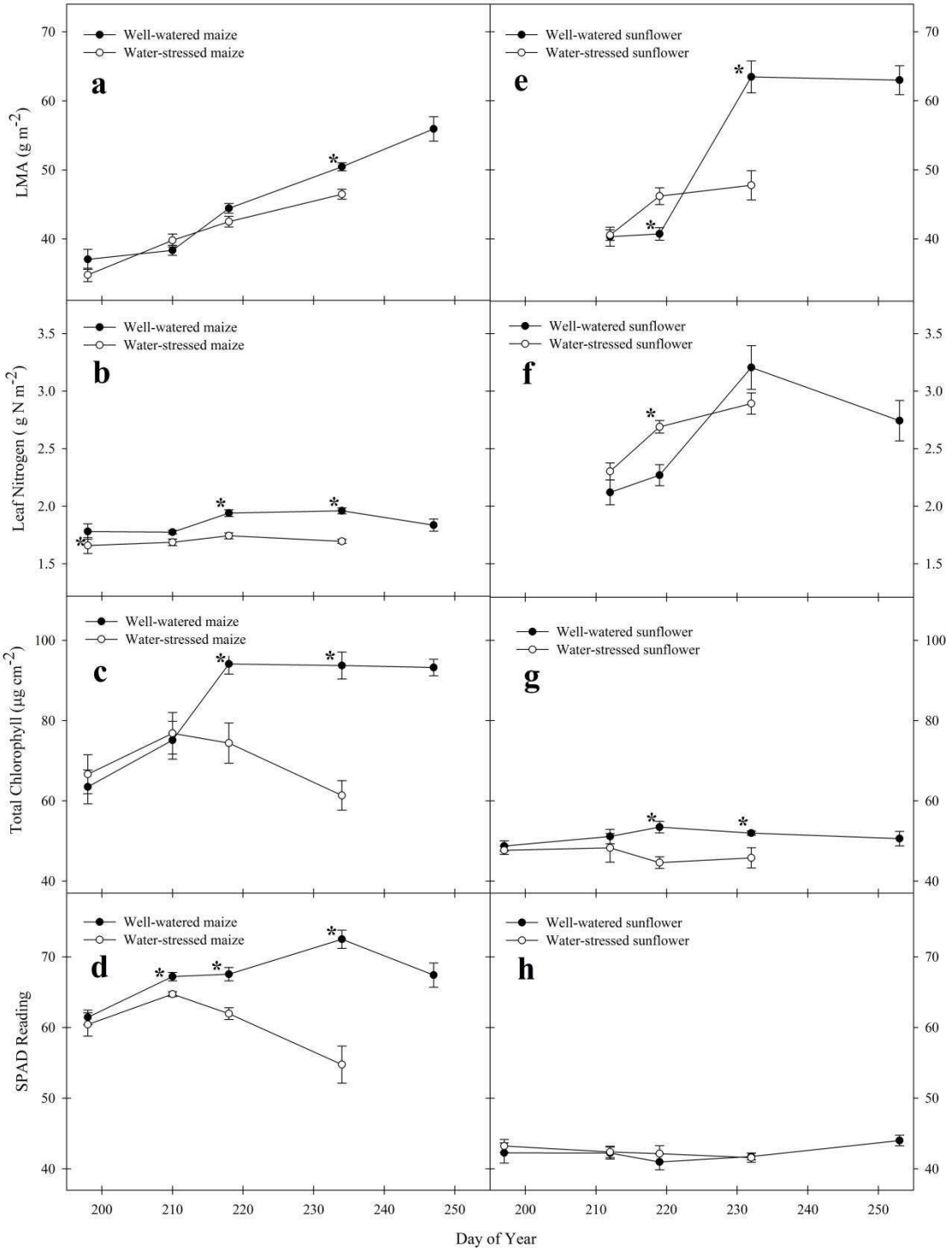

Figure 4. Seasonal changes in leaf mass per area (LMA), area-based leaf nitrogen (N_a), total chlorophyll, and SPAD readings in sunflower and maize under well-watered and water-stressed conditions. Each value represents the mean of five measurements ± SE. Asterisks indicate a significant differences between treatments on that date (Tukey's HSD).

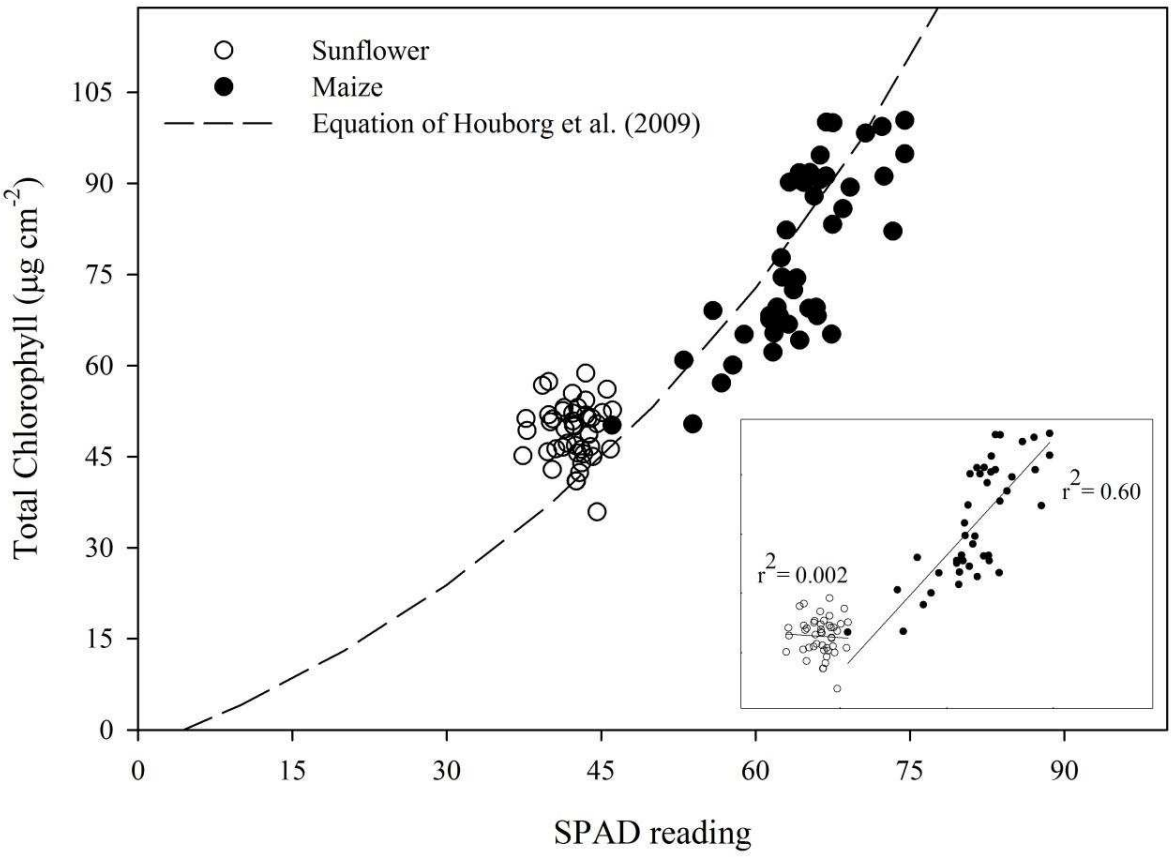

Figure 5. Relationship between total chlorophyll content and SPAD readings for sunflower and maize. Data is pooled over measurement period and treatment for each crop. The dashed line represents the SPAD – Total chlorophyll equation developed for maize by Houborg et al. (2009). The linear regression for maize in the inset box is $y = 1.96x - 48.00$; ($r^2 = 0.60$; $p = <0.0001$).

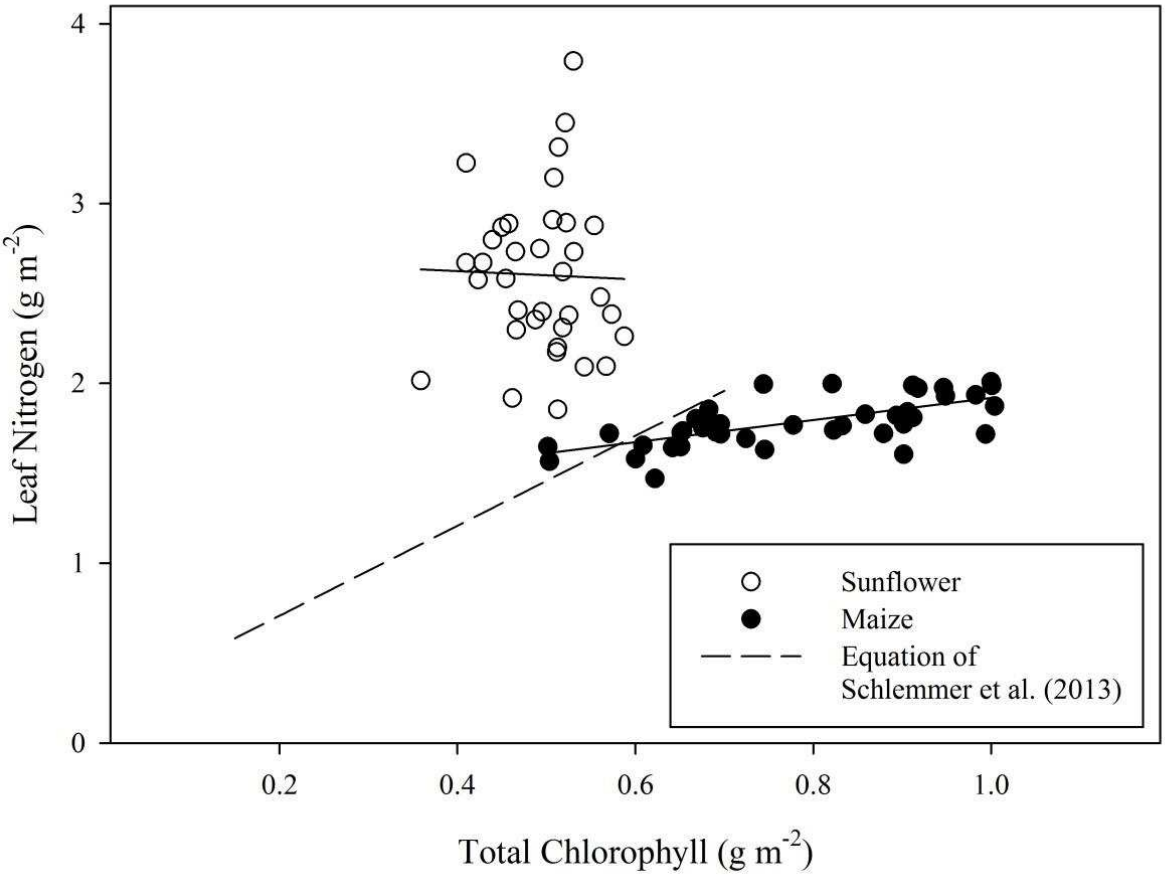

Figure 6. Relationship between leaf nitrogen content and total chlorophyll for sunflower and maize. The data is pooled over measurement period and treatment for each crop. The dashed line represents the equation developed by Schlemmer et al. (2013). The relationship is not significant for sunflower. The linear regression equation for maize is $y = 0.62x + 1.3$; ($R^2 = 0.44$, $p = <0.0001$).

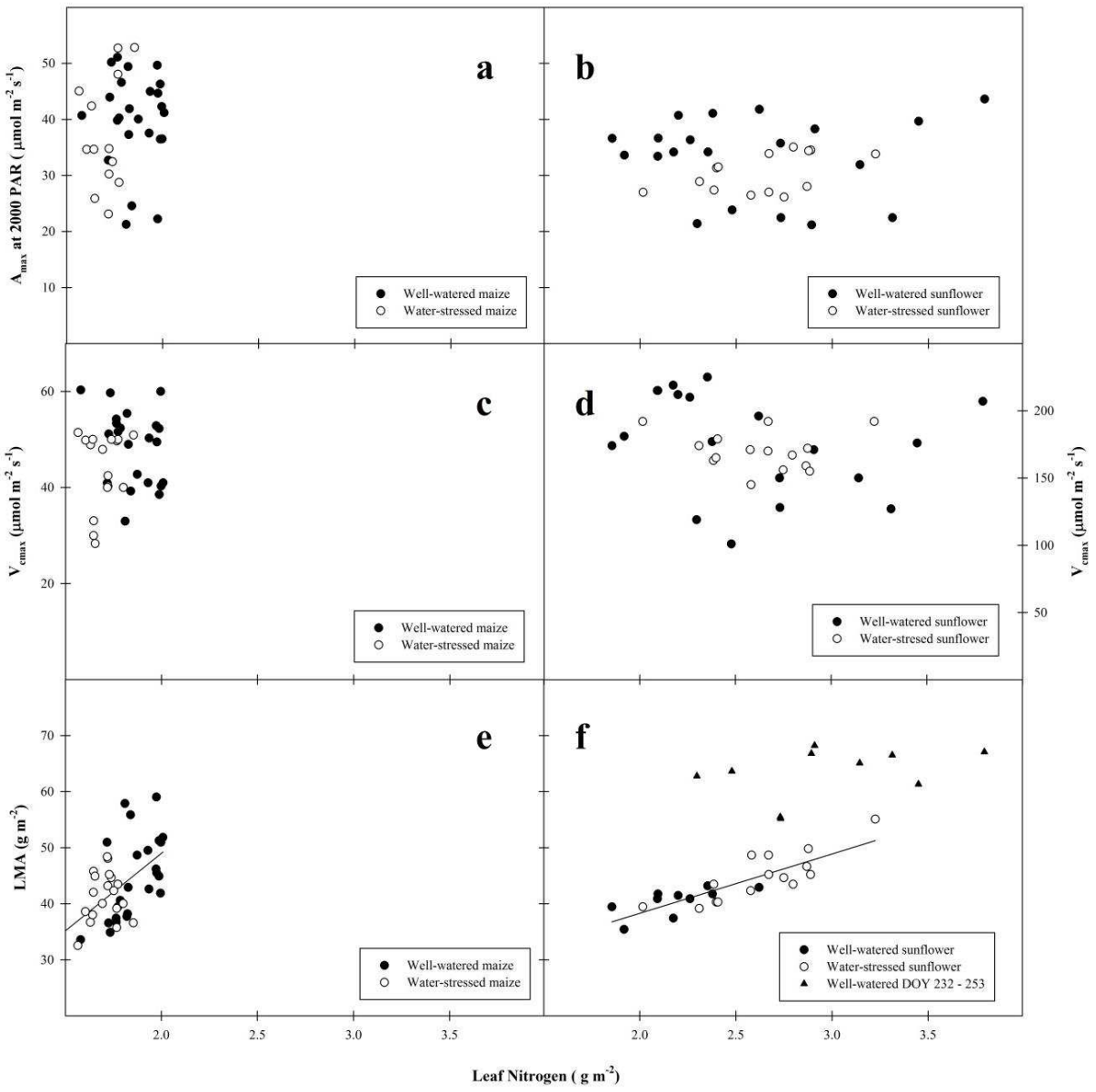

Figure 7. Relationship between area-based leaf nitrogen (N_a) versus the maximum rate of assimilation (A_{max}), the maximum rate of carboxylation (V_{cmax}) and leaf mass per unit area (LMA) for well-watered and water-stressed greenhouse maize and sunflower. The regression equation in panel f excludes triangular data points. Relationships in panels a - d are not significant. The linear regression for LMA in maize is $y = 27.67x – 6.37$ ($R^2 = 0.31$; $p = < 0.0001$. The linear regression for LMA in sunflower (excluding triangular points) is $y = 10.59x +17.11$ ($r^2 = 0.71$; $p = <0.0001$). When triangular points are included, $y = 16.85x + 4.99$ ($R^2 = 0.53$; $p = <0.0001$).

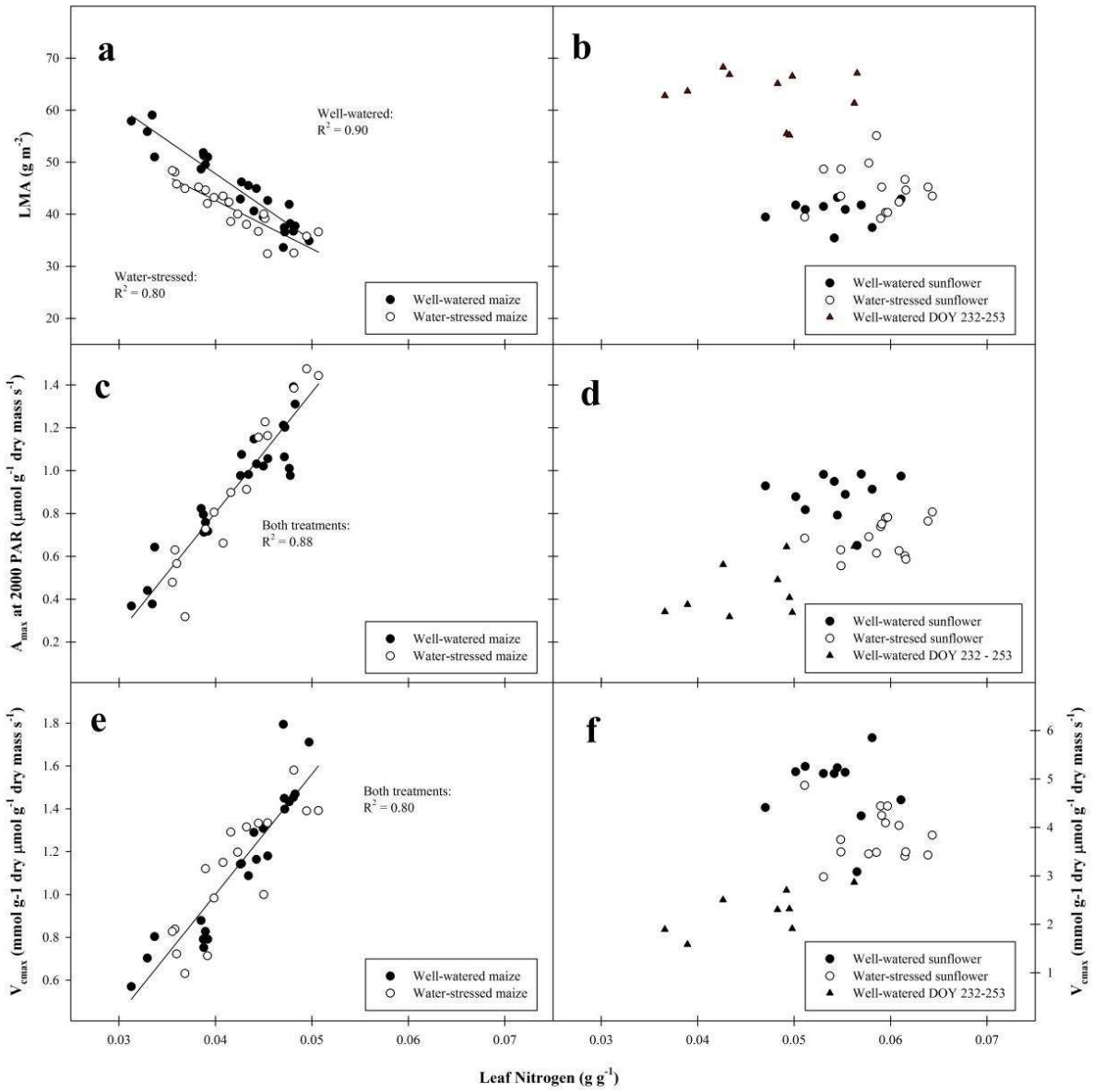

Figure 8. Relationship between LMA, A_{max_mass}, and N_m for well-watered and water-stressed maize and sunflower. The linear regression equation for well-watered maize in panel a is LMA = -1279.18x + 98.98 (r^2 = 0.90, p = <0.0001) and LMA = -929.22 +79.8 (r^2 = 0.80, p = <0.0001) for water-stressed maize. The linear regression equation in panel c for both treatments of maize is y = 56.30x – 1.45 (R^2 = 0.88; p = <0.0001). The relationship in panel e is given by y = 56.15x – 1.25 (R^2 = 0.80; p = <0.0001). The significance of the regressions in panels b, d, and f are dependent on the inclusion of only a few high-leverage points (see text for discussion).

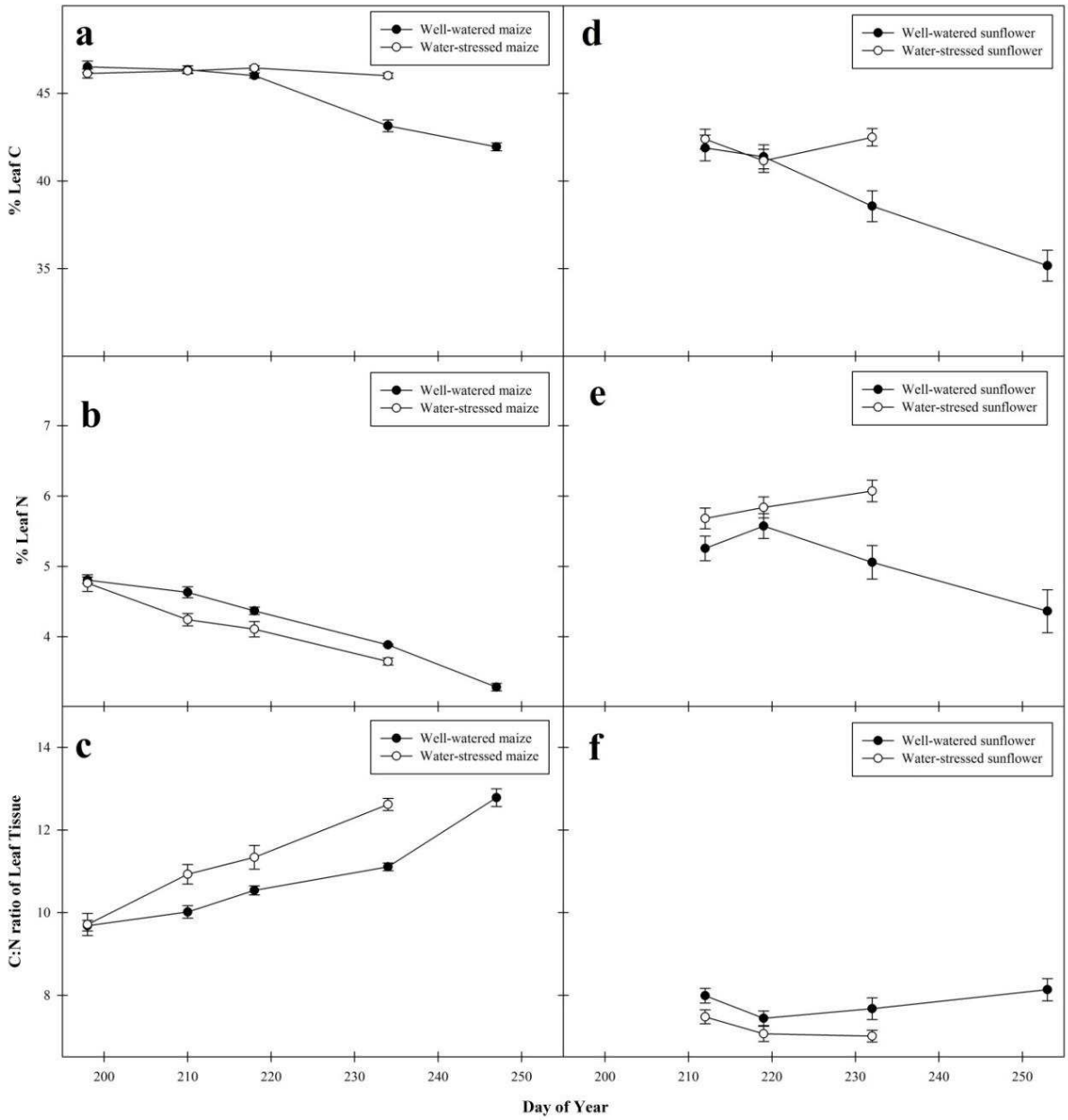

Figure 9. Seasonal changes in % leaf carbon, % leaf N, and the C: N ratio of the tissue for sunflower and maize under well-watered and water-stressed conditions. Error bars represent ± SE.

CITATIONS

Ali, A.A. et al., 2015. Global scale environmental control of plant photosynthetic capacity. Ecol. Appl., 25(8): 2349-2365.

Ball, J.T., 1988. An Analysis of Stomatal Conductance, Stanford University, Stanford.

Ball, J.T., Woodrow, I.E. and Berry, J.A., 1987. A model predicting stomatal conductance and its contribution to the control of photosynthesis under different environmental conditions, pp. 221-224.

Bauerle, W.L. et al., 2012. Photoperiodic regulation of the seasonal pattern of photosynthetic capacity and the implications for carbon cycling. Proceedings of the National Academy of Sciences, 109(22): 8612-8617.

Bauerle, W.L., Oren R., Way, D.A., Qian S.S. Stoy, P.C., Thornton, P.E., Bowden, J.D., Hoffman, F.M, and Reynolds, R.F., 2011. Seasonal patterns of photosynthetic capacity: day length, temperature, and carbon cycling implications. Proceedings of the National Academy of Sciences, In Review.

Berry, J.A., Beerling, D.J. and Franks, P.J., 2010. Stomata: key players in the earth system, past and present. Current opinion in plant biology, 13(3): 232-239.

Boyer, J.S., 1970. Leaf enlargement and metabolic rates in corn, soybean, and sunflower at various leaf water potentials. Plant physiology, 46(2): 233-235.

Buchanan, B.B., Gruissem, W. and Jones, R.L., 2000. Biochemistry & molecular biology of plants, 40. American Society of Plant Physiologists Rockville, MD.

Buckley, T., Farquhar, G. and Mott, K., 1997. Qualitative effects of patchy stomatal conductance distribution features on gas-exchange calculations. Plant, Cell & Environment, 20(7): 867-880.

Chaves, M. and Oliveira, M., 2004. Mechanisms underlying plant resilience to water deficits: prospects for water-saving agriculture. Journal of Experimental Botany, 55(407): 2365-2384.

Chaves, M.M., Maroco, J.P. and Pereira, J.S., 2003. Understanding plant responses to drought—from genes to the whole plant. Functional Plant Biology, 30(3): 239-264.

Chaves, M.M. et al., 2002. How plants cope with water stress in the field? Photosynthesis and growth. Annals of botany, 89(7): 907-916.

Coles, N.D., McMullen, M.D., Balint-Kurti, P.J., Pratt, R.C. and Holland, J.B., 2010. Genetic control of photoperiod sensitivity in maize revealed by joint multiple population analysis. Genetics, 184(3): 799-812.

Collatz, G.J., Ball, J.T., Grivet, C. and Berry, J.A., 1991. Physiological and environmental regulation of stomatal conductance, photosynthesis and transpiration - a model that includes a laminar boundary layer. Agricultural and Forest Meteorology, 54(2-4): 107-136.

Collatz, G.J., Ribas-Carbo, M. and Berry, J., 1992. Coupled photosynthesis-stomatal conductance model for leaves of C4 plants. Functional Plant Biology, 19(5): 519-538.

Dang, Q.-L., Margolis, H.A. and Collatz, G.J., 1998. Parameterization and testing of a coupled photosynthesis–stomatal conductance model for boreal trees. Tree Physiology, 18(3): 141-153.

DeJonge, K.C., Taghvaeian, S., Trout, T.J. and Thomas, L.H., 2015. Comparison of canopy temperature-based water stress indices formaize.

Egea, G., Verhoef, A. and Vidale, P.L., 2011. Towards an improved and more flexible representation of water stress in coupled photosynthesis–stomatal conductance models. Agricultural and Forest Meteorology, 151(10): 1370-1384.

Evans, J.R., 1989. Photosynthesis and nitrogen relationships in leaves of C3 plants. Oecologia, 78(1): 9-19.

Farquhar, G., Caemmerer, S. and Berry, J., 1980. A biochemical model of photosynthetic CO 2 assimilation in leaves of C 3 species. Planta, 149(1): 78-90.

Field, C. and Mooney, H., 1986. photosynthesis--nitrogen relationship in wild plants, On the economy of plant form and function: proceedings of the Sixth Maria Moors Cabot Symposium, Evolutionary Constraints on Primary Productivity, Adaptive Patterns of Energy Capture in Plants, Harvard Forest, August 1983. Cambridge [Cambridgeshire]: Cambridge University Press, c1986.

Flexas, J., Ribas-Carbo, M., DIAZ-ESPEJO, A., GalmES, J. and Medrano, H., 2008. Mesophyll conductance to CO2: current knowledge and future prospects. Plant, Cell & Environment, 31(5): 602-621.

Grassi, G., Vicinelli, E., Ponti, F., Cantoni, L. and Magnani, F., 2005. Seasonal and interannual variability of photosynthetic capacity in relation to leaf nitrogen in a deciduous forest plantation in northern Italy. Tree Physiology, 25(3): 349-360.

Hay, R.K. and Porter, J.R., 2006. The physiology of crop yield. Blackwell Publishing.

Houborg, R., Anderson, M. and Daughtry, C., 2009. Utility of an image-based canopy reflectance modeling tool for remote estimation of LAI and leaf chlorophyll content at the field scale. Remote Sensing of Environment, 113(1): 259-274.

Houborg, R., Cescatti, A., Migliavacca, M. and Kustas, W.P., 2013. Satellite retrievals of leaf chlorophyll and photosynthetic capacity for improved modeling of GPP. Agricultural and Forest Meteorology, 177: 10-23.

Kattge, J., Knorr, W., Raddatz, T. and Wirth, C., 2009. Quantifying photosynthetic capacity and its relationship to leaf nitrogen content for global-scale terrestrial biosphere models. Global Change Biology, 15(4): 976-991.

Kim, S.H. et al., 2007. Temperature dependence of growth, development, and photosynthesis in maize under elevated CO2. Environmental and Experimental Botany, 61(3): 224-236.

Kohanbash, D., Kantor, G., Martin, T. and Crawford, L., 2013. Wireless sensor network design for monitoring and irrigation control: User-centric hardware and software development. HortTechnology, 23(6): 725-734.

Kottkamp, J., Varjabedian, A., Ross, J., Eddy, R. and Hahn, D.T., 2010. Optimizing Greenhouse Corn Production: What Is the Best Fertilizer Formulation and Strength? Purdue Methods for Corn Growth: 14.

Lambers, H., Chapin III, F.S. and Pons, T.L., 2008. Plant water relations. Springer.

Lawlor, D.W. and Tezara, W., 2009. Causes of decreased photosynthetic rate and metabolic capacity in water-deficient leaf cells: a critical evaluation of mechanisms and integration of processes. Annals of Botany.

Le Roux, X., Grand, S., Dreyer, E. and Daudet, F.-A., 1999. Parameterization and testing of a biochemically based photosynthesis model for walnut (Juglans regia) trees and seedlings. Tree Physiology, 19(8): 481-492.

Lea-Cox, J.D. et al., 2013. Advancing wireless sensor networks for irrigation management of ornamental crops: An overview. HortTechnology, 23(6): 717-724.

Leuning, R., Cromer, R. and Rance, S., 1991. Spatial distributions of foliar nitrogen and phosphorus in crowns of Eucalyptus grandis. Oecologia, 88(4): 504-510.

Lichtenthaler, H.K., 1987. Chlorophylls and carotenoids: pigments of photosynthetic biomembranes. Methods enzymol, 148: 350-382.

Lichtenthaler, H.K. and Buschmann, C., 2001. Chlorophylls and Carotenoids: Measurement and Characterization by UV-VIS Spectroscopy. Current protocols in food analytical chemistry.

Lokupitiya, E. et al., 2009. Incorporation of crop phenology in Simple Biosphere Model (SiBcrop) to improve land-atmosphere carbon exchanges from croplands. Biogeosciences, 6(6): 969-986.

Markwell, J., Osterman, J.C. and Mitchell, J.L., 1995. Calibration of the Minolta SPAD-502 leaf chlorophyll meter. Photosynthesis Res., 46(3): 467-472.

Medlyn, B. et al., 1999. Effects of elevated [CO2] on photosynthesis in European forest species: a meta-analysis of model parameters. Plant, Cell & Environment, 22(12): 1475-1495.

Medlyn, B. et al., 2002. Temperature response of parameters of a biochemically based model of photosynthesis. II. A review of experimental data. Plant, Cell & Environment, 25(9): 1167-1179.

Medvigy, D., Jeong, S.J., Clark, K.L., Skowronski, N.S. and Schäfer, K.V., 2013. Effects of seasonal variation of photosynthetic capacity on the carbon fluxes of a temperate deciduous forest. Journal of Geophysical Research: Biogeosciences, 118(4): 1703-1714.

Mott, K., 1995. Effects of patchy stomatal closure on gas exchange measurements following abscisic acid treatment. Plant, Cell & Environment, 18(11): 1291-1300.

Mott, K.A. and Buckley, T.N., 2000. Patchy stomatal conductance: emergent collective behaviour of stomata. Trends Plant Sci., 5(6): 258-262.

Nardini, A., Salleo, S. and Andri, S., 2005. Circadian regulation of leaf hydraulic conductance in sunflower (Helianthus annuus L. cv Margot). Plant, Cell & Environment, 28(6): 750-759.

Niinemets, Ü. and Tenhunen, J., 1997. A model separating leaf structural and physiological effects on carbon gain along light gradients for the shade-tolerant species Acer saccharum. Plant, Cell & Environment, 20(7): 845-866.

Ollinger, S. et al., 2008. Canopy nitrogen, carbon assimilation, and albedo in temperate and boreal forests: Functional relations and potential climate feedbacks. Proceedings of the National Academy of Sciences, 105(49): 19336-19341.

Ollinger, S.V. and Smith, M.-L., 2005. Net primary production and canopy nitrogen in a temperate forest landscape: an analysis using imaging spectroscopy, modeling and field data. Ecosystems, 8(7): 760-778.

Plénet, D., Mollier, A. and Pellerin, S., 2000. Growth analysis of maize field crops under phosphorus deficiency. II. Radiation-use efficiency, biomass accumulation and yield components. Plant Soil, 224(2): 259-272.

Pompelli, M.F. et al., 2013. Spectrophotometric determinations of chloroplastidic pigments in acetone, ethanol and dimethylsulphoxide. Revista Brasileira de Biociências, 11(1).

Reich, P., Ellsworth, D. and Walters, M., 1998. Leaf structure (specific leaf area) modulates photosynthesis–nitrogen relations: evidence from within and across species and functional groups. Funct. Ecol., 12(6): 948-958.

Reich, P.B., Walters, M.B. and Ellsworth, D.S., 1997. From tropics to tundra: global convergence in plant functioning. Proceedings of the National Academy of Sciences of the United States of America, 94(25): 13730-4.

Rey, A. and Jarvis, P., 1998. Long-term photosynthetic acclimation to increased atmospheric CO2 concentration in young birch (Betula pendula) trees. Tree physiology, 18(7): 441-450.

Ritchie, R.J., 2006. Consistent sets of spectrophotometric chlorophyll equations for acetone, methanol and ethanol solvents. Photosynthesis Res., 89(1): 27-41.

Rouphael, Y., Colla, G., Fanasca, S. and Karam, F., 2007. Leaf area estimation of sunflower leaves from simple linear measurements. Photosynthetica, 45(2): 306-308.

Sadras, V., Echarte, L. and Andrade, F., 2000. Profiles of leaf senescence during reproductive growth of sunflower and maize. Annals of Botany, 85(2): 187-195.

Schepers, J.S., Blackmer, T., Wilhelm, W. and Resende, M., 1996. Transmittance and Reflectance Measurements of CornLeaves from Plants with Different Nitrogen and Water Supply. J. Plant Physiol., 148(5): 523-529.

Schlemmer, M. et al., 2013. Remote estimation of nitrogen and chlorophyll contents in maize at leaf and canopy levels. International Journal of Applied Earth Observation and Geoinformation, 25: 47-54.

Schlemmer, M.R., Francis, D.D., Shanahan, J. and Schepers, J.S., 2005. Remotely measuring chlorophyll content in corn leaves with differing nitrogen levels and relative water content. Agronomy Journal, 97(1): 106-112.

Schneiter, A. and Miller, J., 1981. Description of sunflower growth stages. Crop Science, 21(6): 901-903.

Sellers, P.J. et al., 1996a. A revised land surface parameterization (SiB2) for atmospheric GCMs. Part II: The generation of global fields of terrestrial biophysical parameters from satellite data. Journal of climate, 9(4): 706-737.

Sellers, P.J. et al., 1996b. A revised land surface parameterization (SiB2) for atmospheric GCMs. Part I: Model formulation. Journal of Climate, 9(4): 676-705.

Sharkey, T.D., Bernacchi, C.J., Farquhar, G.D. and Singsaas, E.L., 2007. Fitting photosynthetic carbon dioxide response curves for C3 leaves. Plant, Cell & Environment, 30(9): 1035-1040.

Stewart, D. and Dwyer, L., 1999. Mathematical characterization of leaf shape and area of maize hybrids. Crop Science, 39(2): 422-427.

Tait, M.A. and Hik, D.S., 2003. Is dimethylsulfoxide a reliable solvent for extracting chlorophyll under field conditions? Photosynthesis Res., 78(1): 87-91.

Tanaka, K., Kosugi, Y. and Nakamura, A., 2002. Impact of leaf physiological characteristics on seasonal variation in CO< sub> 2</sub>, latent and sensible heat exchanges over a tree plantation. Agricultural and forest meteorology, 114(1): 103-122.

Tardieu, F., Katerji, N., Bethenod, O., Zhang, J. and Davies, W., 1991. Maize stomatal conductance in the field: its relationship with soil and plant water potentials, mechanical constraints and ABA concentration in the xylem sap. Plant, Cell & Environment, 14(1): 121-126.

Tardieu, F. and Simonneau, T., 1998. Variability among species of stomatal control under fluctuating soil water status and evaporative demand: modelling isohydric and anisohydric behaviours. Journal of experimental botany, 49(Special Issue): 419-432.

Terashima, I., Wong, S.-C., Osmond, C.B. and Farquhar, G.D., 1988. Characterisation of non-uniform photosynthesis induced by abscisic acid in leaves having different mesophyll anatomies. Plant and Cell Physiology, 29(3): 385-394.

Thornton, P.E. and Zimmermann, N.E., 2007. An improved canopy integration scheme for a land surface model with prognostic canopy structure. Journal of Climate, 20(15): 3902-3923.

Varble, J.L. and Chávez, J., 2011. Performance evaluation and calibration of soil water content and potential sensors for agricultural soils in eastern Colorado. Agricultural water management, 101(1): 93-106.

Von Caemmerer, S., 2000. Biochemical models of leaf photosynthesis. CSIRO.

Wang, Q., Iio, A., Tenhunen, J. and Kakubari, Y., 2008. Annual and seasonal variations in photosynthetic capacity of Fagus crenata along an elevation gradient in the Naeba Mountains, Japan. Tree physiology, 28(2): 277-285.

Wang, Q. et al., 2004. Simulation and scaling of temporal variation in gross primary production for coniferous and deciduous temperate forests. Global Change Biology, 10(1): 37-51.

Westgate, M.E. and Boyer, J.S., 1985. Carbohydrate reserves and reproductive development at low leaf water potentials in maize. Crop Science, 25(5): 762-769.

Wilson, K., Baldocchi, D. and Hanson, P., 2001. Leaf age affects the seasonal pattern of photosynthetic capacityand net ecosystem exchange of carbon in a deciduous forest. Plant, Cell & Environment, 24(6): 571-583.

Wilson, K.B., Baldocchi, D.D. and Hanson, P.J., 2000. Spatial and seasonal variability of photosynthetic parameters and their relationship to leaf nitrogen in a deciduous forest. Tree Physiology, 20(9): 565-578.

Wise, R.R., Sparrow, D.H., Ortiz-Lopez, A. and Ort, D.R., 1991. Biochemical regulation during the mid-day decline of photosynthesis in field-grown sunflower. Plant Sci., 74(1): 45-52.

Wolf, A., Akshalov, K., Saliendra, N., Johnson, D.A. and Laca, E.A., 2006. Inverse estimation of Vcmax, leaf area index, and the Ball-Berry parameter from carbon and energy fluxes. Journal of Geophysical Research: Atmospheres (1984–2012), 111(D8).

Wullschleger, S.D., 1993. Biochemical limitations to carbon assimilation in C3 plants‚ÄîA retrospective analysis of the A/Ci curves from 109 species. Journal of Experimental Botany, 44(5): 907-920.

Xu, L. and Baldocchi, D.D., 2003. Seasonal trends in photosynthetic parameters and stomatal conductance of blue oak (Quercus douglasii) under prolonged summer drought and high temperature. Tree Physiology, 23(13): 865-877.

CHAPTER 4:

A NEW LOW-COST SAP FLOW GAUGE FOR MEASURING WATER USE IN HERBACEOUS PLANTS

Summary

Sap-flow (SF) measurements provide a unique and valuable tool for studying plant water relations. The heat pulse (HP) SF method can provide logistical advantages over other sap flow techniques due to the low power requirements as well as the fact that one gauge can be used on plants varying different stem diameters. However, while this technique is widely in trees, the literature contains only sparse examples of application of the technique in herbaceous plants. In this study we utilize new developments in HP theory, low-cost electronics, and desktop manufacturing to construct, calibrate, and validate an affordable research-grade HP measurement tool. We also compared the performance of the T_{max} HP method to a new HP technique based on the ratio of the temperature maxima measured by a downstream and tangential probe (HR_{max}).

Gauges were fabricated using 3D-printing technology and low-cost electronics to keep materials cost under $25 per gauge. Each gauge included three needle probes that were inserted into the stem periphery. A central needle contained a resistance heater for applying the heat pulse, while two additional needles measured the resulting temperature increases at positions downstream and tangent to the flow direction. The resultant data was used to calculate sap velocity using two techniques. The T_{max} method used the time to temperature maximum (T_{max}) while a novel heat ratio method (HR_{max}) used the ratio of the temperature increase between the downstream and tangent probes. The data acquisition and control systems were built from low-cost Arduino microcontrollers. Prototype SF gauges were tested and calibrated for corn and

sunflower in the greenhouse, and once calibrated for a specific gauge design and species, the gauges closely tracked gravimetric measurements of plant transpiration. The T_{max} method performed well under high rates of sap flow (i.e., up to 300 g hr^{-1}) in both sunflower and corn, but the accuracy of measurements was poor at low rates of transpiration. The T_{max} method overestimated sap flow when transpiration fell below ≈ 20 g hr^{-1} (corn) ≈ 50 g hr^{-1} (sunflower). The new HR_{max} method was able to accurately track sap flow at high flows and also performed remarkably well at tracking nighttime flows as low as 3 g hr^{-1} in corn. The gauges were also deployed in the field on irrigated corn to validate the calibration coefficients determined in the greenhouse. Estimates of transpiration over a two-week period were within 10% of calculated reference evapotranspiration under the new HR_{max} method, whereas the T_{max} method overestimated transpiration due to overestimation of nighttime flows.

The entire measurement system is 5 to 10 times less expensive than commercial alternatives and can be constructed in-house by researchers, producers, or students interested in the technology. The do-it-yourself simplicity and low cost of the approach make it possible to deploy large numbers of gauges in the field to capture spatial variability, compare water use among agronomic plots, or scale-up sap flow to measure canopy transpiration.

Introduction

Sap flow measurements provide a unique and valuable way to explore and quantify the time course of whole plant water use under field conditions (Smith and Allen, 1996; Wullschleger et al., 1998). The technology is utilized across a wide range of applications on diverse plant types including natural and urban forest trees (Čermák et al., 2004; Granier et al., 2000; Meinzer et al., 2004; Pataki et al., 2011), woody horticultural trees and vines (Alarcón et al., 2003; Bauerle et al., 2002; Fernández et al., 2008; Green and Clothier, 1988; Lu et al., 2002) and agricultural crop

species (Cohen et al., 1988; Cohen and Li, 1996; Cohen et al., 1993; Dugas et al., 1994; Senock et al., 1996). Sap flow measurements can be particularly useful in field crop research, where the potential for water efficiency gains relies on an accurate understanding of how plant transpiration responds to changes in available soil water and weather. When multiple gauges are deployed within a study area, results can be scaled up to estimate canopy transpiration (T) or to partition evapotranspiration (ET) into soil and plant components (Allen and Grime, 1995; Ham et al., 1990; Jara et al., 1998; Sakuratani, 1987; Sauer et al., 2007). Sap flow can provide insights into field-scale water consumption (Cohen et al., 1988; Dugas et al., 1994) as well as aid in the detection of crop water stress (Cohen and Li, 1996) and in determining the effect of elevated CO_2 on plant water use at different scales (Bremer et al., 1996; Senock et al., 1996). It can also be used to evaluate the consistency of field techniques for measuring transpiration as well as the performance of transpiration simulation models (Jara et al., 1998; Stockle and Jara, 1998).

While there are several types of SF gauges, there are two general approaches – the heat balance (HB) and the heat pulse (HP) methods. Both techniques apply heat to the stem and detect the rate of sap flow by monitoring the stem's thermal regime. The HB method solves the heat balance over a stem section by applying constant or variable power to continuously heat the tissue (Baker and Bavel, 1987; Čermák et al., 1973; Sakuratani, 1981; Sakuratani, 1984; Steinberg et al., 1989). A known amount of heat is applied from a flexible heater encircling the stem, and temperature gradients are estimated from thermocouples mounted above and below the heater. The mass flow rate of sap (g h^{-1}) is then computed by determining, by difference, the amount of heat transported in the moving sap. While the HB method has some advantages over the HP technique, it requires significant power inputs, which can be a particular disadvantage at remote sites. The continual application of heat can also result in damage to stems under

conditions of low flow. An additional limitation is that while gauges can accommodate stem sizes as small as 3 mm (Senock and Ham, 1993) individual gauges can also only be used within relatively narrow limits of stem diameters (Smith and Allen, 1996), requiring a number of different sized gauges to accommodate the seasonally shifting stem diameter of herbaceous crops.

The HP technique utilizes needle-like probes that contain line heaters and temperature sensors to determine the apparent heat pulse velocity (V_h). The heater probe releases a short heat pulse that is carried via convection and conduction as a tracer in the transpiration stream. The HP velocity is then calculated by measuring temperature differences at defined locations around the heater. HP measurements are limited to plants with stem diameters large enough to accommodate the insertion of probes. A drawback to the HP method is that because the technique measures velocity (m s^{-1}), not mass flow, and thus an empirical calibration is required to convert results to plant transpiration (kg $plant^{-1}$ s^{-1}). There are also wounding effects due to probe insertion (Green et al., 2003). Thus, researchers have historically developed calibration factors dependent on species, gauge design, and probe insertion depth. Mass SF rates are calculated as the product of V_h and the calibration factor. Fortunately, studies have shown that these calibration factors in herbaceous plants are relatively stable for a given species and gauge design (Cohen and Li, 1996; Cohen et al., 1993). The economic and logistical advantages of this method are the low power requirements as well as the fact that one gauge can be used on plants with widely different stem diameters, allowing the same gauge to be used for multiple species types or across the growth stages of herbaceous crops. Furthermore, recent advances in HP theory have the potential to improve the accuracy and utility of the approach (Kluitenberg and Ham, 2004). Finally, new

developments in electronics and desktop fabrication are particularly well suited for making HP gauges.

One of the most recalcitrant problems in SF research is obtaining enough replication to capture the plant-to-plant differences between neighboring stems. In agricultural work, it often takes more than 10 gauges per plot for statistical comparison of treatments (Senock et al., 1996). Jara et al. (1998) found that between 5 and 17 gauges were needed in corn to estimate sap flow with a ± 10% error, with fewer gauges necessary for obtaining weekly averages and more gauges required for accurately capturing short-term responses (i.e., 20-minute averages). The number of gauges necessary to reduce the error to ± 2.5% increases even more substantially (Jara et al., 1998). Spatial variation in soil-water conditions and micrometeorology can further confound the problem. Thus, researchers that work at these scales need a research grade instrument that can be economically fabricated in large numbers. However, the high cost of commercial gauges coupled with the need for replication can make it impractical to quantify SF in many cases. The ability to deploy low-cost gauges with low maintenance and power requirements would permit the necessary statistical replication and aid in quantifying genotype or treatment differences in transpiration. There is a need for a research-grade instrument that can be economically fabricated in large numbers and that is accessible to researchers who may be working under severe budget limitations.

The developments of free and open source software, low-cost electronics (e.g., Arduino), and low-cost desktop manufacturing technologies (e.g., 3D printing) present a viable and promising solution for lowering the cost of SF research. Open source technologies can also promote and advance scientific research via transparent designs that are clearly documented as well as replicated and improved upon in a collaborative and iterative fashion by the user

community (Pearce 2015). Desktop manufacturing offers an unprecedented opportunity to create tools and custom equipment to meet the exact needs of a particular project or research question. An added benefit of designing and building experimental equipment is a more thorough understanding of the principles and limits of the design (Baden et al., 2015). Additionally, the coupling of low-cost Arduino microcontrollers with 3D printers to create open-source scientific hardware can also result in substantial research savings and empower researchers with limited budgets (Pearce, 2012; Pearce, 2015). This is especially relevant for agricultural research in the developing world were research on drought and plant water relations is needed to address food security issues (Godfray et al., 2010)

The objective of this study was to use new developments in HP theory, low-cost electronics, and desktop manufacturing to deliver an affordable research-grade SF measurement tool for use in water research and education. While there are several different HP techniques that can be used to accommodate various flow conditions, in this study we utilize the T_{max} HP method (Cohen et al., 1988; Cohen et al., 1981) in herbaceous crops, and employ theory recently proposed for a non-instantaneous heat pulse (Kluitenberg and Ham 2004). We also present a new heat ratio method based on the ratio of the temperature maxima of downstream and tangential probes (HR_{max}) that accurately tracks sap flow under both high and low flows. We calibrated and validated the SF technology for both the T_{max} and HR_{max} methods in sunflower (*Helianthus annuus L.)* and corn (*Zea mays* L.). Our goal was not to compete with commercial products, but to essentially create new category of open-source sap flow technology – tools that lay the groundwork for creating a multi-nodal, wide-area sap flow network for measuring crop water use.

Theory

Cohen et al. (1981, 1988) utilized the analytical theory of Marshall (1958) to develop a method to estimate V_h based on the time required for the temperature at an upper (i.e., downstream) temperature sensor to reach a maximum following an instantaneous heat pulse from a heater probe. V_h (m s^{-1}) is calculated as:

$$V_h = \sqrt{\frac{L_d^2 - 4k_x t_{m,d}}{t_{m,d}}} \quad (1)$$

where L_d is the distance to the downstream sensor (m), k_x is the thermal diffusivity of the stem in the axial direction (m^2 s^{-1}), and $t_{m,d}$ is elapsed time (s) to when the temperature at L_d becomes maximal following the heat pulse (i.e., elapsed time to maximum). However, this approach is for an instantaneous heat pulse. In practice the HP duration is usually 4 to 8 seconds, as longer heat durations results in a lower maximum heater temperature and reduce the likelihood of heat injury to plant tissue. Kluitenberg and Ham (2004) introduced a solution for V_h using a non-instantaneous pulse:

$$V_{\mathrm{h}} = \sqrt{\frac{4k_x}{t_o} \ln\left(1 - \frac{t_o}{t_{m,d}}\right) + \frac{L_d^2}{t_{m,d}(t_{m,d} - t_o)}} \quad (2)$$

where t_o is the duration of the heat pulse (s). One problem with both equations 1 and 2 is that k_x is unknown. Some researchers have calculated k_x by simultaneous utilization of the T_{max} and the Compensation Heat Pulse method (Swanson and Whitfield, 1981) at flow rates where both techniques can be used (i.e., Cohen et al. 1988). However, this method requires an upstream

probe, and sometimes results in high and inconsistent values of k_x and large variations between plants (Cohen et al. 1993). Usually k_x is determined by rearranging the velocity equations to solve for k_x at night after assuming V_h is zero or very small. For equation 2 the solution for k_x takes the form:

$$k_x' = \frac{t_o}{4}\left(V^2 - \frac{L_d^2}{t_{m,d}'(t_{m,d}'-t_{m,d}')}\right)\left[ln\left(1-\frac{t_o}{t_{m,d}'}\right)\right]^{-1} \quad (3)$$

where the prime accent on the variables indicates a predawn conditions. The nighttime-based value of k_x is then assumed to hold constant for the following day.

A potential limitation of the HP methods is that some HP techniques perform poorly at low flow rates, whereas others have unresolved limitations under conditions of high flows (Vandegehuchte and Steppe, 2013). For example, the T_{max} method is problematic at low flows. Cohen et al. (1988) found that using equation 1 in cotton was not accurate when the V_h was small. To measure low flows, they switched to the Compensation Heat Pulse method (Swanson and Whitfield, 1981) at flows less than 0.17 mm/s, which required the installation of an additional probe upstream (i.e., below) of the heater. Finite element modeling of low flow conditions in trees has also shown that the relationship between $t_{m,d}$ and V_h is not unique when wounding effects are included (Green et al., 2003). Many of the problems at low flows arise because the observed temperature increase at the downstream probe becomes small with a flat peak and creates uncertainty in determining $t_{m,d}$.

Historically, most HP probe designs included temperature sensors both above and below the heater. This design is necessary if utilizing the Compensation Heat-pulse Velocity method or the Heat Ratio method (Burgess et al., 2001). This configuration is also a requirement if the

investigator needs to measure reverse sap flow, a common occurrence in trees (Burgess et al., 2001), but not a significant process in herbaceous plants like corn and sunflower.

Given these constraints of the T_{max} method, we hypothesized that there may be an advantage to eliminating the upstream (i.e., lower) probe and instead placing a temperature probe to the side (i.e., tangential) of the heater. This configuration could increase the resolution of the T_{max} method by providing a clearer temperature peak under conditions of low flows. Additionally, this configuration permits the utilization of the ratio of the temperature maxima between the downstream and tangential probes to measure V_h. Assuming isotropic properties of the stem,

$$V_h \approx \frac{2k}{L_d} ln\left(\frac{L_d^2 \Delta T_{m,d}}{L_t^2 \Delta T_{m,t}}\right) \tag{4}$$

This equation is first order correct (Gerard Kluitenberg, Kansas State University, personal correspondence). The second order solution is:

$$V_h \approx \frac{4kL_d}{(L_d^2 - L_t^2)}\left[1 - \sqrt{1 - \left(1 - \frac{L_t^2}{L_d^2}\right) ln\left(\frac{L_d^2 \Delta T_{m,d}}{L_t^2 \Delta T_{m,t}}\right)}\right] \tag{5}$$

(Gerard Kluitenberg, Kansas State University, personal correspondence). Using the ratio of the temperature maximum at two locations has certain practical advantages. The value of T_{md} and T_{mt} are relatively easy to determine from temperature data following a heat pulse. Also, unlike the T_{max} method, the temperature ratio is unaffected by the background rate of stem heating or cooling in response to ambient temperature changes. That is, the heat pulse time series data does not have to be detrended to account for changing background conditions. One drawback of the

HR_{max} method is that both equations 4 and 5 are sensitive to errors in probe spacing (L_d and L_t). Also, there is not an easy way to solve for stem thermal properties (k) under zero flow conditions.

Conversion of V_h to flow rate

The measured V_h must be converted to mass or volumetric flow (e.g. kg s^{-1} or m^3 s^{-1}) in order to determine whole plant transpiration. This conversion is difficult in theory for several reasons. First of all, there is interruption of flow and xylem wounding effects on V_h in the region of the needle as well as a lack of information concerning the hydroactive area of stem xylem. While physically based correction factors that account for the blockage of sap streams and sensor thermal properties have been presented, they require complicated numerical approaches to derive the correction coefficients (Green et al., 2003; Swanson and Whitfield, 1981). The heat capacity in the conductive area is also affected by changes in stem water content. Finally, there are model and measurement errors caused by an oversimplified mathematical representation of heat flow and non-ideal response of the needle probes. These factors result in a systematic underestimation in the measured V_h (Cohen et al., 1981; Green et al., 1989). A common and straightforward approach to address these issues is to construct and utilize an empirical calibration using containerized plants, wherein whole plant transpiration (T, kg s^{-1}) is measured gravimetrically while the apparent V_h is measured by sap flow gauge (Cohen et al., 1988; Cohen et al., 1981). A linear relationship is expected between T and ρVA, where A is the cross sectional area of the plant stem (m^2) at the gauge location and ρ is the density of sap (kg/m^3, approximately 1000). Assuming sap density is that of water, the regression analysis reduces to:

$$T = \alpha(\rho AV) \tag{6}$$

where the value of α is the calibration coefficient, determined from the slope of the regression of T versus ρAV over a range of flow rates.

Materials and Methods

Gauge Design and Construction

The gauge design included three needle probes: a central resistance-heater probe to apply a heat pulse, a temperature probe directly above the heater to measure axial heat flow downstream, and a second temperature probe located to the side of the heater to measure tangential heat flow (Fig. 1). The spacing between the thermistors and the heater (L_d and L_t) impacts the unit response and quality of the data – while more pronounced temperature peaks occur when the thermistors are closer to the heater, small construction imperfections or deflections during insertion have larger impacts on the data (Cohen et al., 1988) and errors in V_h estimates are larger for smaller probe spacing (Kluitenberg and Ham 2004). The final design utilized the closest spacing achievable with our fabrication materials and the constraints of the needle hub (L_d = 8.5 mm; L_t = 5.5 mm). The heater probes and temperature sensors were fabricated from 25-mm long 18-AWG hypodermic needles using the techniques in Ham and Benson (2004). The heater was made from two loops (four strands) of enameled heater wire (40 AWG Solid (0.0031), Nichrome 80, 222 Ohms/m; Pelican Wire Company, Florida, Naples, FL). The total resistance of the heaters after fabrication ranged from 26 to 35 ohms. Thermistor probes were made from 10K NTC thermistors (LSMC 700A010K, Selco Products Co, Reno, NV). After the heaters and thermistors were positioned in the needles, an epoxy with high thermal conductivity (TC-2810, 3M, St. Paul, MN or Omega Bond 101, Omega Engineering, Stamford, CT) was injected in order to back-fill the needle air space and secure the sensors.

Thermally conductive epoxy was determined to be necessary for gauge durability, as the heater wire in early prototypes that used standard epoxy failed after repeated use.

The finished heater and temperature probes were mounted into a water-proof plastic chassis fabricated on a 3-D printer (Lulzbot TAZ, Aleph Objects Inc., Loveland, CO, USA) from ABS plastic with three interchangeable parts: probe assembly (containing needles/sensors), a spacer, and a backside clamp (Fig. 1). This allowed the same sensor electronics to be installed on plant stems with different diameters and permitted the adjustment of the needle penetration depth by simply changing the spacer and backside clamp (parts B and C in Figure 1). An example of a sap flow gauge installed on a sunflower plant is shown in Figure 2.

Data Acquisition System

The data acquisition and control system was designed around an Arduino open-source microcontroller board (Arduino, LLC) equipped with a data logger shield from Adafruit industries LLC, NY. The heat pulse (9 to 12V applied for 6 or 8 seconds) was controlled using a MOSFET (FQP30N06L, Fairchild Semiconductor, Sunnyvale, CA, USA) and the current flowing through the heater was measured with high side DC current module (INA219 Breakout, Adafruit Industries, LLC). Typical power applications per length of probe were between 600 and 900 J/m. The thermistors were excited using a precision 2.5V voltage source (LT1460-2.5, Linear Technology, Milpitas, CA, USA) and the transducer output from a 10K half-bridge circuit was measured with 16-bit sigma-delta ADC module (ADS1115 Breakout, Adafruit Industries). Thermistor resistance was converted to temperature with the Steinhart-Hart equation fitted to resistance vs. temperature data provided by Selco Products. The resolution of the temperature measurement was 0.002 ºC. The data logging system was configured to take readings every 10 minutes using the following protocol: 1) sample initial temperature of all sensors, 2) apply heat

pulse for 6 or 8 seconds and monitor heater current and voltage during pulse, 3) measure the resultant temperature lift at all sensors at 2 Hz for a period of 180 seconds. When not taking a sap flow reading, the temperature of the stem was monitored at 1-minute intervals. These data were used to detrend the heat pulse data by knowing the background rate change in stem temperature before the heat pulse. Each data logger system had the capability to read two gauges simultaneously, store time-stamped data on an SD card, and display real-time results on an LCD. A simplified wiring schematic is shown in Figure 3. During the field portion of the study, the dataloggers were powered with 14.8V 7800mAh Li-ion rechargeable batteries that were changed on a weekly basis.

Estimating Sap Velocity

Each sap flow reading resulted in two heat pulse curves, one for the downstream probe (L_d) and one for the side probe (L_t). Each times series was first de-trended to remove the background rate change in stem temperature prior to heating (i.e., remove the effect of natural heating and cooling). The background change in temperature was estimated using stem temperatures collected one minute prior to the application of the heat pulse. After de-trending, the time to maximum ($t_{m,d}$ and $t_{m,t}$) were estimated by first smoothing the data using a Savitzky-Golay (SG) moving-polynomial algorithm (Savitzky and Golay, 1964). This was not done to remove noise from the data acquisition system, but to help identify the true maximum in cases where the temperature peak was relatively flat and there was not a unique value for the time to maximum. This typically occurred during low flow for the downstream probe and during high flow for the side probe. The data were initially smoothed using an 11-point SG window – representing 5 s when sampling at 0.5 s intervals. If a unique peak was not found with the 11-point window, then successively longer SG windows were used (e.g., 15, 19, etc) until a unique

peak was found. The largest window ever required to find $t_{m,d}$ or $t_{m,t}$ was 23 points. For the T_{max} method, diffusivity in the axial direction, k_x, was estimated from predawn data (i.e., between 3 to 5 AM) from the side probe using equation 3. For the HR_{max} method, a diffusivity of 2.4 x 10^{-7} m^2 s^{-1} was used (Cohen et al. 1993). We did not use the T_{max}-based diffusivity for the HR_{max} method because the k determined from equation 3 is an apparent diffusivity used to "zero" the T_{max}-based output and contains the effect of model and measurement errors – i.e., it isnot a true thermal property. The k in the HR_{max} method is essentially a multiplier, and any errors in k will be accounted for in the calibration term α (Eq. 6). The maximum temperatures for use in the HR_{max} method were determined from the 11-point Savitzky-Golay-smoothed temperatures. Once the time to maximum and thermal properties were known, the velocities inferred from the downstream and side probes were estimated using equations 2, 4, and 5.

Greenhouse studies

Calibrations and tests were conducted in 2014 and 2015 on corn (Dekalb hybrid DKC52-04RIV) and sunflower (Syngenta hybrid 2495 NS/CL/DM) in the greenhouse facilities at Colorado State University, Fort Collins, CO. Plants were grown in 26-liter pots filled with a soilless mixture consisting of a 1:4 by volume ratio of Greens Grade™ and Fafard 2SV mix. Greens Grade™ consists of a minimum of 60% medium – course sand, 20-30% of particles ranging from fine sand to clay, and less than 10% very course sand. The Fafard 2SV mix is a fine grade mix of peat moss and fine vermiculite. Plants were kept well-watered during growth via automatic fertigation. Peters' Excel Cal-Mag (15-5-15) was applied at a strength of 200 ppm N through the irrigation lines (Kottkamp et al., 2010). Supplemental lighting throughout the greenhouse was provided for a period of 13 hours (7:00 – 20:00).

Greenhouse measurements were made in December 2014 - January of 2015 when corn plants were in early reproductive growth stages (i.e., R1 - R2). Sunflower greenhouse measurements occurred in January and February of 2015 when plants were flowering (i.e., R5.5 to R6; Schneiter and Miller 1981). Prior to initiation of the SF calibrations and experiments, the pots were sealed with Glad® Press ‘n Seal to eliminate evaporation from the soil surface. Plants were then set on 20- kg capacity digital balances (Adam CBK , Adam Equipment Inc., Bletchley Milton Keynes, UK) connected to a laptop equipped with logging software for the monitoring of gravimetric water loss (Adam Data Capture Utility software, Adam Equipment Inc., Bletchley Milton Keynes, UK). The rates of water loss were measured by automatically weighing the pot to the nearest 0.1 g every minute. To reduce air flow effects on the scale readings, a three-sided transparent plastic wall (1 m x 1.2 m) was placed around the plants. An additional high wattage digital ballast with selectable dimming levels (400W, 600W, and 1000W) mounted above the plants provide further control of light levels (LK1000AC, Lumatek, Novato, CA).

Prior to probe insertion, the printed spacer and the backside clamp were installed on the plant as a temporary jig and plant stems were bored radially with a miniature electric drill (Item #500, General Tools and Instruments LLC, Secaucus, NJ). In corn, probes were installed above the second internode after the removal of the leaf sheath, whereas in sunflower the probes were installed above the second or third node. Insertion depths for the thermistor and heater needles were 6.5 mm and 9 mm, respectively, similar to the depths recommended by Cohen et al. (1996). Stem diameter at the point of insertion was measured via caliper to the nearest 0.1 mm. Stem diameters in greenhouse corn ranged from 16 – 21 mm, whereas stem diameters in sunflower were 26 – 30 mm. Despite this variation in stem diameter, utilizing custom 3D spacers allowed the same gauges to be used on both species. To construct calibration curves, measurements of V_h

over a range of environmental conditions were compared with the rates of water loss (T) measured by the scales.

Field Measurements

Field measurements were made on corn (Dekalb DKC-4620) in August of 2015 in a field near Fort Collins, CO (40° 39′ 19″ N, 104° 59′ 52″ W). Seeds were planted on May 27 2015 with a 0.0254 meter row spacing. Irrigation was applied to meet 100% of ET, and nitrogen was applied at a rate of 168 kg/ha. The target population density was 93,900 plants/ hectare. Density counts for actual population ranged from 94,580 – 95,568 plants/hectare. Four gauges were installed along an 8-meter section of row with installation procedures identical to those performed in the greenhouse, with the addition of a protective rain and irrigation shield. Measurements were made from DOY 234 - 251 when plants were near physiological maturity at the R4 or 'dough' growth stage. The calibration coefficients developed in the greenhouse were tested and applied to the field data. Estimates of sap flow were then compared to reference ET as calculated from a nearby weather station data using the ASCE tall crop formula (Allen et al., 1998). Sap flow was scaled up to a land area basis using plant population.

Results

Example Heat Pulse Data

The temperature increases following a heat pulse is shown in Figure 4. This data demonstrates the precision and fidelity of the temperature measurements made with the low-cost Arduino board. The signal was very steady, with a temperature resolution of 0.002°C. The magnitude and pattern of the temperatures detected at both probes were strongly affected by flow rates. At higher flows, the downstream probe shows a pronounced temperature peak, while the peak for the side probe is smaller (Figure 4; a). However, a low flows, the side probe continues

to provide useful data, whereas the downstream probe becomes extremely flat (Figure 4; b). The T_{max} method relies on sensing changes in time to maximum at the downstream sensor - a shift from 58 s to 150 s between high and low flows. Whereas the HR_{max} method detect changes in ($T_{m,d}/T_{m,t}$), which is approximately (1.4/0.4 =3.5) during high flow and (0.5/1.0 = 0.5) during low flow.

Sunflower

Greenhouse Calibration

Midday maximum sap flow rates for well-watered sunflower were very high, typically ranging from 300 to 400 g h^{-1}. Night time flows were frequently as high as 40 g hr^{-1}. These daytime flow rates for isolated plants are higher than what would occur under field conditions. For example, Howell et al. (2012) reported maximum daily ET rates of 12 – 14 mm d^{-1} for irrigated sunflower grown in the advective environment of the Texas High Plains with a plant population of 56,835 plants per hectare. This equates to a sap flow rate of 230 - 267 g hr^{-1} at peak midday flow. We constrained the data used in the calibration to actual flows of ≤ 300 g hr^{-1}, which is near the upper limit of the flows that would occur under irrigated field conditions. Data less than 30 g hr^{-1} were also excluded from the analysis because the T_{max} method was extremely noisy at low flow and we wanted to span the calibration of the range most relevant to crop water use.

T_{max} method

The relationship between the product of (ρV*a) and gravimetric transpiration for the T_{max} method is shown in Figure 5. The slopes of the regression lines for two gauges, installed on separate plants, are remarkably similar, with intercepts near zero. Cohen and Li (1996) utilized the T_{max} method in sunflower, and reported calibration factors of 0.73 and 1.21 with insertion

depths of 5.5 and 7.8 mm, respectively. Our insertion depth (6.5 mm) is intermediate of these two values, and we obtained calibration factor for combined data of 0.85 (R^2 = 0.94).

The calibration coefficient is a function of wounding, sensor location, gauge design, and stem structure. Additionally, the velocity profile within the stem is not uniform due to uneven distribution of vascular conducting elements (Green et al. 2003). The sensor(s) measure only a small proportion of the stem cross-sectional area, and the V_h measured by the sensor can differ from the average value for the entire cross sectional stem area (Cohen and Li, 1996; Jones et al., 1988). In mature sunflower, the vascular system is confined to a continuous ring at the outer perimeter of the stem (i.e., ≈ the outer 3 mm; Cohen and Li 1996). The high density of conducting elements in the outer perimeter of the sunflower stem means that the needle and thermistor is in good contact with sap conducting tissue, and the measured V_h per unit transpirational flux is high. This contributes to a lower calibration coefficient in sunflower (Cohen and Li 1996), providing a shallow insertion depth is used. We found that an additional motivation for a shallow insertion depth in sunflower is that the interior pith dries out or disintegrates with age, resulting in a hollow stem. Hence, deep insertion depths in sunflower can result in poor and widely varying calibration coefficients and are not recommended.

HR_{max}

The calibration data utilizing the first and second order solutions to the HR_{max} method is shown in Figures 6 and 7, respectively. The linear calibration for combined data with a forced zero intercept is 1.239 (R^2 = 0.88) for the first order HR_{max} method and 0.988 (R^2 = 0.88) second order HR_{max} method. The first order solution appears linear up until flows of approximately 150 g hr^{-1}, after which the data shows upward curvature. While it is possible that transpiration rates are not equal to sap flow when the plant is utilizing stored water above the gauge (i.e., from stem

or leaves). For example, imbalances between changes in leaf transpiration the lagging response of root water absorption can be buffered by stem water storage in order to prevent decreases in leaf water potential (Kitano and Eguchi, 1989). However, that fact that the T_{max} method did not show this upward curvature suggests that this is not the case for this data set. The calibration using the second order solution of the HR_{max} method shows less evidence of curvature, and a calibration coefficient that is almost 1 (i.e., 0.99) (Figure 7).

Performance of the T_{max} and HR_{max} methods under varying flows

The diurnal time course of transpiration versus sap flow between the T_{max} and HR_{max} (2^{nd} order) methods is shown in Figure 8 for a temporally separate set of data than was used in the calibration. While this is not a true independent validation of the method, as the same plants were used, it shows the ability of the gauges to dynamically track changes in transpiration driven by changing environmental conditions. Plants were initially well watered, but allowed to progressively dry down to a state of severe water stress in order to test gauge performance under both high and low flows.

Examination of the T_{max} method shows that it was able to accurately track flows as high as 250 g hr^{-1}, but when transpiration rose above 300 g hr^{-1}, the T_{max} method underestimated transpiration (Figure 8; a). It also considerably overestimated at low flow rates. The HR_{max} method (Figure 8; b) tracked high flows, and also resolved low flows much better than the T_{max} method. A subsample of the data in Figure 8 is shown in Figure 9. Plants were severely water-stressed in this time period, resulting in lower rates of transpiration and sap flow. When compared to the T_{max} method, it is clear that the HR_{max} method substantially improves transpiration estimates under low or nighttime flows.

Corn

Greenhouse Calibration

Midday maximum sap flow rates for well-watered corn were substantially lower than sunflower, typically ranging from 150 - 175 g h^{-1}. Nighttime flows were also much, lower (i.e., ≈ 3 - 4 g hr^{-1}). Calibrations for the T_{max} and HR_{max} methods are shown in Figures 10 – 12. The calibrations from all three methods were highly linear, with intercepts near zero. While both the T_{max} method and the 1st order HR_{max} method had high R^2 values and intercepts close to zero, the calibration for combined data for the second order solution to the HR_{max} method was nearly 1 (i.e., 0.98), whereas the calibration coefficient for the T_{max} method was 1.24. Interestingly, the calibration coefficients we obtained for the T_{max} method were lower substantially lower than those reported by Cohen and Li (1996) for corn. They found the calibration coefficients for the T_{max} method to be 1.59 ± 0.06 with an insertion depth of 5.5 mm, and 1.96 ± 0.148 with an insertion depth of 7.8 mm. These high calibration coefficients indicate that the true V_h is often underestimated by T_{max} techniques in maize. Cohen et al. (1993) traced sap velocity in the vascular bundles of maize, and estimated that sap velocities in these bundles were ≈ 10 times higher than the sap flux densities estimated via the T_{max} HP method. Maize is a monocot with vascular bundles scattered throughout the tissue, and the probability for the sensor to be in contact with conducting tissue is smaller than in sunflower, resulting in a lower measured V_h per unit transpirational flux (i.e., a higher calibration coefficient). The density of bundles also decreases with depth, diminishing the number of vascular bundles in contact with the sensor (Cohen and Li 1996) and increasing the calibration coefficient

Performance of the T_{max} and HR_{max} methods under varying flows

The diurnal time course of transpiration versus sap flow between the T_{max} and HR_{max} (2^{nd} order) methods is shown in Figure 13 for a temporally separate set of data than was used in the calibration. Again, this is not a truly independent validation of the method, as the same plants were used, but demonstrates the capacity of the gauges to dynamically track transpiration.

Similar to the results in sunflower, the T_{max} method was able to accurately track flows as high as 150 g hr^{-1}, but overestimated the low flows that occur at night (Figure 13; a). The HR_{max} method (Figure 13, b) tracked flows high flows, and was able to measure flows as low as 3 g hr^{-1}. A subsample of the data in Figure 13 is shown in Figure 14 to highlight the substantial advantage of the HR_{max} in measuring transpirations under low or nighttime flows.

Field Comparisons

Examination of Figure 15 for field plants shows that there was substantial plant-to-plant variation (e.g., 20%) in estimated transpiration, even in an irrigated field that appeared uniform. This is likely caused by inherent differences in leaf area and interception of radiation among plants. A subset of data from the HR_{max} method is highlighted in Figure 16 to demonstrate how closely the sap flow gauges tracked changes in solar radiation, the overarching driver of plant transpiration in this environment. Solar radiation data was collected on an hourly basis while sap flow was measured every 10 minutes – accounting for some of the observed divergence. All three methods, when averaged over the four gauges in the field, were higher than reference ET calculated from a nearby weather station (Fig 17). Estimates from the T_{max} method were 37% higher than reference ET due to overestimation of nighttime transpiration. However, most corn and sunflower production is under irrigated conditions or in regions in adequate soil moisture where flow rates are high for most of the day. Thus, the T_{max} method could be utilized to study

the daytime water use of these crops if periods of low-flows (i.e., nighttime) are discarded or replaced with data from the HRmax technique. Some users may find it useful to utilize the T_{max} method at high flows, and switch to the HR_{max} method at lower flows. However, the 1st order and second order solutions to the HR_{max} method differed from reference ET (ASCE tall crop formula) by only 12.7% and 9.5%, respectively. The close relationship between sap flow estimates of transpiration and reference ET supports the usefulness of the HP technique for monitoring canopy transpiration in the field.

Conclusions

Large spatial replication of sap flow measurements is often needed to accurately capture spatial variability and allow for statistical comparison of treatments at the field or watershed scale (Jara et al., 1998; Senock et al., 1996). Thus, there is need for low-cost SF gauges that can be easily replicated and deployed. In this study, we developed a novel modular 3D-printed SF gauge, which allows the same electronics to be used on plants of different shapes and stem diameters. In continuance with the pursuit of low-cost open-source technology, we developed a data acquisition and control systems built from low-cost Arduino microcontrollers.

The heat pulse approach was selected due to its low power requirements and flexibility of design for use on multiple stem diameters. Our initial work focused on the T_{max} method, but recent work in trees suggested that the use of a probe tangent to the heater may be beneficial when using the HP methods. While not explored here, data from the three probe design could also be used in a parameter estimate scheme to correct for temporal changes in stem thermal properties over time (Vandegehuchte and Steppe, 2013). Exploration of the heat pulse theory resulted in a new equation for measuring V_h that uses the ratio of the maximum temperature

increase between the downstream and tangential probes, HR_{max}. We found this approach to have distinct advantages in measuring transpiration under low flows.

One of the drawbacks to the T_{max} method is that the temperature trace develops a broad and flat peak at low flows that makes it difficult to identify T_{max}. The T_{max} method performed well during the high daytime flows in both sunflower and corn, but the method performed poorly under low transpiration rates and at night, similar to the result reported by others (Cohen 1988; Cohen et al. 1993). Other studies have also found the T_{max} method to produce very consistent measurements during the day whereas nighttime measurements are noisy (Green et al. 2003). While resolution at low flows can be improved if probe spacing is increased, the trade-off is a smaller temperature rise, a less readily identifiable peak (Green et al. 2003).

While both the T_{max} and HR_{max} methods worked well at higher flows (i.e., > 40 g hr-1), the HR_{max} method worked much better than the T_{max} method under low flows. The new HR_{max} permitted measurement over the entire range of velocities found in maize and sunflower. The HR_{max} method also provides a promising potential tool for measuring low flows under conditions of water stress or at night. Additionally, the HR_{max} method is not sensitive to changes in background temperature of the stem, eliminating the need to detrend the data prior to analysis. A drawback of the HR_{max} method is that it does not allow easy determination of *k* from a zero flow assumption and it is more sensitive to the geometry of the probe spacing than the T_{max} method.

Both methods require the user to develop a calibration coefficient for a specific species, sensor design, and insertion depth. Cohen et al. (1993) found it to be stable across developmental stages in soybean and maize. There could be differences in vasculature arrangement between varieties, but Sass (1977) found that the vasculature was fairly consistent in several hybrids of maize, suggesting that the calibration coefficients for different corn varieties should be similar.

Overall, the literature and our data suggests that one general calibration factor is applicable in a given field crop species for a specific sensor design and insertion depth. Obtaining a genotype or species-specific calibration factor is now simple and straightforward, given the availability of low-cost high resolution scales that log gravimetric water loss (e.g., Adam DU). These scales can be linked via USB to a laptop for continuous measurements of gravimetric water loss without a data logger. While access to a controlled environment greenhouse is convenient, it is not necessary as long as measures are taken to stabilize the scale readings from wind (Cohen et al. 1988).

After calibration for probe spacing and species, the sap flow system was able to estimate canopy transpiration in corn under field conditions to within 10% of reference crop ET estimates. If a sufficient number of gauges are deployed to capture spatial variability, these low-cost user-fabricated gauges should be an excellent tool for estimating field or plot scale canopy transpiration. Future research should address gauge performance and calibration on crops throughout the growing season to account for changes in stem size and vascular anatomy. Larger scale field studies are needed to compare sap-flow estimates of canopy T to independent micrometeorological measurements (e.g., eddy covariance) or lysimeter measurements of ET.

Figures

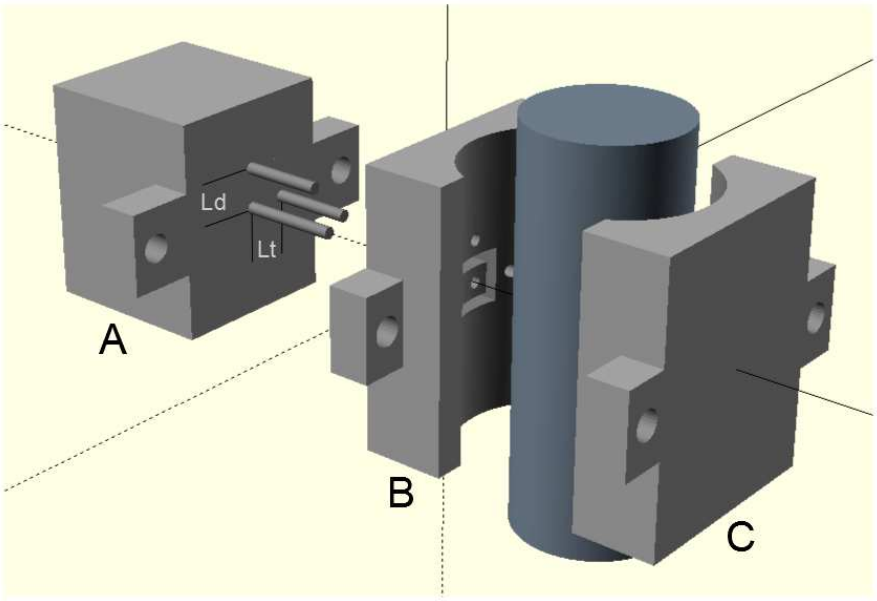

Figure 1. Schematic of a section of a stem demonstrating the components of the sap flow sensor. The 3D printed sensor body (A) contains three needle probes: a central resistance-heater probe to apply a heat pulse, a temperature probe directly above the heater to measure axial heat flow downstream (L_d) and a temperature probe located to the side of the heater to measure tangential heat flow (L_t). The interchangeable 3D printed spacer (B) and backside clamp (C) allows the same sensor body to be installed on stems of different diameters.

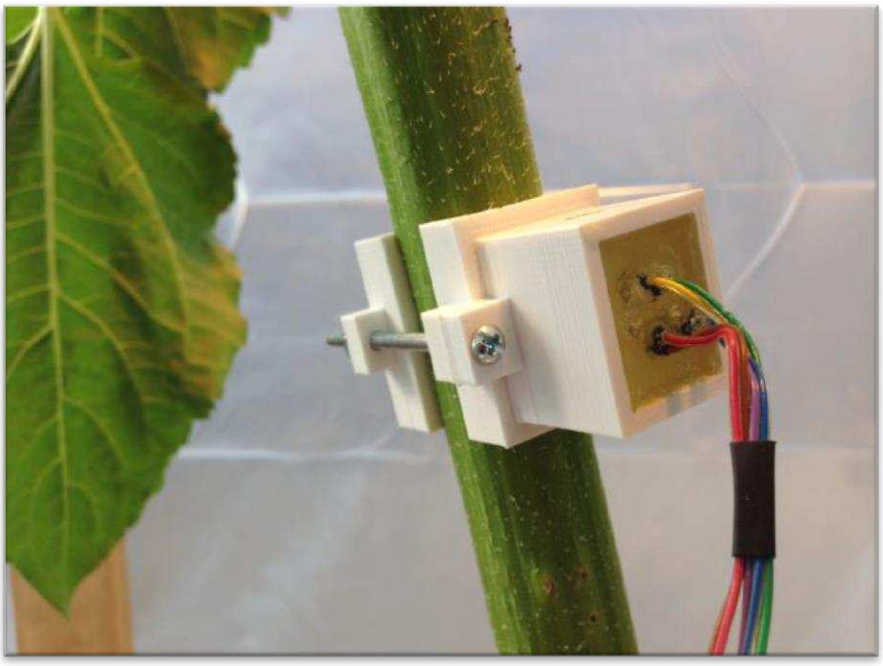

Figure 2. Sap flow gauge attached to a sunflower plant in the greenhouse.

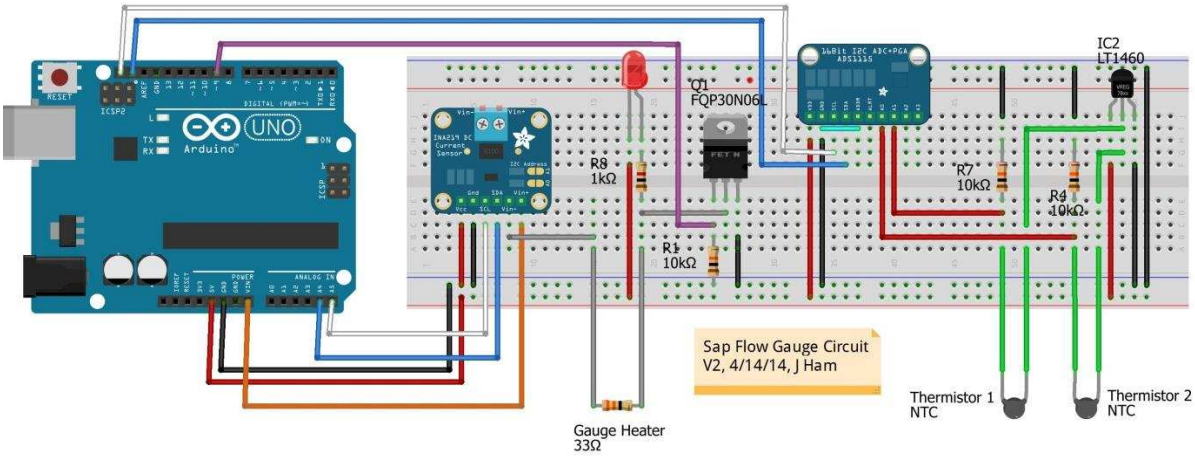

Fig 3. Simplified wiring schematic for reading one sap flow gauge. The Adafruit logger shield that sits atop the Arduino is not depicted, but the wiring is correct. This system can read two gauges (four thermistors), but only one pair of thermistors is shown.

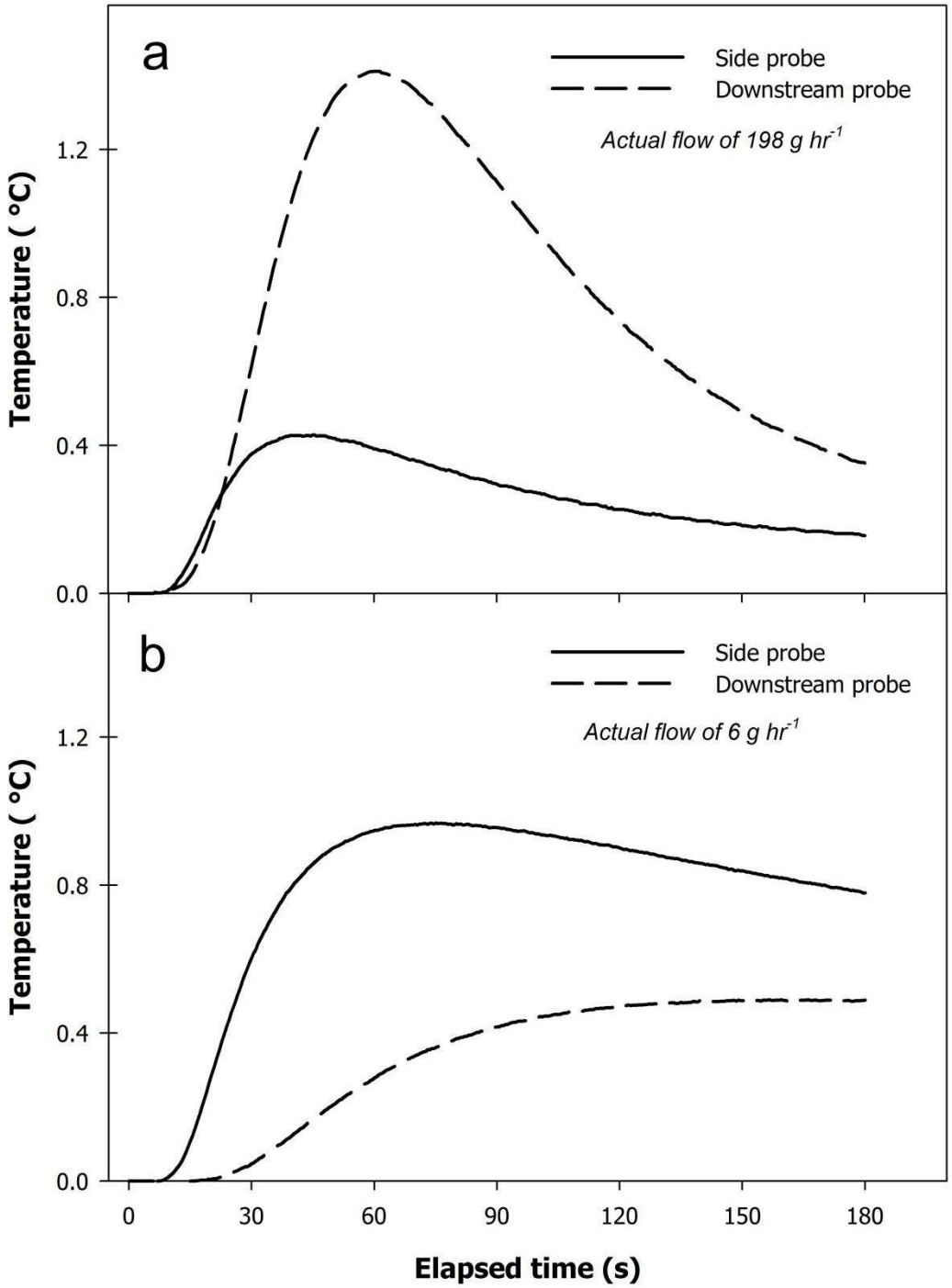

Figure 4. Comparison of the heat pulse signal in corn at two different flow rates. Data in panel (a) represents an actual flow of 198 g hr^{-1}, whereas actual flow rates in panel (b) were 6 g hr^{-1}. The heat pulse was 8 seconds for a total heat input of 825 J m^{-1}.

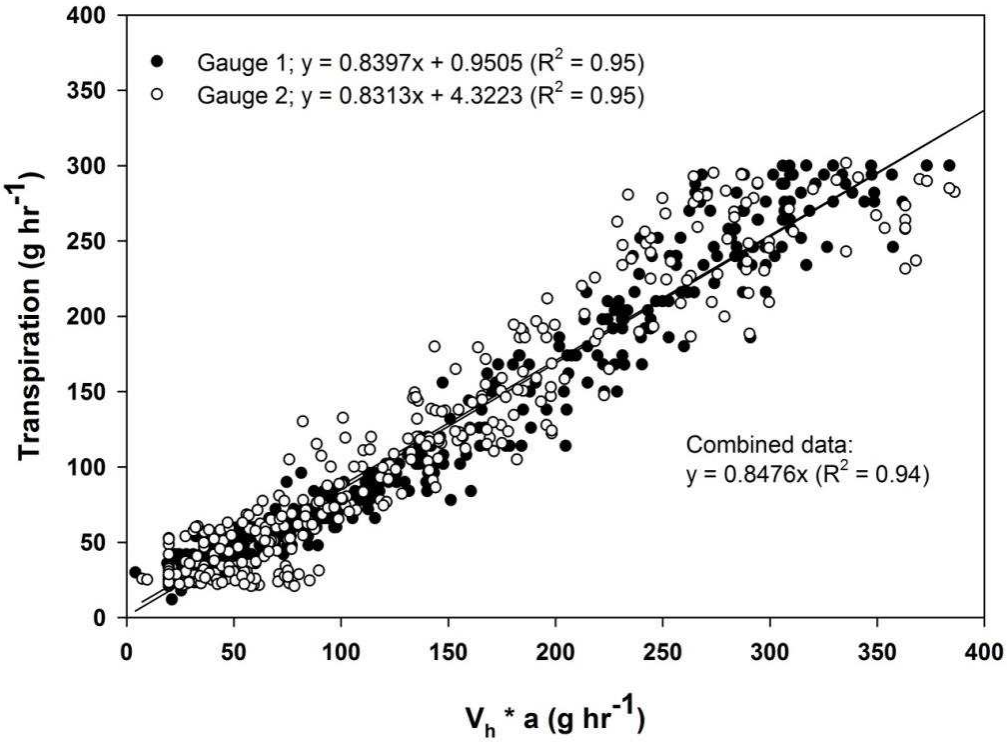

Figure 5. Calibration using the T_{max} method (eq. 2) for two gauges installed on separate sunflower plants. Data is for a five-day period under well-watered conditions. The V_h * a term also includes the density of water and a time adjustment to get to grams per hour.

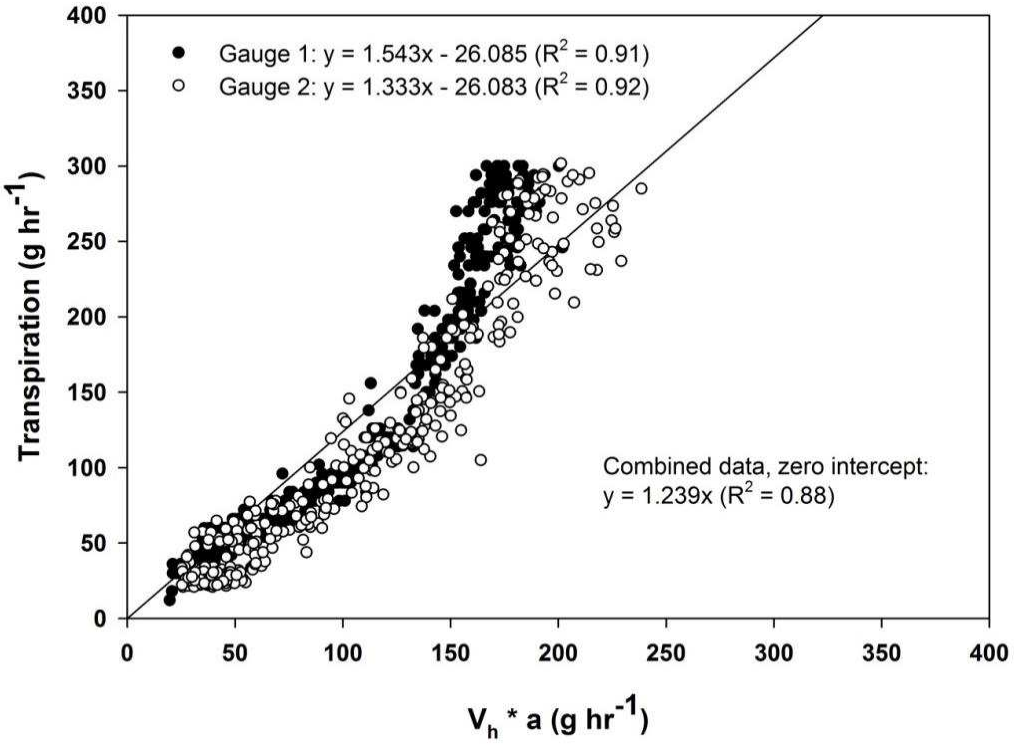

Figure 6. Calibration using the first order HR_{max} method (eq. 4) for two gauges installed on separate sunflower plants. Data is for a five-day period under well-watered conditions. The V_h * a term also includes the density of water and a time adjustment to get to grams per hour.

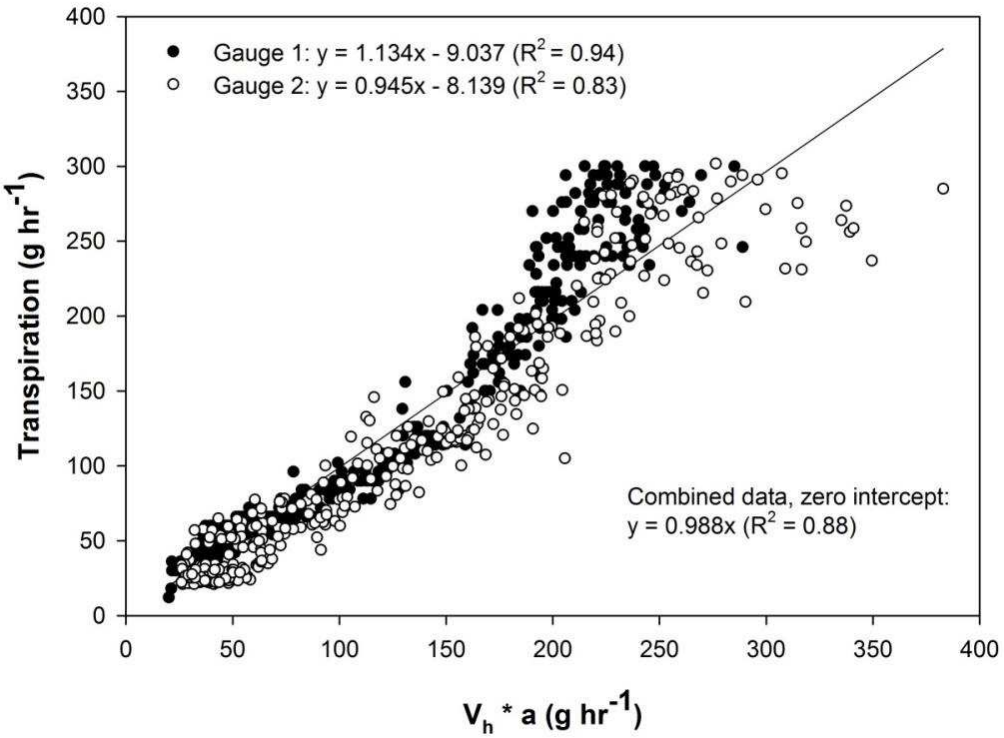

Figure 7. Calibration using the second order HR_{max} method (eq. 5) for two gauges installed on separate sunflower plants. Data is for a five-day period under well-watered conditions. Transpiration rates above 300 g hr^{-1} and less than 30 g hr^{-1} were excluded from the calibration. The V_h * a term also includes the density of water and a time adjustment to get to grams per hour.

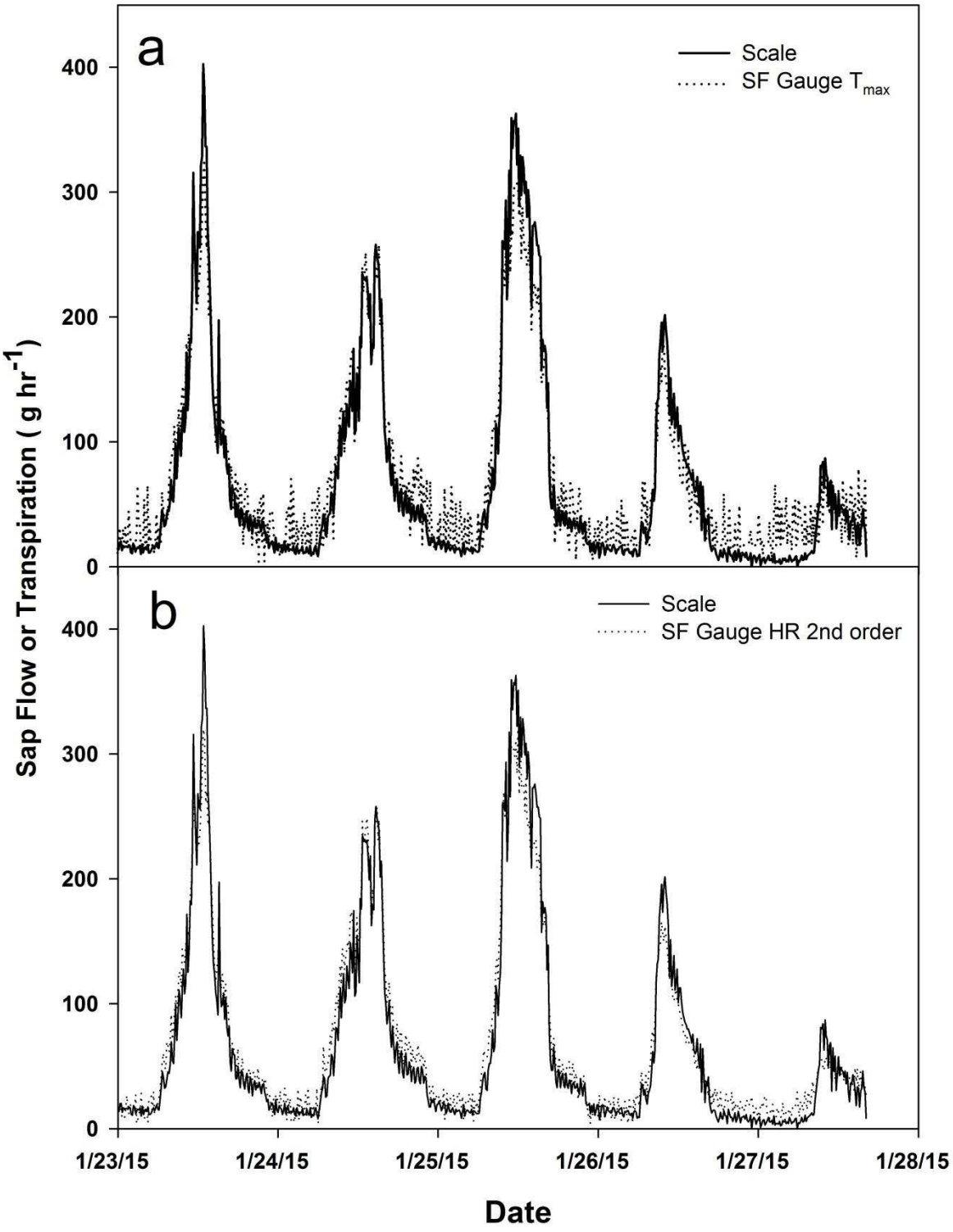

Figure 8. Comparison of the diurnal course of transpiration versus sap flow in sunflower utilizing (a) the T_{max} method (b) the second order HR_{max} method. Plants were initially well-watered, but allowed to progressively dry down to a state of severe water stress.

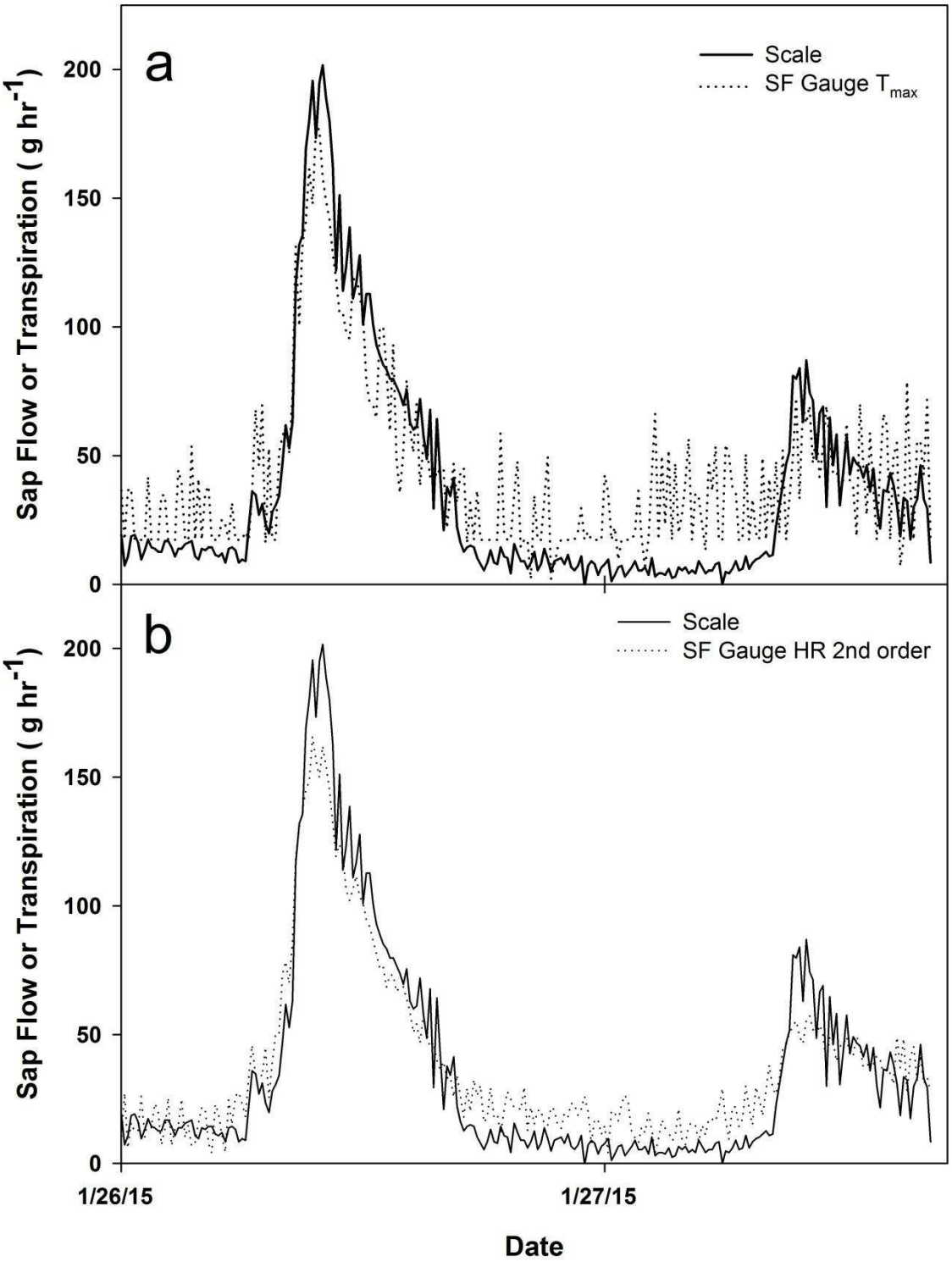

Figure 9. Comparison of the diurnal course of transpiration versus sap flow in sunflower utilizing the Tmax method (a) and the second order HR_{max} method, demonstrating how the method tracks under conditions under low flows or water stress.

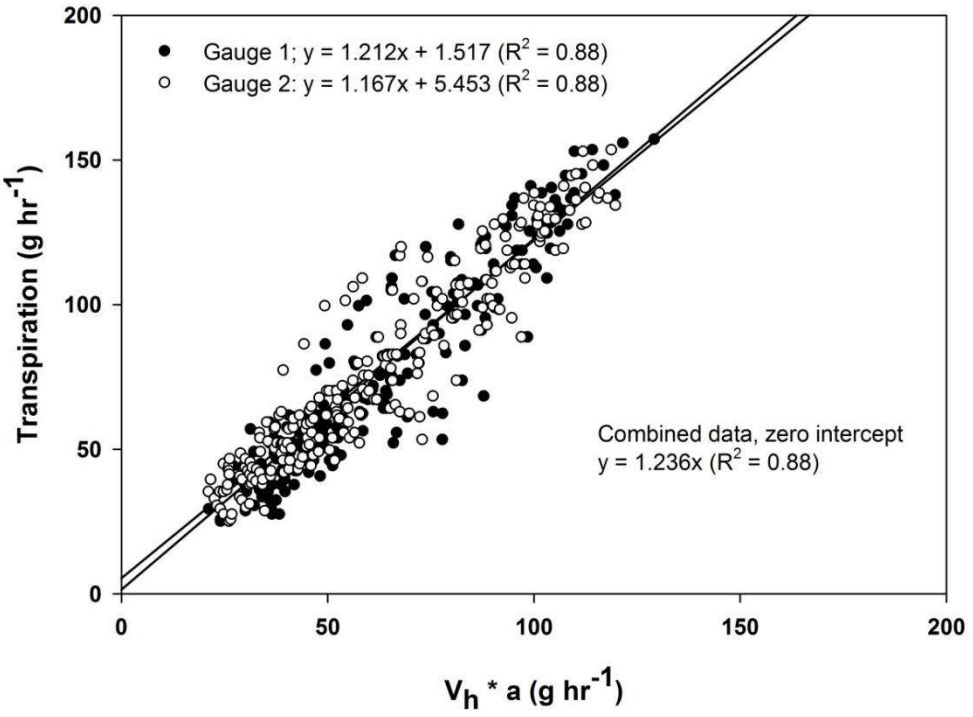

Figure 10. Calibration using the T_{max} method for two gauges on the same corn plant. Data is for a six-day period under well-watered conditions. Transpiration rates less than 30 g hr^{-1} were excluded from the calibration. The V_h * a term also includes the density of water and a time adjustment to get to grams per hr^{-1}.

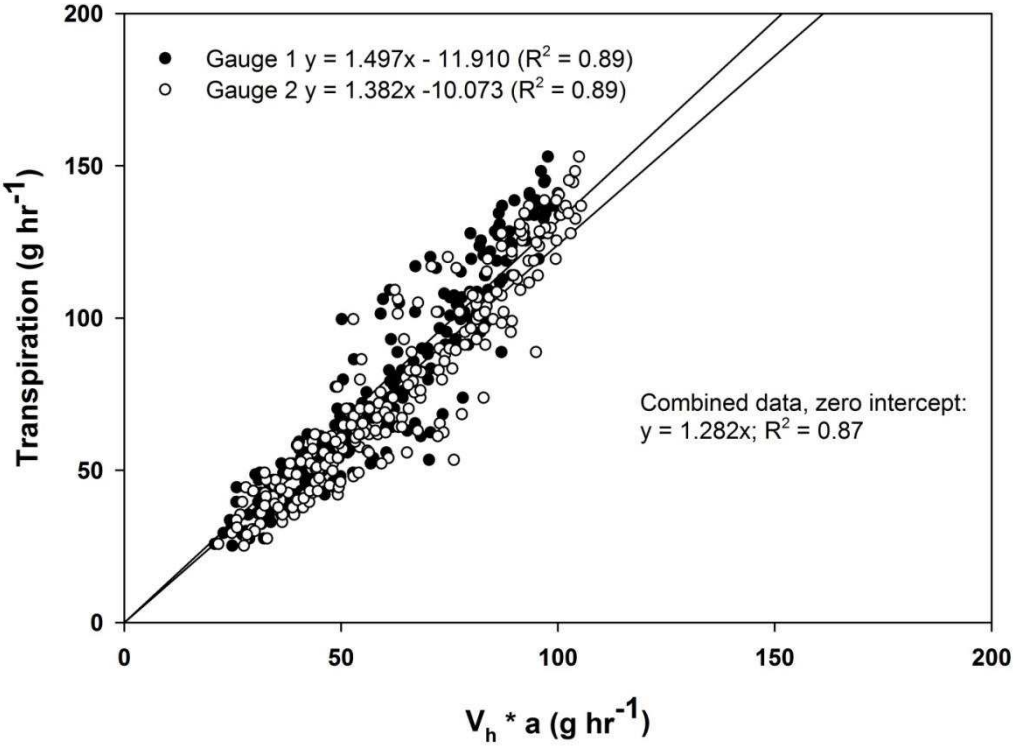

Figure 11. Calibration using the first order HR_{max} method for two gauges installed on the same corn plant. Data is for a six-day period under well-watered conditions. Transpiration rates less than 30 g hr^{-1} were excluded from the calibration. The V_h * a term also includes the density of water and a time adjustment to get to grams per hr^{-1}.

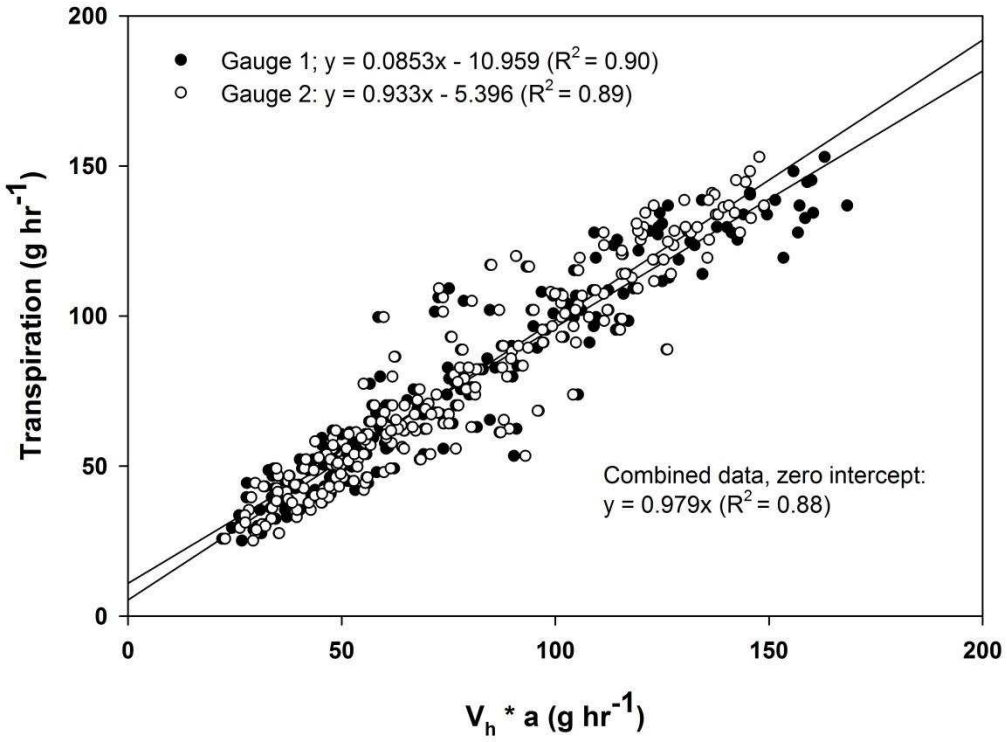

Figure 12. Calibration using the second order HR_{max} method for two gauges installed on the same corn plant. Data is for a six-day period under well-watered conditions. Transpiration rates less than 30 g hr^{-1} were excluded from the calibration. The V_h * a term also includes the density of water and a time adjustment to get to grams per hr^{-1}.

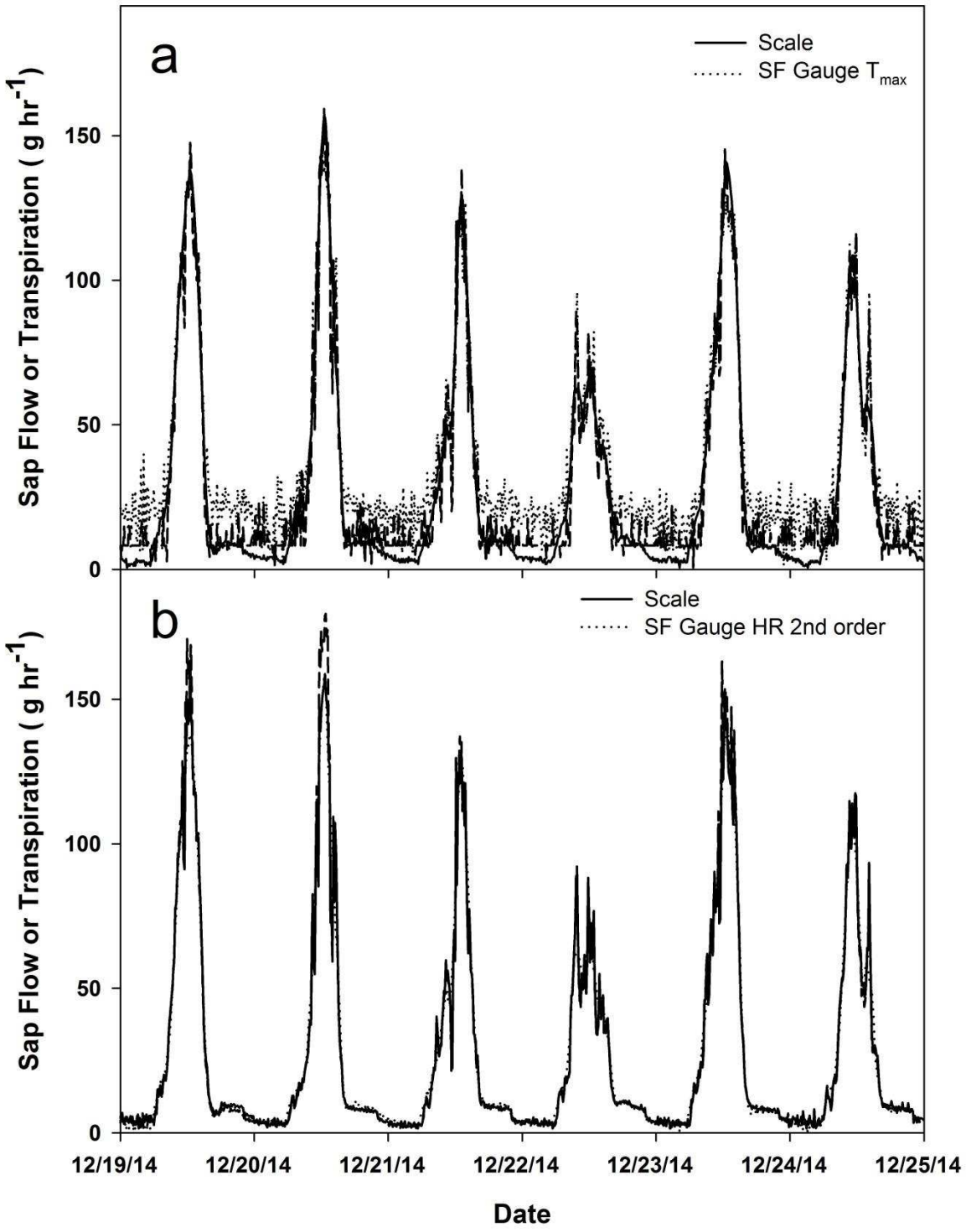

Figure 13. Comparison of the diurnal course of transpiration versus sap flow in corn utilizing (a) the T_{max} method or (b) the second order HR_{max} method.

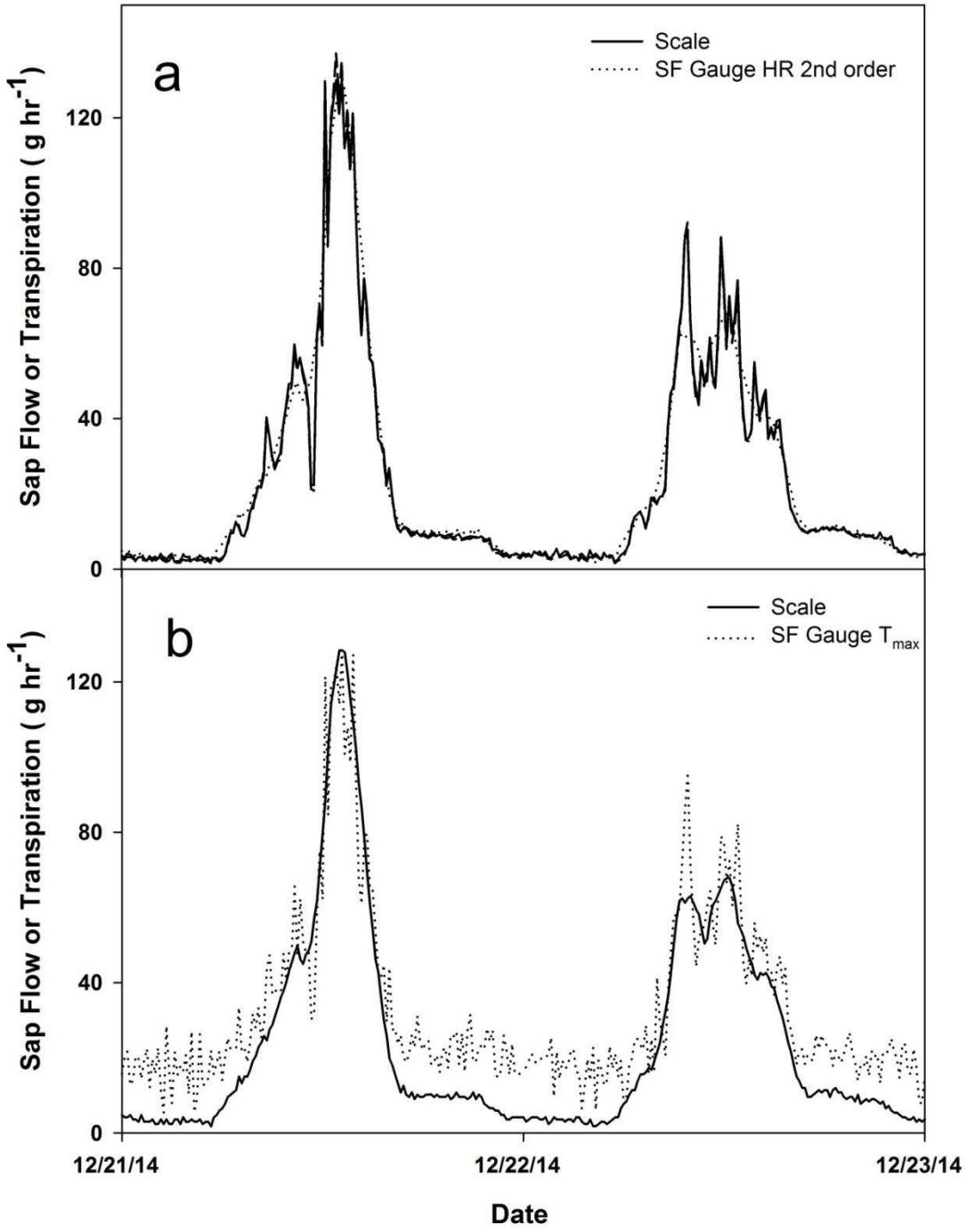

Figure 14. Comparison of the diurnal course of transpiration versus sap flow in greenhouse corn utilizing the second order HR_{max} method (a) or the T_{max} method (b), demonstrating how the methods track under low flows.

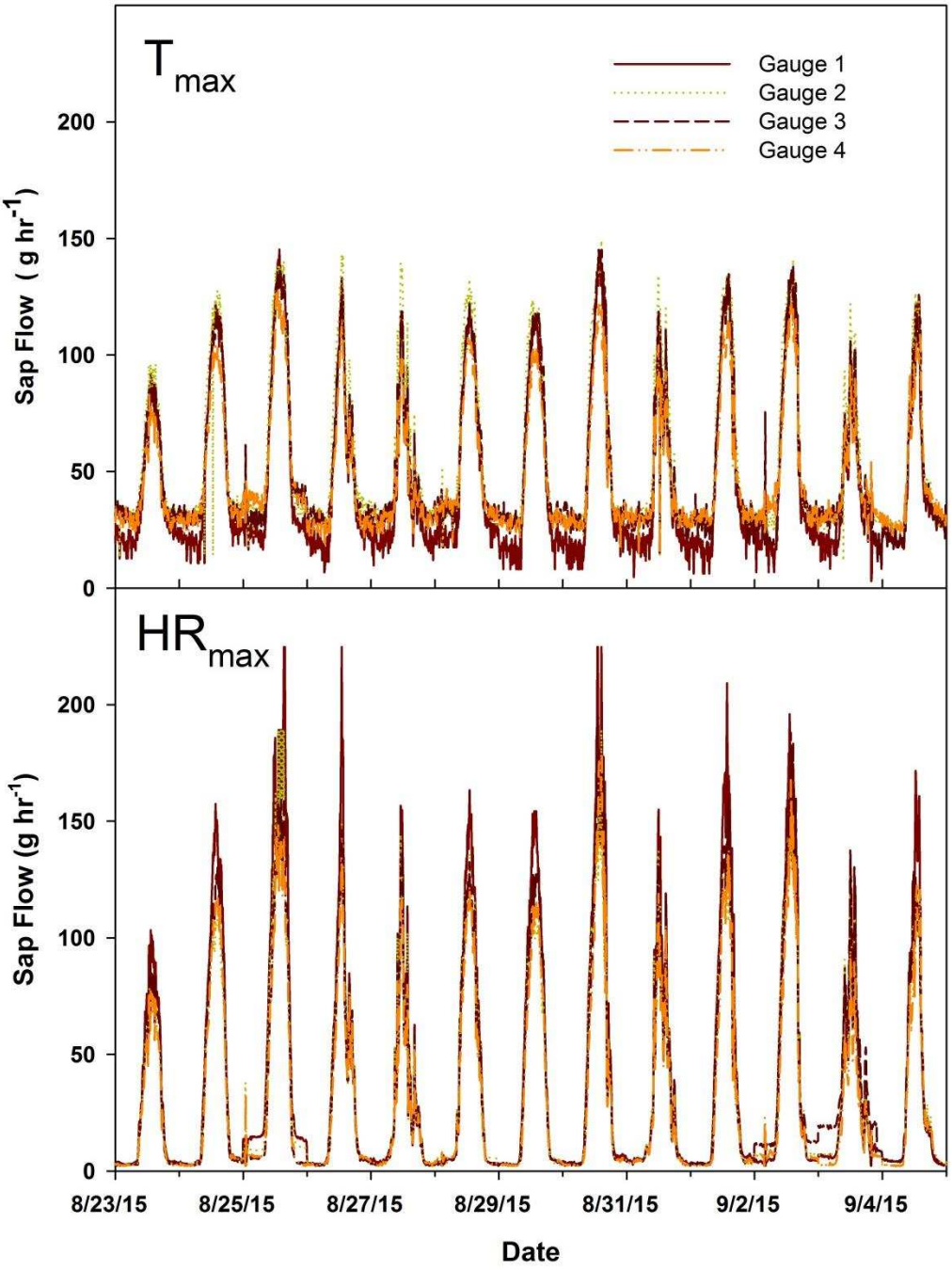

Figure 15. The diurnal course of sap flow over two weeks for four sap flow gauges installed on different corn plants in the field. Estimated sap flow using the T_{max} method is shown in the upper panel, while the results from utilizing the second order solution to the HR_{max} method are shown in the lower panel.

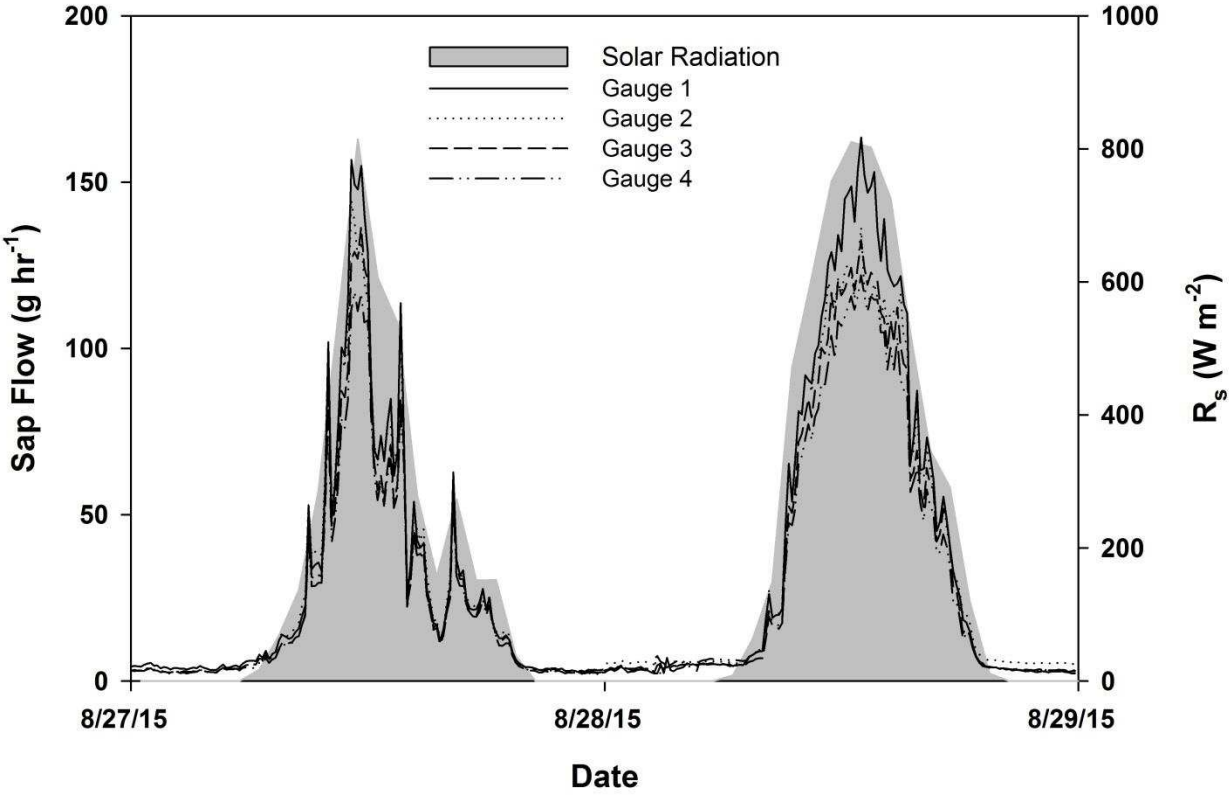

Figure 16. The diurnal course of sap flow for four sap flow gauges installed on different corn plants in the field. Sap flow is estimated using the second order solution to the HR_{max} method. Solar radiation data was collected on an hourly basis while sap flow was measured every 10 minutes, accounting for some of the observed divergence.

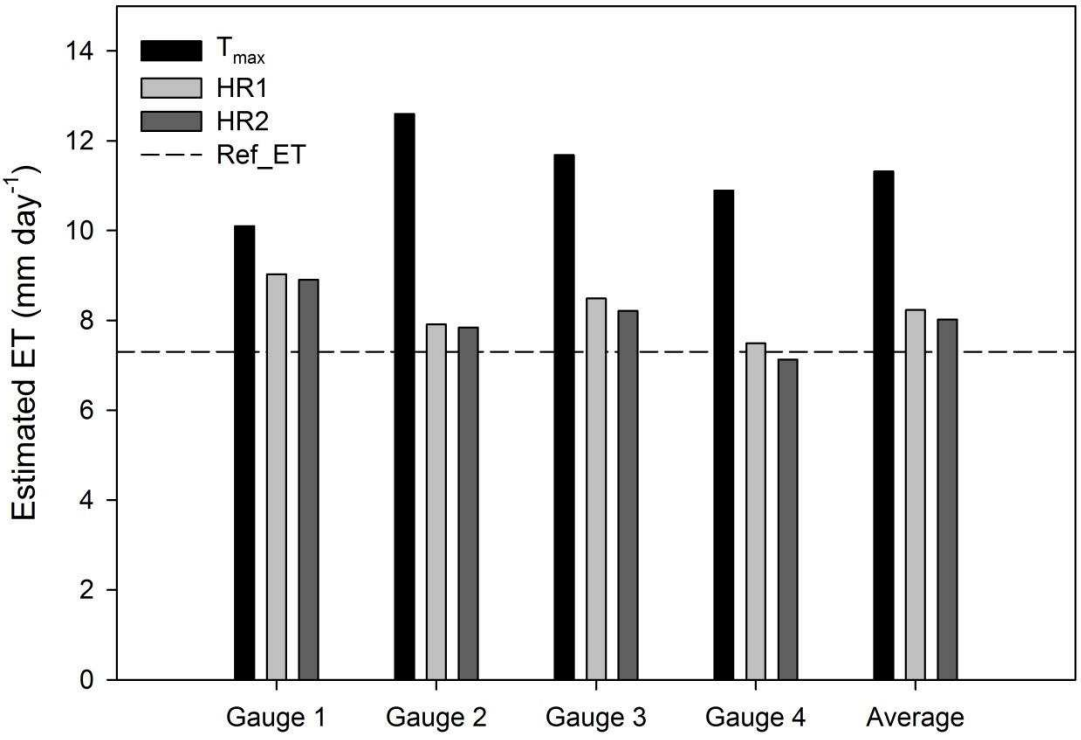

Figure 17. Comparison of estimates of plant transpiration for individual gauges installed on corn in the field for the T_{max} and HR_{max} methods. The average reference ET calculated using from a nearby weather station is shown by the dashed line

CITATIONS

Alarcón, J., Domingo, R., Green, S., Nicolás, E. and Torrecillas, A., 2003. Estimation of hydraulic conductance within field-grown apricot using sap flow measurements. Plant Soil, 251(1): 125-135.

Allen, R.G., Pereira, L.S., Raes, D. and Smith, M., 1998. Crop evapotranspiration-Guidelines for computing crop water requirements-FAO Irrigation and drainage paper 56. FAO, Rome, 300(9): D05109.

Allen, S. and Grime, V., 1995. Measurements of transpiration from savannah shrubs using sap flow gauges. Agricultural and Forest Meteorology, 75(1): 23-41.

Baden, T. et al., 2015. Open Labware: 3-D printing your own lab equipment. PLoS Biol, 13(3): e1002086.

Baker, J. and Bavel, C.v., 1987. Measurement of mass flow of water in the stems of herbaceous plants. Plant, Cell & Environment, 10(9): 777-782.

Bauerle, W.L., Post, C.J., McLeod, M.F., Dudley, J.B. and Toler, J.E., 2002. Measurement and modeling of the transpiration of a temperate red maple container nursery. Agricultural and Forest Meteorology, 114(1-2): 45-57.

Bremer, D.J., Ham, J.M. and Owensby, C.E., 1996. Effect of elevated atmospheric carbon dioxide and open-top chambers on transpiration in a tallgrass prairie. Journal of Environmental Quality, 25(4): 691-701.

Burgess, S.S. et al., 2001. An improved heat pulse method to measure low and reverse rates of sap flow in woody plants. Tree Physiology, 21(9): 589-598.

Caird, M.A., Richards, J.H. and Donovan, L.A., 2007. Nighttime stomatal conductance and transpiration in C3 and C4 plants. Plant Physiology, 143(1): 4-10.

Čermák, J., Deml, M. and Penka, M., 1973. A new method of sap flow rate determination in trees. Biol. Plant., 15(3): 171-178.

Čermák, J., Kučera, J. and Nadezhdina, N., 2004. Sap flow measurements with some thermodynamic methods, flow integration within trees and scaling up from sample trees to entire forest stands. Trees, 18(5): 529-546.

Cohen, Y., Fuchs, M., Falkenflug, V. and Moreshet, S., 1988. Calibrated heat pulse method for determining water uptake in cotton. Agronomy Journal, 80(3): 398-402.

Cohen, Y., Fuchs, M. and Green, G., 1981. Improvement of the heat pulse method for determining sap flow in trees. Plant, Cell & Environment, 4(5): 391-397.

Cohen, Y. and Li, Y., 1996. Validating sap flow measurement in field-grown sunflower and corn. Journal of Experimental Botany, 47(304): 1699-1707.

Cohen, Y., Takeuchi, S., Nozaka, J. and Yano, T., 1993. Accuracy of sap flow measurement using heat balance and heat pulse methods. Agronomy journal, 85(5): 1080-1086.

Dugas, W. et al., 1994. Sap flow measurements of transpiration from cotton grown under ambient and enriched CO 2 concentrations. Agricultural and Forest Meteorology, 70(1): 231-245.

Fernández, J., Green, S., Caspari, H., Diaz-Espejo, A. and Cuevas, M., 2008. The use of sap flow measurements for scheduling irrigation in olive, apple and Asian pear trees and in grapevines. Plant Soil, 305(1-2): 91-104.

Forster, M.A., 2014. How significant is nocturnal sap flow? Tree physiology, 34(7): 757-765.

Godfray, H.C.J., Beddington, J.R., Crute, I.R., Haddad, L., Lawrence, D., Muir, J.F., Pretty, J., Robinson, S., Thomas, S.M. and Toulmin, C., 2010. Food security: the challenge of feeding 9 billion people. Science, 327(5967), pp.812-818.

Granier, A., Biron, P. and Lemoine, D., 2000. Water balance, transpiration and canopy conductance in two beech stands. Agricultural and Forest Meteorology, 100(4): 291-308.

Green, S. and Clothier, B., 1988. Water use of kiwifruit vines and apple trees by the heat-pulse technique. Journal of Experimental Botany, 39(1): 115-123.

Green, S., Clothier, B. and Jardine, B., 2003. Theory and practical application of heat pulse to measure sap flow. Agronomy Journal, 95(6): 1371-1379.

Green, S., McNaughton, K. and Clothier, B., 1989. Observations of night-time water use in kiwifruit vines and apple trees. Agricultural and forest meteorology, 48(3): 251-261.

Ham, J. and Benson, E., 2004. On the construction and calibration of dual-probe heat capacity sensors. Soil Sci. Soc. Am. J., 68(4): 1185-1190.

Ham, J., Heilman, J.L. and Lascano, R.J., 1990. Determination of soil water evaporation and transpiration from energy balance and stem flow measurements. Agricultural and Forest Meteorology, 52(3-4): 287-301.

Howell, T.A., Evett, S.R., Tolk, J.A., Copeland, K.S. and Marek, T.H., 2012. Evapotranspiration and crop coefficients for irrigated sunflower in the Southern High Plains, 2012 Dallas, Texas, July 29-August 1, 2012. American Society of Agricultural and Biological Engineers, pp. 1.

Jara, J., Stockle, C.O. and Kjelgaard, J., 1998. Measurement of evapotranspiration and its components in a corn (Zea Mays L.) field. Agricultural and Forest Meteorology, 92(2): 131-145.

Jones, H.G., Hamer, P.J. and Higgs, K.H., 1988. Evaluation of various heat-pulse methods for estimation of sap flow in orchard trees: comparison with micrometeorological estimates of evaporation. Trees, 2(4): 250-260.

Kitano, M. and Eguchi, H., 1989. Quantitative analysis of transpiration stream dynamics in an intact cucumber stem by a heat flux control method. Plant physiology, 89(2): 643-647.

Kluitenberg, G. and Ham, J., 2004. Improved theory for calculating sap flow with the heat pulse method. Agricultural and Forest Meteorology, 126(1-2): 169-173.

Kottkamp, J., Varjabedian, A., Ross, J., Eddy, R. and Hahn, D.T., 2010. Optimizing Greenhouse Corn Production: What Is the Best Fertilizer Formulation and Strength? Purdue Methods for Corn Growth: 14.

Lu, P., Woo, K.C. and Liu, Z.T., 2002. Estimation of whole-plant transpiration of bananas using sap flow measurements. Journal of Experimental Botany, 53(375): 1771-1779.

Marshall, D., 1958. Measurement of sap flow in conifers by heat transport. Plant physiology, 33(6): 385.

Meinzer, F.C., James, S.A. and Goldstein, G., 2004. Dynamics of transpiration, sap flow and use of stored water in tropical forest canopy trees. Tree Physiology, 24(8): 901-909.

Pataki, D.E., McCarthy, H.R., Litvak, E. and Pincetl, S., 2011. Transpiration of urban forests in the Los Angeles metropolitan area. Ecol. Appl., 21(3): 661-677.

Pearce, J.M., 2012. Building research equipment with free, open-source hardware. Science, 337(6100): 1303-1304.

Pearce, J.M., 2015. Quantifying the value of open source hardware development. Modern Economy, 6(1): 1.

Sakuratani, T., 1981. A heat balance method for measuring water flux in the stem of intact plants. J. Agric. Meteorol, 37(1): 9-17.

Sakuratani, T., 1984. Improvement of the probe for measuring water flux in the stem of intact plants with the stem heat balance method. J. Agric. Meteorol: 177-187.

Sakuratani, T., 1987. Studies on Evapotranspiration from Crops:(2) Separate Estimation of Transpiration and Evaporation from a Soybean Field without Water Shortage. Journal of Agricultural Meteorology, 42(4): 309-317.

Sauer, T.J., Singer, J.W., Prueger, J.H., DeSutter, T.M. and Hatfield, J.L., 2007. Radiation balance and evaporation partitioning in a narrow-row soybean canopy. Agricultural and Forest Meteorology, 145(3): 206-214.

Savitzky, A. and Golay, M.J., 1964. Smoothing and differentiation of data by simplified least squares procedures. Analytical chemistry, 36(8): 1627-1639.

Senock, R. et al., 1996. Sap flow in wheat under free-air CO2 enrichment. Plant, Cell & Environment, 19(2): 147-158.

Senock, R.S. and Ham, J.M., 1993. HEAT-BALANCE SAP FLOW GAUGE FOR SMALL-DIAMETER STEMS. Plant Cell and Environment, 16(5): 593-601.

Smith, D. and Allen, S., 1996. Measurement of sap flow in plant stems. Journal of Experimental Botany, 47(12): 1833-1844.

Steinberg, S., van Bavel, C.H. and McFarland, M.J., 1989. A gauge to measure mass flow rate of sap in stems and trunks of woody plants. J. Am. Soc. Hort. Sci., 114(3): 466-472.

Stockle, C. and Jara, J., 1998. Modeling transpiration and soil water content from a corn (Zea Maize L.) field: 20min vs. daytime integration step. Agricultural and forest meteorology, 92(2): 119-130.

Swanson, R. and Whitfield, D., 1981. A numerical analysis of heat pulse velocity theory and practice. Journal of Experimental Botany, 32(1): 221-239.

Vandegehuchte, M. and Steppe, K., 2013. Sap-flux density measurement methods: working principles and applicability. Functional Plant Biology, 40(10): 213-223.

Wullschleger, S.D., Meinzer, F. and Vertessy, R., 1998. A review of whole-plant water use studies in tree. Tree physiology, 18(8-9): 499-512.